Klaus Halbach, "Matrix Representation of Gaussian Optics," American Journal of Physics, Vol. 32, No. 2, pp. 90-108 (February 1964).

Klaus Halbach, "Berechnung linearer, realisierbarer Netzwerke zur Erzielung optimaler Signal/Rauschverhältnisse," Helvetica Physica Acta, vol. 26, no. 1, pp. 65-74 (January 1953). • Klaus Halbach, "Modulation-Effect Corrections for Moments of Magnetic Resonance Line Shapes," Physical Review, vol. 119, no. 4 (August 1960). • Klaus Halbach and William R. Baker, "Plasma Gun Aspects of an E x B System," The Physics of Fluids Supplement (1964).

PUB-755

VOLUME 2

The Art and Science of Magnet Design

Selected Notes of Klaus Halbach

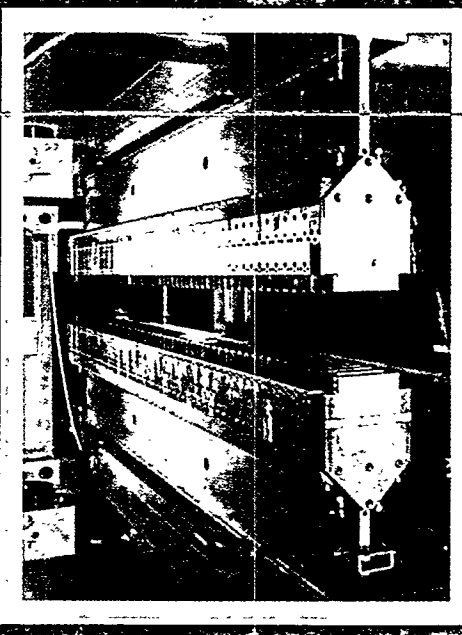

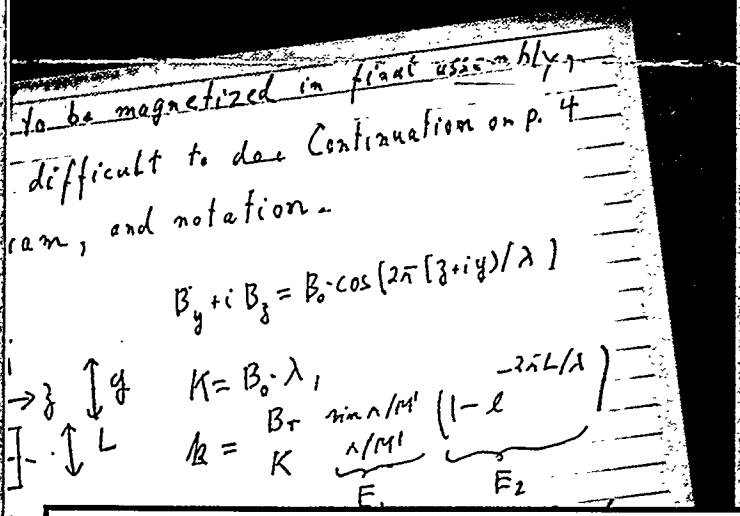

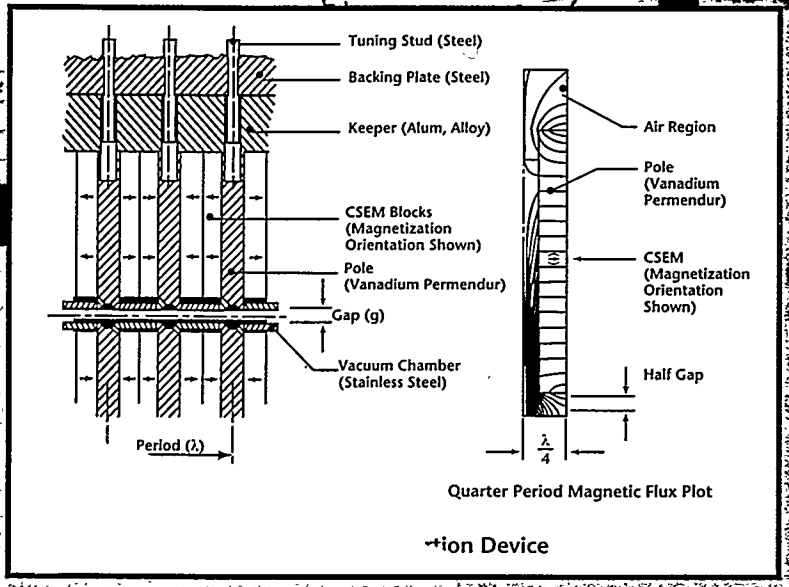

February 1995
Lawrence Berkeley Laboratory
University of California
Berkeley, CA 94720

This is the second of two volumes published in conjunction with the Halbach Symposium on Magnet Technology held at Lawrence Berkeley Laboratory on February 3, 1995, in honor of Klaus Halbach's 70th birthday.
Volume 1 (LBL PUB 754), A Festschrift in Honor of Klaus Halbach, contains technical papers and personal remembrances written by Dr. Halbach's colleagues expressly for the Halbach Symposium and dedicated to him.

VOLUME 2

The Art and Science of Magnet Design

Selected Notes of Klaus Halbach

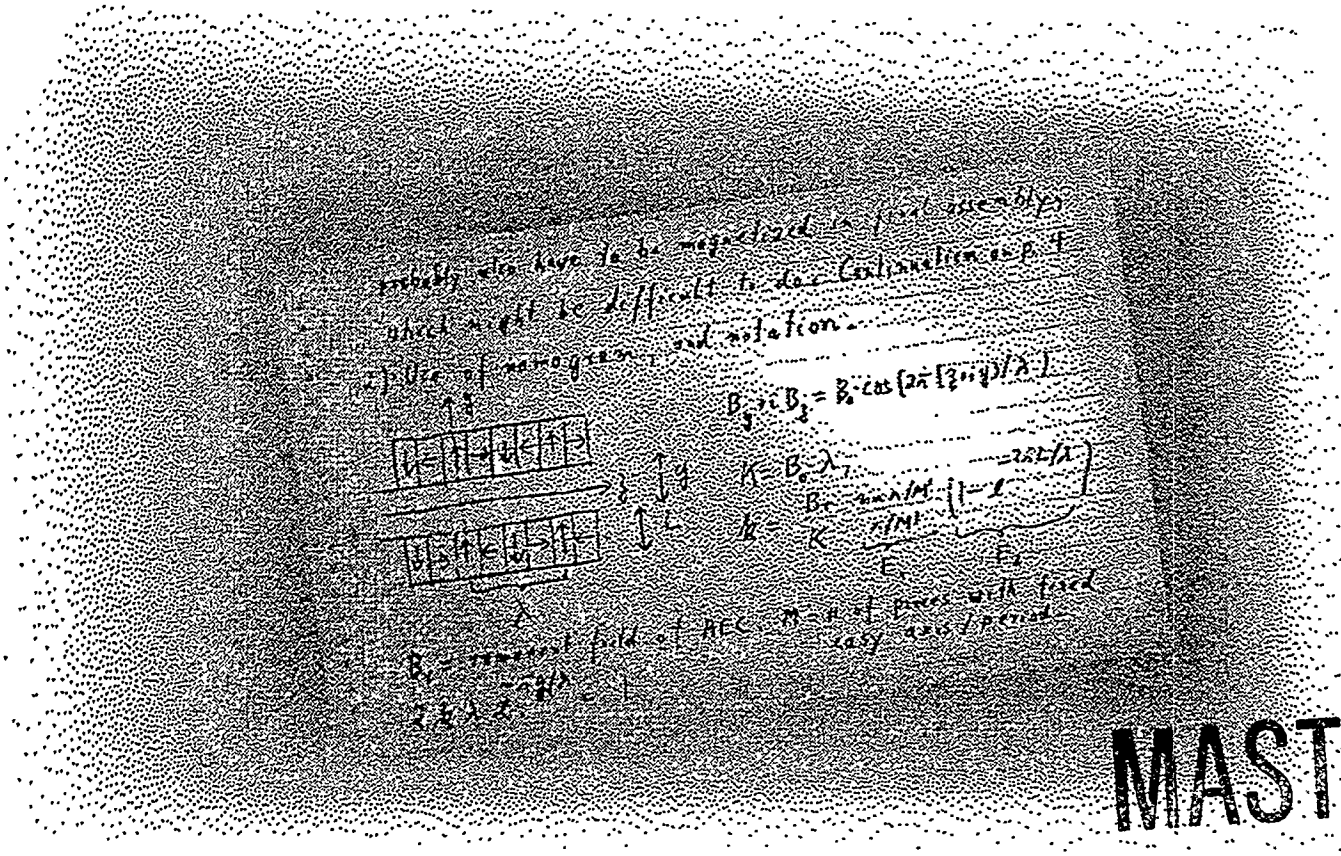

February 1995
Lawrence Berkeley Laboratory
University of California
Berkeley, CA 94720

Prepared for the U.S. Department of Energy under Contract DE-AC03-76SF00098

Preface

This volume contains a compilation of 57 notes written by Dr. Klaus Halbach selected from his collection of over 1650 such documents. It provides an historic snapshot of the evolution of magnet technology and related fields as the notes range from as early as 1965 to the present, and is intended to show the breadth of Dr. Halbach's interest and ability that have long been an inspiration to his many friends and colleagues.

As Halbach is an experimental physicist whose scientific interests span many areas, and who does his most innovative work with pencil and paper rather than at the workbench or with a computer, the vast majority of the notes in this volume were handwritten and their content varies greatly—some reflect original work or work for a specific project, while others are mere clarifications of mathematical calculations or design specifications. As we converted the notes to electronic form, some were superficially edited and corrected, while others were extensively re-written to reflect current knowledge and notation.

The notes are organized under five categories which reflect their primary content: Beam Position Monitors (bpm), Current Sheet Electron Magnets (csem), Magnet Theory (thry), Undulators and Wigglers (u-w), and Miscellaneous (misc). Within the category, they are presented chronologically starting from the most recent note and working backwards in time. The note number, listed in the Table of Contents and at the bottom of each note's first page, comes from a database we have created which includes the titles of the entire collection of notes, and a recently added sixth category, Conformal Transformations (ctr). The appendixes contain a table of all the notes in the database and a list of Dr. Halbach's publications.

The extensive use of hand-written notes by Dr. Halbach leads us to believe that there may be many that were sent to colleagues which were not retained in Dr. Halbach's files, and thus are missing from the database. If you happen to have a note of scientific interest from Dr. Halbach and believe it to be an original, we would appreciate receiving a copy.

Brian M. Kincaid
Simonetta Turek

November 1994

Table of Contents

Theory

Undulator-Wiggler

Halbach Geometries

The Halbach Geometries, referred to in the notes as Gm, are a collection of simple geometric shapes, simple function representations, and 2-dimensional electromagnetic geometries for which conformal mapping calculations have been done to compute basic features such as capacitance, excess flux, etc. For examples of calculations of excess flux, see documents 0336csem (p. 5), 0332csem (p. 11), 0183csem (p. 23), and 0131u-w (p. 175).

The following two pages summarize Dr. Halbach's representations and shorthand notations of his "Geometries." The reader is encouraged to refer back to them when encountering such abbreviations as Gm3 or Gm21 while reading the notes. (Note: Not all the Halbach Geometries are referenced in this collection.)

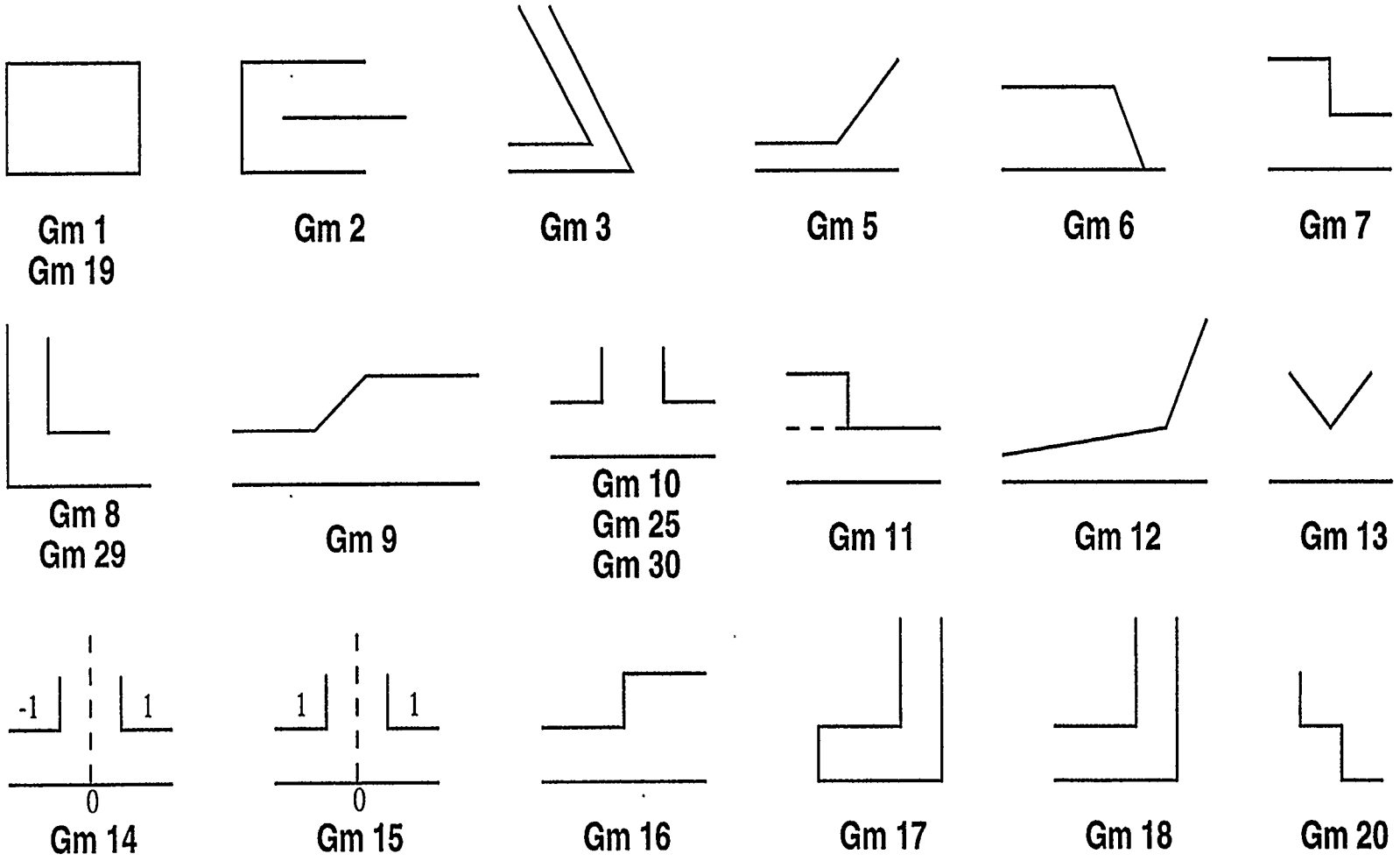
Gm 1
Gm 19
Gm 2
Gm 3
Gm 5
Gm 6
Gm 7
Gm 8
Gm 29
Gm 9
Gm 10
Gm 25
Gm 30
Gm 11
Gm 12
Gm 13
-1
1
0
Gm 14
1
1
0
Gm 15
Gm 16
Gm 17
Gm 18
Gm 20

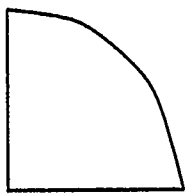

Gm 21

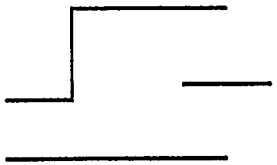

Gm 22

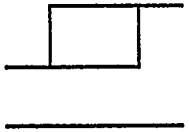

Gm 23

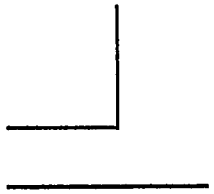

Gm 24

Gm 26

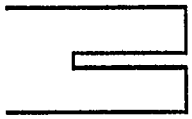

Gm 27

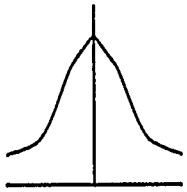

Gm 28

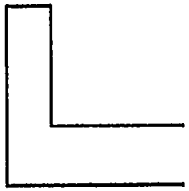

Gm 31

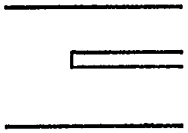

Gm 32

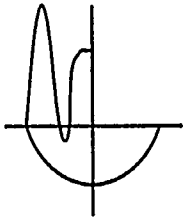

Gm 33

Gm 34

Gm 35

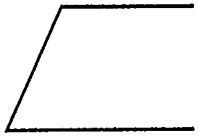

Gm 36

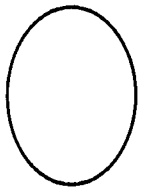

Gm 37

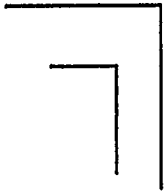

Gm 38

Gm 39

Gm 40

Gm 41

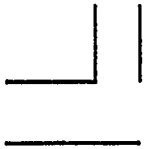

Gm 42

Exact, Complete Proofs of Reciprocity Theorems for Electrostatic and Magnetostatic Beam Monitors

The following is an excercise in Maxwell's equations in a region that is bounded by perfect metal walls and contains nothing but moving electric charges.

$$\nabla \times \mathbf{H} = \mathbf{j} + \dot{\mathbf{D}} \quad \text{and} \quad \nabla \cdot \mathbf{H} = 0, \qquad (1.1), (1.2)$$

where $\mathbf{j}$ comes from the moving charges represented by charge density $\varrho(x, y, z, t)$ in the beam, and

$$\nabla \times \mathbf{E} = -\dot{\mathbf{B}} \quad \text{and} \quad \nabla \cdot \mathbf{D} = \varrho, \qquad (2.1), (2.2)$$

We integrate all equations over time, starting before the front-end wake fields begin, and ending after the end wake fields and RF are gone.

$$\int \dot{\mathbf{D}} dt = 0 \quad \text{and} \quad \int \dot{\mathbf{B}} dt = 0,$$

$$\nabla \times \mathcal{H} = \mathbf{J} \quad \text{and} \quad \nabla \cdot \mathcal{H} = 0, \qquad (3,1), (3.2)$$

$$\nabla \times \mathcal{V} = 0 \quad \text{and} \quad \nabla \cdot \mathcal{V} = R. \qquad (4,1), (4.2)$$

The new symbols stand for integrals over time at every x, y, z.

Electrostatic Pick-up.

The beam with R produces $V_1(x, y, z)$, with $V_1 = 0$ on wall everywhere, including on the electrode. An electrode on V_{20} produces $V_2(x, y, z)$, with $V_2 = 0$ on wall except on the electrode*.

Using (4.1) and (4.2) we notice that V_2 is the actual potential and V_1 is the integrated potential over time. With $\mathcal{H} = -\Delta V$,

$$\begin{aligned} U &= \int \nabla \cdot (V_1 \nabla V_2 - V_2 \nabla V_1)\, dv \\ &= \int \left(V_1 \underbrace{\nabla \cdot \nabla V_2}_{0} - V_2 \underbrace{\nabla \cdot \nabla V_1}_{-R} \right) dv \\ &= \int V_2 R dv. \end{aligned}$$

December, 1986. Note 0022bpm.

* For subscript 2, the quantities are not averaged over time but are time independent, as are all time integrated quantities.

But it is also true that, for the charge q_e,

$$U = \int (V_1 \nabla V_2 - V_2 \nabla V_1) \cdot d\mathrm{a} = V_{20} \cdot Q \quad \text{with} \quad Q = \int q_e dt,$$

induced by electrons on electrode.

The total charge in the bunch, Q_B, is related to $\varrho(x, y, z, t)$ through

$$\int \varrho dt da = Q_B / v,$$

$$\int R v da = \int \varrho dt \, v da = \int Q'_B da,$$

$$Q \cdot V_{20} = \frac{1}{v} \int V_2 Q'_B dv = \boxed{\frac{1}{v} \int Q_B V_2 dz,}$$

where Q'_B is independent of z, and is the charge going through area da, divided by da. The units for $[Q_B] = A$ sec, and $[Q] = A\text{sec}^2$.

Magnetostatic Pick-up.

We use (3.1) and (3.2). The beam with $\mathbf{J}$ produces $\mathbf{A}_1(x, y, z)$, and $\mathcal{H}_1(x, y, z)$. In the coil, the flux from $\mathbf{J}$ integrated over t is

$$\Phi_2 = \int \mu_0 \mathcal{H}_1 \cdot d\mathrm{a} = \int \nabla \times \mathbf{A}_1 \cdot d\mathrm{a} = \mu_0 \oint \mathbf{A}_1 \cdot d\mathrm{s}.$$

In addition, we use a coil with a current, I_2, that produces $\mathbf{A}_2(x, y, z)$, $\mathcal{H}_2(x, y, z)$. We now use, equivalently to the electrostatic case,

$$U = \int \nabla \cdot (\mathbf{A}_1 \times \mathcal{H}_2 - \mathbf{A}_2 \times \mathcal{H}_1) \, dv,$$

where $\mathbf{A}_1$ is the integrated vector potential, and $\mathbf{A}_2$ is the actual potential associated with I_2.

$$\nabla \cdot \mathbf{A}_1 \times \mathcal{H}_2 = \mathcal{H}_2 \cdot \nabla \times \mathbf{A}_1 - \mathbf{A}_1 \cdot \nabla \times \mathcal{H}_2 = \mathcal{H}_2 \cdot \mathcal{H}_1 - \mathbf{A}_1 \cdot \mathbf{J}_2,$$

thus,

$$U = \int (\mathbf{A}_2 \cdot \mathbf{J}_1 - \mathbf{A}_1 \cdot \mathbf{J}_2) \, dv.$$

With

$$\mathbf{J}_1 = J_1 \mathbf{e}_z \quad \text{and} \quad \int J_1 da = \int j_1 da dt = Q_B,$$

we get

$$\int \mathbf{A}_2 \cdot \mathbf{J}_1 dv = Q_B \cdot \int A_{2z} dz,$$

$$\int \mathbf{A}_1 \cdot \mathbf{J}_2 dv = I_2 \int \mathbf{A}_1 \cdot d\mathbf{s} = I_2 \Phi_2 / \mu_0,$$

and get

$$U = Q_B \cdot \int A_{2z} dz - I_2 \Phi_2 / \mu_0 = \int (\mathbf{A}_1 \times \mathcal{H}_2 - \mathbf{A}_2 \times \mathcal{H}_1) \cdot d\mathbf{a}$$

with the last integral taken over the "superconducting" wall.
In the vicinity of the wall we use $\mathcal{H} = -\nabla V$. Thus,

$$U = \int (\mathbf{A}_2 \times \nabla V_1 - \mathbf{A}_1 \times \nabla V_2) \cdot d\mathbf{a}.$$

In general, $\nabla \times (V_1 \mathbf{A}_2) = V_1 \nabla \times \mathbf{A}_2 - \mathbf{A}_2 \times \nabla V_1$, thus

$$U = \int (V_1 \nabla \times \mathbf{A}_2 - V_2 \nabla \times \mathbf{A}_1) \cdot d\mathbf{a} = \int (V_1 \mathcal{H}_2 - V_2 \mathcal{H}_1) \cdot d\mathbf{a} = 0.$$

The last integral vanishes because on the superconducting wall the component of $\mathcal{H}$ perpendicular to the wall (i.e. parallel to $d\mathbf{a}$) is zero. We therefore get

$$\Phi_2 = \mu_0 Q_B \int A_{2z} dz / I_2.$$

The units are $[\Phi_2] = \mu_0 A$ m sec, $[\mathbf{A}_2] = A$, $[\mu_0 Q_B \int A_{2z} dz / I_2] = \mu_0 A$ m sec. It is important to notice that Φ_2 is the integrated flux, and the flux is the integrated induced voltage.

Integral for Excess Flux Calculation

$$J = \int_{t_1}^{t_2} \underbrace{\frac{f(t)}{(t-t_1)^{n_1}(t_3-t)^{n_3}}}_{G} dt$$

We have shown in an earlier note that for $n_1 = n_3 = 1/2$,

$$J = 3\int_{-1}^{1} \frac{f(t)}{\sqrt{4-x^2}} dx, \quad t = \frac{1}{4}(2(t_2+t_1) + (t_2-t_1)x(3-x^2)).$$

For $n_1, n_3 \neq 1/2$, the approach that gave the above equation becomes very complicated, especially if one wants to have generally valid and simple integration. For the general case, we use (arbitrarily, for simplicity)

$$t_2 = 1/2(t_3+t_1) \quad \text{and} \quad J = J_1 + J_3$$

where

$$J_1 = \int_{t_1}^{t_2} G(t)dt \quad \text{and} \quad J_3 = \int_{t_2}^{t_3} G(t)dt,$$

We solve for J_1:

$$A\,dx = (t-t_1)^{-n_1}, \quad Ax = \frac{(t-t_1)^{m_1}}{m_1} \quad \text{and} \quad A = \frac{(t_2-t_1)^{m_1}}{m_1} \quad \text{when} \quad x(t_2) = 1,$$

with

$$m_1 = 1 - n_1 \quad p_1 = \frac{1}{m_1}$$

$$t = t_1 + (t_2-t_1)x^{p_1}, \qquad t_3 - t = (t_2-t_1)(2-x^{p_1}).$$

Thus,

$$J_1 = \frac{(t_2-t_1)^{m_1}}{m1(t_2-t_1)^{n_3}} \int_0^1 \frac{f(t)}{(2-x^{p_1})^{n_3}} dx$$

$$= \boxed{\frac{(t_2-t_1)^{1-n_1-n_3}}{1-n_1} \int_0^1 \frac{f(t)}{(2-x^{p_1})^{n_3}} dx\,.}$$

June, 1993. Note 0336csem.

Equivalently, solving for J_3:

$$-B\,dx = (t_3 - t)^{n_3} dt, \quad Bx = \frac{(t_3 - t)^{m_3}}{m_3} \quad \text{and} \quad B = \frac{(t_2 - t_1)^{m_3}}{m_3},$$

$$t = t_3 - (t_2 - t_1)x^{p_3} \qquad t - t_1 = (t_2 - t_1)(2 - x^{p_3}).$$

Thus,

$$\boxed{J_3 = \frac{(t_2 - t_1)^{1-n_1-n_3}}{1 - n_3} \int_0^1 \frac{f(t)dx}{(2 - x^{p_3})^{n_1}}.}$$

We may now now conclude that

$$J = \int_{t_1}^{t_3} \frac{f(t)}{(t - t_1)^{n_1}(t_3 - t)^{n_3}} dt$$

$$= \boxed{(t_2 - t_1)^{1-n_1-n_3} \left\{ \int_0^1 \frac{f(t_1 + \Delta t x^{\frac{1}{1-n_1}})\,dx}{(2 - x^{\frac{1}{1-n_1}})^{n_3}(1 - n_1)} + \int_0^1 \frac{f(t_3 - \Delta t x^{\frac{1}{1-n_3}})\,dx}{(2 - x^{\frac{1}{1-n_3}})^{n_1}(1 - n_3)} \right\}.}$$

We examine a specific case of excess flux in the pole in the geometry of Figure 1,

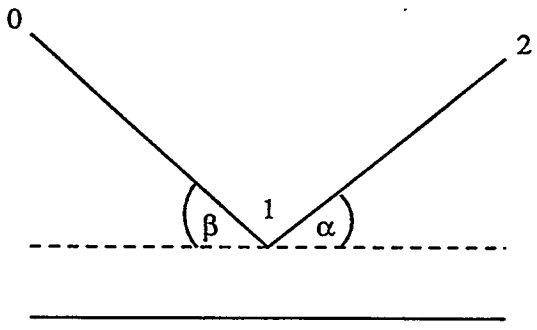

Figure 1.

where,

$$\pi E_{12} = \frac{1}{n_1} \ln\big((n_1 + n_2) I_1\big),$$

$$n_1 = \frac{\alpha}{\pi} \quad \text{and} \quad n_2 = \frac{\beta}{\pi},$$

$$I_1 = \int_0^1 \frac{dt}{t^{n_1}(1-t)^{1-(n_1+n_2)}}$$

$$= \left(\frac{1}{2}\right)^{n_2} \left\{ \frac{1}{1-n_1} \int_0^1 \frac{dx}{\left(2 - x^{\frac{1}{1-n_1}}\right)^{1-(n_1+n_2)}} + \frac{1}{n_1+n_2} \int_0^1 \frac{dx}{\left(2 - x^{\frac{1}{n_1+n_2}}\right)^{n_1}} \right\}.$$

We may conclude that $I_2 = (I_1)_{n_1 \Leftrightarrow n_2}$. Further, the expression $I_1 \frac{\sin\alpha}{\alpha} = I_2 \frac{\sin\beta}{\beta}$ should be true. This is a non-trivial assertion and comes from a derivation of the expression for E_{12} in an earlier note.

H^* at End of CSEM Block

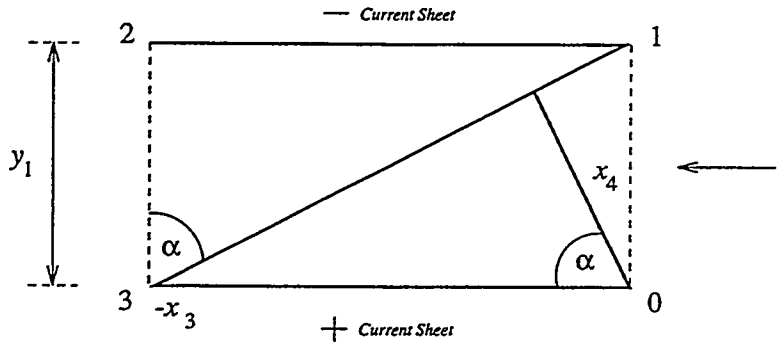

Figure 1.

$$H^*(z) = \frac{I}{2\pi i} \cdot \frac{1}{z - z_0} \longrightarrow -\frac{I'}{2\pi i} \ln \frac{z}{z + x_3} \cdot \frac{z - z_2}{z - z_1}.$$

In the vicinity of $z = 0$,

$$H^* = -\frac{H_c}{2\pi i} \ln \frac{z\, z_2}{z_1 x_3},$$

where

$$\frac{z_1 x_3}{z_2} = \frac{i y_1 x_3}{i y_1 - x_3} = \frac{y_1 x_3}{y_1 + i x_3} = \frac{x_3}{1 + i x_3 / y_1} = x_4 e^{-i\alpha},$$

$$x_4 = \frac{x_3}{\sqrt{1 + x_3^2 / y_1^2}} = x_3 \cos\alpha \quad \text{and} \quad z = r e^{i\varphi}.$$

Thus,

$$\boxed{H^* = -\frac{H_c}{2\pi i} \ln \frac{r e^{i(\varphi+\alpha)}}{x_4} = -\frac{H_c}{2\pi i} \left(\varphi + \alpha + i \ln \frac{x_4}{r}\right).}$$

Field "blows up" at $r = 0$. Thus, for scaling purposes, at location where $\ln \dfrac{x_4}{r} = 2\pi$, $r = x_4 e^{-2\pi} = x_4 \cdot 1.9 \times 10^{-3}$.

There is a strong local field perpendicular to the "current sheet side", which is not problematic when easy axis is parallel to the "current sheet side". It is easier to see with charge sheet, and it leads to the same answer.

Interesting damage results for block not magnetized in either a perpendicular or parallel direction to the sides.

May, 1993. Note 0335csem.

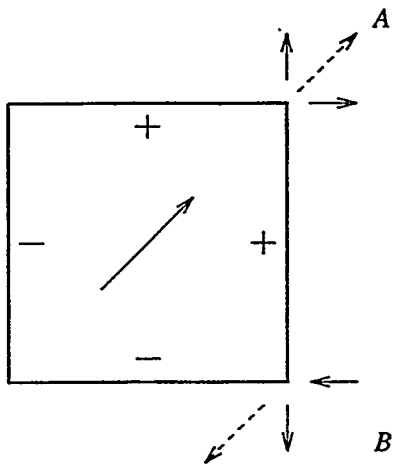

Figure 2.

No damage will result in corner A, but there is a potential of demagnetization at corner B, and at symmetrically located corners.

Summary of Excess Flux Formulae for Gm3, Gm18 and Gm40

Unless otherwise noted, the following definitions hold for all geometries in this Note

$$F = \pi \frac{\Delta A}{V_0}, \quad n = \frac{\alpha}{\pi}, \quad \text{and} \quad a = \frac{h_2}{h_1}.$$

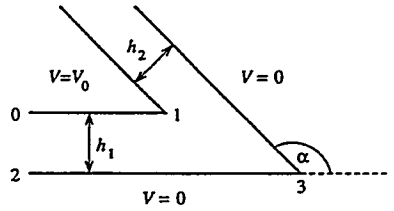

Figure 1.

$$F_{01} = (1+b)\int_0^1 \frac{1-x^n}{(1-x)(b+x)}dx, \tag{1}$$

$$F_{23} = F_{01} + \ln b, \quad \text{with} \quad b = a^{1/n}. \tag{2}$$

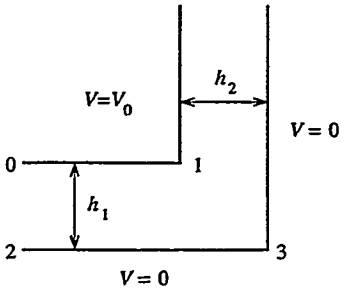

Figure 2.

For Figures 2, 3, and 4 (Gm18 and Gm40) $\alpha = \pi/2$.

$$F_{01} = \ln \frac{1+1/a^2}{4} + 2a \arctan \frac{1}{a}, \tag{3}$$

$$F_{23} = \ln \frac{1+a^2}{4} + 2a \arctan \frac{1}{a}, \tag{4}$$

April, 1989. Note 0332csem.

We summarize here the the sum of excess fluxes for (1) and (3). For (1), we get

$$(F_{01}(a) + F_{01}(1/a)) = (1+b)^2 \int_0^1 \frac{(1-x^n)(1+x)}{(1-x)(b+x)(1+xb)} dx\,. \tag{1D}$$

And for (3), we have

$$(F_{01}(a) + F_{01}(1/a)) = 2\ln\frac{a+1/a}{4} + 2a\arctan(1/a) + 2(1/a)\arctan a\,. \tag{3D}$$

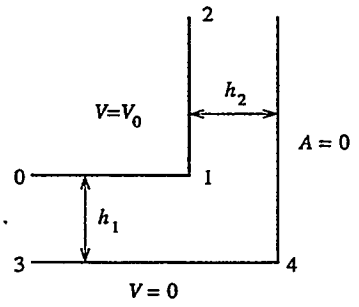

Figure 3.

$$F_{34} = \ln(1+a^2) + 2a\arctan(1/a)\,, \tag{5}$$

$$F_{12} = 2\ln\left(a + \sqrt{1+a^2}\right)\,, \tag{6}$$

$$F_{01} = F_{34} - F_{12}\,. \tag{7}$$

Continued on following page.

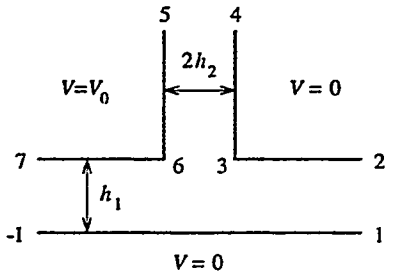

Figure 4.

$$F_{-11} = \ln(1+a^2) + 2a \arctan(1/a)\,, \tag{8}$$

$$F_{67} = \ln \frac{1+a^2}{2a\left(a+\sqrt{1+a^2}\right)} + 2a \arctan \frac{1}{a}\,, \tag{9}$$

$$F_{56} = \ln \frac{\sqrt{1+a^2}\left(a+\sqrt{1+a^2}\right)}{2} + \frac{1}{a} \arctan a\,, \tag{10}$$

$$F_{567} = \ln \frac{\left(\sqrt{1+a^2}\right)^3}{4a} + 2a \arctan \frac{1}{a} + \frac{1}{a} \arctan a\,, \tag{11}$$

$$F_{234} = \ln \frac{\sqrt{1+1/a^2}}{4} + \frac{1}{a} \arctan a\,. \tag{12}$$

Anti-Symmetric Undulator to Make Vertically Polarized or Circularly Polarized Light

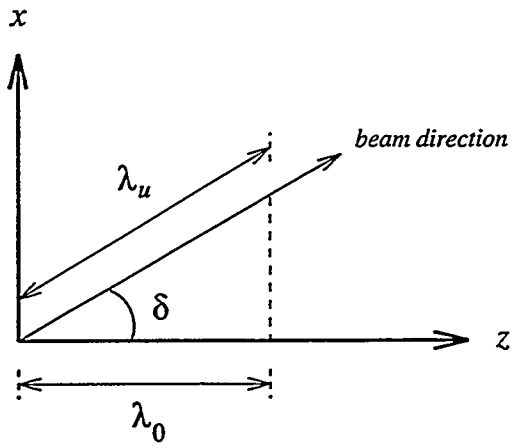

Figure 1.

We have

$$-V = \frac{B_0}{k_0} \sin k_0 z \cosh k_0 y, \tag{1}$$

with fields anti-symmetric to the midplane $y = 0$.

$$B_z = B_0 \cosh k_0 y \cos k_0 z \quad \text{and} \quad B_y = B_0 \sinh k_0 y \sin k_0 z \tag{2}$$

in direction δ relative to the z-axis.

$$\lambda_u = \lambda_0 / \cos \delta, \tag{3.1}$$

$$B_\perp = \underbrace{B_0 \cosh k_0 y \sin \delta}_{B_2} \cos k_0 z, \tag{3.2}$$

$$B_y = \underbrace{B_0 \sinh k_0 y}_{B_1} \sin k_0 z. \tag{3.3}$$

Linearly Polarized Light.

Let $y = 0$, $B_y = 0$,

$$B_2 = \sin \delta B_0 = \sin \delta B_0 \left(\frac{g}{\lambda_u} \cdot \frac{1}{\cos \delta} \right). \tag{4}$$

By the above B_0 is indicated the achievable B_0 as a function of g/λ_0, where λ_0 is the period in the z-direction, and g is the magnet gap.

October, 1984. Note 0208csem.

To have a better understanding, we look at the pure CSEM undulator:

$$B_0 = B_3 e^{-\pi g/\lambda_0},$$

with B_3 equal to the product of $2B_r$, the segmentation factor and the finite height factor.

$$B_2 = B_3 \sin\delta e^{-a/\cos\delta}, \quad \text{with} \quad a = \pi g/\lambda_u. \tag{5.1}$$

We optimize with δ for given g/λ_u. With $B_2' = 0$,

$$\cos\delta - a\tan^2\delta = 0.$$

Instead of solving for given a, we make a table of a *vs.* δ.

$$a = \frac{\cos^3\delta}{\sin^2\delta}, \tag{5.2}$$

$$B_2 = B_3 \sin\delta e^{-\cot^2\delta} = B_3 y. \tag{5.3}$$

Compared to a "normal" undulator:

$$B_{2n} = B_3 e^{-a} = B_3 e^{-\cos\delta/\tan^2\delta} = B_3 y, \tag{5.4}$$

$$\frac{B_2}{B_{2n}} = \sin\delta e^{-\cot^2\delta} e^{\cos\delta\cot^2\delta} = \frac{y}{y_o}, \tag{5.5}$$

δ	g/λ_u	y	y/y_0
30.00	0.83	0.02	0.33
35.00	0.53	0.07	0.40
40.00	0.35	0.16	0.46
45.00	0.23	0.26	0.53
50.00	0.14	0.38	0.60
55.00	0.09	0.50	0.66
60.00	0.05	0.62	0.73

Table 1.

Circularly Polarized Light.

We set $y = y_1$, and $k_0 y_1 = \beta$. From (3.2) and (3.3), we see we need to satisfy $\cosh\beta \sin\delta = \sinh\beta$ for the helical undulator action, thus

$$\sin\delta = \tanh\beta, \tag{6.1}$$

or

$$\cos\delta = \sqrt{1 - \tanh^2\beta} = 1/\cosh\beta, \tag{6.2}$$

or

$$\tan\delta = \sinh\beta, \tag{6.3}$$

$$B_u = B_0 \sinh\beta = B_0 \tan\delta = B_0 \left(\frac{g/\lambda_u}{\cos\delta}\right) \tan\delta. \tag{7}$$

We assess the reasonableness and feasability of the above analysis.

Clearly,

$$\varepsilon = \frac{2y_1}{g} \tag{8.1}$$

is an important parameter.

$$\beta = \frac{2\pi y_1}{\lambda_0} = \frac{2y_1}{g} \cdot \pi \cdot \frac{g}{\lambda_u \cos\delta},$$

and for $p = g/\lambda_u$,

$$\beta = \varepsilon p \frac{\pi}{\cos\delta} = \varepsilon \frac{a}{\cos\delta}, \tag{8.2}$$

$$\varepsilon = \frac{\beta\cos\delta}{a}. \tag{8.3}$$

The indicated procedure is as follows. Given $p = g/\lambda_u$ and $B_0(g/\lambda_0) = B_0(p/\cos\delta)$, we optimize B_u with δ and get ε from (8.3).

For a pure REC undulator,

$$B_0 = B_3 e^{-a/\cos\delta} \quad \text{with} \quad a = \pi g/\lambda_u = \pi p,$$

$$B_u = B_3 \tan\delta \cdot e^{-a/\cos\delta}.$$

With $B_u' = 0$,

$$\frac{1}{\cos^2\delta} - a\tan\delta \cdot \frac{\sin\delta}{\cos^2\delta} = 0,$$

$$a\frac{\sin^2\delta}{\cos\delta} = a\frac{1-\cos^2\delta}{\cos\delta} = 1,$$

$$\boxed{\cos\delta = -\frac{1}{2a} + \sqrt{\frac{1}{4a^2}+1}.} \tag{9.1}$$

For $\cosh\beta = 1/\cos\delta$,

$$\boxed{\beta = \ln\left(\sqrt{\cosh^2\beta - 1} + \cosh\beta\right).} \tag{9.2}$$

$$\boxed{\varepsilon = \beta\cos\frac{\delta}{a}.} \tag{9.3}$$

$$\boxed{\frac{B_u}{B_3} = \tan\delta\cdot e^{-a/\cos\delta}.} \tag{9.4}$$

For extreme "legal" $\varepsilon = 1$:

$$\beta\cos\frac{\delta}{a} = \sin^2\delta\cdot\beta = \sin^2\delta\cdot\ln\left(\sqrt{1+\tan^2\delta}+\tan\delta\right) = \sin^2\delta\cdot\ln\frac{1+\sin\delta}{\cos\delta},$$

$$\beta = 60.27^\circ, \quad g/\lambda_u = .21, \quad \text{and} \quad B_u/B_3 = .46.$$

Hybrid Undulator with Superimposed Quadrupole Field

With the electron beam in the z-direction, and the midplane the xz-plane, the normal undulator fields can be described by

$$B_z = iB_y = B_1^* = iF_1' = iB_1 \cos k(z + iy).$$

For the complex potential $F_1 = A_1 + V_1$, with A_1 and V_1 the vector and scalar potentials respectively, it follows that

$$F_1 = \frac{B_1}{k} \sin k(z + iy) \quad \text{and} \quad V_1 = \frac{B_1}{k} \cos kz \sinh ky.$$

The desired normal quadrupole fields are given by

$$B_0^* = iF_0' = iB_0'z \quad F_0 = \frac{1}{2}B_0'z^2, \quad \text{and} \quad V_0 = B_0'xy.$$

For the scalar potential and the combined undulator and quadrupole fields, we therefore have

$$V = V_1 + V_0 = \frac{B_1}{k} \cos kz \sinh ky + B_0'xy.$$

Setting this equal to a constant gives the associated surface of a pole made with infinitely permeable material. With y_0 the half-gap of the pole at $z = x = 0$,

$$0 = \cos kz \sinh ky - \sinh ky_0 + \frac{B_0'}{kB_1} kxky.$$

With the following substitutions:

$$a = \cos kz, \quad \mathcal{E} = \frac{B_0'}{kB_1}, \quad u = kx, \quad \text{and} \quad v = ky,$$

we arrive at the following equation for the ideal 3D pole:

$$\boxed{a \sinh v - \sinh v_0 + \mathcal{E}uv = G = 0.}$$

To understand what this means, we look at some derived quantities:

$$\boxed{y' = \frac{dy}{dx} = -\frac{G_x'}{G_y'} = -\frac{G_u'}{G_v'} = -\frac{\mathcal{E}v}{a \cosh v + \mathcal{E}u}}$$

January, 1984. Note 0187csem.

is the slope of the pole in the xy-plane. For $x = z = 0$ it is reduced to

$$\boxed{y_0' = -\frac{B_0' y_0 / B_1}{\cosh v_0} = -\frac{\mathcal{E} v_0}{\cosh v_0}.}$$

Looking at the slope just above the axis of the system, i.e. for $x = 0$,

$$\boxed{a \sinh v_1 = \sinh v_0,}$$

and

$$y' = -\frac{\mathcal{E} v_1}{a \cosh v_1},$$

where the subscript 1 refers to the case of $x = 0$ and z equal to anything. For $z = 0$ this reduces to

$$y' = -\frac{B_0' y_0 / B_1}{\cosh v_0} = -\frac{\mathcal{E} v_0}{\cosh v_0}.$$

Eliminating $a = \cos kz$ gives

$$\boxed{y' = -\mathcal{E} v_1 \frac{\tanh v_1}{\sinh v_0}.}$$

For the curvature of the pole in the xy-plane we need

$$\begin{aligned} y'' &= \frac{\partial y'}{\partial x} + \frac{dy}{dx} \cdot \frac{\partial y'}{\partial y} \\ &= k \left(\frac{\partial y'}{\partial u} + y' \frac{\partial y'}{\partial v} \right) \\ &= k \left(\frac{\mathcal{E}^2 v}{(a \cosh v + \mathcal{E} u)^2} + \frac{\mathcal{E}^2 v}{(a \cosh v + \mathcal{E} u)} \cdot \frac{a \cosh v + \mathcal{E} u - a v \sinh v}{(a \cosh v + \mathcal{E} u)^2} \right). \end{aligned}$$

For $u = 0$, this reduces to

$$\begin{aligned} y'' &= \frac{k \mathcal{E}^2 v_1 a}{a^3 \cosh^3 v_1} (2 \cosh v_1 - v_1 \sinh v_1) \\ &= \mathcal{E}^2 k \frac{v_1 \tanh^2 v_1}{\sinh^2 v_0} (2 - v_1 \tanh v_1). \end{aligned}$$

We let $|y'| \ll 1$, and therefore $\sqrt{1 + (y')^2}^3 \approx 1$. With radius of curvature R, we get

$$\frac{1}{k \mathcal{E}^2} \cdot \frac{\sinh^2 v_0}{v_1 \tanh^2 v_1 (2 - v_1 \tanh v_1)} = \boxed{R = \frac{y_0}{\mathcal{E}^2} \cdot \frac{\sinh^2 v_0}{v_0 v_1 \tanh^2 v_1 (2 - v_1 \tanh v_1)},}$$

For $v_1 = v_0$, and $y_0' = -\mathcal{E}v_0/\cosh v_0$:

$$\boxed{R_0 = \frac{y_0}{\mathcal{E}^2} \cdot \frac{\cosh^2 v_0}{v_0^2(2 - v_0 \tanh v_0)} = \frac{y_0}{(y_0')^2} \cdot \frac{1}{v_0^2(2 - v_0 \tanh v_0)}.}$$

We make the following assignments:

$$\frac{1}{k\mathcal{E}^2} = \frac{kB_1^2}{(B_0')^2} = y_0 \frac{B_1^2}{y_0^2(B_0')^2} v_0 \quad \text{and} \quad b = \frac{B_1^2}{y_0^2(B_0')^2},$$

and re-write

$$\boxed{R = y_0 b \cdot \frac{v_0}{v_1} \cdot \frac{\sinh^2 v_0}{\tanh^2 v_1(2 - v_1 \tanh v_1)},}$$

where for $2 - v \tanh v = 0, v = \dfrac{2\pi y}{\lambda} = 2.0653.$

Excess Flux into Gm13

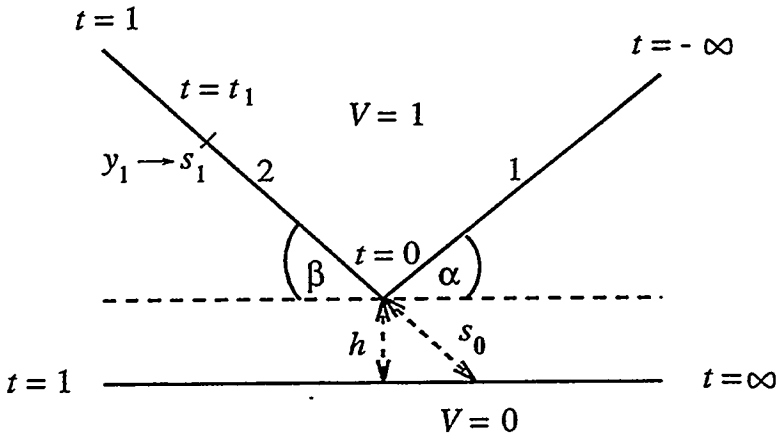

Figure 1.

For the above graph,

$$\frac{\alpha}{\pi} = n_1\,, \quad \frac{\beta}{\pi} = n_2\,, \quad \text{and} \quad n_1 + n_2 = n_3\,.$$

The conformal map is described by

$$\dot{z} = a\frac{t^{n_3}}{(t-1)^{1+n_2}}, \quad a \in \Re\,.$$

From

$$\pi\dot{F} = \frac{1}{t-1} \quad \text{follows} \quad \pi F = \ln(t-1)\,.$$

We describe the flux into surface 2 of Figure 1 as

$$\Phi_2 = -\frac{1}{\pi}\ln(1-t_1) = \int_{s_0}^{s_1}\frac{ds}{\beta s} + \Delta A_2\,.$$

Thus

$$\begin{aligned}\beta\Delta A_2 &= -n_2\ln(1-t_1) - \ln\left(1+\frac{s_1-s_0}{s_0}\right)\\ &= \ln\frac{(1-t_1)^{-n_2}}{\left(1+\dfrac{a}{s_0}\displaystyle\int_0^{t_1}\frac{t^{n_3}\,dt}{(1-t)^{1+n_2}}\right)}\end{aligned}$$

September, 1983. Note 0183csem.

and by l'Hôpital's Rule,

$$= \ln \frac{n_2(1-t_1)^{-n_2-1}}{\left(\frac{a}{s_0} t_1^{n_3}(1-t_1)^{-n_2-1}\right)}$$
$$= \ln \frac{n_2 s_0}{a},$$

and therefore

$$\boxed{\Delta A_2 = \frac{1}{\beta} \ln \left(\frac{h}{\pi} \frac{\beta}{a \sin \beta} \right) .} \tag{1}$$

We need to calculate h/a, and we begin with

$$y_1 = h + a \sin \beta \int_0^{t_1} \frac{t^{n_3} dt}{(1-t)^{n_2+1}} . \tag{2}$$

We now calculate y_1 by going around the singularity at $t = 1$ on circle with $\varrho = \varrho_1 = 1 - t_1$, that is

$$t = 1 + \varrho_1 e^{i\varphi} \quad \text{and} \quad dt = i\varrho_1 e^{i\varphi} d\varphi ,$$

and thus

$$y_1 = \Im i\varrho_1 a \int_0^{\pi} \frac{(1+\varrho_1 e^{i\varphi})^{n_3}}{\varrho_1^{1+n_2} e^{i\varphi(1+n_2)}} e^{i\varphi} d\varphi$$
$$= \Im \frac{ia}{\varrho_1^{n_2}} \int_0^{\pi} (1+\varrho_1 e^{i\varphi})^{n_3} e^{-in_2\varphi} d\varphi .$$

For ϱ_1 sufficiently small,

$$y_1 = \Im \frac{ia}{\varrho_1^{n_2}} \frac{e^{-in_2\pi} - 1}{-in_2} = \frac{a \sin \beta}{n_2 \varrho_1^{n_2}} .$$

Re-writing (2) with $t = 1 - \varrho$

$$y_1 = h + a \sin \beta \int_{\varrho_1}^{1} \frac{(1-\varrho)^{n_3}}{\varrho^{n_2+1}} d\varrho = \frac{a \sin \beta}{n_2 \varrho_1^{n_2}} .$$

Thus

$$\frac{h}{a \sin \beta} = \frac{1}{n_2 \varrho_1^{n_2}} - \int_{\varrho_1}^{1} \frac{(1-\varrho)^{n_3}}{\varrho^{n_2+1}} d\varrho$$
$$= \frac{1}{n_2 \varrho_1^{n_2}} + \frac{(1-\varrho)^{n_3}}{n_2 \varrho^{n_2}} \Bigg|_{\varrho_1}^{1} + \frac{n_3}{n_2} \int_{\varrho_1}^{1} \frac{(1-\varrho)^{n_3-1}}{\varrho^{n_2}} d\varrho ,$$

and

$$\frac{hn_2}{a\sin\beta} = \frac{h\beta}{\pi a\sin\beta} = n_3 I_2$$

where

$$\boxed{I_2 = \int_0^1 \frac{dt}{t^{n_2}(1-t)^{1-n_3}} \quad \text{and} \quad I_1 = \int_0^1 \frac{dt}{t^{n_1}(1-t)^{1-n_3}}.}$$

Therefore we may now summarize from (1) that

$$\boxed{\Delta A_2 = \frac{1}{\beta}\ln(n_3 I_2),}$$

and equivalently

$$\boxed{\Delta A_1 = \frac{1}{\alpha}\ln(n_3 I_1).}$$

Further, since

$$\frac{h}{\pi a} = n_3 I_2 \frac{\sin\beta}{\beta} = n_3 I_1 \frac{\sin\alpha}{\alpha},$$

$$\boxed{n_3 I_1 = n_3 I_2 \frac{\sin\beta/\beta}{\sin\alpha/\alpha}.}$$

A different way to look at what was done earlier:

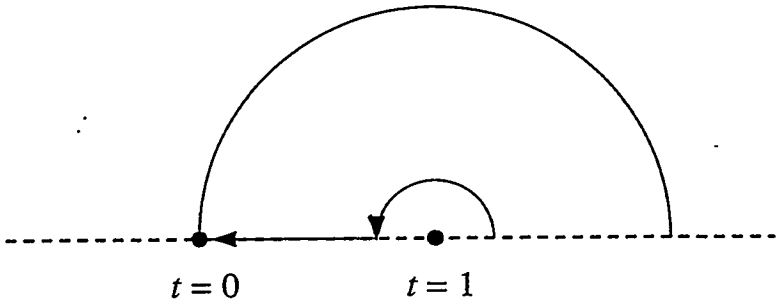

Figure 2.

Since, clearly, $h = \Im \int_{1+}^{0} \dot{z}dt$, one may take a path from any point on the real t-axis to the right of $t = 1$ to $t = 0$.

In this note the path followed a $\varrho_1 \Rightarrow 0$ half-circle around $t = 1$, and then on axis to $t = 0$.

Flux Distribution Symmetry Theorem

Even though this case is the same as the electrostatic case, it is formulated for magnetic fields because of the application to CSEM in hybrid systems.

Theorem.

There are N bodies with $\mu = \infty$. The matrix M, which describes the relationship between potentials V_n on fluxes F_n leaving body n, is symmetrical, i.e.: $F = MV$, $M^t = M$. In this notation, the subscript 0 indicates the reference body on potential $V = 0$. Thus, the theorem states

$$M_{nm} = M_{mn}.$$

Analysis.

Stored energy in the field is unique: it depends only on the initial state (we assume $V_n = 0$) and the end state. By going from the initial to the end state by bringing bodies in any sequence from $V_n = 0$ to the final V_n, and doing so by moving magnetic charges from infinity, we get

$$\mathcal{E} = \int V^t dF = \int V^t M dV.$$

$\mathcal{E}$ must be independent of sequence in which this is done: the right hand side must be a complete differential leading to $M_{nm} = M_{mn}$. We show this explicitly for V_1, V_2 and all other $V_n = 0$:

$$\begin{aligned}\mathcal{E} &= \int \begin{pmatrix} V_1 & V_2 \end{pmatrix} \begin{pmatrix} M_{11}dV_1 - M_{12}dV_2 \\ -M_{21}dV_1 + M_{22}dV_2 \end{pmatrix} \\ &= \int M_{11}V_1 dV_1 + \int M_{22}V_2 dV_2 - \underbrace{\int (M_{12}V_1 dV_2 + M_{21}V_2 dV_1)}_{G}.\end{aligned}$$

We simplify G by making the following substitutions:

$$M_{12} = S + D, \quad M_{21} = S - D, \quad \text{and} \quad S = \frac{1}{2}(M_{12} + M_{21}), \quad D = \frac{1}{2}(M_{12} - M_{21}),$$

$$G = S \int \underbrace{(V_1 dV_2 + V_2 dV_1)}_{(a)} + D \underbrace{\int (V_1 dV_2 - V_2 dV_1)}_{(b)},$$

where (a) is $d(V_1 \quad V_2)$ and is therefore independent of the sequence, and (b) would

November, 1986. Note 0143csem.

be dependent on our sequence. Since G must be independent of the sequence, it follows that $D = 0$.

In a CSEM circuit, $\mathbf{F}$ equals the vector of charges deposited by the CSEM on the surfaces (with all $V = 0$). Therefore, a hybrid system can be represented by magnetic capacitors and sources that deposit DC charges. If one finds this more convenient, one may also do this analysis with capacitors and AC current sources, or with resistors and DC currents.

The theorems known for these circuits apply, such as Kirchhoff's reciprocity theorem, i.e. the nodal equations, etc. One can also use 2×2 matrix methods for systems like ladder networks, and apply them directly to hybrid wigglers. One can use concepts like characteristic impedance of networks and quadrupole theory, i.e. all the tools that have been developed for analog network analysis.

Stored Energy in CSEM

We define the energy density as

$$\mathcal{E} = \int \mathbf{H} \cdot d\mathbf{B}.$$

We can look at the easy-axis direction and the direction perpendicular to the easy-axis separately. The lower integral limit is arbitrary, but must be fixed.

With $B_\parallel = B_r + \mu_0 \mu_\parallel H_\parallel$ and $B_\perp = \mu_0 \mu_\perp H_\perp$:

$$\mathcal{E}_\parallel = \int_{H_\parallel=0}^{H_\parallel} H_\parallel dB_\parallel = \int_{H_\parallel=0}^{H_\parallel} H_\parallel \frac{dB_\parallel}{dH_\parallel} dH_\parallel = \mu_0 \mu_\parallel \int_{H_\parallel=0}^{H_\parallel} H_\parallel dH_\parallel.$$

Thus,

$$\boxed{\mathcal{E}_\parallel = \frac{1}{2} \mu_0 \mu_\parallel H_\parallel^2,}$$

and similarly,

$$\boxed{\mathcal{E}_\perp = \frac{1}{2} \mu_0 \mu_\perp H_\perp^2,}$$

with

$$\boxed{\mathcal{E}_{\text{tot}} = \mathcal{E}_\parallel + \mathcal{E}_\perp.}$$

This obviously gives $H_\parallel$ a unique role.

November, 1982. Note 0142csem.

Earnshaw's Theorem for Non-Permeable Material

Problem: There is an assembly of "frozen" magnetic charges $\varrho(\mathbf{r})$ † in an external magnetic field (produced by solenoid or other REC assembly) without any permeable material in the system.

Question: What is the restoring force for small displacements?

Analysis: The force components in the (x_1, x_2, x_3) coordinate system are

$$F_1 = -\int \varrho V_1' dv, \quad F_2 = -\int \varrho V_2' dv, \quad \text{and} \quad F_3 = -\int \varrho V_3' dv.$$

We displace the system by $\Delta x_1, \Delta x_2, \Delta x_3$, which is the same as displacing the external fields by $-\Delta x_1, -\Delta x_2, -\Delta x_3$ without changing ϱ, and get

$$\begin{aligned} \Delta F_n &= \int \sum \Delta x_m \frac{\partial}{\partial x_m} \varrho \frac{\partial V}{\partial x_n} dv \\ &= \sum M_{nm} \Delta x_m \qquad \text{with} \qquad M_{nm} = \int \varrho \frac{\partial}{\partial x_n} \frac{\partial}{\partial x_m} V dv, \end{aligned}$$

$$\Delta \mathbf{F} = M \cdot \Delta \mathrm{x}.$$

In general, M will not be a diagonal matrix. We assume that it can be made diagonal (by going to a new coordinate system) with matrix C, where

$$C\Delta \mathbf{F} = \Delta \mathbf{F}_d = CMC^{-1} \cdot C\Delta \mathrm{x} = CMC^{-1} \cdot \Delta \mathrm{x}_d,$$

$$CMC^{-1} = M_d = \int \varrho \begin{pmatrix} V_{xx}'' & 0 & 0 \\ 0 & V_{yy}'' & 0 \\ 0 & 0 & V_{zz}'' \end{pmatrix} dv,$$

where x, y, z are the new coordinates. From this, it follows that

$$\boxed{\frac{\Delta F_x}{\Delta x} + \frac{\Delta F_y}{\Delta y} + \frac{\Delta F_z}{\Delta z} = \int \varrho \underbrace{\left(V_{xx}'' + V_{yy}'' + V_{zz}''\right)}_{=\nabla^2 V = 0} dv = 0.}$$

Since a stable system requires a negative restoring force in each of the three coordinate directions, any such system will be unstable.

June, 1981. Note 0076csem.

† REC can be considered this way if one assumes differential permeability $\equiv 1$.

In applications, it will often be clear *a priori* in which coordinate system the matrix M will be diagonal, and the above equation can then be used directly in its final form. This means that for systems with cylindrical symmetry about the z-axis, that because

$$\frac{\Delta F_y}{\Delta y} = \frac{\Delta F_x}{\Delta x} \Rightarrow \frac{\Delta F_r}{\Delta r} \quad \text{and} \quad 2\frac{\Delta F_r}{\Delta r} + \frac{\Delta F_z}{\Delta z} = 0,$$

only one of the stiffnesses needs to be calculated from basics.

It is interesting to note that Earnshaw's Theorem is often stated in an overly broad fashion. For instance, stable support *is* possible if one allows forces not derived from a potential satisfying $\nabla^2 V = 0$. The forces between contacting solid materials, for example, such as mechanical bearings, are due to the quantum nature of solids, and hence do not obey Earnshaw's Theorem. It is also clear without any mathematics that a permanent magnet is stably supported in a superconducting bowl. This is similarly true for an extreme diamagnetic bowl.

Harmonics Produced by Rectangular REC Block

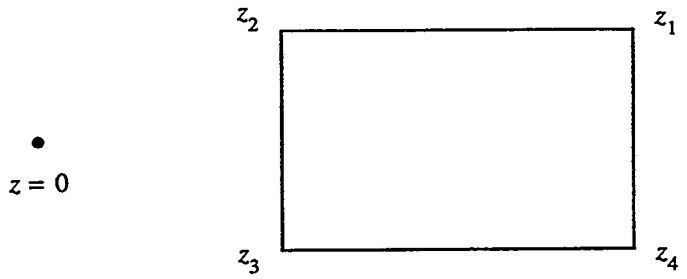

Figure 1.

In this document we refer to the above diagram and (4b) and (16b) of the *Nuclear Instruments and Methods* article†

$$\underline{B}^*(z_0) = \sum_{n=1} b_n z_0^{n-1},$$

$$b_n = \frac{B_r}{2\pi i} \oint \frac{dx}{z^n}.$$

For $n = 1$,

$$b_1 = \frac{B_r}{2\pi i} \ln \frac{z_2}{z_1} \cdot \frac{z_4}{z_3} = \frac{B_r}{2\pi i} \ln \frac{z_2/z_1}{z_3/z_4}$$

$$= \boxed{\frac{B_r}{\pi} \Im \ln \frac{z_2}{z_1}.}$$

For $n \geq 2$,

$$b_n = -\frac{B_r}{2\pi i} \cdot \frac{1}{n-1} \left(\frac{1}{z_2^{n-1}} - \frac{1}{z_1^{n-1}} + \frac{1}{z_4^{n-1}} - \frac{1}{z_3^{n-1}} \right)$$

$$= \boxed{-\frac{B_r}{\pi} \cdot \frac{1}{n-1} \Im \left(\frac{1}{z_2^{n-1}} - \frac{1}{z_1^{n-1}} \right).}$$

October, 1980. Note 0059csem.

† Halbach, H., Nuclear Instruments and Methods 169, 1 (1980).

A Possible REC Undulator for SSRL

I. Reason for REC.

It may be possibe to use some very specific ferrite. All other materials, like the Alnicos, are not only significantly inferior in performance, but would probably also have to be magnetized in final assembly which may be difficult to do.

A potential future advantage is that the permanent magnet undulator can be scaled down in physical size without difficulty. One can therefore envision the following scheme: design a REC undulator for very small gap and λ and have it inside vacuum. Move the two arrays apart to have the large gap necessary during beam formation. When beam is established, move the 2 arrays together to form the design gap that the beam allows. Clearly, this would be nearly impossible with either a conventional, or even a superconducting, undulator.

II. Use of Nomogram and Notation.

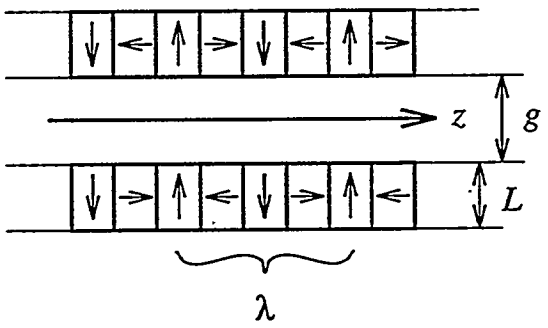

Figure 1.

$$B_y + iB_z = B_0 \cos \frac{2\pi(z+iy)}{\lambda},$$

$$K = B_0 \lambda,$$

$$k = \frac{B_r}{K} \underbrace{\frac{\sin \pi/M'}{\pi/M'}}_{E_1} \underbrace{\left(1 - e^{-2\pi L/\lambda}\right)}_{E_2},$$

where B_r is the remanent field of REC, M' is the number of pieces with fixed easy-axis

April, 1979. Note 0038csem.

per period.

$$2k\lambda e^{-\pi g/\lambda} = 1.$$

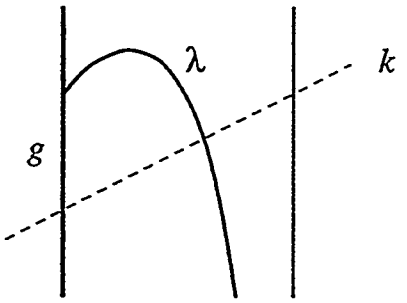

Figure 2.

Because E_1, E_2 are close to 1, and one usually chooses $K \approx 1$ T(cm), k (cm^{-1}) is numerically close to B_r.

In this document, all lengths will be in cm, and B's in Tesla.

III. Design Considerations.

• *End Section*. Normalize center to $z = 0$ and that piece has easy-axis parallel to the y axis. The last pieces at both ends must have the same easy-axis as piece at $z = 0$, but should have only half of normal length in the z-direction. One may want to use coils to fine-tune the end sections, but it would not be surprising if this were unnecessary.

In order to reduce the effects from finite length in x-direction (or to get away with shorter length in that direction) and to avoid 3D fringe effects at the ends in z-direction by cutting end fields off rapidly, one should back-up REC with a soft steel plate with reasonable overhang in z and x directions. This will not affect the amplitude of the $\cos(2\pi(z + iy)/\lambda)$ term, but will introduce a very weak, unnoticeable in the midplane, third harmonic (for $M' = 4$).

• *Length of REC in x-direction*. The present estimate is that it should be approximately the sum of the width of the beam and $2g$. The 3D effects discussed in the previous section are easily analyzed computationally and should be done before ordering materials!

• *Choice of M' and L*. It is recommended , at least for the first undulator, to use $M' = 4$ (giving $E_1 = .9$) and $L = \lambda/2$ (giving $E_2 = .96$) or $L = \lambda/4$ (giving $E_2 = .79$). With these choices, the undulator can be assembled from identical REC pieces with square cross-section and the easy-axis parallel to a side. The exception would be with the end pieces which could be obtained by cutting or grinding the normal pieces.

IV. Specific Calculations.

For a realistic undulator with $g = 2.8\text{cm}$, $B_r = .95\text{T}$, $K = 1\text{Tcm}$ and $M' = 4$:

L (cm)	k (cm^{-1})	λ (cm)
$\lambda/4 = 1.18$	.68	4.73
$\lambda/2 = 2.22$	.82	4.44

Table 1.

Since $\lambda/4$ uses only half the REC of the $\lambda/2$ case and λ is only less than 10% larger, this is the preferable design. The volume for $\lambda/4$ is $V = 3540$ cm^3, and for $\lambda/2$ is $V = 6660$ cm^3.

The REC price would probably be approximately \$1-2/cm^{-3}.

A Simple Derivation of the Lorentz Transformation Without Talking About Light

Postulate: Physics is independent of location, time and uniform motion of the system in which the experiment is performed.

We look at two systems that move with velocity, v, relative to each other. We establish clocks and space (x) markers in each system.

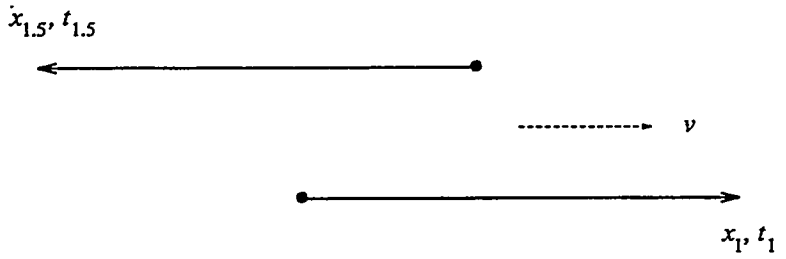

Figure 1.

We locate the origins and synchronize the clocks so that $x_1 = 0$, $t_1 = 0$, $x_{1.5} = 0$, and $t_{1.5} = 0$. Also notice that the "1.5" system has x increasing in the opposite direction from the "1" system.

We want to know $(x_{1.5}, t_{1.5})$ as a function of (x_1, t_1).

We know that $\Delta x_{1.5}/\Delta x_1$, $\Delta x_{1.5}/\Delta t_1$, $\Delta t_{1.5}/\Delta x_1$, and $\Delta t_{1.5}/\Delta t_1$ can not depend on x_1, t_1 because of our postulate. This means that the relationship between the two systems is linear, and can be expressed as a 2 by 2 matrix.

$$\left.\begin{aligned} x_{1.5} &= a_{11}x_1 + a_{12}t_1 \\ t_{1.5} &= a_{21}x_1 + a_{22}t_1 \end{aligned}\right\} \implies r_{1.5} = \begin{pmatrix} x_{1.5} \\ t_{1.5} \end{pmatrix} = A \cdot r_1$$

The velocity of a particle in system "1.5" (e.g. at $x_{1.5} = 0$) as seen from system "1" is $v = -a_{12}/a_{11}$. Thus

$$\boxed{a_{12} = -a_{11}v}$$

with $a_{11} \neq 0$ always true.

The choice of the relative sign of x in the two systems means that the observer in each system sees the other system move in the positive x–direction with velocity v.

July 30, 1992. Note 0287misc.

Therefore,

$$r_1 = A \cdot r_{1.5} = A \cdot A \cdot r_1,$$

and also,

$$A^2 = \begin{pmatrix} 1 & 0 \\ 0 & 1 \end{pmatrix}$$

must be satisfied. By multiplication and substitution,

$$A^2 = \begin{pmatrix} a_{11}(a_{11} - a_{21})v & -a_{11}v(a_{11} + a_{22}) \\ a_{21}(a_{11} + a_{22}) & a_{22}^2 - a_{21}a_{11}v \end{pmatrix}.$$

Therefore,

$$\boxed{a_{11} = -a_{22}}$$

and

$$\boxed{a_{21} = (1 - a_{22}^2)/(a_{22}v).}$$

By further substitution,

$$A = \begin{pmatrix} -a_{22} & a_{22}v \\ (1/a_{22} - a_{22})/v & a_{22} \end{pmatrix}.$$

We introduce $x_2 = -x_{1.5}, t_2 = t_{1.5}$ and

$$r_2 = B \cdot r_1, \quad B = \begin{pmatrix} a_{22} & -a_{22}v \\ (1/a_{22} - a_{22})/v & a_{22} \end{pmatrix}.$$

We further define

$$\gamma = a_{22}.$$

$$g = 1/a_{22}^2 - 1 = 1/\gamma^2 - 1,$$

and therefore

$$B = \gamma \begin{pmatrix} 1 & -v \\ g/v & 1 \end{pmatrix}.$$

It is important to notice that the diagonal elements are identical.

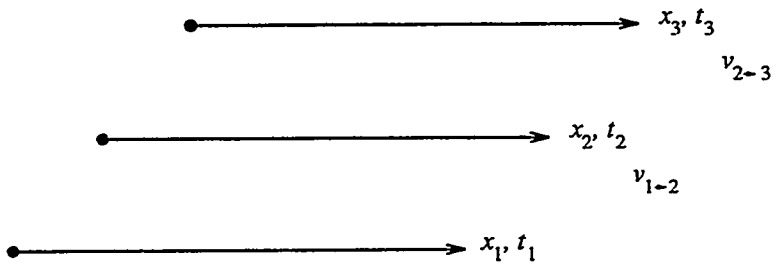

Figure 2.

We define

$$\begin{aligned} r_2 &= B_{1\to 2}\cdot r_1 \\ r_3 &= B_{2\to 3}\cdot r_2 \\ &= B_{2\to 3}\cdot B_{1\to 2}\cdot r_1 \end{aligned}$$

and thus

$$B_{1\to 3} = \gamma_{1\to 2}\gamma_{2\to 3}\begin{pmatrix} 1 & -v_{2\to 3} \\ g_{2\to 3}/v_{2\to 3} & 1 \end{pmatrix}\begin{pmatrix} 1 & -v_{1\to 2} \\ g_{1\to 2}/v_{1\to 2} & 1 \end{pmatrix}$$

and further,

$$B_{1\to 3} = \gamma_{1\to 2}\gamma_{2\to 3}\begin{pmatrix} 1 - v_{2\to 3}g_{1\to 2}/v_{1\to 2} & -(v_{1\to 2}+v_{2\to 3}) \\ g_{2\to 3}/v_{2\to 3} + g_{1\to 2}/v_{1\to 2} & 1 - v_{1\to 2}g_{2\to 3}/v_{2\to 3} \end{pmatrix}.$$

By the identical diagonal elements we have:

$$\frac{v_{2\to 3}g_{1\to 2}}{v_{1\to 2}} = \frac{v_{1\to 2}g_{2\to 3}}{v_{2\to 3}} \implies \frac{g_{1\to 2}}{v_{1\to 2}^2} = \frac{g_{2\to 3}}{v_{2\to 3}^2}.$$

Thus, we may generalize our equation and we have

$$g/v^2 = \frac{(1/\gamma^2 - 1)}{v^2} = k = \text{constant of nature.}$$

Here

$$\boxed{\gamma = \frac{1}{\sqrt{1+kv^2}}.}$$

We have to verify that other relationships are also satisfied (e.g. relation between elements [11] and [12], etc.). We have shown that if the postulate is true, the relationship between x and t of the systems moving with velocity v relative to each other must be

$$\begin{pmatrix} x_2 \\ t_2 \end{pmatrix} = \gamma\begin{pmatrix} 1 & -v \\ kv & 1 \end{pmatrix}\begin{pmatrix} x_1 \\ t_1 \end{pmatrix}, \quad \gamma = \frac{1}{\sqrt{1+kv^2}}.$$

We have not shown that $k \neq 0$, but the value of k can be obtained from "any" experiment, e.g. lifetime of meson, etc., and experiments do not have to use light.

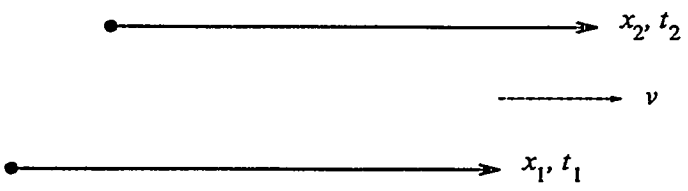

Figure 3.

$$\begin{pmatrix} x_2 \\ t_2 \end{pmatrix} = \gamma \begin{pmatrix} 1 & -v \\ -v/c^2 & 1 \end{pmatrix} \begin{pmatrix} x_1 \\ t_1 \end{pmatrix}, \quad \begin{pmatrix} x_1 \\ t_1 \end{pmatrix} = \gamma \begin{pmatrix} 1 & -v \\ -v/c^2 & 1 \end{pmatrix} \begin{pmatrix} x_2 \\ t_2 \end{pmatrix}$$

$$\gamma = \frac{1}{\sqrt{1 - v^2/c^2}}$$

1) The lifetime of particle at rest at $x_1 = 0$ in system "1" is τ_1. What is it in system "2"?

$$x_1 = 0, \quad t_1 = \tau_1 \quad \Longrightarrow \quad \boxed{t_2 = \tau_2 = \gamma\tau_1}$$

2) The distance x_1 covered by observer at rest at $x_2 = 0$ in time t_2:

$$x_2 = 0, \quad x_1 = \gamma v t_2, \quad \boxed{x_1/t_2 = \gamma v}$$

Note that

$$v\gamma = c \text{ for } \mathrm{v/c} = 1/\sqrt{2}.$$

Dimensional Analysis of the Trajectory of Non-Relativistic Charged Particles in Stationary Electric and Magnetic Fields (MKS units, with and without space charge)

Motivation.

To explain the structure of trajectory equations to engineers working on cyclotron-mass spectrometer.

We use linear scaling length D_0, and represent **B** and **E** fields by the scaling quantities B_0 and $E_0 = V_0 D_0$ times the appropriate dimensionless functions of x/D_0, y/D_0, and z/D_0. We must be able to represent the trajectory $x(t)$ ($t = 0$ at start of trajectory) as the product of D_0 and a function of dimensionless products P_n. The list of parameters to form P's has, in addition to $D_0, B_0, V_0(E_0), t$, the quantity m/e due to the equation of motion. Thus, the complete list consists of $m/e, D_0, B_0, V_0(E_0), t$.

We construct P's by first finding the appropriate physics relationship, then re-writing them in product form with parameters from the above list, and finally by solving for P, i.e.:

$$m\ddot{\mathbf{x}} = e\mathbf{E} \quad \rightarrow \quad m\frac{D_0}{t^2} = e\frac{V_0}{D_0} \quad \rightarrow \quad \boxed{P_1 = t^2 \frac{e}{m}\frac{V_0}{D_0^2}.}$$

For construction of next P, consider the parameter list without e/m:

$$\mathbf{E} = \mathbf{v} \times \mathbf{B} \quad \rightarrow \quad E_0 = B_0 \frac{D_0}{t} \quad \rightarrow \quad P_2 = \frac{B_0}{E_0}\frac{D_0}{t} = \frac{B_0 D_0^2}{V_0 t}.$$

We use P_1 to form P_3 without t, and use P_3 instead of P_2:

$$P_3 = P_2^2 P_1 = \frac{B_0^2}{E_0^2}\frac{e}{m}V_0 \quad \rightarrow \quad \boxed{P_3 = \frac{e}{m}\frac{B_0^2 D_0^2}{V_0}.}$$

We now remove B_0 from the parameter list, leaving only $D_0, V_0(E_0), t$, and we see that no additional P's are possible. Thus, we have

$$\boxed{x(t) = D_0 F_x(P_1, P_3) = D_0 F_x\left(t^2\frac{e}{m}\frac{V_0}{D_0^2}, \frac{e}{m}\frac{B_0^2 D_0^2}{V_0}\right),}$$

and this is equivalently true for $y(t)$ and $z(t)$.

April, 1992. Note 0278misc.

These expressions show the available options for changing the values of parameters if one of these has to be changed in a particular way and if one does not want to change the trajectory. If one does not care how long it takes for the particle to traverse its trajectory, then P_3 is the only P that is to be kept constant. P_1 can be considered to be an expression for the time to traverse the system.

If one wants to include space charge effects, one must include I, e, and ε_0 to the remaining list of parameters D_0, V_0, t. If the magnetic fields produced by the moving charges are important, one must add μ_0 as well.

When writing the P's, we shall use the fact that space charge and magnetic fields for charged particles go to 0 as $1/\varepsilon_0$ and μ_0 go to 0. The space charge effects come from

$$\nabla \cdot \varepsilon_0 \mathbf{E} = \varrho \quad \rightarrow \quad \varepsilon_0 \frac{E_0}{D_0} = I \frac{t}{D_0^3} \quad \rightarrow \quad P_4 = \frac{I}{\varepsilon_0} \frac{t}{V_0 D_0}.$$

We remove t with P_2 to get

$$P_5 = P_4 P_2 = \frac{I}{\varepsilon_0} \frac{1}{V_0} \frac{B_0}{E_0} \quad \rightarrow \quad P_5 = \frac{I}{\varepsilon_0} \frac{B_0 D_0}{V_0^2}.$$

We remove B_0 with P_3 to get

$$P_6 = \frac{P_5^2}{P_3} = \left(\frac{I}{\varepsilon_0}\right)^2 \frac{D_0^2}{V_0^4} \frac{m}{e} \frac{V_0}{D_0^2} \quad \rightarrow \quad \boxed{P_6 = \left(\frac{I}{\varepsilon_0}\right)^2 \frac{m/e}{V_0^3}}$$

with P_4, P_5 discarded.

We remove I from our parameter list and are left with $e, \varepsilon_0, D_0, t, V_0$ for

$$\nabla \cdot \varepsilon_0 \mathbf{E} = \varrho, \quad \varepsilon_0 E_0 = \frac{e}{D_0^2} \quad \rightarrow \quad \boxed{P_7 = \frac{e}{\varepsilon_0 D_0 V_0}.}$$

By removing ε_0 we see that no more P's are possible with just e, D_0, t, V_0. Thus, we have

$$\boxed{\begin{aligned} x(t) &= D_0 F_x(P_1, P_3, P_6, P_7) \\ &= D_0 F_x\left(\frac{e}{m}\frac{V_0 t^2}{D_0}, \frac{e}{m}\frac{B_0^2 D_0^2}{V_0}, \frac{I^2}{\varepsilon_0^2}\frac{m/e}{V_0^3}, \frac{e}{\varepsilon_0 D_0 V_0}\right), \end{aligned}}$$

and this is equivalently true for $y(t)$ and $z(t)$.

We expect that some P's are not significant if ε_0 is large enough so that P_6 and/or P_7 are small enough. For instance, for $D_0 = 10^{-2}$m, $V_0 = 10^3$V, and $e =$ charge of electron, we have $P_7 = 1.8 \times 10^{-9} \ll 1$, thus P_7 is probably not important.

We now add μ_0 to the parameter list, and for e, D_0, t, V_0, μ_0, we have

$$\nabla \times \mathbf{E} = -\dot{\mathbf{B}} \quad \rightarrow \quad \frac{E_0}{D_0} = \frac{V_0}{D_0^2} = \frac{\mu_0 (e/t)/D_0}{t} = \frac{\mu_0 e}{t^2 D_0},$$

$$P_8 = \frac{\mu_0 e D_0}{t^2 V_0}.$$

Using other P's, we get

$$\boxed{P_9 = \frac{\mu_0 I}{D_0 B_0}.}$$

We remove μ_0 from the parameter list, and see that no more P's are possible, and we have

$$\boxed{x(t) = D_0 F_x(P_1, P_3, P_6, P_7, P_9),}$$

and this is equivalently true for $y(t)$ and $z(t)$.

Application to System with Fixed D_0, B_0 (Cyclotrino).

We ignore P_1 since it determines traversal time. Without space charge and current-field effects, we must keep $V_0 m/e$ constant to get same behavior when the particle is changed, i.e. $V_0 \sim e/m$ is necessary. To see how space charge limitation affects "permissible" current, one must look at P_6:

$$\frac{I^2 m/e}{V_0^3} = \frac{I^2 (m/e)^4}{(V_0 m/e)^3} = \text{constant}$$

and this implies that $(m/e)^2 \cdot I$ should be a constant or small enough. As stated earlier, P_7 will be small enough to cause no problems, and the same will be true for P_9.

Further Comments.

While this theory was formulated with scale factors in mind, the P's also have local meaning. That is, if the "local" V † is interpreted as potential energy (divided by e), it becomes clear that P_6 and P_7 (with the local V and D) cannot be sufficiently small to be ignored everywhere since the particles start somewhere with $eV = 0$. But if the ion source is considered as a separate entity the ignorability argument will hold. It is also clear that looking at the P's with subscripted V, V_0 applies not only to applied potentials within the structure, but also to the energy of the incoming beam.‡

† Without the subscript 0 that identifies the "global" scale.

‡ This study was motivated by Tony Young's question about how V_0 has to be changed when B_0 differs from its original design value. Using P_3 we must have $B_0^2/V_0 =$ constant.

Some Practical Numbers.

Use γ sufficiently smaller than 1 to make a P ignorable. Then P_7, $\sqrt{P_6}$ can be ignored if

$$P_7 = \frac{e}{\varepsilon_0 D_0 V_0} < \gamma \quad \rightarrow \quad \boxed{D_0 V_0 = \frac{e}{\varepsilon_0}\frac{1}{\gamma} > \frac{1.8 \times 10^{-8}}{\gamma},}$$

$$\sqrt{P_6} = \frac{I}{\varepsilon_0}\frac{\sqrt{m/e}}{V_0^{3/2}} < \gamma \quad \rightarrow \quad I < V_0^{3/2}\gamma\varepsilon_0\sqrt{e/m}.$$

With e_c = electron charge, and m_p = proton mass,

$$I < V_0^{3/2}\gamma\sqrt{\frac{e/e_c}{m/m_p}}\varepsilon_0\sqrt{\frac{e_c}{m_p}} = V_0^{3/2}\gamma\sqrt{\frac{e/e_c}{m/m_p}}8.7 \times 10^{-8}$$

$$\boxed{I < V_0^{3/2}\gamma\sqrt{\frac{e/e_c}{m/m_p}}8.7 \times 10^{-8}.}$$

Analog Integrator Dynamics

Contrary to conventional analysis, which expresses the output signal in terms of the input signal, the quantity one wants (time integral over input integral) is expressed in terms of output signal (in digital form or as a scope trace), with all dynamic effects taken into account. In addition to dynamic terms being caused by the frequency response of the operational amplifier, the first order sensitivity is also affected by its dynamic behavior.

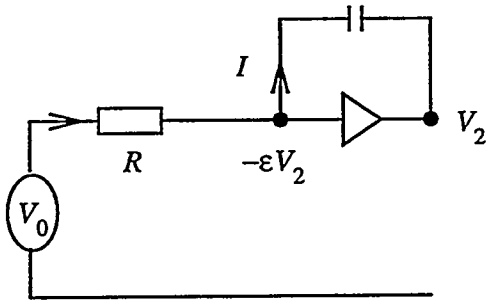

Figure 1.

For p the Laplace transform variable, and $RC = \tau_1$,

$$\frac{V_0 + \varepsilon V_2}{R} = -V_2(1+\varepsilon)pC,$$

where $\mu = 1/\varepsilon \gg 1$ is the open loop gain of the operational amplifier, and

$$V_0 = -V_2(p\tau_1(1+\varepsilon)+\varepsilon) = -V_2 \cdot F.$$

We use the following rough numbers:

$$\varepsilon = 0, \quad \int V_0 dt = 10^{-6}\text{Vsec}, \quad \tau_1 = 10^{-3}\text{sec}, \quad \text{and} \quad -V_2 = \frac{\int V_0 dt}{\tau_1} = 10^{-3}\text{V}.$$

The frequency response of the operational amplifier is

$$\mu_1(p) = \frac{\mu_0}{1+p\tau_0}.$$

It actually behaves in this fashion until the open loop gain is much less than 1. If the operational amplifier were not to behave this way, it would be useless for many

January, 1989. Note 0267misc.

applications. We characterize the frequency response either by the time constant τ_0, or the frequency (times 2π) where the amplitude gain is reduced to 1:

$$1 = \frac{\mu_0}{\omega_2 \tau_0} = \frac{1}{\omega_2 \varepsilon_0 \tau_0} = \frac{1}{\omega_2 \tau_2}$$

with

$$\tau_2 = \frac{1}{\omega_2} \approx 10^{-7}\text{sec}, \quad \mu_0 = 1/\varepsilon_0 \approx 10^6, \quad \text{and} \quad \varepsilon = \varepsilon_0(1 + p\tau_0) = \varepsilon_0 + p\tau_2,$$

and for $\tau_1^* = (\tau_1 + \tau_2)$:

$$\begin{aligned} F &= p\tau_1(1 + p\tau_2) + \varepsilon_0 + p\tau_2 \\ &= p\tau_1^* + \varepsilon_0 + p^2\tau_1\tau_2 \\ &= p\tau_1^* + \varepsilon_0 + p^2\tau_2(\tau_1^* - \tau_2), \end{aligned}$$

$$\boxed{-\frac{V_0}{p\tau_1^*} = V_2\left(1 + \frac{1}{p\mu_0\tau_1^*} + \frac{p\tau_2\tau_1}{\tau_1^*}\right).}$$

In the time domain, the quantity of interest, $\int V_0(\tau)d\tau$, is expressed in terms of the measured quantity $V_2(t)$ by

$$\int V_0(\tau)d\tau = V_2(t) \cdot \tau_1^* + \frac{\int V_2(\tau)d\tau}{\mu_0} + \dot{V}_2(t)\tau_2\tau_1.$$

One has to choose the time constants and open loop gain such that the second and third terms are small compared to the first term so that they can effectively be ignored or corrections can easily be made. It should be noted that the frequency response of the operational amplifier can make a small, but noticeable, correction to the effective time constant τ_1^* through τ_2.

Local Interpolation with Continuous Function and its First N Derivatives

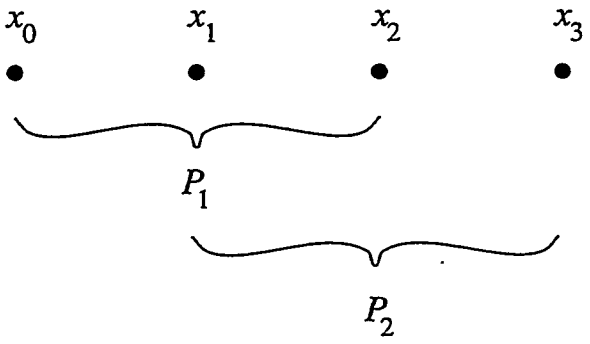

Figure 1.

1. Real function $y_0(x)$ must have known values at $x = x_0, x_1, \ldots, x_n$.

2. Establish interpolation functions $P_{1,\ldots,n-1}(x)$, that have properties appropriate to model $y_0(x)$ in small regions. This necessitates continuous functions, and continuous and meaningful first N derivatives. $P_j(x)$ must reproduce $y_0(x)$ exactly for $x = x_{j-1}$, $x = x_j$ and $x = x_{j+1}$, for $1 \leq j \leq n-1$.

3. Calculate the approximate function $y(x)$ from $y(x) = P_1(x)W_1(x) + P_2(x)W_2(x)$ in interval $x_1 \leq x \leq x_2$, and similarly in other intervals. Make the choices, to some degree arbitrary, for the weight functions $W_{1,\ldots,n-1}(x)$ so that the desired goal is obtained in a reasonable fashion.

4. If, P_1 and P_2 are the same as $y_0(x)$, we do not want the interpolation scheme to destroy the relationship $y(x) = y_0(x)$. Therefore, we must have that

Condition 1: $W_1(x) + W_2(x) = 1\,.$

And if the above is satisfied, it is also true that

Condition 2: $W_1^{(n)}(x) + W_2^{(n)}(x) = 0\,.$

5. We examine $y^{(n)}(x)$:

$$y^{(n)}(x) = P_1^{(n)}W_1 + nP_1^{(n-1)}W_1^{(1)} + \ldots + nP_1^{(1)}W_1^{(n-1)} + P_1W_1^{(n)} + P_2^{(n)}W_2 + nP_2^{(n-1)}W_2^{(1)} + \ldots + nP_2^{(1)}W_2^{(n-1)} + P_2W_2^{(n)}\,,$$

May, 1981. Note 0177misc.

for $n = 1, 2, \ldots, N$. We choose $W^{(1)}$ so that all needed derivatives exist. At $x = x_1$ or $x = x_2$,

$$P_1 W_1^{(n)} + P_2 W_2^{(n)} = P_1(W_1^{(n)} + W_2^{(n)}) = 0$$

because P_1, P_2 fit $y_0(x)$ exactly at $x = x_1$, $x = x_2$, and due to Condition 2. We now choose the weight functions such that at $x = x_1$, $y^{(n)} = P_1^{(n)}$, and at $x = x_2$, $y^{(n)} = P_2^{(n)}$. We do this by requiring that weight functions fulfill

Condition 3: $W_1(x_1) = 1, \quad W_1(x_2) = 0, \quad$ and
$W_2(x_1) = 0, \quad W_2(x_2) = 1,$

and fulfill

Condition 4: $W_1^n(x_1) = W_1^n(x_2) = 0 \quad$ and
$W_2^n(x_1) = W_2^n(x_2) = 0 \quad$ for $\quad n = 1, 2, \ldots, N-1.$

With the above choices, y and its first N derivatives at $x = x_n$ depend only on P_n, independently of whether we get to x_n from an upper or lower interval, i.e., y and its derivatives are continuous everywhere.

6. The construction of the weight functions that satisfy Conditions 1 (and therefore Condition 2), 3, and 4, is not unique. We introduce

$$u(x) = \frac{x - (x_1 + x_2)/2}{(x_2 - x_1)/2} = \frac{2x - (x_1 + x_2)}{(x_2 - x_1)}.$$

This gives us

$$\begin{aligned} u(x_1) &= -1, \\ u((x_1 + x_2)/2) &= 0, \\ u(x_2) &= 1. \end{aligned}$$

We now have that

$$\boxed{W_2(x) = \frac{1}{2}(1 + g_N(x)),}$$

$$\boxed{W_1(x) = \frac{1}{2}(1 - g_N(x)),}$$

$$\boxed{\begin{aligned} y(x) &= \frac{1}{2}(P_2(x) + P_1(x) + (P_2(x) - P_1(x)) \cdot g_N(x)) \\ &= P_1(x)W_1(x) + P_2(x)W_2(x), \end{aligned}}$$

where,

$$\boxed{g_N(x) = a_N \int_0^{u(x)} (1-v^2)^{N-1} dv \quad \text{and} \quad \frac{1}{a_N} = \int_0^1 (1-v^2)^{N-1} dv\,.}$$

We may now conclude that, clearly, Conditions 1 and 3 are satisfied, and from

$$\begin{aligned} W_2^{(1)}(x) &= \frac{g_N(x)}{x_2 - x_1} \\ &= \frac{a_N}{x_2 - x_1}(1-u^2)^{N-1} \\ &= \frac{a_N}{x_2 - x_1}(1-u)^{N-1}(1+u)^{N-1}\,, \end{aligned}$$

it follows that Condition 4 is satisfied as well.

We introduce here some further details. Given

$$\frac{1}{a_N} = \int_0^1 (1-v^2)^{N-1} dv = b_N\,,$$

we have that

$$\begin{aligned} b_N &= \int_0^1 (1-v^2)^{N-2}(1-v^2) dv \\ &= b_{N-1} - \int_0^1 (1-v^2)^{N-2} v^2 dv\,. \end{aligned}$$

For

$$du = -1(1-v^2)^{N-2} v dv \quad \text{and} \quad u = \frac{(1-v^2)^{N-1}}{2(N-1)}\,,$$

$$r = v \quad \text{and} \quad dr = dv\,,$$

we have that

$$b_N = \frac{b_{N-1}}{1 + \dfrac{1}{2(N-1)}}\,,$$

$$\boxed{a_N = a_{N-1}\left(1 + \frac{1}{2(N-1)}\right)\,.}$$

Thus, for $a_1 = 1$

$$\boxed{a_N = a_{N-1}\left(1+\frac{1}{2(N-1)}\right) = \prod_{n=1}^{N-1}\left(1+\frac{1}{2(N-1)}\right).}$$

And further,

$$a_N = \prod_{1}^{N-1}\frac{2n+1}{2n} = \frac{3\cdot 5\cdots(2N-1)}{2^{N-1}(N-1)!} = \frac{(2N-1)!}{2^{N-1}2^{N-1}(N-1)!^2} = \frac{(2N-1)!}{4^{N-1}(N-1)!^2}.$$

Summary.

P_1 fits y_0 exactly at $x = x_0, x_1, x_2$.
P_2 fits y_0 exactly at $x = x_1, x_2, x_3$.

$$\begin{aligned}
y(x) &= P_1(x)W_1(x) + P_2(x)W_2(x),\\
W_2(x) &= \frac{1}{2}(1+g_N(x)),\\
W_1(x) &= \frac{1}{2}(1-g_N(x)),\\
u(x) &= \frac{2x-(x_1+x_2)}{(x_2-x_1)},\\
\frac{1}{a_N} &= \int_0^1 (1-v^2)^{N-1}dv,\\
g_N(x) &= a_N\int_0^{u(x)}(1-v^2)^{N-1}dv.
\end{aligned}$$

Special Cases.

$N = 1$: $\boxed{g_1 \doteq u.}$

$N = 2$: $g_2 = a_2\int_0^u (1-v^2)dv = a_2u(1-u^2/3), \quad 1/a_2 = 2/3$

$$\boxed{g_2 = \frac{1}{2}u(3-u^2).}$$

$N = 3$: $g_3 = a_3\int_0^u (1-2v^2+v^4) = a_3u\left(1-\frac{2}{3}u^2+\frac{u^4}{5}\right), \quad \frac{1}{a^3} = \frac{1}{3}+\frac{1}{5} = \frac{8}{15},$

$$\boxed{g_3 = \frac{1}{8}u(15-10u^2+3u^4).}$$

Linear Least Squares with Erroneous Matrix

When one is dealing with a system in which the relationships between parameter changes, Δp, and the system performance changes, Δs, are in good approximation represented by the linear relationship

$$\Delta s = M\Delta p$$

achieving a desired performance change is simply accomplished by parameter changes

$$\Delta p = M^{-1}\Delta s$$

as long as one has as many parameters as system performance characteristics.

When the desired change, Δs, has more components than Δp, it is often adequate to minimize the weighted sum of the deviations from the desired performance, i.e. one minimizes

$$S = \Delta s^t W \Delta s,$$

where W is a diagonal square matrix with appropriate weights on the diagonal. S is minimized in the first iteration if the parameter vector is changed by

$$\boxed{\Delta p_1 = A\Delta s_1} \quad \text{where} \quad A = (M^tWM)^{-1}M^tW.$$

If the matrix M used for this operation deviates by $\Delta M = M_{\Re} - M$ from the real matrix $M_{\Re}$, the desired change Δs_2 with the new parameters is given by

$$\boxed{\Delta s_2 = \Delta s_1 - (M + \Delta M)\Delta p_1 = (I - MA - \Delta MA)\Delta s_1}$$

If the effort to determine $M_{\Re}$ (often by elaborate measurements) is too large one can iterate the procedure, and it would be of interest to estimate the asymptotic Δs_∞. To obtain this, we introduce

$$\boxed{I - MA = B} \quad \text{and} \quad \boxed{-\Delta MA = D}$$

Thus,

$$\boxed{\Delta s_n = (B + D)^{n-1}\Delta s_1} \quad \text{and} \quad \boxed{\Delta p_n = A(B + D)^{n-1}\Delta s_1}$$

Notice that $AM = I$, $AB = 0$, $DB = 0$ and $B^2 = I - 2MA + MAMA = B$.

November, 1971. Note 0038misc.

Further,

$$(B+D)^2 = B(I+D) + D^2$$

$$(B+D)^3 = B(I+D+D^2) + D^3$$

and so forth such that

$$\boxed{(B+D)^n = B(I-D)^{-1}(1-D^n) + D^n.}$$

Therefore,

$$\boxed{\Delta s_n = (B(I-D)^{-1}(1-D^{n-1}) + D^{n-1})\Delta s_1}$$

$$\boxed{\Delta p_n = AD^{n-1}\Delta s_1}$$

as it must be, because for $\Delta M = 0$ and $n \geq 2$, $\Delta p_n = 0$ and $\Delta s_n = \Delta s_2$.

If ΔM is small enough, the absolute values of the eigenvalues of D will be less than 1, resulting in the following for large enough n:

$$\boxed{\Delta s_\infty = B(I-D)^{-1}\Delta s_1 = (I-MA)(1+\Delta MA)^{-1}\Delta s_1.}$$

Judging whether one is close to this value is possible by observing the decrease in Δp_n with increasing n.

Matrix Describing Second Order Effects to Second Order in One Dimension

No Momentum Errors.

The normalized equation of motion is

$$y'' = y + by^2.$$

Expand y in terms of initial conditions y_0, y_0' up to 2^{nd} order:

$$y = a_{11}y_0 + a_{12}y_0' + a_{13}y_0^2 + a_{14}y_0y_0' + a_{15}{y_0'}^2.$$

Initial conditions for $a(x)$

$$a_{11}(0) = a_{12}'(0) = 1,$$

all others are 0. The equation for $a(x)$ is:

$$a_{11}'' = a_{11}, \quad \text{and} \quad a_{12}'' = a_{12} \quad \Longrightarrow \quad \begin{cases} a_{11} = \cosh x, & a_{12} = \sinh x, \\ a_{21} = \sinh x, & a_{22} = \cosh x. \end{cases}$$

$$a_{13}'' = a_{13} + ba_{11}^2, \quad a_{14}'' = a_{14} + 2ba_{11}a_{12}, \quad \text{and} \quad a_{15}'' = a_{15} + ba_{12}^2.$$

Because in all three cases $a(0) = a'(0) = 0$: $\mathcal{L}(a'') = p^2\mathcal{L}(a)$.

For a_{13},

$$a_{11}^2 = \frac{1}{4}\left(e^{2x} + e^{-2x} + 2\right) \rightleftharpoons \frac{1}{4}\left(\frac{1}{p-2} + \frac{1}{p+2} + \frac{2}{p}\right).$$

In general,

$$\frac{1}{(p-1)(p+1)(p+c)} \rightleftharpoons \frac{e^x}{2(1+c)} + \frac{e^{-x}}{2(1-c)} + \frac{e^{-cx}}{c^2-1},$$

thus,

$$\begin{aligned} \frac{4a_{11}^2}{p^2-1} &\rightleftharpoons \frac{4}{3}\cdot\frac{e^x}{2} + \frac{4}{3}\cdot\frac{e^{-x}}{2} + \frac{e^{2x}+e^{-2x}}{3} - 2 \\ &= \frac{4}{3}\cosh x + \frac{2}{3}\cosh 2x - 2. \end{aligned}$$

Therefore,

$$\boxed{a_{13} = \frac{b}{6}\left(2\cosh x + \cosh 2x - 3\right)} \quad \text{and} \quad \boxed{a_{13}' = a_{23} = \frac{b}{3}\left(\sinh x + \sinh 2x\right).}$$

February, 1966. Note 0006misc.

For a_{14},

$$a_{11}a_{12} = \frac{1}{4}\left(e^{2x} - e^{-2x}\right) \rightleftharpoons \frac{1}{4}\left(\frac{1}{p-2} - \frac{1}{p+2}\right),$$

and thus,

$$\begin{aligned}\frac{4a_{11}a_{12}}{p^2-1} &\rightleftharpoons \frac{-4}{3}\cdot\frac{e^x}{2} + \frac{4}{3}\cdot\frac{e^{-x}}{2} + \frac{e^{2x}-e^{-2x}}{3} \\ &= -\frac{4}{3}\sinh x + \frac{2}{3}\sinh 2x.\end{aligned}$$

Therefore,

$$\boxed{a_{14} = \frac{b}{3}\left(\sinh 2x - 2\sinh x\right)} \quad \text{and} \quad \boxed{a'_{14} = a_{24} = \frac{2b}{3}\left(\cosh 2x - \cosh x\right).}$$

Similarly, for a_{15},

$$a_{12}^2 = \frac{1}{4}\left(e^{2x} + e^{-2x} - 2\right) \rightleftharpoons \frac{1}{4}\left(\frac{1}{p-2} + \frac{1}{p+2} - \frac{2}{p}\right),$$

thus,

$$\begin{aligned}\frac{4a_{12}^2}{p^2-1} &\rightleftharpoons \frac{-8}{3}\cdot\frac{e^x}{2} + \frac{-8}{3}\cdot\frac{e^{-x}}{2} + \frac{e^{2x}+e^{-2x}}{3} + 2 \\ &= -\frac{8}{3}\cosh x + \frac{2}{3}\cosh 2x + 2.\end{aligned}$$

Therefore,

$$\boxed{a_{15} = \frac{b}{6}\left(\cosh 2x - 4\cosh x + 3\right)} \quad \text{and} \quad \boxed{a'_{15} = a_{25} = \frac{b}{3}\left(\sinh 2x - 2\sinh x\right).}$$

Inclusion of Momentum Error α.

The normalized equation of motion is

$$y'' = y + \alpha + by^2.$$

First, add the term linear in α to the expansion in y_0, y_0': add $a_{16}\alpha$. The initial conditions are

$$a_{16}(0) = a_{16}'(0) = 0, \quad a_{16}'' = a_{16} + 1 \quad \Longrightarrow \quad \boxed{a_{16} = \cosh x - 1.}$$

Second, take the terms α^2, αy_0, $\alpha y_0'$ into account, where the procedure is the same as in the calculation of a_{13}, a_{14}, and a_{15}.

Third, do not add any terms, but introduce $z = y + \beta$ (β is a constant) in the differential equation. Thus,

$$z'' = z - \beta + \alpha + b(z^2 - 2z\beta + \beta^2),$$

$$\beta^2 - \frac{\beta}{b} + \frac{\alpha}{b} = 0 \quad \Longrightarrow \quad \beta = \frac{1}{2b}\left(1 - \sqrt{1 - 4\alpha\beta}\right),$$

$$z(1 - 2b\beta) + bz^2 = \boxed{z'' = z\sqrt{1 - 4\alpha\beta} + bz^2.}$$

This procedure requires the calculation of a new matrix for every α of interest, but this will give more insight in return.

General Procedure.

Description of higher order effects with power expansion and the consequences for stability.

We describe deviations from the closed orbit by the column vector

$$\mathbf{v} = \begin{pmatrix} y_1 \\ y_2 \\ \vdots \\ y_k \end{pmatrix}$$

where the components of y_1 are y and y', and components of $y_2, y_3, \ldots, y_k$ are, respectively, the second, third, $\ldots, k^{\text{th}}$ order contributions of y and y'. Then,

$$\mathbf{v}_2 = M\mathbf{v}_1, \quad \text{with} \quad M = \begin{pmatrix} A_{11} & A_{12} & A_{13} & \ldots & A_{1k} \\ 0 & A_{22} & A_{23} & \ldots & A_{2k} \\ 0 & 0 & A_{33} & \ldots & A_{3k} \\ \vdots & \vdots & \vdots & \ddots & \vdots \\ 0 & 0 & 0 & \ldots & A_{kk} \end{pmatrix}.$$

In M, A_{11} describes the first order effects, A_{12} the second order effects, etc. The

other matrices reproduce the higher than first order components of v. The diagonal elements $A_{22}, A_{33}, \ldots, A_{kk}$ depend only on the matrix element of A_{11}. The eigenvalues of M do not depend on $A_{12}, \ldots, A_{1k}$. Thus, the stability of the system does not depend, in this approximation, on the non-linear effects described by these elements. Since stability obviously can depend on non-linear effects, this implies that the power expansion for many passes through the system has a progressively shrinking radius of convergence. One can thus conclude that although this method is worthless to evaluate the effect of non-linearities on stability, it might still yield valuable information provided the system does not become unstable because of the non-linearities.

We show rough numbers for

$$F_3 = a_{13}/b, \quad F_4 = a_{14}/b, \quad F_5 = a_{15}/b,$$

$$F_3' = a_{13}'/b = a_{23}/b, \quad F_4' = a_{14}'/b = a_{24}/b, \quad F_5' = a_{15}'/b = a_{25}/b.$$

x	$\pi/4$	$\pi/2$	π
e^x	2.2	4.8	23
e^{-x}	0.46	0.21	0
$\cosh x$	1.33	2.5	11.5
$\sinh x$	0.87	2.3	11.5

x	$\pi/4$	$\pi/2$
$F_3(x)$	0.77	2.25
$F_4(x)$	0.18	2.3
$F_5(x)$	0.03	0.75

x	$\pi/4$	$\pi/2$
$F_3'(x)$	1.06	4.6
$F_4'(x)$	0.78	6
$F_5'(x)$	0.18	2.3

Curvature of 2D Magnetic Field Lines and Scalar Potential Lines

I. Preparation and Background.

Magnetic fields. 2D magnetic fields can be derived from a scalar potential V or a vector potential A, or the complex potential $F(z) = A + iV$, an analytic function of the complex variable $z = x + iy$, according to

$$B_x - iB_y = B^* = i\frac{dF}{dz} = iF'. \tag{1}$$

Field lines and scalar potential lines in the z-plane are the $z(F)$ maps of straight lines parallel to either the imaginary or real axis of the F-plane.

Modification of the curvature by a conformal map. If a curve in the z-plane has a local tangent in the direction $e^{i\alpha_z}$, the conformal map $w(z)$ of that region has a local tangent in the direction

$$e^{i\alpha_z} = e^{i\alpha_z}\frac{w'}{|w'|}. \tag{2}$$

This equation shows that the angle of intersection of any two curves in the z-plane is preserved under the transformation $w(z)$, hence the name conformal transformation. If the curve at that location in the z-plane is k_z, then the curvature of the map of that point can be shown to be

$$k_w = \frac{\left(k_z + \Im\left(\frac{w''}{w'}e^{i\alpha_z}\right)\right)}{|w'|}. \tag{3}$$

The sign convention used for this formula is such that a positive curvature means that if one proceeds in the direction of the tangent, the curve turns to the left, i.e. the conventional mathematically positive direction.

II. Application of (2).

Fundamental relationships. There are several ways to apply (2) to this problem. The most natural way to do so seems to be, at least at first, to assign quantities w and z in (2) to the the variables F and z of our problem, since we are looking at the map of a region of the F-plane to the z-plane. For most applications, this is not very practical since one then gets the curvature of the maps of constant potential lines as a function of A and V, when in fact one wants the curvature as a function of x and

January, 1994. Note 0611thry.

y. We therefore proceed in the following manner: we assign z and w to z and F, and look in

$$k_F = \frac{\left(k_z + \Im\left(\frac{F''}{F'}e^{i\alpha_z}\right)\right)}{|F'|}, \tag{4}$$

for $k_F = 0$, i.e. the curvature of maps of straight lines in the F-plane is given by

$$k_z = -\Im\left(\frac{F''}{F'}e^{i\alpha_z}\right). \tag{5}$$

To get a more practical formula, we express $e^{i\alpha_z}$ with the help of (2) through

$$e^{i\alpha_z} = e^{i\alpha_F}\frac{|F'|}{F'}, \tag{6}$$

and the derivatives of F through the fields as given in (1), yielding

$$k_z = -\Re\left(\frac{B^{*'}}{B^{*2}}|B|e^{i\alpha_F}\right). \tag{7}$$

For some expressions of the fields, it is more convenient to write this as

$$k_z = +\Re\left(\left(\frac{1}{B^*}\right)'|B|e^{i\alpha_F}\right). \tag{8}$$

In both (7) and (8), $e^{i\alpha_F}$ has the absolute value 1 and is real if one is looking at a scalar potential line, and is purely imaginary if one looks at a field line.

Comments. It is worth noting that in order to calculate the curvatures of interest, one needs only the expressions for the complex field, not the complex potential. Under most circumstances, the expression for the complex potential is not more complicated than the expression for the complex field. There are, however, exceptions. For instance, the field of a modified sextupole is given by

$$B^* = iz^2e^{az^2}. \tag{9}$$

Integrating this to get the complex potential, (1), leads to the error function in the complex plane.

III. Applications.

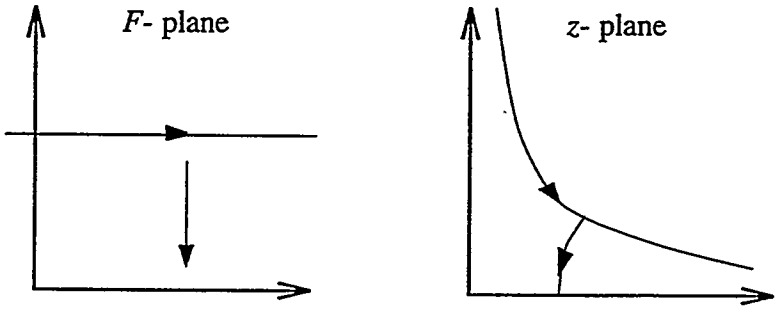

Figures 1(a,b).

(i) *The regular multipole.* For a multipole of order n with the field perpendicular to the midplane, the field is given by

$$B^* = iz^{n-1}. \tag{10}$$

Substituting in (8) gives directly

$$k_z = (n-1)\left|z^{n-1}\right| \Re\left(iz^{-n}e^{i\alpha_w}\right). \tag{11}$$

Using, for $e^{i\alpha_F}$, the phases corresponding to the arrows in Figures 1(a) and 1(b), and using $z = re^{i\varphi}$, gives, for the curvature of the field line and the scalar equipotential:

$$k_z = (n-1)\cos\frac{n\varphi}{r}, \tag{12A}$$

$$k_z = (n-1)\sin\frac{n\varphi}{r}. \tag{12V}$$

(ii) *The modified sextupole.* This particular implementation of a modified sextupole has the field in the midplane perpendicular to the midplane, and behaves like a good sextupole close to the origin, but has a stronger modified field, proportional to $x^2e^{ax^2}$, $a \in \Re$, as one moves away from the origin of the coordinate system. The complex field is therefore given by

$$B^* = ize^{ax^2}.$$

Fringe Field Model Function for Dipoles

For a number of beam optics tasks, it is important to have an analytical function that describes the field in the fringe field region of a dipole†. We restrict ourselves to the simple case of a dipole that has a straght effective field boundary, making this a very simple problem of describing two dimensional fields. Putting the x-axis into the midplane of a dipole whose half gap is normalized to be equal to 1, with large $x > 0$ describing the outside of the magnet, and the far negative end of the x-axis the deep inside region of the magnet, the field in the region of interest can be described by

$$\frac{B_y(x,y) + iB_x(x,y)}{B_0} = G(z) = D_1(z) + D_2(z) + D_3(z), \tag{0.0}$$

$$z = x + iy, \tag{0.1}$$

and the functions D_1, D_2, D_3 chosen such that the asymptotic behavior of $G(z)$ reflects the properties of the fields in the regions deep inside and far outside the magnet. In addition, $G(z)$ should not have any singularities for the space within $-1 < y < 1$. The following functions satisfy these conditions:

$$D_1(z) = \frac{1 + nAe^{\pi z/2}}{\left(1 + Ae^{\pi z/2}\right)^n}, \tag{1}$$

$$D_2(z) = C_1 e^{-C_2(z-x_2)^2}, \tag{2}$$

$$D_3(z) = K_1 \cdot \frac{\left(1 + K_3 e^{-\pi z/2}\right)^m}{\left(1 + K_2(z - x_3)^2\right)^{3/2}}, \tag{3}$$

with all coefficients real, $n \geq 2$, $K_2 > 1$, and $A, C_2, K_3, m > 0$. The fields deep inside the magnet are dominated by the "longest surviving" term $e^{\pi z}$ from $D_1(z)$, while far outside the magnet the field is dominated, as desired, by the "longest surviving" term proportional to $1/z^3$ from D_3, with clearly no singularities for $-1 < y < 1$. $D_2(z)$ has been added (and one could add more such terms) to allow a good fit of $G(z)$ to measured or computed data in the transition region. While this suggested model function $G(z)$ has enough free parameters to fit data, the quality of such a fit has not been tested on a real problem, but the $G(z)$ given here should contain a sufficient number of suggestions that this approach to the Enge function promises to be successful.

December, 1993. Note 0610thry.

† See document 0609thry, *Comments about RAYTRACE.*

Comments about RAYTRACE

Introduction.

Several years ago I was asked at a workshop to comment on the representation of magnetic fields in the RAYTRACE code, a computer program that was developed by H. A. Enge and his students in the 1960's†. Since my comments contained not only some academically interesting points, but also suggestions for improvement of this enormously successful code, several people asked me to put my thoughts on this subject on paper. After describing the specific aspects of the code that I want to discuss, I will elaborate on what I would characterize as shortcomings, together with suggestions for eliminating them, and a description of some mathematical detail at the end.

Fields in RAYTRACE.

Even though it is not a major effort to generalize my comments, I restrict the discussion to the case of the fringe field region of a dipole magnet that has a straight effective field boundary in the region of interest. This means that we are dealing with two dimensional fields, with all the associated simplifications that make it possible to address the core of the problem without unnecessary distractions.

Using the midplane of the magnet as the x-axis of the xy coordinate system, with large positive x representing the region far outside the dipole, and the other extreme the region deep inside the magnet, the field is characterized by the following function, commonly called the Enge function :

$$B_y(x,0) = \frac{B_0}{1+e^{P(x)}}, \tag{1a}$$

where

$$P(x) = C_0 + C_1 x + C_2 x^2 + \ldots + C_n x^n, \tag{1b}$$

with n an odd integer and $C_n > 0$.

The coefficients are obtained by fitting measured or computed field values in the midplane to (1), and fields off the midplane are obtained by using a Taylor series expansion, with the derivatives obtained from (1).

Comments and Suggestions.

I have problems with three tightly linked aspects of this procedure:

December, 1993. Note 0609thry.

† Spencer, J. E. and Enge, H. A., Nuclear Instruments and Methods 49, 181 (1967).

(A) It is true, in general, that if one fits parameters of a function so that the fields on the surface of a volume are well represented by that function, the quality of the fields computed with that function inside the volume is at least as good as (but usually better than) the original data on the surface. It is, of course, assumed that the function and field calculation algorithm satisfy all the relevant vacuum field equations. Conversely, calculating fields in the volume from a function whose free parameters were determined on a line inside the volume gives fields that are not nearly as accurate as the original data. These facts are qualitatively clear if one thinks of the fringe fields in the midplane of the dipole: significantly different pole contours produce very similar fields in the midplane. That means that if one calculates fields off the midplane accurately from the fields in the midplane, small differences in the function there will give significantly different fields far away from the midplane.

(B) Calculating fields off the midplane with a Taylor series expansion makes no sense in this case for the following reasons: since $B_x - iB_y$ or, more conveniently in this case, $B_y + iB_x$, is an analytical function of the complex variable $z = x + iy$, the field at location (x, y) can be obtained directly, without any approximation, by evaluating (1) for complex argument:

$$B_y(x,y) + iB_x(x,y) = B_y(x+iy,0) = \frac{B_0}{1+e^{P(x+iy)}}. \qquad (2)$$

This very simple evaluation of fields from a midplane model function makes it obviously easy to fit the parameters of the model, no matter the nature of that function, to fields off the midplane, thus eliminating the objection raised in (A).

(C) It seems to me that the form of the Enge function is not well suited to this problem for two reasons: 1) the function does not have ther appropriate asymptotic behavior far away from either end of the magnet; and 2) unless one makes a careful study of the Enge function, it may have one or more singularities in the "business" region. Avoiding that kind of disaster by evaluating the field only approximately is clearly not a satisfactory answer to this problem. While it is fairly easy with the help of (2) to make the singularity check (see Appendix), it might be simpler to "design" a function that can not have that kind of singularity, in addition to having the proper asymptotic behavior. I have some very promising candidates but have not made the effort to test them on some real problems.

Appendix.

For the Enge function to have no damaging singularity it is necessary and sufficient that the equation

$$P(z) = im\pi \quad \text{with} \quad m = \text{odd integer} \neq 0 \tag{3}$$

has no solution for z between the midplane and a line parallel to the midplane one half gap, h, away from the midplane. This test is most easily carried out with the argument principle that states, in this case, that the number of zeroes of $w(z)$ within a region of the z-plane equals the number of times $w(z)$ goes around $w = 0$ when z traces the boundary of the region. Since, in this case,

$$w(z) = P(z) + im\pi, \tag{4}$$

with all C_n in $P(z)$ real, it is only necessary to find the locations where the map of the straight line parallel to the midplane at distance h intersects the imaginary axis of P(z), i.e. one has to find $\Im P(z)$ at the locations where $\Re P(x + ih) = 0$. Since $\Re P(x+ih) = 0$ means nothing more than finding the real roots (in x) of a polynomial of order n, this a very simple exercise for a computer. Having these points, it is trivial to see whether $w(z) = 0$ is possible for any odd m. I have carried out that test for the example given by Spencer and Enge, and for four cases given to me by S. Kowalski. I am happy to report that while none of these cases had singularities within one half gap of the midplane, there were some singularities just outside the end of the dipole only a little more than a half gap away from the midplane.

Stored Energy in H-Magnet for $\mu = \infty$

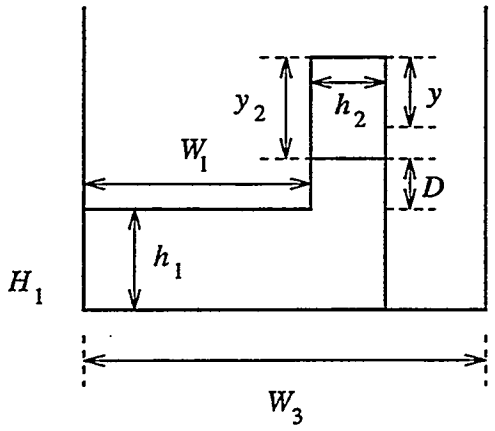

Figure 1.

$$2\mathcal{E} = \int \mathbf{B} \cdot \mathbf{H} dv = \int \mathbf{H} \cdot \nabla \times \mathbf{A} dv.$$

From

$$\nabla \cdot (\mathbf{A} \times \mathbf{H}) = \mathbf{H} \cdot (\nabla \times \mathbf{A}) - \mathbf{A} \cdot (\nabla \times \mathbf{H}),$$

we have that, with $\mathbf{j} = j\mathbf{e}_z$,

$$\begin{aligned} 2\mathcal{E} &= \int \mathbf{A} \cdot \mathbf{j} dv + \int (\mathbf{A} \times \mathbf{H}) \cdot d\mathbf{a} \\ &= \int \mathbf{A} \cdot \mathbf{j} dv + \int \mathbf{A} \cdot (\mathbf{H} \times d\mathbf{a}), \end{aligned}$$

where $\mathbf{H} \times d\mathbf{a} = 0$ on $\mu = \infty$ surface.

In case of a long magnet, $\int j\, da \equiv 0$ which means that we can add any constant to A without changing anything. We make $A = 0$ along the y-axis. We now use $\mathbf{A} = \mu_0 A \mathbf{e}_z$, so that the total energy per unit length is

$$\boxed{\mathcal{E}' = \frac{1}{2}\mu_0 j \int A dx dy}$$

where the integral is evaluated over the coil in the first quadrant.

January, 1993. Note 0607thry.

To get

$$J_1 = \int A(x,y)dxdy$$

we look at

$$J_2(y) = \int_0^{y<y_2} \int_0^{h_2} H_x dxdy = \int\int \frac{\partial A}{\partial y} dydx$$
$$= \int (A(x,y) - A_t)\, dx = \int A(x,y)dx - A_t h_2,$$

where A_t is A at top of the coil slot.

We integrate the original expression for J_2 over x first, and by Ampère's Law,

$$J_2(y) = \int_0^y \frac{I}{y_2} y dy = \frac{Iy^2}{2y_2}.$$

Therefore,

$$\int A(x,y)dx = \frac{Iy^2}{2y_2} + A_t h_2,$$

$$\boxed{J_1 = \int_0^{y_2} \int A(x,y)dxdy = \frac{Iy_2^2}{6} + A_t h_2 y_2.}$$

From *H-Magnet With Minimal Yoke Flux Density*† we know that

$$A_t = I\left(\frac{W_1}{h_1} + \frac{D + y_2/2}{h_2} + E_1\right),$$

and thus we have that

$$J_1 = I h_2 y_2 \left(\frac{W_1}{h_1} + \frac{D + y_2/2}{h_2} + E_1 + \frac{y_2}{6h_2}\right).$$

$$\boxed{jJ_1 = I^2\left(\frac{W_1}{h_1} + \frac{2y_2}{3h_2} + \frac{D}{h_2} + E_1\left(\frac{h_1}{h_2}\right)\right).}$$

$$\boxed{\mathcal{E}' = \frac{1}{2}\mu_0(jJ_1),}$$

† Document 0606thry.

where

$$I = H_1 h_1 = j h_2 y_2,$$

$$E_1(a) = a + \frac{2}{\pi}\left(\ln\frac{a+1/a}{4} + \left(\frac{1}{a} - a\right)\arctan a\right) \quad \text{with} \quad a = h_2/h_1.$$

H-Magnet With Minimal Yoke Flux Density

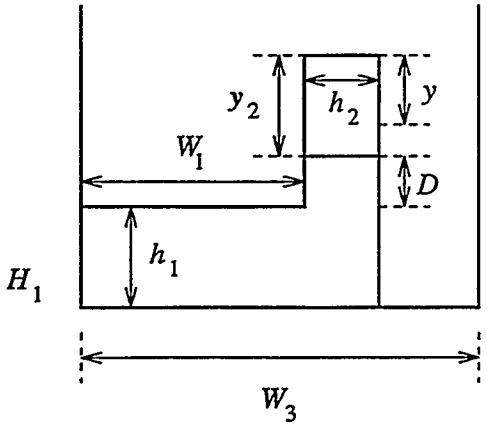

Figure 1.

W_1, H_1, W_3, D, and h_1 are given. We want to minimize $\overline{B}_{\text{yoke,max}}$ for $\mu = \infty$ by chosing the proper h_2.

Procedure.

Calculate flux for 0-thickness coil at top of coil slot using excess flux coefficient E_1 for corner. Subtract "window frame flux" from combination of real coil and 0-thickness coil.

For $V = H_1 h_1 = j h_2 y_2$ we chose h_2 and j. Thus,

$$A = V\left(\frac{W_1}{h_1} + \frac{D + y_2}{h_2} + E_1\left(\frac{h_1}{h_2}\right) - \frac{y_2}{2h_2}\right)\mu_0$$

$$= \boxed{\mu_0 V\left(\frac{W_1}{h_1} + \frac{D + y_2/2}{h_2} + E_1\left(\frac{h_1}{h_2}\right)\right)}$$

$$\boxed{\overline{B}_{\text{yoke,max}} = \frac{A}{W_3 - W_1 - h_2}.}$$

We determine the minimum value of $\overline{B}_{\text{yoke,max}}$ by varying h_2, and we define

$$E_1(a) = a + \frac{2}{\pi}\left(\ln\frac{a + 1/a}{4} + \left(\frac{1}{a} - a\right)\arctan a\right) \quad \text{with} \quad a = h_2/h_1.$$

January, 1993. Note 0606thry.

Dipole with Small Gap Bypass

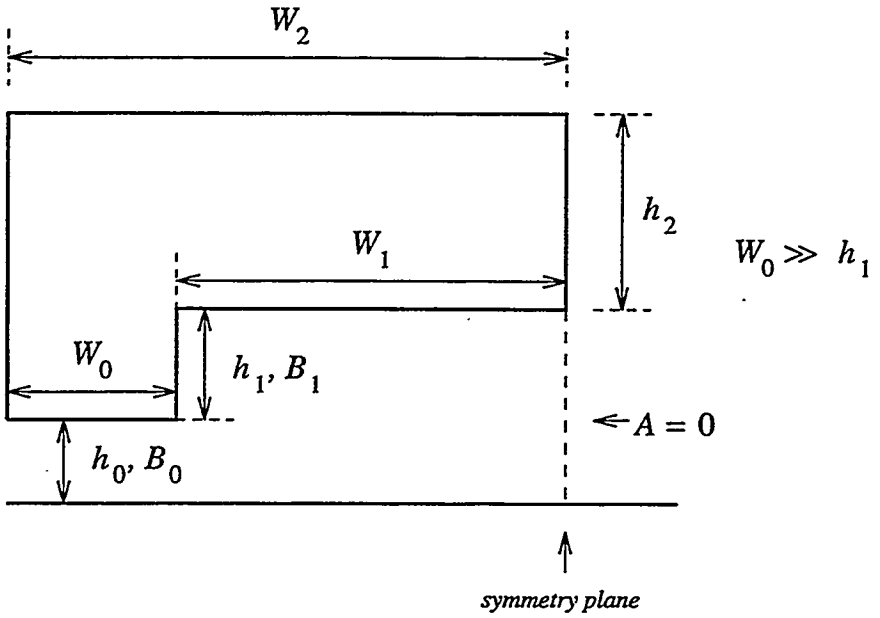

Figure 1.

$$\boxed{B_0 h_0 + h_1 \mu_0 H(B_0) = B_1(h_1 + h_0)} \tag{1}$$

For $W_0/W_2 = \varepsilon_0$,

$$B_2 W_2 = B_0 W_0 + B_1 W_1 \quad \text{and thus} \quad B_2 = B_0 \varepsilon_0 + B_1(1 - \varepsilon_0),$$

$$V_{00} = \frac{B_1}{\mu_0}(h_0 + h_1) + h_2 H(B_0 \varepsilon_0 + B_1(1 - \varepsilon_0))$$

The exact equation

$$\boxed{\mu_0 V_{00} = B_1(h_0 + h_1) + \mu_0 h_2 H(B_0 \varepsilon_0 + B_1(1 - \varepsilon_0))} \tag{2}$$

has the following implementations

$$B_1 \to B_0 \quad \text{and then} \quad B_1, B_0 \to V_{00}.$$

We will now examine three special cases.

June, 1993. Note 0591thry.

In Case 1, V_{00} is so small that $\mu_0 H(B) = \gamma B$,

$$B_0(h_0 + \gamma h_1) = B_1(h_0 + h_1)\,,$$

$$\boxed{\mu_0 V_{00} = B_1 \underbrace{\left(h_0 + h_1 + \gamma h_2 \left(\varepsilon_0 \frac{h_0 + h_1}{h_0 + \gamma h_1} + 1 - \varepsilon_0\right)\right)}_{K}\,,}$$

where

$$\frac{h_0 + h_1}{h_0 + \gamma h_1} = 1 + \frac{(1-\gamma)h_1}{h_0 + \gamma h1} \quad \text{and} \quad K'_{h_0} = 1 - \frac{\gamma h_1 \varepsilon_0 h_2 (1-\gamma)}{(h_0 + \gamma h_1)^2}\,,$$

$$B_1 = \frac{\mu_0 V_{00}}{K}, \quad B_1' = \frac{-\mu_0 V_{00}}{K^2} K' = \frac{\mu_0 V_{00}}{K^2}\left(\frac{\gamma h_1 \varepsilon_0 h_2 (1-\gamma)}{(h_0 + \gamma h_1)^2} - 1\right).$$

For $h_0 \ll \gamma h_1$:

$$B_1' = \frac{\mu_0 V_{00}}{K^2}\left(\frac{\varepsilon_0 h_2 (1-\gamma)}{\gamma h_1} - 1\right) > 0\,.$$

$K' = 0$ for $h_0 + \gamma h_1 = \sqrt{\varepsilon_0 \gamma h_1 h_2 (1-\gamma)}$ such that

$$h_0 = \gamma h_1 \Bigg(\underbrace{\sqrt{\frac{\varepsilon_0 h_2 (1-\gamma)}{\gamma h_1}}}_{\gg 1} - 1\Bigg) \approx \sqrt{\varepsilon_0 h_1 h_2 (1-\gamma)\gamma}\,.$$

For $h_1 = 1$, $h_2 = 5$, $\varepsilon_0 = 1/2$, $\gamma = 10^{-3}$, we have

$$h_0 = \sqrt{1/2 \cdot 1 \cdot 5 \cdot 10^{-3}} = \boxed{\frac{1}{20}\,\text{cm}\,.}$$

In Case 2, we need V_{00} large enough so that $B_0 \approx B_s$, but small enough so that for (2) $\mu_0 H(B) = \gamma B$, thus

$$\mu_0 V_{00} = B_1(h_0 + h_1) + B_1 h_2 \gamma (1 - \varepsilon_0) + B_s h_2 \gamma \varepsilon_0\,,$$

where

$$\boxed{B_1 = \frac{\mu_0 V_{00} - B_s \gamma h_2 \varepsilon_0}{h_0 + h_1 + h_2 \gamma (1 - \varepsilon_0)}\,.}$$

In a third, simple case, Case 3, for a still higher V_{00},

$$B_s \varepsilon_0 + B_1(1 - \varepsilon_0) \to B_s\,,$$

i.e. it is independent of V_{00}, and thus

$$\boxed{B_1 = B_s\,.}$$

Boundary Condition at Iron-Air Interface for AC and Application to 2-Dimensional Cylinder

Interface at $y = 0$,

$$\frac{\partial}{\partial x} = \frac{\partial}{\partial z} = 0 \quad \text{and} \quad \frac{\partial}{\partial y} = {}'.$$

$$\mathbf{H} = H\mathrm{e}_x, \quad \mathbf{j} = \mathrm{e}_z \sigma E \quad \text{and} \quad \mathbf{E} = \mathrm{e}_z E.$$

$$(\nabla \times \mathbf{H})_z = -H' = \sigma E \quad \text{and} \quad E = -\varrho H'.$$

$$(\nabla \times \mathbf{E})_x = E' = -\mu_0 \mu p H = -\varrho H'' \quad \text{and} \quad H'' - k^2 H = 0$$

where, depending on the application, p is either the Laplace transform variable or, for sinusoidal excitation, $i\omega$.

$$\boxed{k = \sqrt{\sigma \mu_0 \mu p} = \frac{1}{D_1}}$$

$$H = H_0 e^{-ky} \quad \text{and} \quad \Phi = \mu_0 \mu \int_0^\infty H dy = \frac{H_0 \mu_0 \mu}{k} = \mu_0 H_0 \mu D_1.$$

Therefore, with

$$\boxed{\mu D_1 = D_2}$$

$$\frac{d\Phi}{dx}\Delta x = \mu_0 D_2 \frac{\partial H_0}{\partial x}\Delta x = \mu_0 H_y \Delta x,$$

$$H_y = D_2 \frac{\partial H_0}{\partial x} \quad \Longrightarrow \quad \boxed{H_\perp = D_2 \frac{\partial H_\parallel}{\partial s_\parallel}}.$$

Given an iron cylinder with D_2, of radius 1, in far-field $\mathbf{H} = H_\infty \mathrm{e}_x$, we try to solve for the complex potential F. Ansatz: the superposition of the macro and micro dipoles, with normalized units.

$$F = -iH_1(z + 1/z) - iH_2(z - 1/z).$$

with $z = x + iy$, normalized with radius r_0 of the cylinder.

May, 1988. Note 0492thry.

On $|z| = 1$

$$F = A + iV = 2H_2 \sin\varphi - i2H_1 \cos\varphi,$$

$$H^* = iF' = H_x - iH_y \quad \text{and} \quad \mathcal{H} = H_r + iH_\varphi = He^{-i\varphi},$$

$$\mathcal{H}^* = H^* e^{i\varphi}.$$

and the boundary condition is, with

$$H_\parallel = H_\varphi \quad \text{and} \quad H_\perp = -H_r,$$

$$\boxed{H_r = -D_2 \frac{\partial H_\varphi}{\partial \varphi}}$$

$$H^* = H_1(1 - 1/z^2) + H_2(1 + 1/z^2) = e^{-i\varphi}\mathcal{H}^*.$$

On the surface,

$$\mathcal{H}^* = H_r - iH_\varphi = 2iH_1 \sin\varphi + 2H_2 \cos\varphi,$$

$$\boxed{H_r = 2H_2 \cos\varphi} \quad \text{and} \quad \boxed{H_\varphi = 2H_1 \sin\varphi}$$

and the boundary condition is, with

$$2H_2 \cos\varphi = D_2 2H_1 \sin\varphi + 2H_2 \cos\varphi \quad \text{and} \quad H_2 = D_2 H_1,$$

$$H_\infty = H_1 + H_2 = H_1(1 + D_2),$$

$$H_1 = \frac{H_\infty}{1 + D_2}, \quad H_2 = \frac{H_\infty D_2}{1 + D_2},$$

$$\boxed{H_r = 2H_\infty \frac{D_2}{1 + D_2} \cos\varphi} \quad \text{and} \quad \boxed{H_\varphi = -2H_\infty \frac{\sin\varphi}{1 + D_2}}$$

normalized with radius r_0 of the cylinder.

Using SI units, we choose $\sigma\mu_0 = 10$, $\mu = 10^4$ and $\omega = 2\pi \cdot 60\text{Hz}$, and therefore we have

$$|D_2| = \sqrt{\frac{\mu}{\sigma\mu_0\omega}} = \frac{10^2}{\sqrt{10^4(.12\pi)}},$$

$$\boxed{|D_2| = 1.6\text{m}}$$

$$\boxed{|D_1| = .16\text{mm}} \quad \text{and} \quad |D_1|\sqrt{2} = .23\text{mm}.$$

For sinusoidal excitation,

$$D_2 = |D_2|\frac{(1-i)}{\sqrt{2}},$$

$$\boxed{|1 + D_2| = \sqrt{\left(1 + \frac{|D_2|}{\sqrt{2}}\right)^2 + \frac{|D_2|^2}{2}} = \sqrt{1 + |D_2|^2 + |D_2|\sqrt{2}}\,.}$$

Normalized, where r_0 is the radius of the cylinder:

$$D_2 = \frac{D_2(\text{m})}{\text{r}_0(\text{m})}\,.$$

That is, for same material and frequency, $|D_2|$ is large for a small cylinder and $|D_2|$ is small for a large cylinder.

Unfortunately, if $H_\perp = D_2\dfrac{\partial H_\parallel}{\partial s_\parallel}$ is valid in z-geometry, it is not satisfied in conformally mapped w-geometry, i.e. dealing with this problem in mapped geometry is not practical.

Flux Into A Rectangular Box

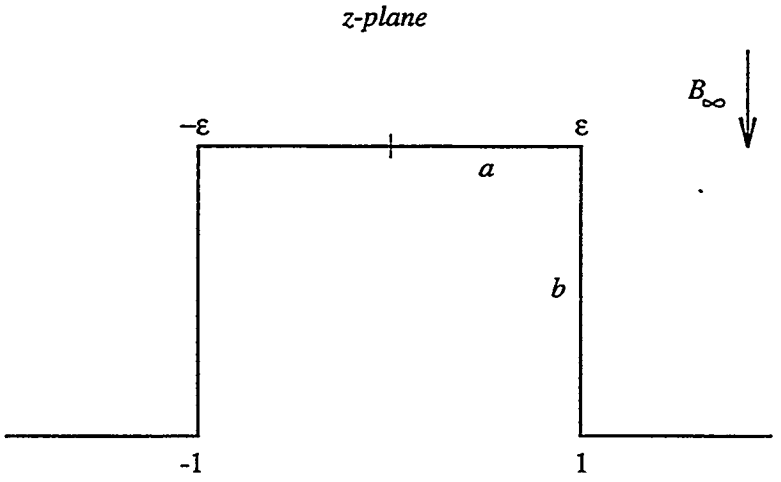

Figure 1.

$$\dot{z} = c\frac{\sqrt{t^2-\varepsilon^2}}{\sqrt{t^2-1}}$$

For

$$t = \varepsilon\sin\varphi, \quad dt = \varepsilon\cos\varphi\, d\varphi \quad \sqrt{1-\varepsilon^2} = \varepsilon_1\,,$$

we have

$$\frac{a}{c} = \int_0^{\varepsilon}\frac{\sqrt{\varepsilon^2-t^2}}{\sqrt{1-t^2}} = \varepsilon^2\int_0^{\pi/2}\frac{\cos^2\varphi\, d\varphi}{\sqrt{1-\varepsilon^2\sin^2\varphi}} = \int_0^{\pi/2}\frac{(1-\varepsilon^2\sin^2\varphi)+(\varepsilon^2-1)}{\sqrt{1-\varepsilon^2\sin^2\varphi}}\,d\varphi$$

$$\frac{a}{c} = \int_0^{\pi/2}\sqrt{1-\varepsilon^2\sin^2\varphi}\,d\varphi - \varepsilon_1^2\int_0^{\pi/2}\frac{d\varphi}{\sqrt{1-\varepsilon^2\sin^2\varphi}}$$

$$\boxed{\frac{a}{c} = E(\varepsilon^2) - \varepsilon_1^2 K(\varepsilon^2)\,.}$$

For

$$t = \cos\varphi, \quad dt = -\sin\varphi\, d\varphi, \quad \varepsilon = \cos\alpha, \quad \varepsilon_1 = \sin\alpha,$$

May, 1988. Note 0491thry.

$$\sin\varphi = \varepsilon_1 \sin\psi, \quad d\varphi = \frac{\varepsilon_1 \cos\psi \, d\psi}{\sqrt{1-\varepsilon_1^2 \sin^2\psi}},$$

we have

$$\frac{b}{c} = \int_{\varepsilon}^{1} \frac{\sqrt{t^2-\varepsilon^2}}{\sqrt{1-t^2}}\, dt = \int_{0}^{\alpha} \sqrt{\varepsilon_1^2 - \sin^2\varphi}\, d\varphi = \varepsilon_1^2 \int_{0}^{\pi/2} \frac{\cos^2\psi}{\sqrt{1-\varepsilon_1^2\sin^2\psi}}\, d\psi$$

$$\boxed{\frac{b}{c} = E(\varepsilon_1^2) - \varepsilon^2 K(\varepsilon_1^2)\,.}$$

Thus

$$\boxed{\frac{a}{b} = \frac{E(\varepsilon^2) - \varepsilon_1^2 K(\varepsilon^2)}{E(\varepsilon_1^2) - \varepsilon^2 K(\varepsilon_1^2)}\,.}$$

For

$$F(t) = cB_\infty t, \quad F' = B_\infty \frac{\sqrt{t^2-1}}{\sqrt{t^2-\varepsilon^2}}, \qquad \boxed{B_0 = \frac{B_\infty}{\varepsilon}\,.}$$

and therefore

$$\boxed{F(\varepsilon) = \frac{aB_\infty \varepsilon}{E(\varepsilon^2) - \varepsilon_1^2 K(\varepsilon^2)}\,,}$$

$$\boxed{F(1) = \frac{aB_\infty}{E(\varepsilon^2) - \varepsilon_1^2 K(\varepsilon^2)}\,.}$$

Given a square box, with dimensions $\varepsilon^2 = 1/2$, $E(1/2) = 1.3506$, $K(1/2) = 1.8541$,

$$F(\varepsilon) = F(\sqrt{1/2}) = 1.67 aB_\infty, \quad F(1) = 2.361 aB_\infty, \quad B_0 = 1.41 B_\infty.$$

Propagation of Fast Perturbation in Dipole

We describe the boundary condition as

$$H_y(h) = D_2 \frac{\partial H_x}{\partial x} \quad \text{with} \quad D_2 = \mu D_1 = \frac{\mu}{\sqrt{i\omega\sigma\mu_0\mu}}.$$

Ansatz:

$$\boxed{H_y(x,y) = \sum a_n \cos k_n y \, e^{-k_n x}}$$

where we look to satisfy the $H_y(-y) = H_y(y)$ symmetry only.

$\nabla^2 H_y = 0$ is obviously satisfied.

$$\frac{\partial H_x}{\partial y} = \frac{\partial H_y}{\partial x} = -\sum a_n k_n \cos k_n y \, e^{-k_n x}$$

$$\boxed{H_x = -\sum a_n \sin k_n y \, e^{-k_n x}.}$$

At the boundary we have

$$\sum a_n \cos k_n h \, e^{-k_n x} = \sum a_n D_2 k_n \sin k_n h \, e^{-k_n x}.$$

For

$$D_2 k_n \tan k_n h = 1 \quad \text{and} \quad \boxed{\alpha_n = k_n h,}$$

we therefore have

$$\boxed{\alpha_n \tan \alpha_n = \frac{h}{D_2}}$$

where

$$\frac{1}{D_2} = \sqrt{\frac{i\omega\sigma\mu_0}{\mu}}.$$

November, 1987. Note 0489thry.

Case 1: "normal" case, $\mu \to \infty$ $\alpha_n = n\pi$.
Case 2: superconducting case, $\sigma \to \infty$ $\alpha_n = (n+1/2)\pi$.
Case 3: using iron with $\omega = 2\pi 60\text{Hz}$, and given that $D_1 = \dfrac{1}{\sqrt{i\omega\sigma\mu_0\mu}}$,

$$|D_1| = \frac{1}{\sqrt{2\pi \cdot 60 \cdot 10^{1+3}}} = 5.2 \cdot 10^{-4}\text{m} = .52\text{mm}$$

$$|D_2| = \mu |D_1| = 52\text{cm}\,.$$

We introduce

$$\alpha_0 \tan\alpha_0 = \frac{h}{D_2} = \varepsilon = h\sqrt{\frac{i\omega\sigma\mu_0}{\mu}}$$

and for $|\varepsilon| << 1$, $\boxed{\alpha_0 \approx \sqrt{\varepsilon}\,.}$ Thus, for $\alpha_n = n\pi + \delta_n$,

$$(n\pi + \delta_n)\tan\delta_n = \varepsilon \quad \Longrightarrow \quad \boxed{\delta_n \approx \frac{\varepsilon}{n\pi}\,.}$$

For a better notation of α_0 we have that, for

$$\alpha_0^2 + \alpha_0^4/3 = \varepsilon \quad \Longrightarrow \quad \alpha_0^2 = -3/2 + \sqrt{9/4 + 3\varepsilon}\,.$$

and it follows that

$$\boxed{\alpha_0^2 = \frac{3\varepsilon}{\frac{3}{2} + \sqrt{\frac{9}{4} + 3\varepsilon}} = \frac{2\varepsilon}{1 + \sqrt{1 + \frac{4\varepsilon}{3}}}\,,}$$

$$\boxed{\alpha_0^2 = \frac{2\varepsilon}{2 + \frac{2\varepsilon}{3}} = \frac{\varepsilon}{1 + \frac{\varepsilon}{3}}\,.}$$

To determine a_n from $H_y(y)$ at $x = 0$ we try

$$\int_0^h H_y(y)\cos k_m y\, dy = \sum a_n \int_0^h \cos k_n y\, \cos k_m y\, dy\,.$$

Since $2\cos k_n y \cos k_m y = \cos(k_n + k_m)y + \cos(k_n - k_m)y$,

$$\begin{aligned}
\frac{2}{h}\int_0^h \cos k_n y \cos k_m y\, dy &= \frac{\sin(\alpha_n + \alpha_m)}{\alpha_n + \alpha_m} + \frac{\sin(\alpha_n - \alpha_m)}{\alpha_n - \alpha_m} \\
&= \frac{\alpha_n(\sin(\alpha_n + \alpha_m) + \sin(\alpha_n - \alpha_m))}{\alpha_n^2 - \alpha_m^2} \\
&\qquad - \frac{\alpha_m(\sin(\alpha_n + \alpha_m) - \sin(\alpha_n - \alpha_m))}{\alpha_n^2 - \alpha_m^2} \\
&= \frac{2(\alpha_n \sin\alpha_n \cos\alpha_m - \alpha_m \cos\alpha_n \sin\alpha_m)}{\alpha_n^2 - \alpha_m^2} \\
&= \frac{2\cos\alpha_n \cos\alpha_m(\alpha_n \tan\alpha_n - \alpha_m \tan\alpha_m)}{\alpha_n^2 - \alpha_m^2} \\
&= 0 \quad \text{for} \quad n \neq m.
\end{aligned}$$

Note: this orthogonality condition is not satisfied for $\int_0^h \sin k_n y \sin k_m y\, dy$. So, for instance, $V(0, y)$ would not work "directly". One would have to first calculate $H_y(0, y)$.

Description of the Properties of an Ellipse

For many problems, one needs integrals over the circumference of an ellipse, whose equation is

$$\frac{x^2}{a^2} + \frac{y^2}{b^2} = 1.$$

One may describe the ellipse by the parametric representation

$$z = a\cos\varphi + ib\sin\varphi,$$

and use φ as the integration variable.

However, in many cases, it is mathematically more convenient to use z on the circumference as the integrations variable. If one can represent all quantities of interest *on the circumference* as analytic functions of z, one can then use the Cauchy Theorem to execute the integration.

In using the parametric representation, one usually does something similar by introducing $e^{i\varphi}$ as the new integration variable. While this oftens works very well, it can lead to difficulties: for example, when e^{kz} appears in the function to be integrated.

In general, problems are much simpler for circles, where $a = b$. When $b \neq a$ it often becomes so difficult to execute the integral that it is most convenient to expand in a quantity that is equivalent to $a - b$ and thus the formulas will be easily written and therefore the expansion will be similarly easy.

Thus,

$$z = a\cos\varphi + ib\sin\varphi = e^{i\varphi}\frac{a+b}{2} + e^{-i\varphi}\frac{a-b}{2}, \tag{1}$$

$$\begin{aligned} 0 &= e^{i\varphi} - 2\frac{z}{a+b} + e^{-i\varphi}\frac{a-b}{a+b} = 0 \\ &= e^{2i\varphi}(a+b)^2 - 2ze^{i\varphi}(a+b) + \varepsilon, \end{aligned}$$

$$\boxed{\varepsilon = a^2 - b^2} \quad \text{and} \quad \boxed{W_1 = \sqrt{1 - \varepsilon/z^2}.} \tag{2}$$

$$e^{i\varphi} = \frac{z + \sqrt{z^2 - \varepsilon}}{a+b} = z\frac{1+W_1}{a+b}, \tag{3.1}$$

January, 1988. Note 0476thry.

$$e^{-i\varphi} = 2\frac{z}{a-b} - e^{i\varphi}\frac{a+b}{a-b}$$
$$= \frac{z-\sqrt{z^2-\varepsilon}}{a-b} = z\frac{1-W_1}{a-b} \tag{3.2}$$
$$= \frac{(a+b)/z}{1+W_1}. \tag{3.3}$$

For $\cos\varphi$, $\sin\varphi$:

$$\frac{1}{a+b}+\frac{1}{a-b}=\frac{2a}{\varepsilon} \quad \text{and} \quad \frac{1}{a+b}-\frac{1}{a-b}=\frac{-2b}{\varepsilon},$$

$$\cos\varphi = \frac{az-b\sqrt{z^2-\varepsilon}}{\varepsilon} = \frac{z^2+b^2}{az+b\sqrt{z^2-\varepsilon}} = \frac{z^2+b^2}{z(a+bW_1)}, \tag{4.1}$$

$$i\sin\varphi = \frac{-bz+a\sqrt{z^2-\varepsilon}}{\varepsilon} = \frac{z^2-a^2}{bz+a\sqrt{z^2-\varepsilon}} = \frac{z^2-a^2}{z(b+aW_1)}. \tag{4.2}$$

$$ds = \sqrt{a^2\sin^2\varphi + b^2\cos^2\varphi}\,d\varphi. \tag{5}$$

From (3.1) we have

$$ie^{i\varphi}d\varphi = \frac{\left(1+(z/\sqrt{z^2-\varepsilon})\right)dz}{a+b} = \frac{e^{i\varphi}dz}{zW_1},$$

$$d\varphi = \frac{1}{i}\frac{dz}{zW_1}. \tag{6.0}$$

Thus,

$$\varepsilon^2 G = \varepsilon^2(a^2\sin^2\varphi + b^2\cos^2\varphi)$$
$$= z^2(b^2(a-bW_1)^2 - a^2(b-aW_1)^2)$$
$$= z^2(W_1^2(b^4-a^4) + 2abW_1(a^2-b^2))$$
$$= z^2\left(\frac{\varepsilon(a^2+b^2)}{z^2} - (a-b)^2 - 2ab\frac{1-W_1^2}{1+W_1}\right),$$

$$G = a^2+b^2-z^2\frac{\varepsilon}{(a+b)^2} - \frac{2ab}{1+W_1},$$

where

$$\frac{2}{1+W_1} = 1 + \frac{1-W_1}{1+W_1}$$

and thus

$$\begin{aligned} G &= a^2+b^2-ab-z^2\frac{\varepsilon}{(a+b)^2}-ab\frac{1-W_1}{1+W_1} \\ &= (a-b)^2+ab-z^2\frac{\varepsilon}{(a+b)^2}-ab\frac{1-W_1}{1+W_1} \\ &= \frac{\varepsilon^2}{(a+b)^2}+ab-z^2\frac{\varepsilon}{(a+b)^2}-ab\frac{1-W_1}{1+W_1} \\ &= \boxed{ab-\varepsilon\frac{z^2-\varepsilon}{(a+b)^2}-ab\frac{1-W_1}{1+W_1}.} \end{aligned} \tag{7.1}$$

To expand an expression like

$$\frac{1-W_1}{1+W_1} \quad \text{with} \quad W_1=\sqrt{1-\varepsilon/z^2},$$

in ε, it is often convenient to break it up into an even and odd part in ε:

$$2F(\varepsilon)=F(\varepsilon)+F(-\varepsilon)+F(\varepsilon)-F(-\varepsilon) \quad \text{with} \quad W_2=\sqrt{1+\varepsilon/z^2},$$

$$2\frac{1-W_1}{1+W_1}=2H=\frac{1-W_1}{1+W_1}+\frac{1-W_2}{1+W_2}+\frac{1-W_1}{1+W_1}-\frac{1-W_2}{1+W_2},$$

$$\begin{aligned} 2H(1+W_1W_2+W_1+W_2) &= (1-W_1)(1+W_2)+(1+W_1)(1-W_2) \\ &\quad +(1-W_1)(1+W_2)-(1+W_1)(1-W_2) \\ &= 2(1-W_1W_2+W_2-W_1), \end{aligned}$$

$$\frac{1-W_1}{1+W_1}=\frac{1-\sqrt{1-\varepsilon^2/z^4}+\sqrt{1+\varepsilon/z^2}-\sqrt{1-\varepsilon/z^2}}{1+\sqrt{1-\varepsilon^2/z^4}+\sqrt{1+\varepsilon/z^2}+\sqrt{1-\varepsilon/z^2}}.$$

To second order in ε:

$$\boxed{\frac{1-W_1}{1+W_1}=\frac{\varepsilon}{z^2}\frac{1+\varepsilon/2z^2}{4}.} \tag{7.2}$$

A comment about the expansion in ε and subsequent integration: the expansion has to be valid and good for z on the ellipse. If, to carry out the integration, one later modifies the integration path (in particular, to a very small circle around $z=0$), this will *not* invalidate the original expansion.

Addendum. A different way to derive G.

For

$$W_0 = \sqrt{z^2 - \varepsilon},$$

$$\varepsilon = a^2 - b^2 \quad \text{and} \quad s = a^2 + b^2,$$

$$s^2 - \varepsilon^2 = 4a^2b^2 \quad \text{and} \quad 2ab = \sqrt{s^2 - \varepsilon^2},$$

we have

$$\begin{aligned}
\varepsilon^2 G &= (b\varepsilon\cos\varphi + ia\varepsilon\sin\varphi)(b\varepsilon\cos\varphi - ia\varepsilon\sin\varphi) \\
&= W_0(2abz - W_0(a^2 + b^2)) \\
&= sW_0\left(z\sqrt{1 - \varepsilon^2/s^2} - W_0\right) \\
&= sW_0\frac{z^2(1 - \varepsilon^2/s^2) - z^2 + \varepsilon}{z\sqrt{1 - \varepsilon^2/s^2} + W_0},
\end{aligned}$$

$$G = sW_0\frac{1 - \varepsilon z^2/s^2}{z\sqrt{1 - \varepsilon^2/s^2} + W_0} = \boxed{sW_1\frac{1 - \varepsilon z^2/s^2}{\sqrt{1 - \varepsilon^2/s^2} + W_1}.}$$

To first order in ε:

$$G = s\frac{1}{2}\left(1 - \frac{\varepsilon}{2z^2}\right)\left(1 - \frac{\varepsilon z^2}{s^2}\right)\left(1 + \frac{\varepsilon}{4z^2}\right) = \frac{s}{2}\left(1 - \varepsilon\left(\frac{z^2}{s^2} + \frac{1}{4z^2}\right)\right),$$

for $s = 2a^2$ and $s^2 = 4a^4$,

$$\boxed{\sqrt{G} = a\left(1 - \frac{\varepsilon}{2}\left(\frac{z^2}{s^2} + \frac{1}{4z^2}\right)\right),}$$

$$\boxed{\sqrt{G} = a\left(1 - \frac{\varepsilon}{8a^2}\left(\frac{z^2}{a^2} + \frac{a^2}{z^2}\right)\right).}$$

Characterization of Dipole Fringe Fields with Field Integrals

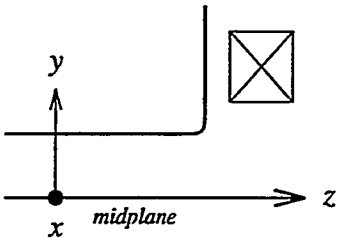

Figure 1.

Background and Introduction.

The quantity $\int B_y(x,y,z)dz$ was measured as a function of y for a fixed x, with integration region beginning in the homogenous field region inside the dipole magnet and reaching into the essentially field-free region outside. This resulted in the approximate plotted curve of Figure 1 below.

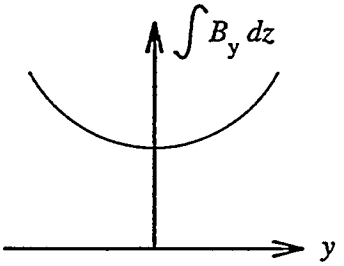

Figure 2.

The conclusion reached pointed to the coil being too close to or too far from the midplane. For didactic purposes this is a very interesting problem for two reasons.

(1) The coil position is only indirectly responsible. The fact that $\int B_y dz$ depends on y indicates that this is a 3D problem: namely, $\int B_y(x,0,z)dz$ will have a curvature of opposite polarity (i.e. effective field boundary is curved). This is due either to a curvature of the pole ends (when projected into the xz-plane) or to the finite width in the x-direction. If the latter is the cause, the problem is magnified by the absence (or incorrect design) of the field clamp *and* by a coil that is too far from the midplane.

(2) The characterization of the fringe field by measuring $\int B_y(x,0,z)dz$ gives, in case of midplane symmetry, more information than $\int B_y(0,y,z)dz$ alone.

May, 1986. Note 0438thry.

Analysis.

We assume midplane symmetry. Violation of midplane symmetry should be detected and/or measured, preferably with null method.

In vacuum, full 3D, the following hold:

$$\frac{\partial B_y}{\partial x} - \frac{\partial B_x}{\partial y} = 0, \tag{1.1}$$

$$\frac{\partial B_x}{\partial x} + \frac{\partial B_y}{\partial y} + \frac{\partial B_z}{\partial z} = 0. \tag{1.2}$$

We now investigate the properties of

$$\int_{z_1}^{z_2} B_x(x,y,z)dz/L = b_x(x,y) \quad \text{and} \quad \int_{z_1}^{z_2} B_y(x,y,z)dz/L = b_y(x,y) \tag{2a, b}$$

where z_1, z_2 are constants, i.e. they are not considered variables; L is a convenient length that is used only for normalization purposes. Integration is performed over (1.1). Integration and differentiation can be interchanged and thus

$$\frac{\partial b_y}{\partial x} - \frac{\partial b_x}{\partial y} = 0. \tag{3.1}$$

Integration is performed over (1.2) and

$$\frac{\partial b_x}{\partial x} + \frac{\partial b_y}{\partial y} = (B_z(x,y,z_1) - B_z(x,y,z_2))/L. \tag{3.2}$$

If, independently of x and y, B_z at the two end-points is the same†, we have

$$\frac{\partial b_x}{\partial x} + \frac{\partial b_y}{\partial y} = 0. \tag{3.3}$$

(3.1) and (3.2) mean that b_x and $-b_y$ satisfy the Cauchy-Riemann conditions of real and imaginary parts of the analytic function of $Z = x + iy$:

$$b_x - ib_y = b^*(Z). \tag{4}$$

We use the Taylor series to represent $b^*(Z)$:

$$b^*(Z) = -i\sum_0^n a_n Z^n,$$

where n = multipole order -1, i.e. $n = 0 \Longrightarrow$ dipole, $n = 1 \Longrightarrow$ quadrupole, etc. Because of midplane symmetry all a_n must be real. Notice that for $y = 0$,

† In the case under discussion here, $B_z = 0$ at both ends even though $B_z \neq 0$ in the fringe field region.

$b_y(x,0) = \sum a_n x^n$, i.e. all harmonics contribute; while for $x = 0$, only a_n with even n contributes to $b_y(0,y)$. If one measures for $x = 0$ both b_y and b_x, then one gets information about all harmonics. There is an advantage to measuring both $b_y(0,y)$ and $b_x(0,y)$ since one gives only the odd harmonics and the other only the even, while they are all mixed when calculating $b_y(x,0)$.

Looking at (5) it is obvious that if $b_y(0,y)$ is not constant, but depends on y, then $b_y(x,0)$ must depend on x. That is, one is in fact dealing with 3D fields which must be due to curved (in projection on xy-plane) poles or poles of insufficient width in the $x-$direction, and failure to use a field clamp. It is also qualitatively clear that these 3D effects get more pronounced with increasing distance of the coils from the midplane.

Specifically, for a known value of $b_y(0,y)$, what is $b_y(x,0)$?

$$b_y(0,y) = \sum_0^m a_{2m} y^{2m} (-1)^m, \tag{6.1}$$

$$b_y(x,0) = \sum_0^m a_{2m} x^{2m} + \sum_0^m a_{2m+1}, \tag{6.2}$$

where in (6.2) a_{2m+1} is not obtainable from $b_y(0,y)$, but can be obtained from $b_x(0,y)$. If one measures $b_x(0,y)$, one gets

$$b_x(0,y) = \sum_0^m a_{2m+1} y^{2m+1} (-1)^m. \tag{6.3}$$

For simple analysis, one should plot $b_y(0,y)$ *vs* y^2, and $b_x(0,y)/y$ *vs* y^2. One has to be careful to make the measurements in such a way that they really mean something. The flux loop and integrator method is perhaps best because it can practically always be done in such a way that one makes a null measurment.

Penetration of Solenoidal Field through Conducting Shell

Preliminaries: Solenoid, shield infinitely long. Thin shell, circular cross-section: treat eddy currents in it in plane geometry with proper boundary values. Only one shell: matrix formulation not needed.

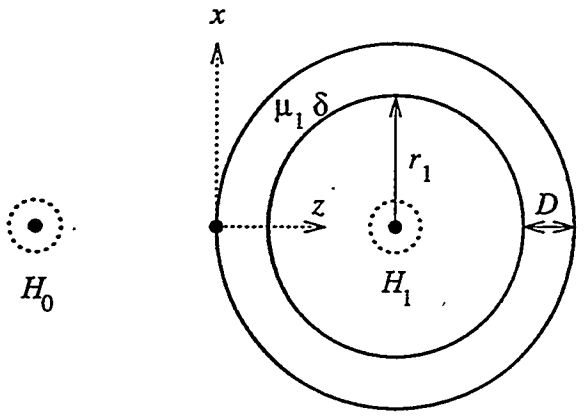

Figure 1.

At $z = 0$,

$$H_y = H_0(p) = \text{given solenoid current.}$$

At $z = D$,

$$E_x = \frac{\mu_0 p H_1 \pi r_1^2}{2\pi r_1} = \frac{r_1}{2}\mu_0 p H_1.$$

In shell,

$$\mathbf{H} = \mathbf{e}_y H, \quad \mathbf{E} = \mathbf{e}_x E, \quad \text{and} \quad \sigma = \frac{\partial}{\partial z}.$$

$$\nabla \times \mathbf{H} = \sigma \mathbf{E} \implies -H' = \sigma E,$$

$$\nabla \times \mathbf{E} = -\mu_0 \mu p \mathbf{H} \implies E' = -\mu_0 \mu p H.$$

For $\mu_0 \mu \sigma p = k^2$,

$$H'' = -\sigma E' = \mu_0 \mu \sigma p H = k^2 H,$$

$$H = H_0 \cosh kz + b \sinh kz,$$

and for $\gamma = kD$,

$$H_1 = H_0 \cosh \gamma + b \sinh \gamma, \quad \text{and thus} \quad b = \frac{H_1 - H_0 \cosh \gamma}{\sinh \gamma},$$

May, 1986. Note 0437thry.

$$E_1 = \frac{r_1}{2}\mu_0 p H_1 = -\frac{H_1'}{\sigma} = -\frac{k}{\sigma}(H_0 \sinh\gamma + b\cosh\gamma),$$

$$H_1 = \frac{\mu_0 \sigma p r_1}{2k} = -\left(H_0 \sinh\gamma + \frac{\cosh\gamma(H_1 - H_0\cosh\gamma)}{\sinh\gamma}\right),$$

where, for

$$\frac{\mu_0\sigma p r_1}{2k} = \frac{k^2 r_1/\mu}{2k} = \frac{r_1}{2}\frac{k}{\mu} = \gamma\varepsilon, \quad \text{and thus} \quad \boxed{\varepsilon = \frac{r_1}{2\mu D},}$$

where diffusion occurs for $\mu \gg 1$. Thus, for

$$H_1(\varepsilon\gamma\sinh\gamma + \cosh\gamma) = H_0,$$

$$\boxed{H_1(p) = \frac{H_0}{\cosh\gamma + \varepsilon\gamma\sinh\gamma}.}$$

The zeroes of $\cosh\gamma + \varepsilon\gamma\sinh\gamma$ are given, with

$$\gamma_n = D\sqrt{\mu_0\mu\sigma p_n} = i\alpha_n.$$

And

$$\cosh\gamma + \varepsilon\gamma\sinh\gamma = \cos\alpha_n - \varepsilon\alpha_n\sin\alpha_n = 0,$$

$$\boxed{\frac{1}{\varepsilon} = \alpha_n\tan\alpha_n,}$$

$$\boxed{p_n = \frac{-\alpha_n^2}{\mu_0\mu\sigma D^2}.}$$

One may expect difficulties for some calculations because $\gamma = D\sqrt{\mu_0\mu\sigma p}$, but this is not so, for

$$\cosh\gamma + \varepsilon\gamma\sinh\gamma = 1 + \gamma^2\left(\frac{1}{2} + \varepsilon\right) + \gamma^4\left(\frac{1}{4!} + \frac{\varepsilon}{3!}\right) + \gamma^6\left(\frac{1}{6!} + \frac{\varepsilon}{5!}\right) + \cdots$$
$$= 1 + \sum_{n=1}^{\infty}\gamma^{2n}\left(\frac{1}{(2n)!} + \frac{\varepsilon}{(2n-1)!}\right),$$

and $\cosh\gamma + \varepsilon\gamma\sinh\gamma$ is a simple function of γ^2, not a complicated function of γ. For

$$\varepsilon \gg 1 \implies \alpha_0^2 \approx \frac{1}{\varepsilon} = \mu_0\mu\sigma p_0 D^2 = \frac{2\mu D}{r_1} \implies \boxed{\mu_0\sigma D r_1 p_0 = 2,}$$

with σD implying non-diffusion.

The roots, in quadrants 1 and 3, are given by,

$$\tan \alpha_n = \frac{1}{\alpha_n \varepsilon}.$$

Where, for $\alpha_n \varepsilon \gg 1$, $\alpha_n = n\pi + \sigma_n$, and thus

$$\boxed{\sigma = \frac{1}{\varepsilon(n\pi + \sigma_n)} \approx \frac{1}{\varepsilon n \pi}.}$$

The residue contribution from $\cosh\gamma + \varepsilon\gamma \sinh\gamma$ is given by

$$\frac{1}{\cosh\gamma + \varepsilon\gamma\sinh\gamma} \quad \Longrightarrow \quad R = \frac{1}{\dfrac{d\gamma}{dp}(\sinh\gamma + \varepsilon\sinh\gamma + \varepsilon\gamma\cosh\gamma)},$$

where $d\gamma/dp = \gamma/2p$ and $\varepsilon\gamma = -\cosh\gamma/\sinh\gamma$. Thus,

$$R = \frac{2p}{\gamma}\frac{\sinh\gamma}{\varepsilon\sinh^2\gamma - 1} = \frac{2p}{\gamma^2}\frac{\gamma\sinh\gamma}{\varepsilon\sinh^2\gamma - 1} = \frac{2p}{\gamma^2}\frac{\alpha_n \sin\alpha_n}{\varepsilon\sin^2\alpha_n + 1}.$$

For $\cot\alpha_n = \alpha_n\varepsilon$, and $\sin\alpha_n = 1/\sqrt{1+\cot^2\alpha^2} = 1/\sqrt{1+\alpha_n^2\varepsilon^2}$,

$$\boxed{R_n = \frac{2}{\mu_0\mu D^2\sigma}\frac{\alpha_n}{\sqrt{1+\alpha_n^2\varepsilon^2}\left(1 + \dfrac{\varepsilon}{1+\alpha_n^2\varepsilon^2}\right)} = \frac{2}{\mu_0\mu D^2\sigma}\frac{\alpha_n\sqrt{1+\alpha_n^2\varepsilon^2}}{1+\alpha_n^2\varepsilon^2+\varepsilon}.}$$

For $\alpha_0^2 = 1/\varepsilon$,

$$R_0 = \frac{2}{\mu_0\mu\sigma D^2}\frac{1}{\sqrt{\varepsilon}}\frac{\sqrt{1+\varepsilon}}{1+2\varepsilon} = \frac{1}{\mu_0\mu\sigma D^2\varepsilon}\frac{\sqrt{1+1/\varepsilon}}{1+1/2\varepsilon}.$$

Rogowski Dipole

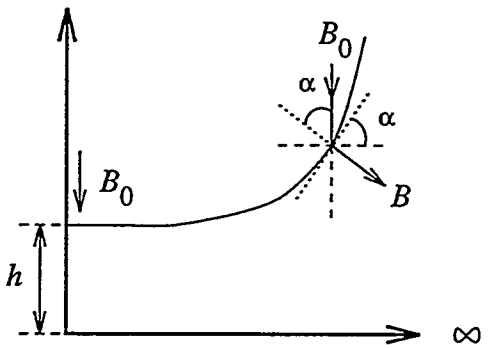

Figure 1.

$$B = B_0 \cos\alpha \cdot \frac{e^{i\alpha}}{i} \quad \text{and} \quad B^* = iB_0 \cos\alpha \cdot e^{-i\alpha},$$

$$\frac{iB_0}{B^*} = \boxed{G = \frac{e^{i\alpha}}{\cos\alpha} = 1 + i\tan\alpha} \cdot \text{with} \quad G = \frac{1}{F'} = \frac{\dot{z}}{\dot{F}}\,.$$

On pole: $\Re G = 0$. On $0, 1, \infty : \Im G = 0$.

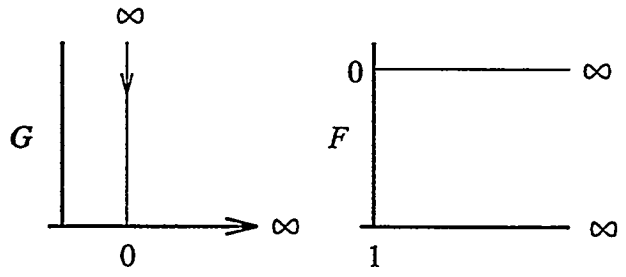

Figures 2(a,b).

$$\dot{G} = \frac{a/2}{\sqrt{t}} \quad \text{and} \quad \boxed{G = 1 + a\sqrt{t},}$$

$$\dot{F} = \frac{b/2}{\sqrt{t}\sqrt{t-1}} \quad \text{and} \quad \boxed{F = b\ln\left(\sqrt{t} + \sqrt{t-1}\right).}$$

Thus

$$\dot{z} = \dot{F}G = \frac{b}{2}\left(\frac{1}{\sqrt{t}\sqrt{t-1}} + \frac{a}{\sqrt{t-1}}\right) \quad \text{and} \quad \boxed{z = b\left(\ln\left(\sqrt{t} + \sqrt{t-1}\right) + a\sqrt{t-1}\right).}$$

February, 1981. Note 0397thry.

Since $ih = b(\ln i + ia) = ib(\pi/2 + a)$, we let

$$\boxed{\pi/2 + a = C} \quad \text{and} \quad \boxed{h = bC.}$$

On pole: $t = -\tau < 0$,

$$x + iy = b(i\pi/2 + \ln(\sqrt{\tau} + \sqrt{\tau + 1}) + ia\sqrt{\tau + 1}),$$

with

$$\boxed{\tau = \sinh^2 \alpha,} \quad \boxed{x = b\alpha,}$$

$$b\left(\frac{\pi}{2} + a\cosh\alpha\right) = \frac{h}{C}\left(C + a\left(\cosh\frac{x}{b} - 1\right)\right) = \boxed{y = h\left(1 + \frac{a}{c}\left(\cosh C\frac{x}{h} - 1\right)\right),}$$

and

$$G(1) = 1 + a = \frac{B(z = ih)}{B(z = 0)}.$$

Rogowski Quadrupole: Formulation of Problem

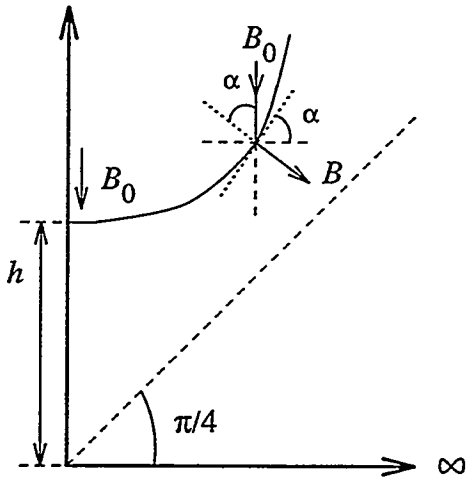

Figure 1.

$$\mu = \infty, \quad \text{and} \quad B^* = +iB_0.$$

$$B = B_0 \cos\alpha \cdot \frac{e^{i\alpha}}{i}, \quad \text{and} \quad B^* = iB_0 \cos\alpha \cdot e^{-i\alpha}.$$

Thus,

$$\frac{iB_0}{B^*} = G = \frac{e^{i\alpha}}{\cos\alpha} = 1 + i\tan\alpha,$$

on the pole, with $\Re G = \text{constant} = 1$, and

$$|G| = \frac{B_0}{|B|}.$$

On the 45° line,

$$B \approx e^{i\pi/4}/i, \quad B^* \approx ie^{i\pi/4}, \quad \text{and} \quad G \approx e^{i\pi/4}.$$

February, 1981. Note 0326thry.

Observe Figures 2(a,b,c):

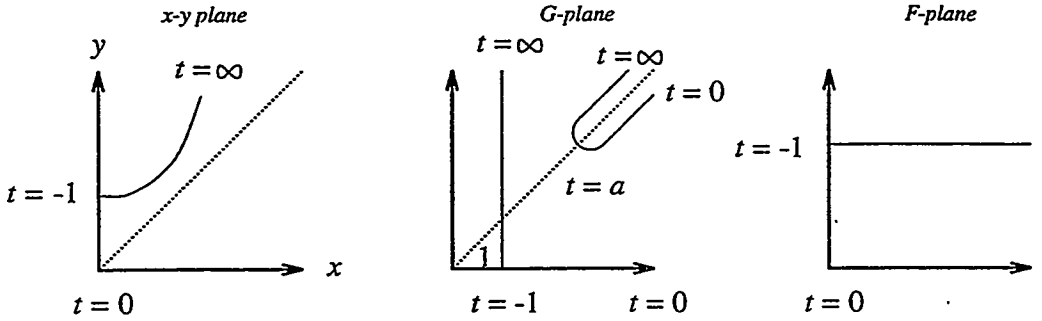

Figures 2(a,b,c).

$$\boxed{\frac{dG}{dt} = b\frac{t-a}{t^{5/4}\sqrt{t+1}}e^{i\pi/4}.}$$

$$B^* = iB_0\frac{dF}{dz}, \quad \frac{dz}{dF} = \frac{\dot{z}}{\dot{F}} = G \quad \text{and} \quad \boxed{\dot{z} = G(t)\cdot\dot{F}.}$$

In the F-plane, for $-1 \le t \le 0$:

$$\boxed{\pi\dot{F} = \frac{c:}{\sqrt{t}\sqrt{t+1}}.}$$

The mathematical difficulty arises in the integration of $\dot{G}$. For

$$t = w^4, \quad dt = 4w^3dw, \quad \frac{dt}{t^{5/4}} = \frac{4w^3dw}{w^5} = \frac{4dw}{w^2},$$

we solve the elliptic integral

$$\boxed{G = b\int\frac{w^4-a}{w^2\sqrt{1+w^4}}dw.}$$

The integration of $\dot{z} = (\dot{G}F) - \dot{G}F$ leads to

$$\boxed{z = GF - be^{i\pi/4}\int\frac{t-1}{t^{5/4}\sqrt{t+1}}Fdt}$$

and therefore

$$\boxed{F = 2C\ln\left(\sqrt{t}+\sqrt{t+1}\right).}$$

Eddy Currents for Fast Permanent Magnet Magnetization

Sometimes permanent magnets are magnetized by "hitting" them for a short time with high H. It is of interest to know how the magnetization front propagates through the material. Since this is a highly non-linear problem, a strongly simplified model is used in this document, but one which has all the essential features of the real process.

At the left edge of the material, assume a step function excitation starting at $t = 0$, with amplitude H_{00}. Our model is a 1-dimensional block of material with the left edge at $x = 0$, and

$$\frac{\partial}{\partial y} = \frac{\partial}{\partial z} = 0, \quad \mathbf{H} = \mathbf{e}_y H, \quad \mathbf{E} = \mathbf{e}_z E, \quad \text{and} \quad \mathbf{j} = \sigma \mathbf{E}.$$

For the times of interest, $H \geq 0$ everywhere. We use a strongly simplified $B(H)$ curve.

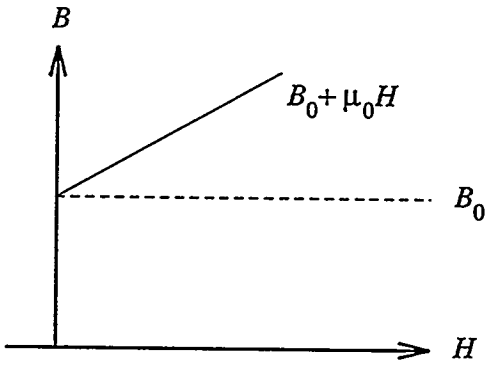

Figure 1.

Figure 1 shows that in the beginning, the material "sees" no H and $B = 0$. As soon as it "sees" $H > 0$, it becomes magnetized according to the above curve.

To reach an initial understanding of the problem, only the propagation in a medium that is, at least at first, unlimited to the right is treated.

$$\nabla \times \mathbf{H} = \mathbf{j} \quad \Longrightarrow \quad H' = \sigma E, \quad \text{with} \quad H' = \frac{\partial}{\partial x}.$$

$$\nabla \times \mathbf{E} = -\dot{\mathbf{B}} \quad \Longrightarrow \quad +E' = +\dot{B}.$$

August, 1977. Note 0264thry.

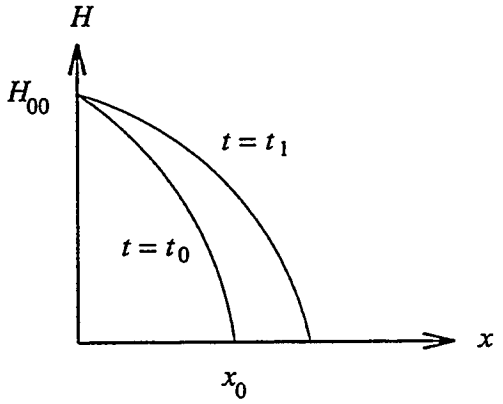

Figure 2.

The "location" of the front is designated by $x_0(t)$. We integrate $E' = \dot{B}$ over x across $x_0(t)$:

$$E(x_0 + \varepsilon) - E(x_0 - \varepsilon) = -E(x_0) = \int \dot{B} dx = B_0 \dot{x}_0,$$

giving the equation of the front for both **Case I** and **Case II** below.

Case I: $B(H) = B_0$.

For $x < x_0$:

$$E' = 0, \quad \text{and} \quad E = -B_0 \dot{x}_0 = \varrho H'.$$

$$H(x) = H_{00} - \sigma B_0 x \dot{x}_0,$$

meaning that for this $B(H)$ model, the $H(x)$ curves of Figure 2 are straight lines.

$$H(x_0) = 0 = H_{00} - \sigma B_0 x_0 \dot{x}_0.$$

Integrating over t gives $H_{00}t - \sigma B_0 x_0^2/2$, giving the following result for the propagation of the front:

$$\frac{2tH_{00}}{B_0\sigma} = \frac{B_{00}}{B_0} \cdot \frac{2t}{\mu_0\sigma} = \boxed{x_0^2 = r\frac{2t}{\mu_0\sigma},} \quad \text{with} \quad r = \frac{\mu_0 H_{00}}{B_0} = \frac{B_{00}}{B_0}.$$

Case II: $B = B_0 + \mu_0 H$.

For $x < x_0$: $\quad H' = \sigma E, \quad$ and $\quad E' = \mu_0 \dot{H}$ †.

For $x = x_{0_+}$: $\quad H = 0.$

† The right side of this last equation is now non-zero in contrast to Case I where $\dot{B} = 0$ in the magnetized part of the material; i.e. $\dot{B} \neq 0$ only at the propagating front.

For $x = x_{0\_}$: $\quad B = B_0, \quad E = -B_0\dot{x}_0 = \varrho H'.$

For $x = 0$: $\quad H = H_{00}.$

The differential equation is $\boxed{H'' = \mu_0\sigma\dot{H}.}$

We introduce

$$\sqrt{\frac{t}{\mu_0\sigma}} = \tau \quad \text{and thus} \quad t = \tau^2\mu_0\sigma,$$

and get

$$\dot{H} = \frac{\partial H}{\partial \tau}\cdot\frac{d\tau}{dt} = \frac{\partial H}{\partial \tau}\cdot\frac{1}{2\tau\mu_0\sigma}, \quad \text{and} \quad \frac{\partial^2 H}{\partial x^2} = \frac{\partial H}{\partial \tau}\cdot\frac{1}{2\tau}.$$

We use the dimensional analysis argument that x and τ are the only dimensional quantities entering the problem. This means that H must be a function of x/τ. We let $u = x/2\tau$. For $H = F(u)$:

$$\frac{\partial^2 H}{\partial x^2} = \frac{F''}{4\tau^2} = \frac{1}{2\tau}\cdot F'\cdot\frac{-u}{\tau} = \frac{-F'u}{2\tau^2}, \quad \text{and thus} \quad F'' + 2uF' = 0,$$

$$\ln\frac{F'}{F_0'} + u^2 = 0, \quad \text{and} \quad \boxed{F' = -ae^{-u^2},}$$

with $F_0' = -a$ because F' has to be less than 0.

The boundary conditions, with fixed $\tau > 0$, are

$$\boxed{F = H(u) = H_{00} - a\int_0^u e^{-u^2}du.}$$

$u_0 = x_0/2\tau$ and x_0 refer to the location of front.

$$H(u_0) = H_{00} - a\int_0^{u_0} e^{-u^2}du = 0, \quad \text{with} \quad a = \frac{H_{00}}{\int_0^{u_0} e^{-u^2}du}.$$

Just as in **Case I**, the location x_0 of the front is proportional to $\sqrt{t}$. Thus,

$$\frac{\partial H(u_0)}{\partial x} = \frac{-ae^{-u_0^2}}{2\tau} = \sigma E = -B_0\sigma\dot{x}_0 = -B_0\sigma\cdot\frac{dx_0}{d\tau}\cdot\frac{1}{2\tau\mu_0\sigma}$$

$$\boxed{a = e^{u_0^2}\cdot\frac{B_0}{\mu_0}\cdot\frac{dx_0}{d\tau}} \quad \text{and} \quad \boxed{\frac{B_{00}}{B_0} = \tau = \frac{dx_0}{d\tau}\cdot e^{-u_0^2}\cdot\int_0^{u_0} e^{-u^2}du.}$$

Since $u_0 = x_0/2\tau$, this is a first order differential equation that looks difficult at first.

However, it is obvious that from dimensional considerations the solution must be

$$\boxed{x_0 = 2\tau g(r),}$$

where the factor of 2 is for neatness. That is, $u_0 = g(r)$, and then $g(r)$ is determined by

$$\boxed{r = 2ge^{g^2} \int_0^g e^{-u^2} du.}$$

For small g:

$$r = 2g^2 \quad \Longrightarrow \quad g = \sqrt{r/2}, \quad \text{and} \quad x_0 = \tau\sqrt{2r} = \sqrt{r \cdot \frac{2t}{\mu_0\sigma}},$$

where x_0 has the same solution as the case of $B = B_0$, as it has to be.

Evaluation with a $TI59$ gives the following results:

g	0.01	0.1	0.2	0.3	0.4	0.6	0.8	1.0
r	2.0×10^{-4}	2.01×10^{-2}	8.22×10^{-2}	.191	.356	.920	2.00	4.06

g	1.1	1.2	1.3	1.4	1.5	1.6	1.8	2.0
r	5.76	8.17	11.7	16.8	24.4	35.8	80.6	193

If r is of order 4, then

$$g \approx 1 \quad \Longrightarrow \quad \boxed{x_0 = 2\tau = 2\sqrt{\frac{t}{\mu_0\sigma}}.}$$

Case **III:** H after complete penetration of the slab.

When the front has reached $x_0 = x_1$, where $2x_1$ is the slab thickness, the boundary conditions change. In contrast to our earlier analysis, a given length x_1 enters the problem implicitly, and thus the dimensional analysis argument that H must be equal to $F(x/2\tau)$ is no longer valid. If time is counted anew, with $t = 0$ when $x_0 = x_1$, we are dealing with a linear system with boundary condition

$$H(x_1 + \Delta x) = H(x_1 - \Delta x) \quad \text{for} \quad t \geq 0,$$

with known and given $H(x)$ for $t = 0$ and $0 \leq x \leq 2x$.

If $H(x) - H_{00}$ is defined to be an odd function of x with respect to $x = 0$, and an even function with respect to $x = \pm x_1$, and this function is expanded into a Fourier series, then the period is $4x_1$, and

$$H(x) - H_{00} = \sum a_n(t) \sin\left(n\frac{2\pi}{4x_1}x\right).$$

To satisfy these symmetry conditions n must be odd, and we get

$$H(x) = H_{00} + \sum a_{2m+1}(t) \sin\left((2m+1)\frac{\pi x}{2x_1}\right)$$

and $a_{2m+1}(0)$ from known $H(x)$ at $t = 0$, the time of complete penetration.
Recalling the differential equation, $H'' = \mu_0 \sigma \dot{H}$, with $n = 2m + 1$ we have

$$-a_n\left(\frac{n\pi}{2x_1}\right)^2 = \mu_0 \sigma \dot{a}_n,$$

$$\boxed{a_n(t) = a_n(0) \cdot e^{-\left(\frac{n\pi}{2x_1}\right)^2 \frac{t}{\mu_0 \sigma}},}$$

$$\boxed{a_{2m+1}(t) = a_{2m+1}(0) \cdot e^{-(2m+1)^2 \frac{\pi^2 t}{4x_1^2 \mu_0 \sigma}}.}$$

At $t = 0$:

$$H(x) = H_{00} - H_{00}\frac{\int_0^u e^{-u^2}du}{\int_0^{u_0} e^{-u^2}du} = H_{00}\left(1 - \frac{\int_0^{g\frac{x}{x_1}} e^{-u^2}du}{\int_0^g e^{-u^2}du}\right),$$

$$\boxed{-H_{00}\frac{\int_0^{g\frac{x}{x_1}} e^{-u^2}du}{\int_0^g e^{-u^2}du} = \sum a_{2m+1}(0) \sin\left((2m+1)\frac{\pi x}{2x_1}\right).}$$

To determine $a_{2m+1}(0)$ we let

$$a_n(0) \cdot \int_0^1 \sin^2\left(n\frac{\pi}{2}v\right)dv = -\frac{H_{00}}{\int_0^g e^{-u^2}du} \cdot \int_0^1 \underbrace{\left(\int_0^{gv} e^{-u^2}du\right)}_{\zeta} \underbrace{\sin\left(n\frac{\pi}{2}v\right)dv}_{d\eta},$$

with

$$\int_0^1 \sin^2\left(n\frac{\pi}{2}v\right)dv = \frac{1}{2}\int_0^1 (1 - \cos(n\pi v))dv = \frac{1}{2},$$

$$\zeta = \int_0^{gv} e^{-u^2}\,du, \quad \text{and} \quad d\zeta = ge^{-g^2v^2},$$

$$d\eta = \sin\left(n\frac{\pi}{2}v\right)dv, \quad \text{and} \quad \eta = -\frac{\cos\left(n\frac{\pi}{2}v\right)}{n\frac{\pi}{2}v},$$

$$\left(\int_0^1 \zeta d\eta\right)_{n=\text{odd}} = \frac{2g}{n\pi}\int_0^1 e^{-g^2v^2}\cos\left(n\frac{\pi}{2}v\right)dv.$$

Thus,

$$\boxed{a_{2m+1} = -H_{00}\cdot\frac{4}{(2m+1)\pi}\cdot\frac{\displaystyle\int_0^1 e^{-g^2v^2}\cos\left((2m+1)\frac{\pi}{2}v\right)dv}{\displaystyle\frac{1}{g}\int_0^g e^{-u^2}\,du}.}$$

One would let

$$\frac{1}{g}\int_0^g e^{-u^2}\,du = \int_0^1 e^{-g^2v^2}\,dv,$$

if one wants to evaluate it with the integral of the numerator. Otherwise, one may return to the definition of g and use

$$\frac{1}{g}\int_0^g e^{-u^2}\,du = \frac{re^{-g^2}}{2g}.$$

The total time required to get good magnetization is determined as follows:

(1) Time to reach $x = x_1$: $\quad t_1 = \mu_0\sigma(x_1^2/4)$.

(2) Time for a_1 to decay by a factor of e : $\quad t_2 = \mu_0\sigma x_1^2(4/\pi^2)$.

Thus,

$$\mu_0\sigma x_1^2\left(\frac{1}{4}+\frac{4}{\pi^2}\right) = \boxed{t_{\text{total}} \approx .65\mu_0\sigma x_1^2.}$$

(3) If time for a_1 to decay by e^π is used, $t_2 = \mu_0\sigma x_1^2(4/\pi)$, and

$$\mu_0\sigma x_1^2(0.25+1.27) = \boxed{t_{\text{total}} \approx 1.5\mu_0\sigma x_1^2.}$$

Change of Determinant for Small Changes of One Element of the Matrix that Describes a System that Is Least Squares Optimized with Restraints and Has Least Squares Limitations on Parameters

We let

$$\boxed{A = \begin{pmatrix} M^t W M + V & N^t \\ N & 0 \end{pmatrix}}$$

and consider only those terms linear in ΔM_{nm} or ΔN_{nm}.

1)

$$\Delta M_{ik} = \Delta M_{nm}\delta(i-n)\delta(k-m) \quad \text{with} \quad \Delta M_{nm} = a.$$

Here and below we sum over indices appearing more than once.

$$\begin{aligned}\left(M^t W M\right)_{ik} &= M_{li} W_{ll} M_{lk} \\ &\rightarrow \quad \left(M_{li} + a\delta(l-n)\delta(i-m)\right) W_{ll} \left(M_{lk} + a\delta(l-n)\delta(k-m)\right) \\ &= M_{li} W_{ll} M_{lk} + a W_{nn} \left(M_{ni}\delta(k-m) + M_{nk}\delta(i-m)\right) + a^2.\end{aligned}$$

To get $\| A + \Delta A \|$ to first order in a, one must differentiate $\| A + \Delta A \|$ with respect to a and then evaluate, knowing that A^{-1} is Hermitian.

$$\| A + \Delta A \| = \| A \| + a W_{nn} \cdot 2 M_{nk} K_{mk},$$

where K is the co-factor, and summation over k is done only over values consistent with the number of rows in M.

$$\boxed{\frac{\| A + \Delta A \|}{\| A \|} = 1 + \frac{\Delta M_{nm}}{M_{nm}} \cdot 2 W_{nn} M_{nm} \cdot \sum_k M_{nk} A^{-1}_{km}}$$

where $W_{nn} \sum_k M_{nk} A^{-1}_{km} = (A^{-1} M^t W)_{mn}$.

2)

$$\Delta N_{ik} = \Delta N_{nm}\delta(i-n)\delta(k-m),$$

$$\| A + \Delta A \| = \| A \| + 2\Delta N_{nm} K_{nm},$$

$$\boxed{\frac{\| A + \Delta A \|}{\| A \|} = 1 + \frac{\Delta N_{nm}}{N_{nm}} \cdot 2 N_{nm} A^{-1}_{mn}.}$$

November, 1968. Note 0072thry.

Sensitivity of Solution of Linear Equations to Change of an Individual Matrix Element

We let

$$MP = S, \quad M^{-1} = N \quad \text{and} \quad P = NS,$$

$$(M + \Delta M)(P + \Delta P) = M(I + A)(P + \Delta P) = S \quad \text{where} \quad A = N\Delta M,$$

$$P + \Delta P = (I + A)^{-1}P \quad \text{and} \quad \Delta P = \left((I + A)^{-1} - I\right) P.$$

Further

$$\Delta M_{nm} = a\delta(n - n_0)\delta(m - m_0) \quad \text{where} \quad a = \Delta M_{n_0 m_0},$$

$$A_{km} = N_{kn}\Delta M_{nm} = aN_{kn}\delta(n - n_0)\delta(m - m_0) = aN_{kn_0}\delta(m - m_0),$$

$$A^2_{km} = A_{ki}A_{im} = a^2 N_{kn_0}\delta(i - m_0)N_{in_0}\delta(m - m_0),$$

where $A^2 = aN_{m_0 n_0}A$, and we let $\alpha = aN_{m_0 n_0}$.

$$(I + A)^{-1} = I + \gamma A \quad \text{and} \quad (I + A)(I + \gamma A) = I + A(I + \gamma + \gamma\alpha) = I,$$

thus,

$$\boxed{\gamma = -\frac{1}{1 + \Delta M_{n_0 m_0} N_{m_0 n_0}}} \quad \text{with} \quad \boxed{\Delta M_{n_0 m_0} N_{m_0 n_0} \neq -1}$$

$$\boxed{\Delta P = \gamma A P}$$

$$\Delta P_k = \gamma A_{km} P_m = \gamma a N_{kn_0}\delta(m - m_0)P_m,$$

$$\boxed{\Delta P_k = -\frac{\Delta M_{n_0 m_0} P_{m_0}}{1 + \Delta M_{n_0 m_0} N_{m_0 n_0}} \cdot N_{kn_0}}$$

That the matrix M becomes exactly singular for $\Delta M_{n_0 m_0} = -1/N_{m_0 n_0}$ is easily shown with *Cramer's Rule*. Let K_{nm} be the co-factor to the nm element, and $\|M + \Delta M\| = \|M\| + \Delta M_{n_0 m_0} K_{m_0 n_0}$:

$$\Delta M_{n_0 m_0} \cdot \frac{K_{n_0 m_0}}{\|M\|} = \Delta M_{n_0 m_0} N_{m_0 n_0} = -1$$

which is the necessary condition for a singular matrix.

November, 1968. Note 0071thry.

This condition can easily be used to judge whether a matrix is "close" to being singular. One would test

$$\frac{M_{n_0 m_0}}{\Delta M_{n_0 m_0}} = -M_{n_0 m_0} N_{m_0 n_0}$$

and when the result is large compared to the inverse of the relative error of $M_{n_0 m_0}$, one is likely to be in trouble. This is of particular importance when the matrix elements are experimentally determined.

Fourier Analysis of Numerical Data

We assume that the spacing between data points is uniform, $2\pi/N$. Representing $F(\varphi)$ by a Fourier series with unknown coefficients and making the coefficients such that

$$\sum_{\varphi_n}\left(F(\varphi_n)-\sum_m a_m e^{im\varphi_n}\right)^2=\min$$

gives the same coefficients that one obtains by evaluating the integral

$$\int F(\varphi)e^{-im\varphi}d\varphi$$

with trapezoidal rule applied to the whole integrand:

$$a_m^*=\frac{1}{2\pi}\int F(\varphi)e^{im\varphi}d\varphi \quad\Longrightarrow\quad \frac{\Delta\varphi}{2\pi}\sum F(\varphi_n)e^{im\varphi_n}=\frac{1}{N}\sum F(\varphi_n)e^{im\varphi_n}.$$

A better way to integrate would be to assume that not the whole integrand changes linearly over an individual interval, but that only $F(\varphi)$ changes linearly over the interval.

For one interval,

$$\int F(\varphi)e^{i(m\varphi+\alpha)}d\varphi=\int(a+b\varphi)e^{i(m\varphi+\alpha)}d\varphi=(a+b\varphi)\frac{e^{i(m\varphi+\alpha)}}{im}+\frac{be^{i(m\varphi+\alpha)}}{m^2}.$$

When summing over the whole range of φ, the first term contributions cancel. With $b=(F_2-F_1)/\Delta\varphi$, we get

$$\begin{aligned}I&=\int_{\text{interval}}F(\varphi)e^{i(m\varphi+\alpha)}d\varphi\\&=\frac{F_2-F_1}{m^2\Delta\varphi}\left(e^{i(m\varphi_2+\alpha)}-e^{i(m\varphi_1+\alpha)}\right)\\&=\frac{F_2e^{i(m\varphi_2+\alpha)}\left(1-e^{-im\Delta\varphi}\right)-F_1e^{i(m\varphi_1+\alpha)}\left(e^{im\Delta\varphi}-1\right)}{m^2\Delta\varphi}.\end{aligned}$$

August, 1968. Note 0059thry.

When summing over the whole circle, we get:

$$\int_0^{2\pi} F(\varphi)e^{i(m\varphi+\alpha)}d\varphi = \sum \frac{F(\varphi_n)\left(1-e^{-im\Delta\varphi}-e^{im\Delta\varphi}+1\right)}{m^2\Delta\varphi}e^{i(m\varphi_n+\alpha)}$$

$$= \sum \frac{F(\varphi_n)4\sin^2\varepsilon}{m^2\Delta\varphi}e^{i(m\varphi_n+\alpha)} \quad \text{with} \quad \varepsilon = \frac{m\Delta\varphi}{2}$$

$$= \boxed{\left(\frac{\sin\varepsilon}{\varepsilon}\right)^2 \Delta\varphi \sum F(\varphi_n)e^{i(m\varphi_n+\alpha)}}$$

with

$$\frac{m\Delta\varphi}{2} = \boxed{\varepsilon = m\frac{\pi}{N}.}$$

A parabolic approximation for F over two intervals, $-\Delta\varphi \le \varphi \le \Delta\varphi$, without $e^{i\alpha}$, gives after some calculation:

$$\boxed{I_2 = \left(\frac{\sin^4\varepsilon}{\varepsilon^2} + \cos\varepsilon\left(\frac{\sin\varepsilon}{\varepsilon}\right)^3\right) \cdot \Delta\varphi \cdot \sum_n F(\varphi_n)e^{i(m\varphi_n+\alpha)}}$$

with $\varepsilon = m\pi/N$, and

$$\left(\frac{\sin^4\varepsilon}{\varepsilon^2} + \cos\varepsilon\left(\frac{\sin\varepsilon}{\varepsilon}\right)^3\right) = t = \left(\frac{\sin\varepsilon}{\varepsilon}\right)^2 \cdot \left(\sin^2\varepsilon + \cos\varepsilon\frac{\sin\varepsilon}{\varepsilon}\right).$$

Program to Calculate t, and Results.

```
5  CLS
10 FOR N=1 TO 18
15 E=N*3.14159265/36
20 PRINT ((SIN(E)/E)^2*((SIN(E))^2+COS(E)*SIN(E)/E)
30 NEXT N
```

For ε = N*5:

ε	5°	10°	15°	20°	25°	30°	35°	40°	45°
t	.9999	.9998	.9988	.9962	.9911	.9821	.9682	.9482	.9213

ε	50°	55°	60°	65°	70°	75°	80°	85°	90°
t	.8870	.8450	.7957	.7397	.6780	.6120	.5434	.4739	.4053

Program to Calculate K_1/ε^2 and K_2/ε^2, and Results.

```
5  CLS
10 FOR N=1 TO 18
20 E=N*3.14159265/36
30 PRINT N*5, (3+COS(4*E)-SIN(4*E)/E)/(4*E^2), (SIN(2*E)/(2*E)-COS(2*E))/(E^2)
40 NEXT N
```

ε	K_1/ε^2	K_2/ε^2
5°	.67069299	1.3292762
10°	.68235368	1.3171576
15°	.70042915	1.2971353
20°	.72300072	1.2694693
25°	.74761149	1.2345172
30°	.77147163	1.1927287
35°	.79169091	1.1446375
40°	.80551841	1.0908528
45°	.81056947	1.0320491
50°	.8050208	.96895504
55°	.78775796	.90234147
60°	.75866353	.83300908
65°	.71763969	.76177546
70°	.6665645	.68946226
75°	.60718709	.61688241
80°	.54197173	.54482766
85°	.47370526	.47405682
90°	.40528474	.40528474

Curvature of Field Lines in a Quadrupole

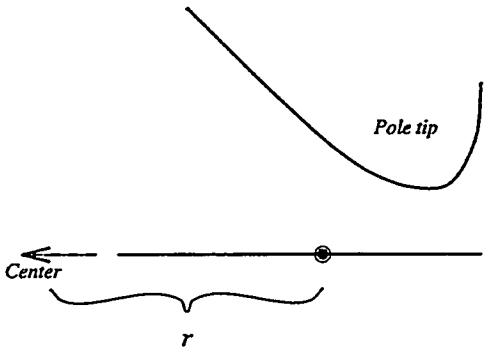

Figure 1.

$$F(z) = (z+r)^2 \quad \text{with} \quad r = 1/K.$$

The field line is described by $\Re(z+r)^2 = (x+r)^2 - y^2 = \text{constant}$, thus

$$(x+r)^2 - y^2 = (x_0+r)^2 \quad \rightarrow \quad x = -r + \sqrt{y^2 + (x_0+r)^2}.$$

Further, $1/R = x''/\left(1+(x')^2\right)^{3/2}$, with

$$x' = \frac{y}{\sqrt{y^2+(x_0+r)^2}} \quad \text{and} \quad x'' = \frac{(x_0+r)^2}{\left(y^2+(x_0+r)^2\right)^{3/2}}$$

$$1+(x')^2 = \frac{2y^2+(x_0+r)^2}{\sqrt{y^2+(x_0+r)^2}}, \quad \text{and} \quad \left(1+(x')^2\right)^{3/2} = \frac{\left(2y^2+(x_0+r)^2\right)^{3/2}}{\left(y^2+(x_0+r)^2\right)^{3/2}}.$$

Thus,

$$\frac{1}{R} = \frac{(x_0+r)^2}{\left(2y^2+(x_0+r)^2\right)^{3/2}} \quad \text{and} \quad \boxed{R = (x_0+r)\left(1+\frac{2y^2}{(x_0+r)^2}\right)^{3/2}}$$

for field line starting at x_0.

May, 1986. Note 0009thry.

The field line at x, y is described by

$$\frac{\left((x+r)^2+y^2\right)^{3/2}}{(x+r)^2-y^2} = \boxed{R = (x+r)\frac{\left(1+\left(\frac{y}{x+r}\right)^2\right)^{3/2}}{1-\left(\frac{y}{x+r}\right)^2}.}$$

We make the following substitutions:

$$\frac{y}{x+r} = \tan\alpha, \quad 1+\tan^2\alpha = \frac{1}{\cos^2\alpha}, \quad \text{and} \quad 1-\tan^2\alpha = \frac{\cos 2\alpha}{\cos^2\alpha},$$

and thus,

$$\boxed{R = \frac{(x+r)}{\cos\alpha\cos 2\alpha}.}$$

Also,

$$\sqrt{(x+r)^2+y^2}\left(\frac{1+\tan^2\alpha}{1-\tan^2\alpha}\right) = \boxed{R = \frac{\sqrt{(x+r)^2+y^2}}{\cos 2\alpha}.}$$

Skin Effect in Fe

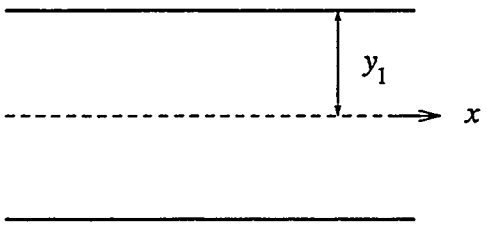

Figure 1.

We introduce initial conditions and definitions:

$$\mathbf{E} = \mathbf{e}_x E, \quad \text{and} \quad \mathbf{B} = \mathbf{e}_z B \quad \text{with} \quad B = \mu_0 \mu_{\text{rel}} H = \mu H,$$

$$\frac{\partial}{\partial z} = \frac{\partial}{\partial x} = 0, \quad \text{and} \quad \frac{\partial}{\partial y} \neq 0,$$

$$\nabla \times \mathbf{H} = H' = \sigma E = j, \quad \text{and} \quad \nabla \times \mathbf{E} = -E' = -i\omega\mu H,$$

$$\sigma E' = j' = i\omega\mu\sigma H.$$

We let $i\omega\mu\sigma = k^2$, and

$$H'' - k^2 H = 0, \quad \boxed{H = H_0 \cosh ky,} \quad \text{and} \quad \boxed{j = H_0 k \sinh ky.}$$

The average field in the sheet, $\overline{H}$, compared to the field outside, H_1, is given by

$$\overline{H} = \frac{1}{2y_1} \int_{-y_1}^{y_1} H\,dy = H_0 \frac{\sin ky_1}{ky_1}, \quad H_1 = H_0 \cosh ky_1, \quad \text{and} \quad H_0 = \frac{H_1}{\cosh ky_1},$$

$$\boxed{\frac{\overline{H}}{H_1} = \frac{\tanh ky_1}{ky_1}.} \tag{1}$$

In (1), we let $x = ky_1$, and solve

February, 1966. Note 0007thry.

$$\frac{\overline{H}}{H_1} = \frac{\tanh x}{x} \approx \frac{1 + x^2/6 + x^4/120}{1 + x^2/2 + x^4/24}$$
$$\approx \left(1 + \frac{x^2}{6} + \frac{x^4}{120}\right)\left(1 - \frac{x^2}{2} + \frac{5x^4}{24} + \cdots\right)$$
$$\approx \boxed{1 - \frac{1x^2}{3} + \frac{2x^4}{15}.} \qquad (2)$$

The power dissipation per cubic meter is given by

$$P = \frac{\varrho}{2}|j|^2 = \frac{1}{2}\varrho H_0^2 |k|^2 |\sinh^2 ky|.$$

We let $ky = \alpha + i\alpha$ where $\alpha = |k|/\sqrt{2}$ thus

$$\sinh(\alpha + i\alpha) = \sinh\alpha\cos\alpha + i\cosh\alpha\sin\alpha,$$

$$\begin{aligned} |\sinh(\alpha + i\alpha)|^2 &= \sinh^2\alpha\cos^2\alpha + \cosh^2\alpha\sin^2\alpha \\ &= \sinh^2\alpha\cdot(1 - \sin^2\alpha) + (1 - \sinh^2\alpha)\cdot\sin^2\alpha \\ &= \sinh^2\alpha + \sin^2\alpha \\ &= \frac{1}{2}(1 - \cos 2\alpha + \cosh 2\alpha - 1) \\ &= \frac{1}{2}(\cosh 2\alpha - \cos 2\alpha), \end{aligned}$$

and

$$\begin{aligned} \overline{|\sinh(\alpha + i\alpha)|^2} &= \frac{1}{2y_1}\int_0^{y_1}(\cosh 2\alpha - \cos 2\alpha)dy \\ &= \frac{1}{2\alpha_1}\int_0^{\alpha_1}(\cosh 2\alpha - \cos 2\alpha)d\alpha \\ &= \frac{1}{4\alpha_1}(\sinh 2\alpha_1 - \sin 2\alpha_1). \end{aligned}$$

Thus,

$$\boxed{\overline{P} = \frac{H_0^2\mu}{2}\cdot\omega\cdot\frac{\sinh 2\alpha_1 - \sin 2\alpha_1}{4\alpha_1}} \quad \text{with} \quad \alpha_1 = y_1\sqrt{\frac{\omega\mu\sigma}{2}}.$$

For

$$\frac{\sinh x - \sin x}{x} \approx \frac{2\cdot\left(\frac{x^3}{3!} + \frac{x^7}{7!}\right)}{x} = \frac{x^2}{3}\left(1 + \frac{x^4}{7!/3!}\right) = \frac{x^2}{3}\left(1 + \frac{x^4}{840}\right) \approx \frac{x^2}{3},$$

and thus,

$$\frac{\sinh 2\alpha_1 - \sin 2\alpha_1}{4\alpha_1} = \frac{(2\alpha_1)^2}{6} = \frac{(\sqrt{2}\gamma_1)^2}{6} = \frac{\gamma_1^2}{3}, \quad \text{with} \quad \gamma_1 = y_1\sqrt{\omega\mu\sigma} = \sqrt{2}\alpha_1.$$

Therefore,

$$\boxed{\overline{P} = \frac{H_0^2\mu}{2} \cdot \omega \cdot \frac{y_1^2\omega\mu\sigma}{3}.}$$

For $H_0\mu = B_0$,

$$\boxed{\overline{P} = \frac{B_0^2}{2} \cdot \frac{y_1^2\omega^2\sigma}{3} = \frac{B_0^2}{2} \cdot \frac{(2y_1)^2\omega^2\sigma}{12}.}$$

Resulting, thermally, in a trivial geometry:

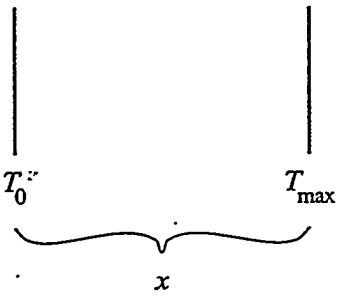

Figure 2.

For heat conductivity, $S = \lambda T'$ in power/m^2,

$$\Delta S(x) = \overline{P}\Delta x, \quad \text{and thus} \quad \overline{P} = S' = \lambda T'',$$

and thus,

$$\boxed{T_{\max} - T_0 = \frac{x^2\overline{P}}{2\lambda}.}$$

Typical Numbers for Dynamo Steel.

We let

$$\varrho = 46\mu\Omega\,\text{cm} = 4.6 \times 10^{-7}\Omega\,\text{m},$$

$$\mu(14\text{kG}) = 2100, \quad \text{and} \quad \mu(18\text{kG}) = 125,$$

$$\lambda = 27\text{–}36\ \frac{\text{BTU/h}}{\text{ft}\,^\circ F} \quad \text{with} \quad 1\ \frac{\text{BTU/h}}{\text{ft}\,^\circ F} = \frac{0.293}{1.84}\ \frac{\text{Watts}}{\text{m}\,^\circ C}$$
$$= 47.5\text{–}63.5\ \text{Watts/m}\,^\circ C.$$

(1) For $|x^2|/3 = 1/10$ we have

$$\frac{|x^2|}{3} = \frac{\omega\mu}{3\varrho}\cdot y_1^2 = \frac{1}{10}, \quad \text{and} \quad y_1 = \sqrt{\frac{0.3\varrho}{\omega\mu}} = 10^{-3}\sqrt{\frac{2.3}{16.8}} = 0.37\times 10^{-3}\text{m} = 0.37\text{mm},$$

$$\boxed{2y_1 = 0.74\text{mm}.}$$

(2) For $B_0 = 14$ kG =1.4T and the above $2y_1$,

$$\boxed{\overline{P} = \frac{60}{4.6}\times 10^3 = 13\times 10^3\text{Watts/m}^3 = 13\times 10^{-3}\text{Watts/cm}^3.}$$

(3) For $x = 0.4$m and the above $\overline{P}$,

$$\Delta T = \frac{(.16)(13\times 10^3)}{(2)(50)} = (13)(.16)^\circ C \approx 21^\circ C.$$

If the field is a sinusoidal function between $B = 0$T and 14kG, one has to use $B_0 = 7$kG.

A More Detailed Expression for $\overline{H}/H_1$.

With $2y_1 = D$, we let

$$x = \frac{kD}{2} = \frac{D}{2}\sqrt{i\omega\mu\sigma} = \frac{D}{2}\sqrt{2}\sqrt{i\frac{\omega\mu\sigma}{2}}.$$

With $\lambda = \sqrt{2/\omega\mu\sigma}$,

$$x = \sqrt{i}\frac{D}{\sqrt{2}\lambda} = \sqrt{i}\varepsilon, \quad \text{where} \quad \varepsilon = \frac{D}{\sqrt{2}\lambda}.$$

Therefore,

$$\frac{\overline{H}}{H_1} = 1 - i\frac{\varepsilon^2}{3} - \frac{2\varepsilon^4}{15} \quad \text{and} \quad \boxed{\tan\varphi \approx \frac{\varepsilon^2}{3} = \frac{(D/\lambda)^2}{6},}$$

$$\left|\frac{\overline{H}}{H_1}\right|^2 = 1 - \frac{7\varepsilon^4}{45}, \quad \text{and} \quad \left|\frac{\overline{H}}{H_1}\right| = 1 - \frac{7\varepsilon^4}{90},$$

and thus,

$$\boxed{\left|\frac{\overline{H}}{H_1}\right| = 1 - \frac{7}{(4)(90)}\frac{D^4}{\lambda}.}$$

Results for Al, Cu and Fe at 60Hz.

For Al and Cu, we let

$$\lambda = \sqrt{\frac{2\varrho}{\sigma\mu_0}} = \sqrt{\frac{10^4\varrho}{2.4}}.$$

$$\varrho_{\mathrm{Al}} = 2.8 \times 10^{-8} \quad \text{and} \quad \lambda_{\mathrm{Al}} = 1.08\mathrm{cm},$$

$$\varrho_{\mathrm{Cu}} = 1.7 \times 10^{-8} \quad \text{and} \quad \lambda_{\mathrm{Cu}} = 0.84\mathrm{cm},$$

and $D = (1/4)\mathrm{in} = 0.635\mathrm{cm}$:

	D/λ	$(D/\lambda)^2$	$(D/\lambda)^2/6$	$0.7\,(D^2/6\lambda^2)^2$
Cu	0.755	0.570	0.095	0.00635
Al	0.587	0.345	0.0575	.0023

For Fe with $\mu \approx 2000$,

$$\varrho_{\mathrm{Fe}} = 4.6 \times 10^{-7} \quad \text{and} \quad \lambda_{\mathrm{Fe}} \approx 1\mathrm{mm},$$

and $D = 14\mathrm{mm}$:

	D/λ	$(D/\lambda)^2$	$(D/\lambda)^2/6$	$0.7\,(D^2/6\lambda^2)^2$
Al	0.350	0.1225	0.0205	0.00029

Magnetic Field Energy Calculations

$$E = \frac{1}{2}\int (\mathbf{B}\cdot\mathbf{H})d\tau = \frac{1}{2}\int (\mathbf{B}\cdot\nabla V)d\tau = \frac{1}{2}\int \mathbf{H}\cdot(\nabla\times\mathbf{A})d\tau,$$

with

$$\mathbf{B}\cdot\nabla V = \nabla\cdot(V\mathbf{B}) - V\nabla\cdot\mathbf{B} = \nabla\cdot(V\mathbf{B}),$$
$$\mathbf{H}\cdot(\nabla\times\mathbf{A}) = \mathbf{A}\cdot(\nabla\times\mathbf{H}) = \mathbf{A}\cdot\mathbf{j}.$$

Field Energy in the Airspace of a Long, Symmetrical Bending Magnet.

The airspace is bounded by the midplane, an equipotential and two field lines (lines starting at two locations on the midplane).

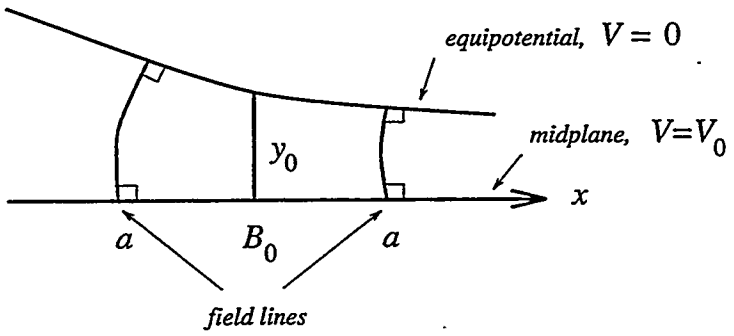

Figure 1.

Derive B from the potential: $\mathbf{B} = \nabla V$,

$$2\mu_0 E = \int (\mathbf{B}\cdot\nabla V)d\tau = \int \nabla\cdot(V\mathbf{B})d\tau = \int V\mathbf{B}\cdot d\sigma.$$

Normalize $V = 0$ on equipotential, then contribution on equipotential is 0, as well as being 0 along the field lines:

$$2\mu_0 E = LV_0\int B_y dx,$$

where L is the length of the magnet.

February, 1966. Note 0006thry.

For $B_y = B_0(1+Kx)$:

$$\int_{-a}^{a} B_y dx = 2aB_0, \quad \text{and} \quad V_y'|_{x=0} = B_y = B_0 \quad \Longrightarrow \quad V_0 = yB_0.$$

Thus,

$$2\mu_0 E = LB_0 y_0 2aB_0 \quad \Longrightarrow \quad \boxed{\frac{E}{L} = \frac{B_0^2}{2\mu_0} 2ay_0.}$$

y_0 equipotential is the hyperbola tangent to an ellipse with half-axis a:

$$y_0 = \frac{c}{r_0} = \frac{b}{r_0 a}\sqrt{(x+r_0)^3 x} = b\frac{r_0}{a}\sqrt{\frac{x}{r_0}\left(\frac{x}{r_0}+1\right)^3}.$$

For $a/r_0 = \varepsilon$,

$$s = \frac{x}{r_0} = \frac{2\varepsilon^2}{1+\sqrt{1+8\varepsilon^2}} = \frac{1}{4}\left(\sqrt{1+8\varepsilon^2}-1\right),$$

we redefine $y_0 = bF(\varepsilon)$, where

$$\boxed{F(\varepsilon) = \sqrt{\frac{s(s+1)^3}{\varepsilon^2}} = \sqrt{\frac{2}{1+\sqrt{1+8\varepsilon^2}}\left(\frac{3+\sqrt{1+8\varepsilon^2}}{4}\right)^3}.}$$

For $8\varepsilon^2 \ll 1$:

$$\sqrt{1+8\varepsilon^2} = 1+4\varepsilon^2.$$

$$F^2(\varepsilon) = \frac{2}{2+4\varepsilon^2}\left(\frac{4+4\varepsilon^2}{4}\right)^3 = (1-2\varepsilon^2)(1+3\varepsilon^2),$$

$$\boxed{F(\varepsilon) = 1+\varepsilon^2/2.}$$

For $\varepsilon = 1/2$, $F(1/2) = 1.2$, while if $\varepsilon = 1$, $F(1) = 1.3$.

Magnetic Energy of 2D Vacuum Field Inside Arbitrary Boundary.

Represent **B** by scalar potential: $\mathbf{B} = \nabla V$,

$$2\mu_0 E = \int (\mathbf{B} \cdot \nabla V) d\tau = \int \nabla \cdot (V\mathbf{B}) d\tau = \int V (\mathbf{B} \cdot d\boldsymbol{\sigma}) .$$

The expression for scalar product of two vectors in 2-dimensional space, when vectors are expressed by the complex numbers $a = a_x + ia_y$ and $b = b_x + ib_y$, is

$$\mathbf{a} \cdot \mathbf{b} = a_x b_x + a_y b_y = \Re a b^* = \Re a^* b.$$

Thus, for $d\boldsymbol{\sigma} = iLdz$:

$$\boxed{2\mu_0 E/L = \Re \int V i B^* dz.}$$

For $V = v$, and $iB^* = F'$:

$$2\mu_0 E/L = \Re \int v F' dz = \Re \int v dF = \Re \int v(du + idv)$$
$$= \boxed{\int v du = \int v(u'_x + u'_y y') dx.}$$

Special Case.

The energy of field derived from $F = (B_0 K/2)(z + r_0)^2$, with $r_0 = 1/K$, inside the ellipse described by $(x/a)^2 + (y/b)^2 = 1$, is given by

$$F = \frac{1}{2} B_0 K \left((x + r_0)^2 - y^2 + 2iy(x + r_0) \right) .$$

With

$$u'_x = B_0 K(x + r_0), \quad u'_y = -B_0 K y, \quad v = B_0 K y (x + r_0), \quad y' = -\frac{b^2}{a^2}\frac{x}{y},$$

and

$$x = a \sin\varphi, \quad dx = a \cos\varphi d\varphi, \quad y = b\sqrt{1 - (x/a)^2} = b \cos\varphi,$$

and $a/r_0 = \varepsilon$,

$$
\begin{aligned}
2\mu_0 E/L &= B_0^2 K^2 \int y(x+r_0)\left(x + r_0 + y\frac{b^2 x}{a^2 y}\right) dx \\
&= B_0^2 K^2 \int (x+r_0)\left(r_0 + x\left(1+\frac{b^2}{a^2}\right)\right) y dx \\
&= B_0^2 ab \int_0^{2\pi} (1+\varepsilon\sin\varphi)\left(1+\varepsilon\sin\varphi\left(1+\frac{b^2}{a^2}\right)\right)\cos^2\varphi d\varphi \\
&= B_0^2 ab \int_0^{2\pi} \left(1+\varepsilon\sin\varphi\left(2+\frac{b^2}{a^2}\right)+\varepsilon^2\sin^2\varphi\left(1+\frac{b^2}{a^2}\right)\right)\cos^2\varphi d\varphi \\
&= B_0^2 ab\left(\pi + 0 + \varepsilon^2\frac{\pi}{4}\left(1+\frac{b^2}{a^2}\right)\right) \\
&= \boxed{B_0^2 ab\pi\left(1+\frac{a^2+b^2}{4r_0^2}\right).}
\end{aligned}
$$

Scalar Potential for 3D Fields in "Business Region" of Insertion Device with Finite Width Poles

Task.

In the absence of random errors, we are interested in the formulation of 3-dimensional $V(x,y,z)$ (with $\nabla^2 V = 0$) for $\mathbf{B}$ in the "business region" of an insertion device (hybrid or electro-magnetic) with finite width poles, and containing only a small number of free, easily measured constants.

Notation and Coordinate System.

The beam will be in the direction of the z-axis. The midplane will be in the xz-plane. The field will be in the y-direction in the midplane.

Field Symmetries.

B_y will be the even function of x,y and B_x will be the odd function of x,y.

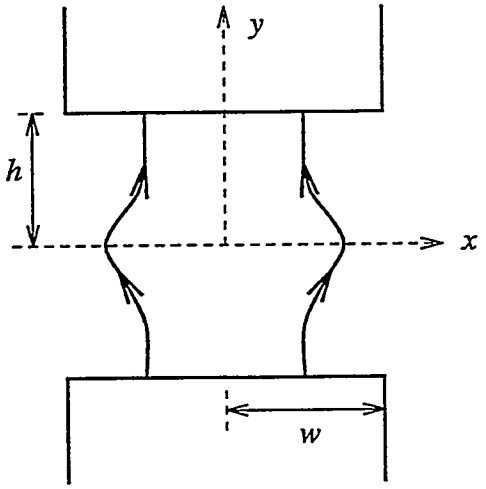

Figure 1.

Representation of $V(x,y,z)$.

We represent $V(x,y,z)$ by a Fourier series in z:

$$V(x,y,z) = \sum_{n=\text{odd}} \cos nk_3 z \cdot G_n(x,y) \quad \text{with} \quad k_3 = 2\pi/\lambda, \tag{1}$$

where

$$\nabla^2 = 0 \quad \Longrightarrow \quad \nabla^2 G_n = n^2 k_3^2 G_n. \tag{2}$$

February, 1992. Note 0144u-w.

For an infinitely wide pole:

$$\partial G_n/\partial x = 0 \quad \Longrightarrow \quad G_n(x,y) = a_n \sinh nk_3 y,$$

which is a standard 2D solution. The effect of the finite width pole is described by

$$G_n = a_n \sinh nk_3 y + g_n(x,y),$$

where g_n is the effect of the finite width pole. Thus

$$\nabla^2 g_n = n^2 k_3^2 g_n. \tag{3}$$

Case 1:

$$\mu_{\mathrm{Fe}} = \infty \quad \Longrightarrow \quad B_x(x, \pm h, u\lambda/2) = 0 \tag{4}$$

where u is an integer.

1.1) We initially assume that

$$G_n = g_n = 0 \quad \text{for} \quad n > 1$$

and we see that the symmetries and (4) give $g'_{1x}(x,0) = g'_{1x}(x,\pm h) = 0$. We expand $g'_{1x}(x,y)$ in a Fourier series in y with a $2h$ period, and see that

$$g'_{1x}(x,y) = b'_m(x) \sin mk_2 y \quad \text{with} \quad k_2 = \pi/h. \tag{5}$$

We now substitute (5) into (3). We have $b'''_m = b'_m(m^2k_2^2 + n^2k_3^2)$, with $n = 1$. A solution which satisfies this equation and the symmetries is given by

$$b_m(x) = c_m \cosh k_{nm} x, \quad \text{where} \quad k_{nm} = (m^2k_2^2 + n^2k_3^2)^{1/2}. \tag{6}$$

A complete solution is given by

$$V(x,y,z) = \cos k_3 z \cdot a_0 \left(\sinh k_3 y + \sum_{m=1} \sin mk_2 y \cosh k_{1m} x \cdot \frac{a_m}{\cosh k_{1m} w} \right). \tag{7}$$

c_m is chosen such that a_m can be expected to be only weakly dependent on w.

1.2) We now assume that

$$G_n = g_n \neq 0 \quad \text{for} \quad n \geq 1.$$

(7) can be generalized, but one must realize that the resulting formula does not have the same force of logic that was inherent in its original derivation. This generalized

formula allows the possibility that contributions from many n could combine to make $B_x(x, \pm h, u\lambda/2) = 0$.

$$V(x,y,z) = \sum_{n=\text{odd}} \cos nk_3 z \cdot G_n(x,y)$$

$$G_n(x,y) = A_{n0}\left(\sinh nk_3 y + \sum_{m=1} \sin mk_2 y \cosh k_{nm} x \cdot \frac{a_{nm}}{\cosh k_{nm} w}\right) \tag{8}$$

$$k_{nm} = (n^2 k_3^2 + m^2 k_2^2)^{1/2} \quad \text{with} \quad k_3 = 2\pi/\lambda \quad \text{and} \quad k_2 = \pi/h.$$

Notice that in the above set of equations A_{n0} has units of Tesla-meters and a_{nm} is dimensionless.

We expect that a_{nm} is of the first order, the finite width effects decrease with increasing n and m, and further, that only a few a_{nm} are needed.

Case 2:

$$\mu_{\text{Fe}} < \infty \quad \Longrightarrow \quad B_x(x, \pm h, u\lambda/2) = -B_x(-x, \pm h, u\lambda/2) \neq 0. \tag{9}$$

The contributions from Fe alone are given by the addition of $Q_n(x,y)$:

$$V = \sum \cos nk_3 z \cdot Q_n(x,y) \quad \text{where} \quad \nabla^2 Q_n = n^2 k_3^2 Q_n.$$

For the sake of simplification, we shall look at one Q_n, normalize lengths so that $nk_3 = 1$, and denormalize at the end

$$\nabla^2 Q = Q. \tag{10}$$

We follow the logic of **Case 1** as well as also satisfying $Q'_y(x,0) \approx x^2$ for sufficiently small x. Thus, we start with

$$Q(x,y) = (\cosh \eta x - 1)P_1(y) + P_2(y), \tag{11}$$

where η is real and arbitrary. Later we will let $\eta \to 0$. We substitute (11) into (10) and get

$$\begin{aligned} \nabla^2 Q &= \eta^2 c P_1 + (c-1)P_1'' + P_2'' \\ &= Q \\ &= (c-1)P_1 + P_2. \end{aligned}$$

where $c = \cosh \eta x$ and P_1, P_2 are unknown. Separating into terms with and without

c, we have

$$\eta^2 P_1 + P_1'' = P_1, \quad P_2'' - P_1'' = P_2 - P_1, \tag{12}$$

$$p^2 = 1 - \eta^2, \quad P_1'' - p^2 P_1 = 0 \quad \Longrightarrow \quad P_1 = \sinh py, \tag{13}$$

$$P_2'' - P_2 = P_1'' - P_1 = -\eta^2 P_1 = -\eta^2 \sinh py,$$

$$P_2 = \sinh py - p \sinh y, \tag{14}$$

in which the second term serves to satisfy the condition $P_{2y}'(0) = 0$.

$$Q(x,y) = (\cosh \eta x - 1) \sinh py + \sinh py - p \sinh y, \tag{15}$$

with $\eta \to 0$ and $p \to (1 - \eta^2/2)$.

$$Q(x,y) = \frac{\eta^2}{2}(x^2 \sinh y - y \cosh y + \sinh y). \tag{16}$$

We denormalize (16) and drop $\eta^2/2$ and get

$$Q_n(x,y) = (nk_3 x)^2 \sinh nk_3 y - nk_3 y \cosh nk_3 y + \sinh nk_3 y, \tag{17}$$

$$V(x,y,z) = \sum_{n=\text{odd}} \cos nk_3 z (G_n(x,y) + Q_n(x,y)). \tag{18}$$

Magnetic Measurements.

First, the simplest implementation consists of measuring the Fourier coefficients of the expansion of B_z, B_y, B_x in $\sin nkz$ and $\cos nkz$ and determining the value of the free coefficients in G_n and Q_n that best fit the data. Use a "filter" to remove the random errors from the data sets.

Second, choose x, y very carefully for each of these sets of measurements in order to take advantage of the properties of $G_n(x,y)$ and $Q_n(x,y)$ and its derivatives with respect to x, y. This is particularly important for the contributions originating from $\sin mk_2 y$ in $G_n(x,y)$.

Third, investigate suitability of less conventional magnetic measurements, like a Hall probe or flux loop that vibrates in the x-direction, with phase sensitive de-modulation.

Use of Model.

After verification of the validity region of the model is completed, it can be used for trajectory calculations. Furthermore, one can use this model to determine the maximal narrowness of the pole before detrimental effects become intolerable.

In application to existing hardware, one can break up the total field into the ideal 3D field and the random errors.

Magnetic Measurement and Data Reduction to Identify Some Specific Error Field Consequences

Measurement of Steering in Wigglers and Undulators.

Prefer null measurement method, if it can be done.

In "body" of wiggler or undulator: use coil with length equal to the product of period and integer.

In the end-region, from the field-free region to the periodic part: measure using long coil reaching from the outside to the periodic part, together with an attached compensation coil in the periodic part. This gives a signal that depends only on the steering integral, and is independent of position in the periodic part. It is an important tool for correcting the ends.

Normalized sensitivity of system, for $\varphi = kz = 2\pi z/\lambda$ is given by

$$S(\varphi) = S_0(\varphi) + S_1(\varphi),$$

where S_0 refers to the main coil, and S_1 to the compensation coil. With $\varphi = 0$ referring to the end of the main coil, and $\varphi = -\alpha$ to the center of the correction coil (of length $2\varphi_1$) relative to the end of the main coil, we have, in the coil coordinate system,

$$\begin{aligned} &S_0(\varphi) = 1 \text{ at } -\infty \le \varphi \le 0, \\ &S_0(\varphi) = 0 \text{ at } 0 \le \varphi, \\ &S_1(\varphi) = \varepsilon \text{ at } -\alpha - \varphi_1 \le \varphi \le -\alpha + \varphi_1, \\ &S_1(\varphi) = 0 \text{ at } \varphi \text{ outside the above region.} \end{aligned}$$

For the periodic region, $\varphi > 0$ and

$$B = \sum_{n=\text{odd}} n a_n \cos n\varphi = \Re \sum n a_n e^{in\varphi},$$

with the end of main coil at $\varphi_0 > \pi$ in the field coordinate system, the signal from the main coil is

$$F_0 = \int_{-\infty}^{0} B d\varphi + \int_{0}^{\varphi_0} \Re \sum n a_n e^{in\varphi} d\varphi = \text{Steering} \int + \Re \sum a_n \left(e^{in\varphi_0} - 1\right)/i,$$

and similarly, the signal from the compensating coil is

$$F_1 = \varepsilon \int_{\varphi_0-\alpha-\varphi_1}^{\varphi_0-\alpha+\varphi_1} \sum n a_n e^{in\varphi} d\varphi = \Re \sum a_n e^{in(\varphi_0-\alpha)} 2\varepsilon \sin\varphi_1,$$

September, 1993. Note 0142u-w.
Presented at the ID Measurement Workshop, ANL, September, 1993.

$$F_0 - F_1 = \text{Steering} \int + \Re \sum a_n e^{in\varphi_0} \left(\frac{1}{i} - 2\varepsilon e^{-in\alpha} \sin n\varphi_1 \right).$$

We want $F_0 - F_1$ independent of φ_0, thus

$$2\varepsilon \sin n\alpha \sin n\varphi_1 = 1, \quad \text{and} \quad 2\varepsilon \cos n\alpha \cos n\varphi_1 = 0.$$

When harmonics are weak (undulator), we need to satisfy these conditions only for $n = 1$, but when strong harmonics are present (wiggler), we need to satisfy them for all odd n: to get

$\cos n\alpha = 0$ choose $\boxed{\alpha = \pi/2,}$

$\sin n\alpha = (-1)^{(n-1)/2}$ choose $\boxed{\varphi_1 = \pi/2,}$ $\varepsilon = 1/2.$

$\varphi_1 = \pi/2$ needs to be done by hardware, $\alpha = \pi/2$, $\varepsilon = 1/2$, can be done by "tuning" if one provides for it. Other solutions should be obvious.

This scheme can also be implemented with simple coil (or Hall probes) and software. However, software implementation is *not* a null method and therefore suffers much more from equipment imperfections.

Phase Shifts of Emitted Light Due to Error Fields.

This is one of a number of ways to develop more insight into why or how synchrotron light properties deteriorate because of error fields.

We make the following definitions:

$$x'' = \frac{g}{\gamma} B, \quad \text{with} \quad g = \frac{e}{m_0 c},$$

$$' = \frac{\partial}{\partial z}, \quad \varphi = kz, \quad \text{and} \quad k = \frac{2\pi}{\lambda}.$$

For the reference trajectory:

$$B(\varphi) = B_0 \cos \varphi,$$

$$x_0' = \frac{gB_0}{\gamma k} \sin \varphi = \frac{K}{\gamma} \sin \varphi, \quad \text{with} \quad \frac{gB_0}{k} = K = .934 \cdot B_0(\text{T}) \cdot \lambda(\text{cm}),$$

$$x_0 = -\frac{K}{k\gamma} \cos \varphi,$$

$$\boxed{x_W = \frac{K}{k\gamma}.}$$

We define the trajectory length error as

$$\begin{aligned}\Delta s &= \int_{-\infty} \left(\sqrt{1+(x_0'+\Delta x')^2} - \sqrt{1+x_0'^2}\right) dz \\ &= \int \left(x_0'\Delta x' + \frac{1}{2}\Delta x'^2\right) dz \\ &= x_0\Delta x' - \int x_0 \Delta x'' dz + \frac{1}{2}\int \Delta x'^2 dz.\end{aligned}$$

For $D = \Delta B/B_0$ as a function of φ:

$$\Delta x'' = \frac{gB_0}{\gamma}\frac{\Delta B}{B_0} = \frac{gB_0}{\gamma}D = \frac{Kk}{\gamma}D,$$

$$\Delta x' = \frac{K}{\gamma}\int D d\varphi.$$

Thus,

$$\Delta s = \left(\frac{K}{\gamma}\right)^2 \frac{1}{k}\left(-\cos\varphi \int D d\varphi + \int \cos\varphi D d\varphi + \frac{1}{2}\int \left(\int D d\varphi\right)^2 d\varphi\right),$$

With $\Delta t = \Delta s/c$, $\Delta\Phi = \omega_L \Delta t = \Delta s \omega_L/c = \Delta s k_L$, and

$$\lambda_L = \frac{\lambda}{2\gamma^2}\left(1+\frac{K^2}{2}\right) = \frac{\lambda K^2}{4\gamma^2}\left(1+\frac{2}{K^2}\right),$$

$$\boxed{\Delta\Phi = P\left(\underbrace{-\cos\varphi \int D d\varphi}_{(G_1)} + \underbrace{\int \cos\varphi D d\varphi}_{(G_2)} + \underbrace{\frac{1}{2}\int \left(\int D d\varphi\right)^2 d\varphi}_{(G_3)}\right),}$$

where

$$P = \frac{4}{1+2/K^2}.$$

Notice that, as a function of K, $\Delta\Phi \approx K^2$ for $K^2 \ll 2$, and $\Delta\Phi$ is independent of K^2 for $K^2 \gg 2$. G_1 produces harmonics and reduces the intensity of the fundamental, but only if steering is not 0. The $G_2 \neq 0$ contribution depends on symmetry of D, not on the presence or absence of steering. In G_3 only steering errors contribute and it always gives $\Delta\Phi$ of the same sign. G_3 being of second order, we may expect a significant contribution only for a long undulator. We will see below that G_3 can be surprisingly large even for a short undulator.

We present order of magnitude estimates for $\overline{G_2^2}, \overline{G_3^2}$, for the ensemble.

For G_2 from one primary source:

$$G_2 = \varepsilon_2 D_2 \frac{\lambda}{2} \frac{2\pi}{\lambda} = \varepsilon_2 D_2 \pi.$$

For n_2 sources per period: after $N_1 = z/\lambda$ periods

$$\overline{G_2^2} = \overline{(\varepsilon_2 D_2 \pi)^2} n_2 \frac{z}{\lambda} = \overline{D_2^2} \pi^2 \varepsilon_2^2 n_2 \frac{z}{\lambda}.$$

Without $\cos\varphi$ in the integrand, we may expect from steering:

$$\overline{G_0^2} = \overline{D_0^2} \pi^2 \varepsilon_0^2 n_0 \frac{z}{\lambda} = \overline{D_0^2} \pi^2 \varepsilon_0^2 n_0 N_1.$$

$$\overline{G_3} = \frac{1}{2} \overline{D_0^2} \pi^2 \varepsilon_0^2 n_0 \int_0^{L=N_1\lambda} \frac{z}{\lambda} dz \frac{2\pi}{\lambda} = \frac{1}{2} \overline{D_0^2} \pi^3 \varepsilon_0^2 n_0 N_1^2.$$

$$\varepsilon_4 = \frac{\overline{G_3}}{\sqrt{\overline{G_2^2}}} = \frac{\overline{D_0^2} \pi^3 \varepsilon_0^2 n_0 N_1^2/2}{\sqrt{\overline{D_2^2}} \pi \varepsilon_2 \sqrt{n_2} \sqrt{N_1}} = \frac{\varepsilon_0^2 n_0 \overline{D_0^2}}{\sqrt{\varepsilon_2 n_2 \overline{D_2^2}}} \frac{\pi^2}{2} N_1^{3/2}.$$

To get a feeling for the order of magnitude, we assume that the first order term, $\sqrt{\overline{G_2^2}}$, contributes twice the contribution of the second order term, $\overline{G_3}$, i.e. $\varepsilon_4 = 1/2$, and further, $\varepsilon_0 = \varepsilon_2 = 1$ $n_0 = n_2 = 4$, $N_1 = 10^2$ $\overline{D_0^2} = \overline{D_2^2}$, then

$$\sqrt{\overline{D_0^2}} = \frac{1}{20 \times 10^3} = 5 \times 10^{-5}$$

has to be satisfied. And for $\sqrt{\overline{D_0^2}} = 10^{-3}$, $\varepsilon_0 = 1$, $n_0 = 4$, $N_1 = 10^2$,

$$\Delta\Phi = .6 \text{ radians}.$$

$\Delta\Phi$ over-estimates the damage done to the emitted light because $\Delta\Phi = a + bz$ causes no real damage. We subtract the straight line from the original $\Delta\Phi(z) = f(z)$, and

then normalize the length of the undulator to 1:

$$H = \int_0^1 (a + bz - f(z))^2 dz$$

and minimize H with a, b,

$$\int f(z)dz = F_0, \quad \int zf(z)dz = F_1, \quad \text{and} \quad \int f^2(z)dz = F_2.$$

The solution gives

$$\boxed{a = 2(2F_0 - 3F_1),} \quad \text{and} \quad \boxed{b = 6(2F_1 - F_0),}$$

and this gives

$$\boxed{H = F_2 - 4(F_0^2 + 3F_1(F_1 - F_0)).}$$

For a specific function $f(z) = u\sqrt{z} + vz^2$, corresponding to the ensemble model used above, and after optimization (see Appendix A for details),

$$H = \left(\frac{1}{180}\right)\frac{2u^2}{5} - \frac{8uv}{7} + v^2,$$

With $\alpha = v/u$, we get the following improvement factor:

$$\frac{H}{F_2} = \left(\frac{1}{36}\right)\frac{\alpha^2 - 8\alpha/7 + 2/5}{\alpha^2 + 20\alpha/7 + 5/2}.$$

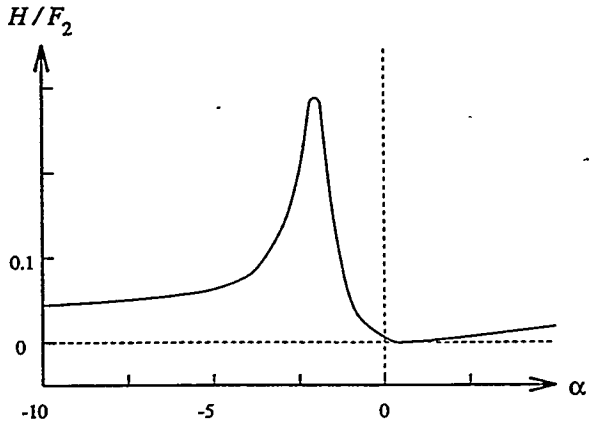

Figure 1.

For Figure 1,

$$(H/F_2)_{\min} = 4.5 \times 10^{-4} \qquad \text{at } \alpha = .605,$$

$$(H/F_2)_{\max} = .274 \qquad \text{at } \alpha = -1.65,$$

Even if one does not consider the model of $f(z) = u\sqrt{z} + vz^2$ a realistic one, it is quite clear that (a) one should optimize not $\Delta\Phi(z)$, but $\Delta\Phi(z)$ minus "best" straight line, and that (b) gains can be remarkable. In other words, the quality of the light generated may be much better than one would think if one were to only look at $\Delta\Phi(z)$ or $D(z)$. We make a trivial, but interesting observation: since H (before or after subtraction of straight line) is a quadratic function of u, v, an *increase* in the G_2 or G_3 contribution may lead to a *decrease* of H.

For the measurement of $G_2 = \int \cos\varphi D d\varphi$, consider the following 2-coil configuration:

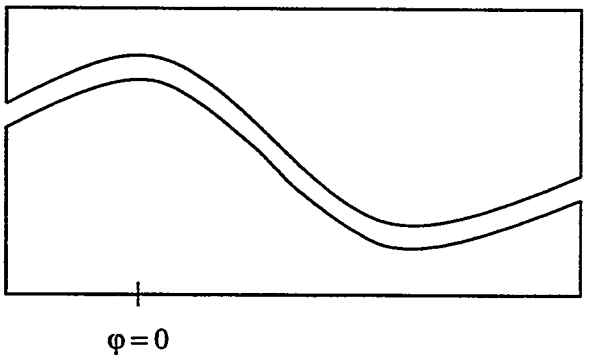

Figure 2.

The above design will measure the integral over $\cos\varphi \cdot B(\varphi)$. But, $\cos\varphi \cdot B_0 \cos\varphi$ gives a large signal, therefore the null-coil system is needed. The proposed system cancels $B_0 \cos\varphi$ but also "sees" steering; thus, it is fine only if steering is small enough or known. Therefore, we give below only the basic design and performance equations for system components, and one system.

Since $\Delta\Phi$ is only relevant for undulator, we ignore the harmonics.

The compensation coil is the same for measurement of steering at ends.

The main coil sensitivity is $S_0 = \cos(\alpha_0+\varphi)$ at $-\varphi_2 \le \varphi \le \varphi_2$, and $S_0 = 0$ outside this region. At the center of the coil, sensitivity is $\cos\alpha_0$, and $B = \cos\varphi_0 = \Re e^{i\varphi_0} = B$.

$$F_0 = \Re \int_{-\varphi_2}^{\varphi_2} e^{i(\varphi_0+\varphi)} \cos(\alpha_0+\varphi) d\varphi$$

$$= \frac{1}{2}\Re e^{i\varphi_0} \int_{-\varphi_2}^{\varphi_2} \left(e^{i\alpha_0} e^{2i\varphi} + e^{-i\alpha_0}\right) d\varphi$$

$$= \boxed{\frac{1}{2}\Re e^{i\varphi_0} \left(e^{i\alpha_0} \sin 2\varphi_2 + e^{-i\alpha_0} 2\varphi_2\right).}$$

The compensation coil sensitivity is $S_1(\varphi) = \varepsilon_1$ at $-\varphi_1 \le \varphi \le \varphi_1$, and $S_1(\varphi) = 0$ outside this region. At the center of the coil, $B = \cos(\varphi_0 + \beta) = \Re e^{i(\varphi_0+\beta)}$.

$$F_1 = \Re\varepsilon \int_{-\varphi_1}^{\varphi_1} e^{i(\varphi_0+\beta+\alpha)} d\varphi$$

$$= \boxed{2\varepsilon_1 \Re e^{i(\varphi_0+\beta)} - \sin\varphi_1.}$$

With $\varepsilon = 4\varepsilon_1 \sin\varphi_1$ and $2\varphi_2 = \gamma$,

$$F_0 + F_1 = \frac{1}{2}\Re e^{i\varphi_0}\left(e^{i\alpha_0}\sin\gamma + e^{-i\alpha_0}\gamma + \varepsilon e^{i\beta}\right).$$

To get no signal for all φ_0, we must satisfy

$$\cos\alpha_0(\sin\gamma + \gamma) = -\varepsilon\cos\beta, \quad \text{and} \quad \sin\alpha_0(\sin\gamma - \gamma) = -\varepsilon\sin\beta,$$

and since there are four parameters to satisfy two equations there are many possible solutions. We pick one with $\beta = 0$ and $\alpha_0 = 0$ and have

$$\varepsilon = 4\varepsilon_1 \sin\varphi_1 = -(\gamma + \sin\gamma), \quad \boxed{\varepsilon_1 = -\frac{2\varphi_2 + \sin 2\varphi_2}{4\sin\varphi_1}.}$$

If $|\varepsilon_1| > 1$, we can use a combined coil system as follows, with $\varphi_2 = \varphi_1 = 3\pi/2$ and therefore $\varepsilon_1 = 3\pi/4$.

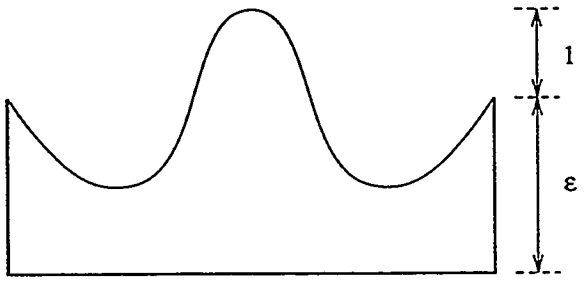

Figure 2.

This is not the ultimate answer, but only a first step, and it may start similar thinking on other issues.

Appendix A.

For the execution of the optimization of H, we let

$$a + b/2 = F_0, \quad 2F_1 - F_0 = b/3, \quad a/2 + b/3 = F_1,$$

$$\boxed{b = 6(2F_1 - F_0)} \quad \boxed{a = 2(2F_0 - 3F_1).}$$

With the above, we have

$$\begin{aligned} H &= a^2 + b^2/3 + F_2 - 2aF_0 - 2bF_1 + ab \\ &= a\underbrace{(a + b/2)}_{F_0} + b\underbrace{(b/3 + a/2)}_{F_1} + F_2 - 2aF_0 - 2bF_1 \\ &= F_2 - aF_0 - bF_1 \\ &= F_2 - 2F_0(2F_0 - 3F_1) - 6F_1(2F_1 - F_0) \\ &= \boxed{F_2 - 4F_0^2 - 12F_1^2 + 12F_0F_1.} \end{aligned}$$

For the special case of $f(z) = \sqrt{z} + \alpha z^2$:

$$F_0 = 2/3 + \alpha/3 = (\alpha + 2)/3, \quad \text{and} \quad F_1 = 2/5 + \alpha/4,$$

and for $f^2(z) = z + \alpha^2 z^4 + 2\alpha z^{2.5}$, $F_2 = \frac{1}{2} + \frac{\alpha^2}{5} + \frac{4\alpha}{7}$. Therefore,

$$\begin{aligned} F_2 - H &= \frac{4}{9}(\alpha + 2)^2 + 12\left(\frac{\alpha}{4} + \frac{2}{5}\right)^2 - 4(\alpha + 2)\left(\frac{\alpha}{4} + \frac{2}{5}\right) \\ &= \frac{7\alpha^2}{36} + \frac{26\alpha}{45} + \frac{112}{225}, \end{aligned}$$

$$\begin{aligned} H &= \alpha^2\left(\frac{1}{5} - \frac{7}{36}\right) + \alpha\left(\frac{4}{7} - \frac{26}{45}\right) + \frac{1}{2} - \frac{112}{225} \\ &= \boxed{\frac{1}{180}\left(\alpha^2 - \frac{8\alpha}{7} + \frac{2}{5}\right)} = \boxed{\frac{1}{180}\left(v^2 - \frac{8uv}{7} + \frac{2u^2}{5}\right).} \end{aligned}$$

$$\boxed{\frac{H}{F_2} = \frac{1}{36}\frac{\alpha^2 - 8\alpha/7 + 2/5}{\alpha^2 + 20\alpha/7 + 5/2}.}$$

Least Square Fit of $f(z)$ with $a+bz$ in $0 \le z \le 1$

Origin and Purpose of Study. If $f(z)$ = phase shift, the difference between $f(z)$ and $a+bz$ is the only damaging property of $f(z)$ since a would be an irrelevant shift of phase reference, and b represents a shift of center of line without any broadening.

We define

$$S = \int (a + bz - f(z))^2 dz.$$

For $S'_a = 0$: $\quad a + b/2 = F_0 = \int f(z)dz,$
For $S'_b = 0$: $\quad a/2 + b/3 = F_1 = \int z f(z)dz.$

Therefore,

$$\boxed{b = 12F_1 - 6F_0} \quad \text{and} \quad \boxed{a = 4F_0 - 6F_1.}$$

For $\int f(z)^2 dz = F_2$,

$$\begin{aligned} S &= a^2 + b^2/3 + F_2 + ab - 2aF_0 - 2bF_1 \\ &= a(a + b/2) + b(a/2 + b/3) - 2aF_0 - 2bF_1 + F_2 \\ &= F_2 - aF_0 - bF_1 \\ &= F_2 - F_0(4F_0 - 6F_1) - F_1(12F_1 - 6F_0) \\ &= \boxed{F_2 - 4(F_0^2 + 3F_1^2 - 3F_0F_1).} \end{aligned}$$

For a specific function, $f(z) = \sqrt{z} + \alpha z^2$,

$$f(z)^2 = z + 2\alpha z^{5/2} + \alpha^2 z^4,$$

$$F_0 = \frac{2}{3} + \frac{\alpha}{3}, \quad F_1 = \frac{2}{5} + \frac{\alpha}{4}, \quad \text{and} \quad F_2 = \frac{1}{2} + \frac{4\alpha}{7} + \frac{\alpha^2}{5},$$

thus,

$$\begin{aligned} S &= \frac{\alpha^2}{5} + \frac{4\alpha}{7} + \frac{1}{2} - 4\left(\frac{1}{9}(\alpha^2 + 4\alpha + 4) + 3\left(\frac{\alpha^2}{16} + \frac{\alpha}{5} + \frac{4}{25}\right) - (\alpha + 2)\left(\frac{\alpha}{4} + \frac{2}{5}\right)\right) \\ &= \alpha^2\left(\frac{1}{180}\right) - \alpha\left(\frac{2}{315}\right) + \frac{1}{450} \\ &= \alpha^2 a_2 + \alpha a_1 + a_0 \end{aligned}$$

with

$$a_2 = \frac{1}{180}, \quad a_1 = -\frac{2}{315}, \quad \text{and} \quad a_0 = \frac{1}{450},$$

August, 1993. Note 0141u-w.

therefore,

$$\boxed{S = \frac{1}{180}\left(\alpha^2 - \frac{8\alpha}{7} + \frac{2}{5}\right),}$$

$$\boxed{\frac{S}{F_2} = \frac{1}{36} \cdot \frac{\alpha^2 - \frac{8\alpha}{7} + \frac{2}{5}}{\alpha^2 + \frac{20\alpha}{7} + \frac{5}{2}}.}$$

For $\alpha \gg 1$, $\sqrt{S/F_2}$ is improved by a factor of 6, and for $\alpha \ll 1$, $\sqrt{S/F_2}$ is improved by a factor of 15.

S/F_2 is a strongly peaked function:

$(S/F_2)_{max} \approx .274$ at $\alpha \approx -1.65$,
$S/F_2 \approx .125$ at $\alpha \approx -3$,
$S/F_2 \approx .004$ at $\alpha \approx 0$.
$(S/F_2)_{min} \approx 4.5 \times 10^{-4}$ at $\alpha \approx .605$,

Since $a + bz$ represents the error-free condition, looking at the deviation of phase shift from the straight line may represent the best way to characterize the consequences of the error fields.

$$S_{min} = \frac{1}{180}\left(\frac{2}{5} - \frac{16}{49}\right) = \frac{1}{50 \cdot 49} \quad \text{with} \quad \alpha = \frac{4}{7},$$

and the values for a, b are

$$a = 4F_0 - 6F_1 = \frac{4}{3}(\alpha + 2) - 6\left(\frac{\alpha}{4} + \frac{2}{5}\right) = \boxed{-\frac{\alpha}{6} + \frac{4}{15},}$$

$$b = 12F_1 - 6F_0 = 3\left(\alpha + \frac{8}{5}\right) - 2(\alpha - 2) = \boxed{\alpha + \frac{4}{5}.}$$

Normalizations Factors ε_1 and ε_2 for Comparison of First and Second Order Phase Shifts, with Analytical Model of $b(z)$

At the center

$$\Delta B = b(0)$$
$$= \frac{V_1}{h}\frac{1}{k_0(x_2-x_1)}\ln\frac{\cosh k_0 x_2 + 1}{\cosh k_0 x_1 + 1}$$
$$= \boxed{\frac{V_1}{h}\cdot\underbrace{\frac{\left(\ln\dfrac{\sinh k_0 x_2/2}{\sinh k_0 x_1/2}\right)}{\left(\dfrac{k_0(x_2-x_1)}{2}\right)}}_{g_0},}$$

with $k_0 = \pi/h$ and $k_1 = 2\pi/\lambda$. Further,

$$\int b(z)\cos(k_1 z)k_1 dz = \frac{V_1}{h}\cdot\frac{2}{\pi}\cdot k_1\cdot\frac{2\pi}{k_0}\cdot\int_{x_1}^{x_2}\frac{\sin k_1 x}{\sinh(\pi k_1/k_0)}\cdot\frac{dx}{x_2-x_1}$$
$$= \boxed{\frac{V_1}{h}\cdot\underbrace{\frac{4k_1}{k_0}\cdot\frac{\sin(k_1\Delta x/2)/(k_1\Delta x/2)}{\sinh(\pi k_1/k_0)}}_{g_1},}$$

$$\boxed{\frac{V_1}{h} = \frac{\Delta B}{g_0},}$$

$$\boxed{\int b(z)\cos(k_1 z)k_1 dz = \frac{\Delta B}{g_0}g_1,}$$

$$\boxed{\int b\,dz = \frac{V_1}{h}\cdot\frac{\lambda}{2}} = \frac{\Delta B\cdot\lambda/2}{g_0}.$$

Thus,

$$\int\frac{\Delta B}{B_0}k_1 dz = \varepsilon_2\pi\frac{\Delta B}{B_0} = \frac{\Delta B}{B_0}\frac{\lambda/2}{g_0}\frac{2\pi}{\lambda},$$

August, 1993. Note 0140u-w.

$$\boxed{\varepsilon_2 = \frac{1}{g_0}.}$$

Similarly,

$$\frac{1}{B_0}\int b\cos(k_1 z)k_1 dz = \frac{\Delta B}{B_0}\frac{g_1}{g_0} = \varepsilon_1 \pi \frac{\Delta B}{B_0},$$

$$\boxed{\varepsilon_1 = \frac{g_1}{\pi g_0}.}$$

Thus,

$$\boxed{\frac{\varepsilon_1}{\varepsilon_2^2} = \frac{g_0 g_1}{\pi},}$$

and

$$\frac{g_0 g_1}{\pi} = \frac{4}{\pi}\cdot \ln\left(\frac{\sinh k_0 x_2/2}{\sinh k_0 x_1/2}\right)\cdot \frac{\sin(k_1\Delta x/2)}{\sinh(\pi k_1/k_0)}\cdot \frac{(k_1/k_0)^2}{(k_1\Delta x/2)^2}.$$

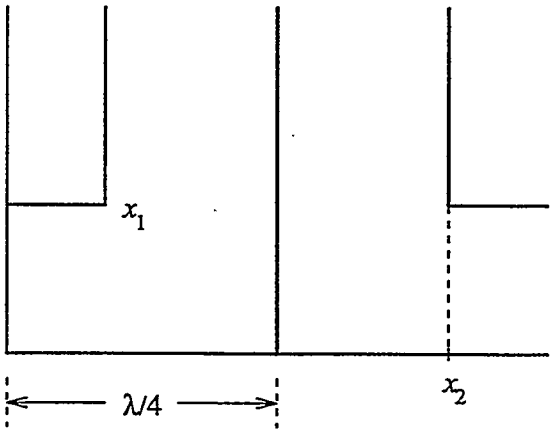

Figure 1.

For the above figure,

$$x_1 + \frac{1}{2}(x_2 - x_1) = \frac{\lambda}{4} = \frac{x_1 + x_2}{2},$$

$$\frac{\lambda/4}{x_1} = 3, \quad \boxed{x_1 = \frac{\lambda}{12},}$$

$$x_2 = \frac{\lambda}{2} - x_1 = \lambda\frac{5}{12}.$$

Further,

$$k_1\frac{\Delta x}{2}=\frac{2\pi}{\lambda}\cdot\frac{1}{2}\cdot\frac{4\lambda}{12}=\boxed{\frac{\pi}{3},}$$

$$k_0\frac{x_2}{2}=\frac{\pi}{h}\cdot\frac{5\lambda}{24}=\boxed{\frac{\lambda}{h}\cdot\frac{5\pi}{24},}$$

$$k_0\frac{x_1}{2}=\frac{\pi}{h}\cdot\frac{\lambda}{24}=\boxed{\frac{\lambda}{h}\cdot\frac{\pi}{24},}$$

$$\frac{k_1}{k_0}=\frac{2h}{\lambda},\quad \frac{\lambda}{h}=a.$$

Thus,

$$\frac{g_0g_1}{\pi}=\frac{36\cdot 4}{\pi^3}\cdot\frac{\sqrt{3}}{2}\cdot\ln\left(\frac{e^{a5\pi/12}-1}{e^{a\pi/12}-1}\right)\cdot\frac{1}{a^2}\cdot\frac{1}{\sinh(2\pi/a)},$$

where for $\dfrac{2h}{\lambda}=b=\dfrac{2}{a}$, and $a=\dfrac{2}{b}$,

$$\frac{g_0g_1}{\pi}=\frac{36\sqrt{3}}{\pi^3}\cdot b^2\cdot\ln\left(\frac{e^{5\pi/6b}-1}{e^{\pi/6b}-1}\right)\cdot\frac{1}{2\sinh(\pi b)}.$$

Comparison of First and Second Order Contributions of Error Fields to Phase Shift

We introduce, for $kz = \varphi$, $kdz = d\varphi$, and $\frac{\Delta B}{B_0} = D$,[†]

$$\Delta\Phi = P\left(\underbrace{-\cos\varphi\int Dd\varphi}_{(A_1)} + \underbrace{\int\cos\varphi Dd\varphi}_{(B_1)} + \underbrace{\frac{1}{2}\int\left(\int Dd\varphi\right)^2 d\varphi}_{(B_2)}\right),$$

where

$$P = \frac{4}{1+2/K^2}.$$

Notice that $\Delta\Phi \approx K^2$ for $K^2 \ll 2$, and $\Delta\Phi$ is independent of K^2 for $K^2 \gg 2$.
We denote the "typical" case of B_1 as

$$B_1 = \varepsilon_1 D\frac{\lambda}{2}\frac{2\pi}{\lambda} = \varepsilon_1\pi D.$$

At every error source, B_1 changes by the above "typical" value of B_1[‡]. We assume n contributions per period. After $N = z/\lambda$ periods, the total expectation value is

$$\overline{B_1^2} = n\frac{z}{\lambda}\overline{(\varepsilon_1\pi D)^2}.$$

When

$$B_1 = \int Dd\varphi,$$

we expect

$$\overline{B_1^2} = n\frac{z}{\lambda}\overline{(\varepsilon_2\pi D)^2}.$$

At the end of insertion device with N periods we expect

$$\langle B_1^2\rangle = \varepsilon_1^2\pi^2\overline{D^2}nN,$$

August, 1993. Note 0139u-w.

† See document 0138u-w for the origins of this equation.

‡ See document 0140u-w for derivations of ε_1 and ε_2.

$$\begin{aligned}\langle B_2\rangle &= \frac{1}{2}\varepsilon_2^2\pi^2\overline{D^2}n\frac{(N\lambda)^2}{2\lambda}\frac{2\pi}{\lambda}\\ &= \frac{1}{2}\varepsilon_2^2\pi^3\overline{D^2}nN^2\\ &= \varepsilon_3\sqrt{\langle B_1^2\rangle} \quad \text{with} \quad \varepsilon_3 < 1.\end{aligned}$$

This means that

$$\frac{1}{2}\varepsilon_2^2\pi^3\overline{D^2}nN^2 = \varepsilon_3\varepsilon_1\pi\sqrt{\overline{D^2}}\sqrt{n}\sqrt{N},$$

$$\boxed{\sqrt{\overline{D^2}} = \frac{2\varepsilon_3\varepsilon_1/\varepsilon_2^2}{\pi^2\sqrt{n}\left(\sqrt{N}\right)^3}.}$$

We make the following definitions:

$$\varepsilon_1 = \varepsilon_2 = 1, \quad 2\varepsilon_3 = 1, \quad n = 4 \quad \text{and} \quad N = 81.$$

Thus,

$$\sqrt{\overline{D^2}} \approx \frac{1}{20\times 10^3} \approx 5\times 10^5.$$

This means that the second order contributions will dominate. Or, similarly

$$\varepsilon_3 = \frac{\pi^2}{2}\frac{\varepsilon_2^2}{\varepsilon_1}\sqrt{\overline{D^2}}\sqrt{n}\left(\sqrt{N}\right)^3,$$

and for $\sqrt{\overline{D^2}} = 10^{-3}$,

$$\varepsilon_3 \approx 5\times 2\times 10^{-3+}\times 10^3 \approx 10$$

still demonstrating that second order contributions will dominate.

The magnitude of the $\Delta\Phi$ shift along the length of the insertion device with second order contributions is

$$\begin{aligned}\Delta\Phi &= 4\frac{1}{2}\varepsilon_2^2\pi^3\overline{D^2}nN^2\\ &\approx 2\times 30\times 10^{-6}\times 4\times 6.5\times 10^3\\ &\approx 30\times 50\times 10^{-3}\\ &\approx 1.5 \text{ radians.}\end{aligned}$$

Thus,

$$\frac{\varepsilon_1}{\varepsilon_2^2} \approx .5 \rightarrow D$$

for equal contributions (i.e.: $\varepsilon_3 = 1$), and for

$$D \approx 5\times 10^{-5} \rightarrow D \approx 5\times 10^{-3} \rightarrow \alpha = 100$$

for representation of phase shift by straight line.

Connection Between Undulator Field Errors and Optical Phase

We begin with the following definitions:

$$x'' = \frac{g}{\gamma}B \quad \text{and} \quad g = \frac{e}{m_0 c}.$$

We introduce the following references:

$$B(z) = B_0 \cos kz,$$

$$x_0' = \frac{gB_0}{\gamma k}\sin kz = \frac{K}{\gamma}\sin kz \quad \text{with} \quad \frac{gB_0}{k} = K,$$

$$x_0 = -\frac{K}{k\gamma}\cos kz,$$

$$\boxed{x_W = \frac{K}{k\gamma}.}$$

We now proceed with the analysis.

$$\Delta s = \int \left(\sqrt{1+(x_0'+\Delta x')^2} - \sqrt{1+(x_0')^2}\right) dz = \int \left(x_0'\Delta x' + \frac{1}{2}\Delta(x')^2\right) dz.$$

By integration by parts, with $du = x_0' dz$, $u = x_0$, $v = \Delta x'$, and $dv = \Delta x'' dz$,

$$\Delta s = x_0 \Delta x' - \int x_0 \Delta x'' dz + \frac{1}{2}\int \Delta(x')^2 dz,$$

with

$$\Delta x' = \frac{gB_0}{\gamma k}\int \frac{\Delta B}{B_0} k dz \quad \text{and} \quad \Delta x'' = \frac{gB_0}{\gamma}\frac{\Delta B}{B_0},$$

where $gB_0/\gamma k = K/\gamma$, and thus

$$\Delta s = \frac{K^2}{\gamma^2 k}\left(-\cos kz \int \frac{\Delta B}{B_0} k dz + \int \cos(kz)\frac{\Delta B}{B_0} k dz + \frac{1}{2}\int \left(\int \frac{\Delta B}{B_0} k dz\right)^2 k dz\right).$$

Furthermore,

$$\Delta t = \frac{\Delta s}{c},$$

August, 1993. Note 0138u-w.

$$\Delta\varphi = \omega\Delta t = \Delta s\frac{\omega}{c} = \Delta s \cdot k_L,$$

where,

$$\lambda_L = \frac{\lambda}{2\gamma^2}\left(1+\frac{K^2}{2}\right),$$

$$k_L = k\frac{4\gamma^2}{K^2\left(1+\frac{2}{K^2}\right)},$$

and therefore,

$$\Delta\varphi = P\left(\underbrace{-\cos kz\int\frac{\Delta B}{B_0}kdz}_{(a)} + \underbrace{\int\cos(kz)\frac{\Delta B}{B_0}kdz}_{(b)} + \underbrace{\frac{1}{2}\int\left(\int\frac{\Delta B}{B_0}kdz\right)^2 kdz}_{(c)}\right),$$

with

$$P = \frac{4}{1+2/K^2}.$$

Term (c) is of second order and is important only for a long insertion device. Term (a) gives harmonics and reduces line intensity for steering errors, but produces no effect if there is no steering. Term (b) produces phase shift and line broadening. Whether or not it is equal 0 depends on such elements as symmetry, but not on presence of net steering.

ϱ, A_0/B_1 for Hybrid Insertion Device

This note is a result of ANL lecture notes, and from *Simple Analytical Model For Fields From One Pole Of Hybrid Insertion Device*,† with $k_1 = 2\pi/\lambda$ and $k_n = nk_1$, and

$$\boxed{B(x) = \sum_{n=\text{odd}} B_n \cos k_n x,}$$

from poles with $\pm$ "1", and

$$\boxed{B_n = \frac{2}{\pi} \int_{-\infty}^{\infty} b(x) \cos k_n x \, dk_1 x,}$$

where $b(x)$ is the field from one pole with excitation $+1$.

For V from 0 to V_1 at the edge of pole going from $-x_1$ to x_1,

$$\boxed{B_n = 4\frac{k_1}{k_0} \frac{\sin k_n x_1}{\sinh(\pi k_n/k_0)} \frac{V_1}{h}} \quad \text{with} \quad k_0 = \pi/h.$$

For V going linearly from 0 to V_1 over thickness of CSEM $= (x_2 - x_1)/2$, we have

$$\boxed{A_0 = \int_{-\infty}^{\infty} b(x)dx = \frac{V_1}{h}\frac{\lambda}{2},}$$

$$\boxed{B_n = 4\frac{k_1}{k_0}\frac{V_1}{h}\frac{\sin(k_n(x_2 - x_1)/2)}{(k_n(x_2 - x_1)/2)}\frac{1}{\sinh(\pi k_n/k_0)}.}$$

For $k_1(x_2 - x_1)^2/6 \ll 1$,

$$\boxed{B_1 = 4\frac{k_1}{k_0}\frac{V_1}{h}\frac{1}{\sinh(\pi k_1/k_0)} = \frac{4}{\pi}\frac{V_1}{h}\frac{\alpha}{\sinh\alpha}} \quad \text{with} \quad \alpha = \pi\frac{k_1}{k_0} = 2\pi\frac{h}{\lambda} = \pi\frac{g}{\lambda}.$$

We may now conclude that

$$\boxed{\frac{A_0}{B_1} = \lambda\frac{\pi}{8}\frac{\sinh\alpha}{\alpha}.}$$

August, 1993. Note 0137u-w.

† Document 0136u-w

For

$$\varrho = \frac{A_0}{\int_{-\lambda/4}^{\lambda/4} B_1 \cos k_1 x \, dx} = \frac{B_1 \lambda \frac{\pi}{8} \frac{\sinh \alpha}{\alpha}}{B_1(2/k_1)} = \frac{k_1 \lambda \pi}{16} \frac{\sinh \alpha}{\alpha} = \frac{\pi^2}{8} \frac{\sinh \alpha}{\alpha},$$

we have

ϱ	1.5	2.0	2.5	3.0	4.0	5.0
g/λ	.35	.57	.70	.79	.94	1.05

Simple Analytical Model for Fields from One Pole of Hybrid Insertion Device

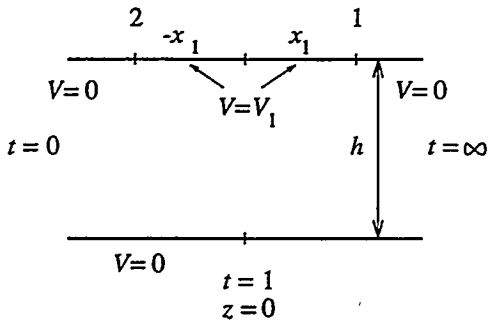

Figure 1.

Model: midplane on $V = 0$, and pole from $-\infty$ to $+\infty$ on $V = 0$, except on $V = V_1$ for $-x_1 \le x \le x_1$.

The above geometry is described by the following conformal map

$$\pi \dot{z} = \frac{h}{t},$$

and the following elements

$$k_0 z = \ln t, \quad t = e^{k_0 z} \quad \text{and} \quad k_0 = \frac{\pi}{h},$$

and where x_1 is the half-width of the pole. Putting $\pm$ current filaments at $x = \pm x_1$,

$$\pi F = V_1 \ln \frac{(t - t_1)}{(t - t_2)},$$

$$\begin{aligned} F' &= \frac{V_1}{h}\left(\frac{t}{t - t_1} - \frac{t}{t - t_2}\right) \\ &= \frac{V_1}{h}\left(\frac{1}{t/t_1 - 1} - \frac{1}{t/t_2 - 1}\right). \end{aligned}$$

where $t = e^{k_0 z}$, $t_1 = e^{k_0(x_1 + ih)} = -e^{k_0 x_1}$. Thus,

---

August, 1993. Note 0136u-w.

$$F'\frac{h}{V_1} = \frac{1}{e^{k_0(z+x_1)}+1} - \frac{1}{e^{k_0(z-x_1)}+1}$$
$$= -\frac{e^{k_0 z}\left(e^{k_0 x_1} - e^{-k_0 x_1}\right)}{e^{2k_0 z}+1+e^{k_0 z}\left(e^{k_0 x_1}+e^{-k_0 x_1}\right)}$$
$$= \boxed{-\frac{\sinh k_0 x_1}{\cosh k_0 z + \cosh k_0 x_1}} = -b(z). \tag{1}$$

The odd harmonics of the field are described by

$$B_N = a\int_{-\infty}^{\infty} b(x)\cos(Nk_1 x)dx, \tag{2}$$

where $N = 2n+1$, $k_N = k_1 N = k_1(2n+1)$, $k_1 = 2\pi/\lambda$, and a is a constant, thus

$$\frac{B_N}{a} = \sinh k_0 x_1 \int_{-\infty}^{\infty} \frac{\cos(k_N x)dx}{\cosh k_0 x + \cosh k_0 x_1}$$
$$= \sinh k_0 x_1 \cdot G_N, \tag{3}$$

$$G_N = \Re\int_{-\infty}^{\infty} \frac{e^{ik_N x}}{\cosh k_0 x + \cosh k_0 x_1}dx, \tag{4}$$

That is, to evaluate this integral, one can integrate a line integral along the real axis of the complex z-plane, and close it at ∞ in the upper half-plane without changing its value.

There are singularities at $\cosh k_0 z = -\cosh k_0 x_1$ in the upper half-plane, with $k_0 z = \pm k_0 x_1 + i\pi(2m+1)$, for $m = 0, 1, 2, \ldots$. We take the first singularity at $k_0 z = +k_0 x_1 + i\pi M$ and do others later by replacing x_1 by $-x_1$. We integrate over the upper half-plane:

$$
\begin{aligned}
G_{N+} &= \Re \int \frac{e^{ik_N z}dz}{\cosh k_0 z + \cosh k_0 x_1} \\
&= \Re \sum_{m=0} \frac{e^{ik_N(x_1+i\pi M/k_0)}}{k_0 \sinh k_0 z_m} \cdot 2\pi i \\
&= +\frac{2\pi}{k_0} \cdot \frac{\sin k_N x_1}{\sinh k_0 x_1} \cdot \sum_{m=0} e^{-\pi(k_N/k_0)(2m+1)} \\
&= +\frac{2\pi}{k_0} \cdot \frac{\sin k_N x_1}{\sinh k_0 x_1} \cdot \frac{e^{-\pi k_N/k_0}}{1-e^{-2\pi k_N/k_0}} \\
&= +\frac{2\pi}{k_0} \cdot \frac{\sin k_N x_1}{\sinh k_0 x_1} \cdot \frac{1}{2\sinh(\pi k_N/k_0)} \\
&= \frac{\pi}{k_0} \cdot \frac{\sin k_N x_1}{\sinh k_0 x_1} \cdot \frac{1}{\sinh(\pi k_N/k_0)}.
\end{aligned}
$$

One solves for G_{N-} similarly. Thus, we may re-write (3),

$$
\frac{B_N}{a} = \frac{2\pi}{k_0} \cdot \frac{\sin k_N x_1}{\sinh(\pi k_N/k_0)}, \tag{5}
$$

and further,

$$
\boxed{\frac{B_{(2n+1)}}{B_1} = \frac{\sin(k_1(2n+1)x_1)}{\sinh((\pi k_1/k_0)(2n+1))} \cdot \frac{\sinh(\pi k_1/k_0)}{\sin(k_1 x_1)},} \tag{6}
$$

$$
\text{with} \quad k_0 = \frac{\pi}{h}, \quad k_1 = \frac{2\pi}{\lambda}, \quad \text{and thus} \quad \pi\frac{k_1}{k_0} = 2\pi\frac{h}{\lambda}.
$$

This model of $b(z)$, and the resultant B_N, assume that the potential increases like a step function at the edge of the pole. As a next approximation, to improve this model, one would assume that the potential increases linearly over the size of the CSEM and represent this by the operation

$$
\frac{1}{x_2 - x_1} \int_{x_1}^{x_2} dx_1,
$$

which is easily executed on both $b(z)$ and B_N. For $b(z)$ we have

$$
\int \frac{\sinh k_0 x_1}{\cosh k_0 z + \cosh k_0 x_1} \cdot \frac{dx_1}{(x_2 - x_1)} = \frac{1}{k_0(x_2 - x_1)} \ln \frac{\cosh k_0 z + \cosh k_0 x_2}{\cosh k_0 z + \cosh k_0 x_1}, \tag{7}
$$

and for B_N we have

$$\int \sin(Nk_1x_1)\frac{dx_1}{(x_2-x_1)} = \frac{\cos Nk_1x_1 - \cos Nk_1x_2}{Nk_1(x_2-x_1)}$$

$$= -\sin\left((2n+1)k_1\frac{x_2+x_1}{2}\right)\frac{\sin\left((2n+1)k_1\dfrac{x_2-x_1}{2}\right)}{\dfrac{(2n+1)}{k_1}\cdot\dfrac{x_2-x_1}{2}} \quad (8)$$

where

$$-\sin\left(k_1(2n+1)\left(\frac{x_2+x_1}{2}\right)\right) = (-1)^{n+1},$$

$$\frac{x_2+x_1}{2} = \frac{\lambda}{4} \quad \text{and} \quad (2n+1)k_1\frac{x_2-x_1}{2} = \frac{\pi}{2} + n\pi.$$

The argument of the log function can, and should be, operated on in the same manner, such that for

$$\cosh k_0 z = C_0, \quad \cosh k_0 x_1 = C_1, \quad \text{and} \quad \cosh k_0 x_2 = C_2,$$

$$\frac{C_0+C_2}{C_0+C_1} = \frac{C_0+a+b}{C_0+a-b} = \frac{1+\dfrac{b}{C_0+a}}{1-\dfrac{b}{C_0+a}}$$

where

$$a = \frac{C_2+C_1}{2}, \quad b = \frac{C_2-C_1}{2}, \quad \text{and} \quad \ln\frac{H\varepsilon}{1-\varepsilon} = 2\left(\varepsilon + \frac{\varepsilon^3}{3} + 10\right).$$

Wiggler Parameter K Definitions

For $v = c$ we have

$$m_0 \gamma v^2 x'' = evB = evA',$$

$$x' = \frac{1}{\gamma}\frac{e}{m_0 v}A \quad \text{and} \quad x'_{\max} = \frac{K_1}{\gamma}.$$

Definition 1:

$$\boxed{K_1 = \frac{e}{m_0 c}A_{\max} = \frac{e}{2\pi m_0 c}2\pi A_{\max}.}$$

For a pure sinusoidal field we have

$$B = B_0 \sin kz \quad \text{and} \quad A = \frac{B_0}{k}\cos kz\,.$$

Thus

$$A_{\max} = \frac{B_0}{k} \quad \Longrightarrow \quad \boxed{K_1 = \frac{e}{2\pi m_0 c}B_0 \lambda_u\,.}$$

Definition 2:

The "path length" slippage in λ_u equals λ_{light}. (We shall refer to λ_{light} as λ_{L} for the remainder of this document.)

$$\Delta t = \frac{s}{c\beta} - \frac{\lambda_u}{c} = \frac{\lambda_{\text{L}}}{c} \quad \text{and thus} \quad \lambda_{\text{L}} = \lambda_u\left(\frac{s}{\lambda_u \beta} - 1\right)$$

where $s =$ path length over one period, and $s' = \sqrt{1 + x'^2}$.

Proceeding from above, we now have that

$$\frac{\lambda_{\text{L}}}{\lambda_u} = \frac{1}{\beta\lambda_u}\int_0^{\lambda_u}\left(1 + \frac{x'^2}{2}\right)dz - 1$$

$$= \frac{1}{\beta} - 1 + \frac{1}{2\lambda_u}\int_0^{\lambda_u} x'^2\,dz\,.$$

June, 1993. Note 0135u-w.

By introducing

$$\beta^2 + \frac{1}{\gamma^2} = 1 \quad \text{and thus} \quad \beta^{-1} = \left(1 - \frac{1}{\gamma^2}\right)^{-1/2} = 1 + \frac{1}{2\gamma^2},$$

we further simplify

$$\begin{aligned}\frac{\lambda_L}{\lambda_u} &= \frac{1}{2\gamma^2} + \frac{1}{2\lambda_u}\int_0^{\lambda_u} x'^2 dz \\ &= \frac{1}{2\gamma^2}\left(1 + \underbrace{\left(\frac{e}{m_0 c}\right)^2 \frac{\int_0^{\lambda_u} A^2 dz}{\lambda_u}}_{K_2^2/2}\right).\end{aligned}$$

and we now arrive at our definition

$$\boxed{K_2^2 = \left(\frac{e}{m_0 c}\right)^2 \frac{2}{\lambda_u}\int_0^{\lambda_u} A^2 dz\,.}$$

For $A = \dfrac{B_0}{k}\cos kz$ we have

$$K_2^2 = \left(\frac{e}{m_0 c}\right)^2 \frac{2}{\lambda_u}\frac{B_0^2}{k^2}\frac{\lambda_u}{2} = \left(\frac{e}{2\pi m_0 c} B_0 \lambda_u\right)^2$$

where $(e/2\pi m_0 c) = .934 \cdot 10^2$ in SI units.

We define $(2\pi m_0 c/e) = A_e$ and thus $1/A_e = .934 \cdot 10^2$ MKS.
We now reformulate our **Definitions 1** and **2** such that

$$\boxed{K_1 = \frac{2\pi}{A_e} A_{\max}}$$

and

$$\boxed{K_2 = \frac{2\pi}{A_e}\sqrt{\frac{2\int_0^{\lambda_u/4} A^2 dz}{\lambda_u/4}}\,.}$$

Definition 3:

$$K_3 = \frac{B_0 \lambda_u}{A_e} = \frac{V_0}{A_e}\, 4\frac{\lambda_u/4}{D_4}\,.$$

Where D_4 refers to the NPOLE1.BAS program variable which describes the distance factor in the transformation from scalar potential to the field.

NPOLE

A recreation, with "Korea modification," of a program (for HP71B) to design and analyze $\lambda/4$ of hybrid insertion device.

We will begin by establishing some background information for the conformal map and the limits for t_1 and t_2.

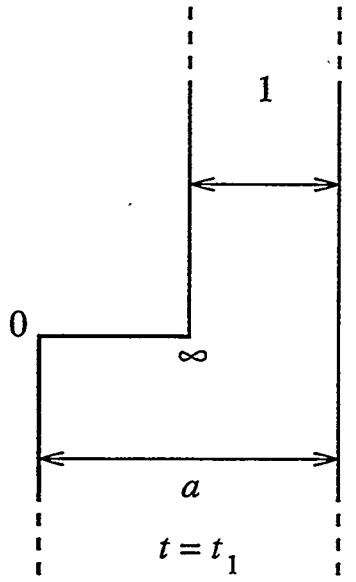

Figure 1.

For the map of Figure 1,

$$\pi \dot{z} = -i \frac{1 - t_1}{\sqrt{t}(t - t_1)(t - 1)}$$

$$a = \frac{1}{\sqrt{t_1}} \quad \text{and thus} \quad t_1 = \frac{1}{a^2}.$$

June, 1993. Note 0134u-w.

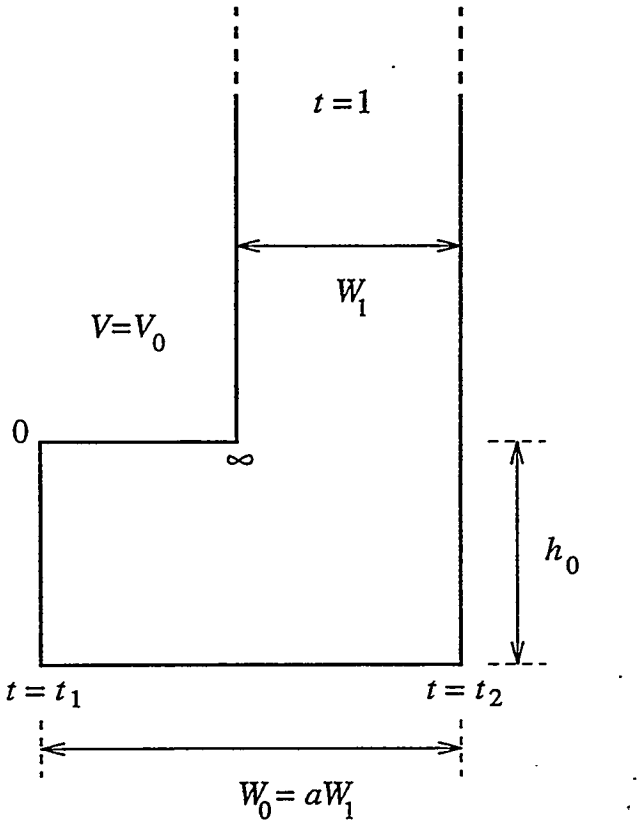

Figure 2.

We proved in Korea in 1987 that

$$0 < t_1 < 1/a^2 < t_2 < 1 \quad \text{and} \quad \frac{1}{a^2} = \left(\frac{W_1}{W_0}\right)^2$$

for the geometry of Figure 2.

Therefore, in program NPOLE1.BAS (included at the end of this document),

$$t_1 = \frac{1}{a^2}\text{RANG(C1)}, \quad t_2 = \frac{1}{a^2} + \left(1 - \frac{1}{a^2}\right)\text{RANG(C2)},$$

with $0 < \text{RANG}(x) < 1$ as used in the first version, and $\text{RANG}(x) = 1/(1 + e^x)$ as specifically used now.

The map for geometry with corners at t_1, t_2 is described by

$$\boxed{\dot{z} = -iW_1 \frac{Q_1}{\sqrt{t}\sqrt{t - t_1}\sqrt{t - t_2}(t - 1)}} \quad \text{and} \quad \boxed{Q_1 = \frac{\sqrt{1 - t_1}\sqrt{1 - t_2}}{\pi}.}$$

We determine t_1 and t_2 from

$$\boxed{\frac{h_0}{W_1} = Q_1 \int_0^{t_1} \frac{dt}{\sqrt{t}\sqrt{t_1 - t}\sqrt{t_2 - t}(1-t)}}$$

$$\boxed{\frac{W_0}{W_1} = Q_1 \int_{t_1}^{t_2} \frac{dt}{\sqrt{t}\sqrt{t - t_1}\sqrt{t_2 - t}(1-t)}.}$$

To evaluate the integrals, we use

$$\boxed{\int_{t_1}^{t_2} \frac{f(t)dt}{\sqrt{t - t_1}\sqrt{t_2 - t}} = 3 \int_{-1}^{1} \frac{f(t)}{\sqrt{4 - x^2}}\, dx\,,}$$

$$\boxed{t = \frac{2(t_2 + t_1) + (t_2 - t_1)\, x(3 - x^2)}{4}}$$

We use Gaussian integration with segmented intervals for testing and accuracy purposes. We use a "2D" secant equation solver to determine t_1 and t_2 from the above integrals.

We describe the complex potentials for fluxes, fields:

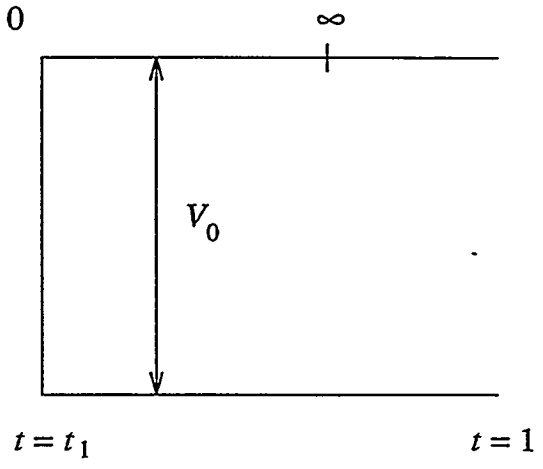

Figure 3.

$$\dot{F} = -\frac{Q_2 V_0}{\sqrt{t}\sqrt{t - t_1}\,(t-1)} \quad \text{and} \quad Q_2 = \frac{\sqrt{1 - t_1}}{\pi}.$$

We therefore have

$$F = -Q_2 V_0 \int \frac{dt}{t^2\sqrt{1-t_1/t}\,(1-1/t)} = -Q_2 \int \frac{2du}{t_1\,(1-(1-u^2)/t_1)} V_0$$

where

$$\sqrt{1-\frac{t_1}{t}} = u, \quad \frac{t_1}{t} = 1-u^2, \quad \text{and thus} \quad \frac{dt}{t^2} = \frac{2udu}{t_1}$$

$$\boxed{1-t_1 = t_3^2\,.}$$

Thus,

$$\begin{aligned}
\frac{1}{V_0}F &= -Q_2 \int \frac{2du}{u^2-t_3^2} \\
&= -Q_2 \int \left(\frac{1}{u-t_3} - \frac{1}{u+t_3}\right)\frac{du}{t_3} \\
&= \frac{Q_2}{t_3}\ln\frac{u+t_3}{u-t_3} \\
&= \boxed{\frac{Q_2}{t_3}\ln\frac{\sqrt{1-t_1/t}+t_3}{\sqrt{1-t_1/t}-t_3}\,.}
\end{aligned}$$

Flux into pole / V_0:

$$\begin{aligned}
E_p &= \frac{Q_2}{t_3}\ln\left|\frac{\sqrt{1+t_1/\tau}+t_3}{\sqrt{1+t_1/\tau}-t_3}\right|\Bigg|_0^\infty \\
&= \boxed{\frac{Q_2}{t_3}\ln\frac{1+t_3}{1-t_3}\,.}
\end{aligned}$$

Flux into midplane (for K):

$$\begin{aligned}
E_M &= \left(F(t_2)-F(t_1)\right)/V_0 \\
&= \boxed{\frac{Q_2}{t_3}\ln\frac{t_3+\sqrt{1-t_1/t_2}}{t_3-\sqrt{1-t_1/t_2}}\,,}
\end{aligned}$$

with $K_1 = 2\pi V_0 E_M(1/A_e)$ where $(1/A_e) = .934\cdot 10^2$ MKS.

We calculate the excess flux coefficient for the side of the pole ($V_0 = 1$):

$$\left(A(t)-A(\infty) = \frac{y(t)-y(\infty)}{W_1} + E_s\right)_{t\to 1}$$

$$E_s = \int_1^\infty \left(-\dot{F} + \frac{\dot{z}}{i}\right) dt = \int_1^\infty \frac{1}{\sqrt{t}\sqrt{t-t_1}(t-1)} \underbrace{\left(Q_2 - \frac{Q_1}{\sqrt{t-t_2}}\right)}_{G_1} dt$$

where

$$\begin{aligned} G_1 &= Q_2\left(1 - \frac{\sqrt{1-t_2}}{\sqrt{t-t_2}}\right) \\ &= \frac{Q_2}{\sqrt{t-t_2}}(\sqrt{t-t_2} - \sqrt{1-t_2}) \\ &= \frac{Q_2(t-1)}{\sqrt{t-t_2}\,(\sqrt{t-t_2} + \sqrt{1-t_2})} \end{aligned}$$

and thus

$$E_s = Q_2 \int_1^\infty \frac{dt}{\sqrt{t}\sqrt{t-t_1}\sqrt{t-t_2}\,(\sqrt{t-t_2} + \sqrt{1-t_2})}$$

$$= \boxed{Q_2 \int_0^1 \frac{dt}{\sqrt{1-t_1 t}\sqrt{1-t_2 t}\,(\sqrt{t-t_2 t} + \sqrt{t}\sqrt{1-t_2})}.}$$

The field B_0 at $t = t_1$ is $(\dot{F}/\dot{z})$. With V_0 on pole,

$$B_0 = \frac{V_0}{W_1}\frac{Q_2}{Q_1}\sqrt{t_2 - t_1} = \frac{V_0}{W_1}\frac{\sqrt{t_2 - t_1}}{\sqrt{1-t_2}} = \frac{V_0}{D_4}$$

where D_4 is an old notation and

$$\boxed{D_4 = W_1 \frac{\sqrt{1-t_2}}{\sqrt{t_2 - t_1}}.}$$

For the second definition of K,

$$K_2 = 2\pi \frac{1}{A_e}\sqrt{\frac{2\int_0^{\lambda_u/4} A^2 dz}{\lambda_u/4}}.$$

We need $\int F^2 dz$, thus,

$$\int A^2 dz = \int_{t_1}^{t_2} F^2 \dot{z}\, dt = G_2\,.$$

Therefore, we have that

$$G_2 = \frac{Q_1 Q_2^2}{t_3^2} V_0^2 W_1 \int_{t_1}^{t_2} \left(\ln \frac{t_3 + \sqrt{1 - t_1/t}}{t_3 - \sqrt{1 - t_1/t}}\right)^2 \frac{dt}{\sqrt{t}\sqrt{t-t_1}\sqrt{t_2 - t}(1-t)}.$$

$$\frac{G_2}{\lambda_u/4} = \frac{G_2}{W_0} = V_0^2 \frac{W_1}{W_0} \frac{Q_1 Q_2^2}{t_3^2} J$$

where

$$J = \int_{t_1}^{t_2} \left(\ln \frac{t_3 + \sqrt{1 - t_1/t}}{t_3 - \sqrt{1 - t_1/t}} \right)^2 \frac{dt}{\sqrt{t}\sqrt{t - t_1}\sqrt{t_2 - t}(1 - t)},$$

and thus we may summarize

$$\boxed{K_2 = 2\pi V_0 \frac{1}{A_e} \sqrt{\frac{2W_1 Q_2^2 Q_1}{t_3^2 W_0} J}\ .}$$

Program NPOLE1.BAS

```
PRINT:PRINT DATE$;"  ";TIME$;"  NPOLE1"
'GOTO BYPASS
PRINT "Determines parameter values and evaluates flux into midplane (Em) and"
PRINT "pole (Ep) of ID, and excess flux coefficient for side of pole (Es)."
PRINT "K1,K2,K3 are obtained by multiplying the printed values by the scalar"
PRINT "potential of pole in Tcm.  K1 is for maximum deflection angle, K2 for"
PRINT "trajectory length effect, and K3 for B0*period.  D4=V0/B0 for V0=1."
REM--List of P1() elements:0>W01^(-2),1>T1,2>T2,3>T3,5>Q1,6>Q2,9>Function ID
BYPASS:
DEFINT J:DEFDBL A-Z
PI=4*ATN(1):A1$="##.###^^^^ ":TAP=0
A2$="  Em          Ep          Es          K1          K2          K3          D4"
A3$="                 H0=##.##   W0=##.##   W1=##.##"
DIM P1(0:9),GX(1:4),GW(1:4)
SHARED PI,GX(),GW(),P1(),A1$
REM--GX,GW=(normalized) abscissas; P1=parameters for Gauss integrator
DATA .1834346425,.3626837834,.5255324099,.3137066459
DATA .7966664774,.2223810345,.9602898565,.1012285363
FOR J1=1 TO 4:READ GX(J1),GW(J1):NEXT J1:REM--Abscissas, weights for Gauss
REM------------------------------------------------------------------------
'C10=1:C20=1
PRINT:PRINT TAB(TAP);:PRINT A2$

DO
AGAIN:
INPUT;"H0,W0,>W1=",H00,W00,W10:REM--INPUT unnormalized 1/2gap, period/4,
IF H00>0 THEN H0=H00:REM--pole to symmetry line distance, stored temporarily
IF W00>0 THEN W0=W00:REM--in H00,W00,W10, then in H0,W0,W1(=not-normalized).
IF W10>0 THEN W1=W10:REM--H01,W01=normalized with W1, used in program.
IF H00=0 AND W00=0 AND W10=0 THEN END
IF W0<W1 THEN PRINT TAB(20);:PRINT "W0 must be larger than W1!":GOTO AGAIN
PRINT TAB(24);:PRINT USING A3$;H0;W0;W1
H01=H0/W1:W01=W0/W1:P1(0)=1/(W01*W01):DC1=.1:DC2=.1
GOSUB SOLVIT
PRINT TAB(TAP);:PRINT USING A1$;EM;EP;ES;K1;K2;K3;D4
LOOP

SOLVIT:
C11=C10+DC1:C21=C20:C12=C10:C22=C20+DC2
CALL EVAL(C10,C20,S10,S20):S10=S10-H01:S20=S20-W01:S00=ABS(S10)+ABS(S20)
CALL EVAL(C11,C21,S11,S21):S11=S11-H01:S21=S21-W01:S01=ABS(S11)+ABS(S21)
CALL EVAL(C12,C22,S12,S22):S12=S12-H01:S22=S22-W01:S02=ABS(S12)+ABS(S22)
DO
```

```
REM--REARR puts "worst" set into last column, to be discarded later
GOSUB REARR
N1=1/((S11-S10)*(S22-S20)-(S12-S10)*(S21-S20)):  REM--Start of 2D secant
D1=N1*(S20*S12-S10*S22):D2=N1*(S10*S21-S20*S11):REM--equation solver
DC1=(C11-C10)*D1+(C12-C10)*D2:DC2=(C21-C20)*D1+(C22-C20)*D2
C12=C11:C22=C21:C11=C10:C21=C20:S12=S11:S22=S21:S11=S10:S21=S20
S02=S01:S01=S00:C10=C10+DC1:C20=C20+DC2:REM--Recommended new parameters
CALL EVAL(C10,C20,S10,S20):S10=S10-H01:S20=S20-W01:S00=ABS(S10)+ABS(S20)
LOOP UNTIL S00<.001
P1(9)=3:CALL SGAUSSINT8(0,1,G2,-.001):Q2=P1(6):T1=P1(1):T2=P1(2):T3=P1(3)
Q1=P1(5):ES=Q2*G2:EP=Q2/T3*LOG((1+T3)/(1-T3)):D4=W1*SQR((1-T2)/(T2-T1))
EM=Q2/T3*LOG(2/(1-SQR(1-T1/T2)/T3)-1):K1=2*PI*EM*.934:K3=4*W0/D4*.934
P1(9)=4:CALL SGAUSSINT8(-1,1,K2,-.001):K2=2*PI*Q2/P1(3)*SQR(2*Q1*3*K2/W01)*.934
RETURN

REARR:
IF S00>S01 THEN GOSUB SW01
IF S01>S02 THEN GOSUB SW12
RETURN

SW01:
SWAP S00,S01:SWAP S10,S11:SWAP S20,S21:SWAP C10,C11:SWAP C20,C21:RETURN
SW12:
SWAP S01,S02:SWAP S11,S12:SWAP S21,S22:SWAP C11,C12:SWAP C21,C22:RETURN

SUB EVAL(C1,C2,S1,S2):REM--Calculates H01,W01 for set of parameters C1,C2>T1,T2
T1=P1(0)*RANG(C1):T2=P1(0)+(1-P1(0))*RANG(C2)
T3=SQR(1-T1):P1(1)=T1:P1(2)=T2:P1(3)=T3
Q2=T3/PI:Q1=Q2*SQR(1-T2):P1(5)=Q1:P1(6)=Q2
P1(9)=1:CALL SGAUSSINT8(-1,1,G2,-.001):S1=3*Q1*G2
P1(9)=2:CALL SGAUSSINT8(-1,1,G2,-.001):S2=3*Q1*G2
END SUB

SUB SGAUSSINT8(X0,X3,G2,DG):REM--Gauss integrator, with interval segmentation
IF DG>0 THEN E1=DG:E2=0 ELSE E1=0:E2=-DG:REM--For DG>/<0,DG=absol./rel.  error
CALL GAUSSINT8(X0,X3,G2):J1=1:J4=16:REM--J4=largest # subdiv.
DO
  G1=G2:G2=0:J1=2*J1:DX=(X3-X0)/J1:REM--G1/G2=last/next computed integral
  IF J1>J4 THEN PRINT "   Not converged":END
  FOR J2=0 TO J1-1
    CALL GAUSSINT8(X0+J2*DX,X0+(J2+1)*DX,G3)
    G2=G2+G3:REM---------------------------------G2=integral
  NEXT J2
LOOP UNTIL ABS(G2-G1)<E1+E2*ABS(G2) OR J1>J4
END SUB
```

```
SUB GAUSSINT8(X1,X2,G2):REM--------------Integrator; G2=value of integral
X0=.5*(X2+X1):X3=X0-X1:G2=0
ON P1(9) GOTO INTEGRAND1,INTEGRAND2,INTEGRAND3,INTEGRAND4
INTEGRAND1:
FOR J1=1 TO 4
 DX=GX(J1)*X3:G2=G2+GW(J1)*(GCT1(X0+DX)+GCT1(X0-DX))
NEXT J1:G2=G2*X3
EXIT SUB
INTEGRAND2:
FOR J1=1 TO 4
 DX=GX(J1)*X3:G2=G2+GW(J1)*(GCT2(X0+DX)+GCT2(X0-DX))
NEXT J1:G2=G2*X3
EXIT SUB
INTEGRAND3:
FOR J1=1 TO 4
 DX=GX(J1)*X3:G2=G2+GW(J1)*(GCT3(X0+DX)+GCT3(X0-DX))
NEXT J1:G2=G2*X3
EXIT SUB
INTEGRAND4:
FOR J1=1 TO 4
 DX=GX(J1)*X3:G2=G2+GW(J1)*(GCT4(X0+DX)+GCT4(X0-DX))
NEXT J1:G2=G2*X3
END SUB

FUNCTION GCT1(X):REM---------------First of functions to be integrated.
TT=P1(1)*(2+X*(3-X*X))/4:GCT1=1/SQR((P1(2)-TT)*(4-X*X))/(1-TT)
END FUNCTION

FUNCTION GCT2(X)
TT=((P1(2)+P1(1))*2+(P1(2)-P1(1))*X*(3-X*X))/4
GCT2=1/SQR(TT*(4-X*X))/(1-TT)
END FUNCTION


FUNCTION GCT3(X)
S1=SQR(1-P1(2)*X):GCT3=1/SQR(1-P1(1)*X)/(S1*(S1+SQR(X*(1-P1(2)))))
END FUNCTION

FUNCTION GCT4(X)
TT=((P1(2)+P1(1))*2+(P1(2)-P1(1))*X*(3-X*X))/4:T4=SQR(1-P1(1)/TT)/P1(3)
GCT4=(LOG((1+T4)/(1-T4)))^2/(1-TT)/SQR(TT*(4-X*X))
END FUNCTION
```

```
FUNCTION RANG(X):REM----------------------------0<RANG(X)<1
RANG =1/(1+EXP(X))
END FUNCTION

DEF FNPOLE(X)=((X+1)*LOG(X+1)-(X-1)*LOG(X-1))/PI
```

Program Results

```
06-28-1993  10:14:02  NPOLE1
Determines parameter values and evaluates flux into midplane (Em) and
pole (Ep) of ID, and excess flux coefficient for side of pole (Es).
K1,K2,K3 are obtained by multiplying the printed values by the scalar
potential of pole in Tcm.  K1 is for maximum deflection angle, K2 for
trajectory length effect, and K3 for B0*period.  D4=V0/B0 for V0=1.

    Em          Ep          Es          K1          K2          K3          D4
H0, W0,>W1 = .5,1.4                       H0= 0.50    W0= 1.00    W1= 0.40
 1.373E+00  1.515E+00  2.532E-01  8.055E+00  7.890E+00  7.310E+00  5.111E-01
```

Error of Flux Calculation for Finite Pole Width with Excess Flux Coefficient

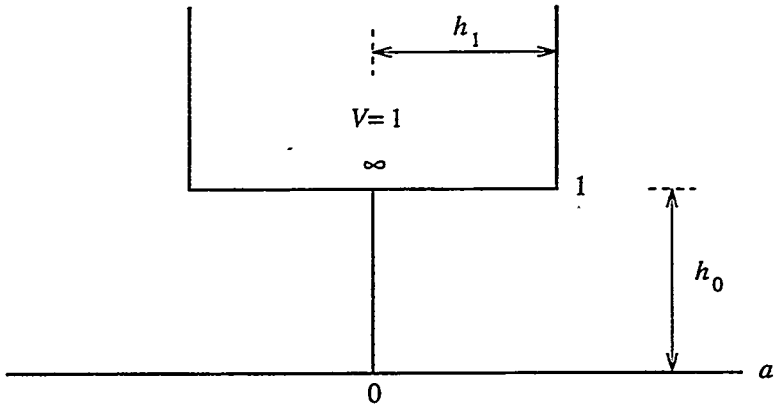

Figure 1.

$$\boxed{\dot{z} = -\frac{\sqrt{t^2-1}}{\sqrt{t^2-a^2}^3}}$$

We have

$$h_0 = \int_0^\infty \frac{\sqrt{1+t^2}}{\sqrt{a^2+t^2}^3}\,dt \quad \text{and} \quad h_1 = \int_1^\infty \frac{\sqrt{1-t^2}}{\sqrt{t^2-a^2}^3}\,dt\,.$$

We introduce

$$\sqrt{a^2+t^2} = \frac{1}{u}, \quad t = \sqrt{\frac{1}{u^2}-a^2} = \frac{\sqrt{1-a^2u^2}}{u}$$

$$dt = -\frac{\dfrac{a^2u^2}{\sqrt{1-a^2u^2}} + \sqrt{1-a^2u^2}}{u^2}\,du = -\frac{1}{u^2\sqrt{1-a^2u^2}}\,du$$

$$1+t^2 = 1-a^2+\frac{1}{u^2} = b^2+\frac{1}{u^2}, \qquad b^2 = 1-a^2$$

we therefore have

$$h_0 = -\frac{1}{a}\int_0^{1/a} \frac{\sqrt{1+b^2u^2}}{\sqrt{1-a^2u^2}}\,du\,.$$

June, 1993. Note 0133u-w.

And given $au = \sin\varphi$, and $du = \dfrac{\cos\varphi\, d\varphi}{a}$,

$$\begin{aligned} h_0 &= -\frac{1}{a}\int_0^{\pi/2} \sqrt{1 + \frac{b^2}{a^2}\sin^2\varphi}\, d\varphi \\ &= -\frac{1}{a}\int_0^{\pi/2} \sqrt{1 + \frac{b^2}{a^2} - \frac{b^2}{a^2}\cos^2\varphi}\, d\varphi \\ &= -\frac{1}{a^2}\int_0^{\pi/2} \sqrt{1 - b^2\cos^2\varphi}\, d\varphi \\ &= \boxed{-\frac{1}{a^2}E(b^2)\,.} \end{aligned}$$

For $t = \dfrac{1}{u}$, $dt = -\dfrac{du}{u^2}$, and $u = \sin\alpha$

$$\begin{aligned} h_1 &= -\int_0^1 \frac{\sqrt{1/u^2 - 1}}{\sqrt{1/u^2 - a^2}^3}\,\frac{du}{u^2} \\ &= -\int_0^1 \frac{\sqrt{1-u^2}}{\sqrt{1-a^2u^2}^3}\, du \\ &= -\int_0^{\pi/2} \frac{\cos^2\alpha\, d\alpha}{\sqrt{1-a^2\sin^2\alpha}^3} \end{aligned}$$

From Jahnke and Emde[1]:

$$\boxed{h_1 = -\frac{K(a^2) - E(a^2)}{a^2}}$$

and therefore

$$\boxed{\frac{h_1}{h_0} = \frac{K(a^2) - E(a^2)}{E(1-a^2)}\,.}$$

1 *Table of Functions with Formulae and Curves,* Dover Publications, 1945: p. 56.

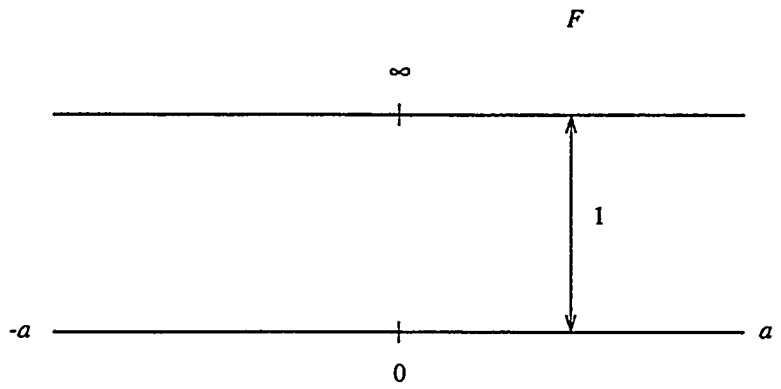

Figure 2.

$$\pi \dot{F} = -\frac{2a}{t^2 - a^2} = \frac{1}{t+a} - \frac{1}{t-a}$$

$$\boxed{\pi F = \ln \frac{t+a}{t-a} = \ln \frac{1 + a/t}{1 - a/t}}$$

The flux into the poleface is

$$A(1) - A(\infty) = A_{\text{ideal}} = \boxed{\frac{1}{\pi} \ln \frac{1+a}{1-a}.}$$

Comparing this flux to the homogeneous flux and the excess flux for the end of a semi-infinite pole with half-gap $= h_0$, we have

$$\begin{aligned} A_{\text{approx}} &= \frac{h_1}{h_0} + \frac{1}{\pi}(2 - \ln 4) \\ &= \boxed{\frac{K(a^2) - E(a^2)}{E(1-a^2)} + .195.} \end{aligned}$$

Therefore we have

$$G\left(\frac{h_1}{h_0}\right) = \frac{A_{\text{approx}} - A_{\text{ideal}}}{A_{\text{ideal}}} = \frac{A_{\text{approx}}}{A_{\text{ideal}}} - 1 = \boxed{\frac{\frac{h_1}{h_0} + \frac{1}{\pi}(2 - \ln 4)}{\frac{1}{\pi} \ln \frac{1+a}{1-a}} - 1.}$$

Program EXCFLTST.BAS

```
CLS
DEFDBL A-Z
PRINT DATE$ ;"  ";TIME$ ;"  EXCFLTST"
REM--Error of flux calculation for finite width pole with excess flux
REM--coefficient.    INPUT parameter = 1/2-width of pole / 1/2-gap.
PI=4*ATN(1):A1$="dA=##.###^^^^  dA/A=##.###^^^^  dX/H1=##.###^^^^"
E1=(2-LOG(4))/PI:X2=1:DY=1E-6
DIM P1(0:2)
DO
INPUT;"H1/H0=",H0
X1=.9*X2:P1(0)=H0:REM--G1=2/(1+EXP(PI*H0+2)):E1=2/PI*(1-G1-LOG(2-G1))
CALL SECANTS(X1,X2,DY,Y2,P1())
A1=1/SQR(1+EXP(X2)):A0=LOG((1+A1)/(1-A1))/PI:AE=H0+E1
PRINT TAB(15);:PRINT USING A1$;AE-A0;AE/A0-1;(AE-A0)/H0
LOOP

SUB SECANTS(X1,X2,DY,Y2,P1())
CALL FCTY(X1,Y1,P1()):CALL FCTY(X2,Y2,P1())
IF ABS(Y1)<ABS(Y2) THEN SWAP Y1,Y2:SWAP X1,X2
J1%=0
DO
DX=Y2*(X1-X2)/(Y2-Y1)
X1=X2:Y1=Y2:X2=X1+DX:J1%=J1%+1
CALL FCTY(X2,Y2,P1())
LOOP UNTIL ABS(Y2)<DY OR J1%=15
IF J1%=15 THEN PRINT "NOT CONVERGED"
END SUB

SUB FCTY(X1,Y1,P1())
A2=1/(1+EXP(X1))
Y1=(ELLK(A2)-ELLE(A2))/ELLE(1-A2)-P1(0)
END SUB

FUNCTION ELLK(X1)
X=1-X1:S1=.01451196212*X+.03742563713:S1=S1*X+.03590092383
S1=S1*X+.09666344259:S1=S1*X+1.38629436112:S2=.00441787012*X+.03328355346
S2=S2*X+.06880248576:S2=S2*X+.12498593597:S2=S2*X+.5
ELLK=S1-S2*LOG(X)
END FUNCTION
```

```
FUNCTION ELLE(X1)
X=1-X1:S1=.01736506451*X+.04757383546:S1=S1*X+.0626060122
S1=S1*X+.44325141463:S2=X*.00526449639+.04069697526
S2=S2*X+.09200180037:S2=S2*X+.2499836831
ELLE=X*S1+1-X*S2*LOG(X)
END FUNCTION
```

Program Results

```
06-16-1993  09:09:24  EXCFLTST
H1/H2=.1      dA= 4.832E-02  dA/A= 1.956E-01  dX/H1= 4.832E-01
H1/H2=.2      dA= 2.240E-02  dA/A= 6.022E-02  dX/H1= 1.123E-01
H1/H2=.3      dA= 1.129E-02  dA/A= 2.331E-02  dX/H1= 3.762E-02
H1/H2=.4      dA= 5.848E-03  dA/A= 9.920E-03  dX/H1= 1.462E-02
H1/H2=.5      dA= 3.074E-03  dA/A= 4.441E-03  dX/H1= 6.149E-03
H1/H2=.6      dA= 1.627E-03  dA/A= 2.050E-03  dX/H1= 2.712E-03
H1/H2=.7      dA= 8.645E-04  dA/A= 9.665E-04  dX/H1= 1.235E-03
H1/H2=.8      dA= 4.602E-04  dA/A= 4.626E-04  dX/H1= 5.752E-04
H1/H2=.9      dA= 2.452E-04  dA/A= 2.239E-04  dX/H1= 2.725E-04
H1/H2=1       dA= 1.307E-04  dA/A= 1.094E-04  dX/H1= 1.307E-04
H1/H2=2       dA= 3.008E-07  dA/A= 1.370E-07  dX/H1= 1.504E-07
```

Excess Flux Into Pole and Flux Into Side of Gm40

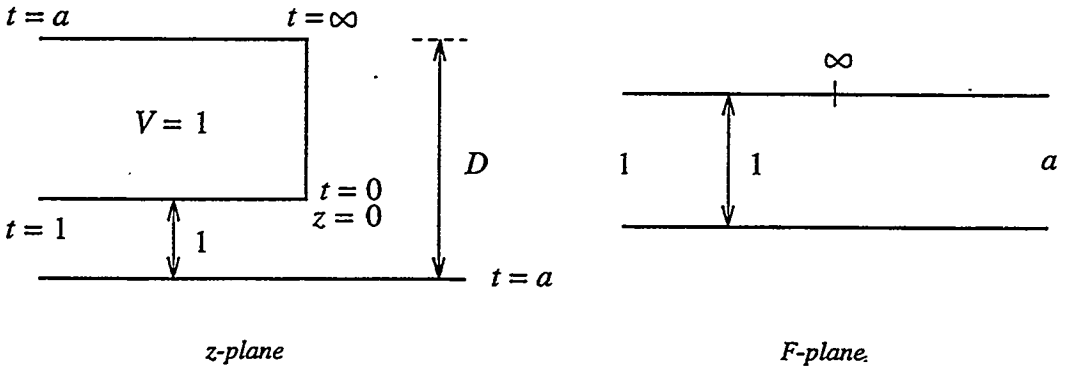

Figure 1.

The conformal map is described by

$$\pi \dot{z} = \frac{\sqrt{t}(a-1)^2}{(t-1)(t-a)^2}.$$

To determine the value a that produces the desired D, we use $t = a + \tau$, $|\tau| \ll a$. Expanding in τ gives

$$\pi \frac{dz}{d\tau} = \frac{(a-1)^2\sqrt{a}\left(1+\frac{\tau}{2a}\right)}{(a-1)\left(1+\frac{\tau}{a-1}\right)} \cdot \frac{1}{\tau^2}.$$

Expanding more, and then integrating over the half-circle around $t = a$, we get

$$\begin{aligned} D &= -(a-1)\sqrt{a}\left(\frac{1}{2a} - \frac{1}{a-1}\right) \\ &= \sqrt{a} \cdot \frac{a+1}{2a} \\ &= \boxed{\frac{1}{2}\left(\sqrt{a} + \frac{1}{\sqrt{a}}\right).} \end{aligned}$$

By substitution and integration, we have

$$\frac{\pi z}{(a-1)^2} = \frac{\partial}{\partial a}\int \frac{\sqrt{t}\,dt}{(t-1)(t-a)} = \frac{\partial}{\partial a} J,$$

April, 1993. Note 0131u-w.

where, for $t = W^2$ and $dt = 2W\,dW$,

$$\begin{aligned} J &= \int \frac{2t\,dW}{(t-1)(t-a)} \\ &= \int \frac{2}{a-1}\left(\frac{a}{t-a} - \frac{1}{t-1}\right) dW \\ &= \frac{1}{a-1}\int \left(\sqrt{a}\left(\frac{1}{W-\sqrt{a}} - \frac{1}{W+\sqrt{a}}\right) - \left(\frac{1}{W-1} - \frac{1}{W+1}\right)\right) dW \\ &= \boxed{\frac{1}{a-1}\left(\sqrt{a}\ln\frac{\sqrt{a}-W}{\sqrt{a}+W} + \ln\frac{1+W}{1-W}\right) :} \end{aligned}$$

Further, we have that

$$\sqrt{a}\,\frac{\partial}{\partial a}\ln\frac{\sqrt{a}-W}{\sqrt{a}+W} = \frac{1}{2}\left(\frac{1}{\sqrt{a}-W} - \frac{1}{\sqrt{a}+W}\right) = \frac{W}{a-t}.$$

$$\left(\frac{1}{\sqrt{a}-1/\sqrt{a}}\right)' = -\frac{1}{2a}\cdot\frac{\sqrt{a}+1/\sqrt{a}}{(\sqrt{a}-1/\sqrt{a})^2} = -\frac{D}{(a-1)^2},$$

$$\left(\frac{1}{a-1}\right)' = -\frac{1}{(a-1)^2}.$$

Thus,

$$J' = -\frac{1}{(a-1)^2}\left(\ln\frac{1+W}{1-W} + D\ln\frac{\sqrt{a}-W}{\sqrt{a}+W}\right) + \left(\frac{1}{a-1}\cdot\frac{W}{a-t}\right),$$

and therefore,

$$\boxed{\pi z = (a-1)\frac{W}{a-t} + D\ln\frac{\sqrt{a}+W}{\sqrt{a}-W} - \ln\frac{1+W}{1-W}.}$$

Further, for

$$\pi\dot{F} = -\frac{a-1}{(t-1)(t-a)} = \frac{1}{t-1} - \frac{1}{t-a},$$

$$\boxed{\pi F = \ln\frac{1-t}{1-t/a}.}$$

The flux into the side of the pole, for $-\infty \le t \le 0$, is

$$\boxed{A_S = \frac{1}{\pi}\ln(a).}$$

We describe the excess flux into the poleface by

$$\Delta A_P = F(0) - F(1-\varepsilon) - (z(0) - z(1-\varepsilon)) \quad \text{follows} \quad \varepsilon \to 0\,,$$

$$\pi \Delta A_P = \ln \frac{1-1/a}{\varepsilon} + \left(1 + D \ln \frac{\sqrt{a}+1}{\sqrt{a}-1} - \ln \frac{2}{\varepsilon/2}\right),$$

$$\frac{a-1}{\varepsilon a}\frac{\varepsilon}{4} = \frac{a-1}{4a},$$

$$\boxed{\Delta A_P = \frac{1}{\pi}\left(1 + \ln \frac{a-1}{4a} + D \ln \frac{\sqrt{a}+1}{\sqrt{a}-1}\right).}$$

The definition of ΔA_P means that the flux into the pole surface is the same as the uniform flux into a pole whose width is increased, on both sides, by the product of the half-gap and the expression for ΔA_P. The definition of A_S means that the total flux into each side of the pole equals the product of the scalar potential of the pole and the expression for A_S.

From our expression for D, and $a - 2D\sqrt{a} + 1 = 0$, we have

$$\boxed{\sqrt{a} = D + \sqrt{D^2 - 1}\,.}$$

We may now eliminate a from A_S and ΔA_P. Thus,

$$\boxed{A_S = \frac{2}{\pi} \ln(D + \sqrt{D^2 - 1})\,,}$$

and further,

$$1/\sqrt{a} = D - \sqrt{D^2 - 1}\,,$$

$$\frac{\sqrt{a}+1}{\sqrt{a}-1} = \frac{D+1+\sqrt{D^2-1}}{D-1+\sqrt{D^2-1}} = \frac{\sqrt{D+1}}{\sqrt{D-1}} \cdot \frac{\sqrt{D+1}+\sqrt{D-1}}{\sqrt{D-1}+\sqrt{D+1}} = \sqrt{\frac{D+1}{D-1}},$$

$$\frac{a-1}{4a} = \frac{\sqrt{a}-\sqrt{1/a}}{4\sqrt{a}} = \frac{\sqrt{D^2-1}}{2(D+\sqrt{D^2-1})} = \frac{1}{2(1+1/\sqrt{1-1/D^2})},$$

$$\boxed{\Delta A_P = \frac{1}{\pi}\left(1 + \frac{D}{2} \ln \frac{D+1}{D-1} - \ln\left(2\left(1 + \frac{D}{\sqrt{D^2-1}}\right)\right)\right).}$$

Flux Transport Along Axial Direction of Electro-Magnetic Wiggler

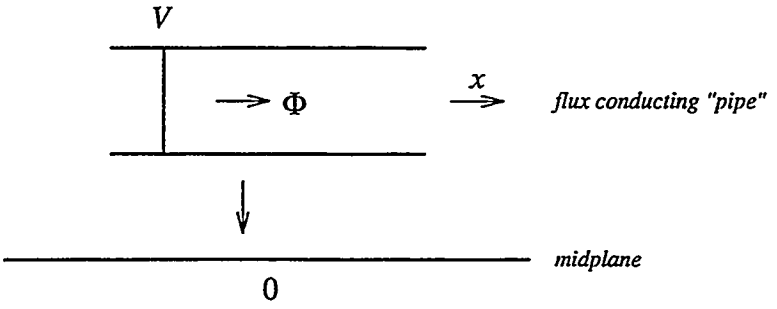

Figure 1.

Status characterized by status vector $v = \begin{pmatrix} V \\ \Phi \end{pmatrix}$, where V is the scalar potential with respect to the midplane, and Φ is the flux transported to the right. Going "downstream", V and Φ change because of the $\int Hds$ "loss" in iron (and due to small gaps), and because of flux going to the midplane. Over a short distance,

$$\frac{d\Phi}{dx} = -V \cdot \varepsilon \,, \tag{1}$$

with ε to 0th approximation (detailed later in this note) is given by

$$\varepsilon = \frac{W}{h} \,, \tag{2}$$

with h having the value of the half-gap, and W being the width over which the flux "escapes" to the midplane.

$$\frac{dV}{dx} = -\Phi \cdot k_2 \,, \tag{3}$$

April, 1993. Note 0129u-w.

with k_2 in 0th approximation (also detailed later) given by

$$k_2 = \frac{1}{a\mu} = \gamma/a\,, \tag{4}$$

where a is the cross-section area of the flux "duct", and μ is the permeability. The voltage drop due to small gaps perpendicular to the flux flow will be added later. Within the section with constants k_2 and ε, we get

$$V'' = -k_2\Phi' = Vk^2 \quad \text{with} \quad k^2 = \varepsilon k_2\,. \tag{5}$$

The solution within the uniform section of length x is

$$V = \alpha C + \beta S \quad \text{with} \quad C = \cosh kx \ \text{ and } \ S = \sinh kx\,,$$

$$\Phi = -V'/k_2 = -(\alpha S + \beta C)k/k_2\,,$$

$$v(x) = \begin{pmatrix} C & S \\ -Sk/k_2 & -Ck/k_2 \end{pmatrix}\begin{pmatrix}\alpha\\ \beta\end{pmatrix} \quad \text{with} \quad \begin{pmatrix}\alpha\\ \beta\end{pmatrix} = \begin{pmatrix} 1 & 0 \\ 0 & -k_2/k \end{pmatrix} v(0)\,,$$

$$v(x) = M\cdot v(0)\,, \quad v = \begin{pmatrix} V \\ \Phi \end{pmatrix} \text{ and } M = \begin{pmatrix} C & -Sk_2/k \\ -Sk/k_2 & C \end{pmatrix}. \tag{6}$$

By reversing the direction arrow of Φ, i.e., by re-defining the sign of Φ, the off-diagonal minus signs disappear. The sequence of sections with different properties are taken into account by multiplying their matrices. v remains unchanged when crossing the interface from one section to the next unless there is a (steering) coil, or a local field clamp, thus introducing an additive Δv when going through that interface.

It is clear that $1/k$ is the important scaling distance that describes how transported flux decays.

Structure of Solution to Simple Problem.

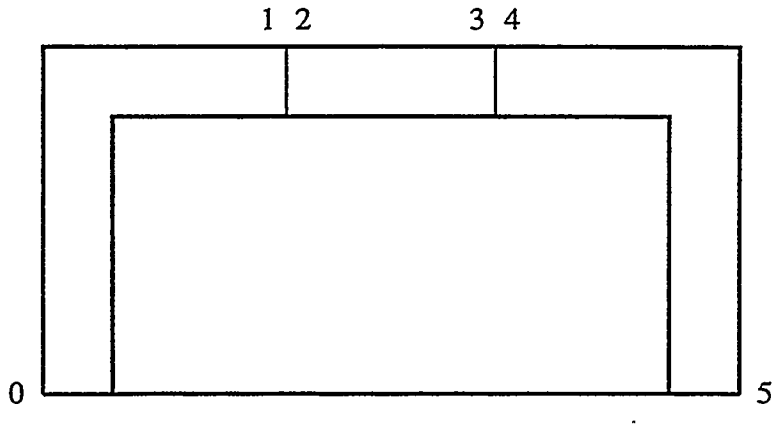

Figure 2.

There are field clamps at each end, i.e. at point 0 and point 5. There are $\pm\Delta V$ coils at the interfaces between points 1 and 2, and between points 3 and 4. The status vectors $v_0 = \begin{pmatrix} 0 \\ \Phi_0 \end{pmatrix}$ and $v_5 = \begin{pmatrix} 0 \\ \Phi_5 \end{pmatrix}$ describe that the points 0 and 5 are located in the midplane, and that they contain the to-be-determined values Φ_0 and Φ_5 which represent the fluxes going to the midplane through the field clamps. Of similar interest are the Φ-components of v_2 and v_4.

Given $\Delta v_0 = \begin{pmatrix} \Delta v_0 \\ 0 \end{pmatrix}$, we describe the coil(s) by

$$v_2 = M_{01} v_0 + \Delta v_0 \,. \tag{7.1}$$

$$v_4 = M_{23} v_2 - \Delta v_0 = M_{23} M_{01} v_o + (M_{23} - I)\Delta v_0 \,, \tag{7.2}$$

where I is the unit matrix.

$$v_5 = M_{45} v_4 = \underbrace{M_{05}}_{a_{ik}} v_0 + \underbrace{M_{45}(M_{23} - I)}_{b_{ik}} \Delta v_0 \,, \tag{7.3}$$

where a_{ik} and b_{ik} are elements of these matrices, and thus

$$v_5 = \Phi_0 \begin{pmatrix} a_{12} \\ a_{22} \end{pmatrix} + \begin{pmatrix} b_{11} \\ b_{21} \end{pmatrix} \Delta V_0 = \begin{pmatrix} 0 \\ \Phi_5 \end{pmatrix} .$$

$$\boxed{\Phi_0 = -\Delta V_0 b_{11}/a_{12} .} \tag{7.4}$$

$$\Phi_5 = \Phi_0 a_{22} + \Delta V_0 b_{21} = \Delta V_0 (b_{21} - a_{22} b_{11}/a_{12})$$

$$\boxed{\Phi_5 = \Delta V_0 (a_{12} b_{21} - a_{22} b_{11})/a_{12} .} \tag{7.5}$$

With Φ_0 and Φ_5 now known, (7.1) and (7.2) give the flux produced by the coils in the section delimited by points 2 and 3.

Details of k_2.

One has to be careful to use the correct value for μ. If the field associated with this flux is parallel to the pre-existing field, one has to use $\mu = \dfrac{dB}{dH}$. If it is perpendicular to the pre-existing flux, one must use $\mu = \dfrac{B}{H}$ which is the "normal μ".

Now we must look at the effect of a thin gap over a large area. ΔV across that gap from flux Φ is gotten from $\Phi = \displaystyle\int \frac{\Delta V \, da}{g}$ and thus $\Delta V = \dfrac{\Phi}{\displaystyle\int \frac{da}{g}}$. If a gap-less length L of μ is associated with this gap, the total ΔV is given by

$$\Delta V = \Phi \left(\frac{1}{\int \frac{da}{g}} + \gamma \frac{L}{A} \right) = \Phi L \left(\frac{\gamma}{a} + \frac{1/L}{\int \frac{dg}{a}} \right) ,$$

$$\boxed{k_2 = \frac{\gamma}{a} + \frac{1/L}{\int \frac{da}{g}} .} \tag{8}$$

Details of ε.

Only the general approach and the results derived in a separate note are given here. There are three contributions to ε: flux from the top, from the sides, and from the poles facing the midplane.

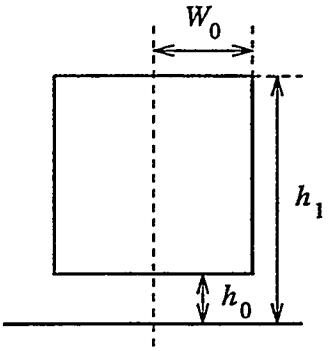

(a)

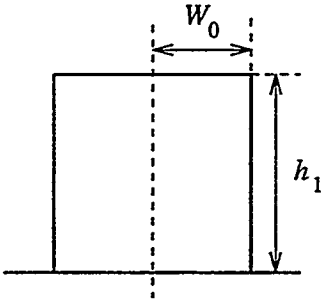

(b)

Figures 3(a) and 3(b).

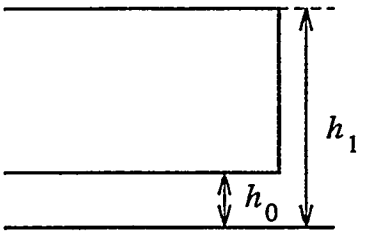

(c)

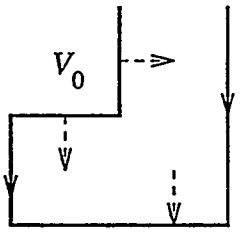

(d)

Figures 3(c) and 3(d).

To get the flux into the top per unit length in direction perpendicular to the paper plane, we use as a model the solid block that touches the midplane of Figure 3(b). For the flux into each side, we use the geometry of Figure 3(c) and calculate the flux into the side. If the side has "pole structure" we take it into account with an excess voltage drop coefficient approximation (if necessary). For flux from the poles to the midplane, we calculate the flux for the geometry of Figure 3(d), and we use

the excess flux coefficient for a solid block of Figure 3(c) to correct the width $2W_0$ of the cross-section shown in Figure 3(a).

Results for the Geometry of Figure 3(d).

$$\boxed{\varepsilon_P = \frac{\Phi(\lambda/4)}{V_0}\frac{4}{\lambda}(W_0 + \Delta W_0)\,2\,,} \tag{9.1}$$

with $\dfrac{\Phi(\lambda/4)}{V_0}$ calculated by POISSON or an analytical program.

We calculate ΔW_0 from the geometry of Figure 3(c), with

$$\boxed{D = h_1/h_0\,,} \tag{9.2}$$

$$\boxed{\Delta W_0 = h_0\frac{1}{\pi}\left(1 + \frac{D}{2}\ln\left(\frac{D+1}{D-1}\right) - \ln\left(2\left(1 + \frac{D}{\sqrt{D^2-1}}\right)\right)\right)\,.} \tag{9.3}$$

The contribution from the flux into the top is

$$\varepsilon_T = \frac{2}{\pi}\ln\frac{1+a_1}{1-a_1}\,, \tag{10.1}$$

where a_1 is determined from

$$\frac{h_1}{W_0} = \frac{E(b) - a_1^2 K(b)}{E(a_1) - b^2 K(a_1)} \tag{10.2}$$

with $b^2 = 1 - a_1^2$, and

$$E(a_1) = \int_0^{\pi/2}\sqrt{1 - a_1^2\sin^2\varphi}\,d\varphi \quad \text{and} \quad K(a_1) = \int_0^{\pi/2}\frac{d\varphi}{\sqrt{1 - a_1^2\sin^2\varphi}}\,. \tag{10.3}$$

The flux into the sides contributes

$$\varepsilon_S = \frac{4}{\pi}\ln\left(D + \sqrt{D^2-1}\right)\,,$$

with D given by (9.2).

(11.1) assumes smooth sides, i.e., the excess potential drop is ignored. It should be noted that the area a in (8) is smaller than the cross-section shown in Figure 3(a), the latter includes the poles, while the former does not.

We make here further clarifications on units. If we were to deal with a uniform field over a width W of a flat pole, at distance h_0 from the midplane, ε would be exactly $\varepsilon = \frac{W}{H}$. That is, $\frac{d\Phi}{dx}$ and V have the same dimensions, meaning that either $\mu_0 = 4\pi \cdot 10^{-7}$ is incorporated in the vector potential V, or μ_0 is left out of the definition of Φ. The meaning of ε is the flux per unit length in the axial direction of the structure on potential V, divided by V.

ε_S with excess potential drop is given by

$$\varepsilon_S = \frac{4}{\pi} \ln\left(D_1 + \sqrt{D_1^2 - 1}\right) \tag{11.2}$$

with

$$D_1 = \frac{h_1 + \frac{2}{\pi}\Delta L}{h_0 + \frac{2}{\pi}\Delta L}. \tag{11.3}$$

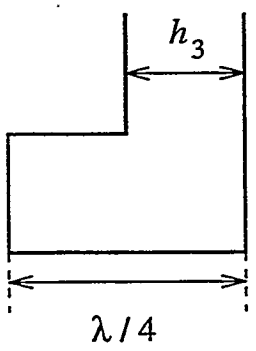

Figure 4.

$$\alpha = \frac{\lambda/4}{h_3} \quad \text{and} \quad \Delta L = \frac{h_3}{\pi}\left((\alpha+1)\ln(1+1/\alpha) + (\alpha-1)\ln(1-1/\alpha)\right). \tag{11.4}$$

The effect of ΔL will be very small under most circumstances. The excess flux

potential drop is too small to be of concern for ε_T.

3D Scalar Potential for Saturation-Caused Fields in the Insertion Device

This entails the same approach as for the case of $\mu = \infty$, except that the condition $\partial V/\partial x = 0$ at $y = h$ is to be dropped:

$$V = \sum \cos nk_z z \cdot g_n(x, y)\,,$$

$$\nabla^2 V = 0 \quad \Longrightarrow \quad \nabla^2 g_n = n^2 k_z^2 g_n\,.$$

We introduce $nk_z x = u$, and $nk_z y = v$:

$$\nabla^2_{u,v} g = g\,. \tag{1}$$

We construct $g(u, v)$ that has the following properties: odd in y, $g(-v) = -g(v)$, and gives field approximating $\cosh \varepsilon u - 1$ for $y = 0$. ε is arbitrary, real or imaginary, and the field equals 0 for $u = 0$ when letting $\varepsilon \to 0$ at end.

We try $g = \cosh \varepsilon u \sinh av$. To satisfy (1):

$$\varepsilon^2 + a^2 = 1 \quad \text{and thus} \quad \boxed{a = \sqrt{1 - \varepsilon^2}}$$

has to hold. We add a function of v, such that g'_v is proportional to $\cosh \varepsilon u - 1$ for $v = 0$. The only odd function of v that will satisfy this requirement and also satisfy (1) is $-a \sinh v$, thus

$$\boxed{g = \cosh \varepsilon u \sinh av - a \sinh v\,.} \tag{2}$$

One can use the superposition of such functions with different ε, but this would probably not be practical.

The expansion for $\varepsilon \to 0$ is

$$\boxed{g = \frac{\varepsilon^2}{2}\left(u^2 \sinh v - v \cosh v + \sinh v\right).} \tag{3}$$

For $v = 0$, we obtain the expected sextupole field:

$$g'_v(u, 0) = \frac{\varepsilon^2}{2} u^2\,. \tag{4}$$

At the pole, where $v_h = nk_z h$,

$$g'_u(u, v_h) = \frac{\varepsilon^2}{2} 2u \sinh v_h, \tag{5}$$

It is this field in the x-direction that is responsible for the sextupole field in the midplane.

February, 1992. Note 0125u-w.

(5) allows us to make an estimate of the saturation effects in the midplane during the design phase. Thus,

$$\frac{g'_v(u,0)}{g'_u(u,v_h)} = \frac{u}{2\sinh v_h} = \frac{nk_z x}{2\sinh nk_z h} = \frac{x}{2h}\cdot\frac{nk_z h}{\sinh nk_z h}. \tag{6}$$

It is interesting to note that every additional expansion of (2) in ε^2 leads to a new solution to (1) describing the fields in the midplane to the highest orders $\sim x^4, x^6$, etc.

To check on (3), its expansion in k_z up to the 3rd order terms in $\{u,v\}$ gives, as expected,

$$\begin{aligned} g &= \frac{\varepsilon^2}{2}\left(u^2 v - v\left(1+\frac{v^2}{2}-\left(1+\frac{v^2}{6}\right)\right)\right) \\ &= \frac{\varepsilon^2}{2}\left(u^2 v - \frac{v^3}{3}\right) \\ &= \frac{\varepsilon^2}{6}\Im(u+iv)^3. \end{aligned} \tag{7}$$

Scalar Potential for 3D Insertion Device Fields

In the 2D case,

$$(1) \qquad V = \sum_{n=\text{odd}} b_n \cos nk_z z \cdot \sinh nk_z y \quad \text{with} \quad k_z = \frac{2\pi}{\lambda}.$$

In order to simplify matters, we drop the sum, and re-introduce it at the end.
The effects of lateral ends are equally periodic in z, thus $nk_z \Rightarrow k_z$, and

$$(2) \qquad V_{LE} = \cos k_z z \cdot g(x,y)\,.$$

Where $g(x,y)$ is valid only in the vacuum region of the $\{x,y\}$ space.
Further, we have that

$$(3) \qquad \nabla^2 V = 0 \quad \Longrightarrow \quad \nabla^2 g = k_z^2 g\,,$$

where g is the Fourier expansion coefficient as a function of x, y,
At the pole surface, for integer μ, $z = \mu\lambda/2$ and $y = h =$ half gap, $B_x = B_y = 0$. We expand g in a Fourier series in y. We have that $g \sim \sin mk_y y$ for $k_y = \pi/h$, and

$$g = \sum a_m \sin mk_y y \cdot \cosh k_m x\,,$$

with $k_m^2 = k_z^2 + m^2 k_y^2$. We use $a_m = b_0 b_m / \cosh k_m W$, where W is half the pole width, and we expect b_m to be only weakly dependent on W.

$$(4) \qquad \begin{cases} V = \displaystyle\sum_{n=\text{odd}} b_{n_0} \cos nk_z z \cdot (\sinh nk_z y + g_n), \\ g_n = \displaystyle\sum_{m=1} \frac{b_{nm} \sin mk_y y \cdot \cosh k_{nm} x}{\cosh k_{nm} W}, \\ k_{nm}^2 = n^2 k_z^2 + m^2 k_y^2, & \text{with } k_z = 2\pi/\lambda,\ k_y = \pi/h, \\ k_{nm}^2 = m^2 k_y^2 \left(1 + \dfrac{n^2}{m^2}\left(\dfrac{k_z}{k_y}\right)^2\right), & \text{with } \dfrac{k_z}{k_y} = \dfrac{2h}{\lambda} = \dfrac{\text{gap}}{\lambda}. \end{cases}$$

Under most circumstances, $\dfrac{k_z}{k_y} \leq .5$. For $n = 1$, $k_{nm} \approx mk_y$.

February, 1992. Note 0124u-w.

We want to measure $\partial B_y/\partial x$. We move a B_y-coil in the x direction that is long in

In the region of interest, only the case of $m = 1$ is of importance. That is, the dominant term is

$$g_1 = \frac{b_{11} \sin k_y y \cdot \cosh k_{11} x}{\cosh k_{11} W}. \tag{5}$$

We may now proceed to conclude that

$$-H_y = k_z \sum n b_{n_0} \cos n k_z z \left(\cosh n k_z y + \sum b_{nm} \frac{m k_y}{n k_z} \cdot \frac{\cos m k_y y \cdot \cosh k_{nm} x}{\cosh k_{nm} W} \right). \tag{6}$$

From (6), we expect $b_{nm} < 0$, and $\frac{m k_y}{n k_z} |b_{nm}|$ to be in the order of 1, but probably less than 1.

Suggestions for Magnetic Measurements.

Make all measurements as function of z, filter out random errors, and then do the harmonic analysis by measuring the quantities derived from $\sinh n k_z y + g_n$. To measure field components, measure B_y at $y = 0$ for a number of values of x close enough to the lateral edge to get values of b_{n1} and b_{n2}. Then measurements of B_x close to the lateral ends are made, at $y \simeq h/2$, to check the validity of $V(x, y, z)$. If agreement is reached, an investigatation of whether b_{nm} are more easily obtained from B_x measurements is to be done. To verify the model, compare the measurements at individual points, without the harmonic analysis, to the model calculations.

After sufficient measurements, make a table that lists the b_{nm} coefficients as functions of two dimensionless products (i.e. h/λ and W/h), and possibly find a practical formula to represent the data. A possible complication may result from saturation in the iron which may dominate the behavior of the field as a function of x.

Examination of experimental data shows that decay of field errors as one moves away from the lateral edge of the insertion device can be much slower than this description indicates. A possible cause of this may be H_x at pole surface caused by saturation.

(11.1) assumes smooth sides, i.e., the excess potential drop is ignored. It should be noted that the area a in (8) is smaller than the cross-section shown in Figure 3(a), the latter includes the poles, while the former does not.

We make here further clarifications on units. If we were to deal with a uniform field over a width W of a flat pole, at distance h_0 from the midplane, ε would be exactly $\varepsilon = \frac{W}{H}$. That is, $\frac{d\Phi}{dx}$ and V have the same dimensions, meaning that either $\mu_0 = 4\pi \cdot 10^{-7}$ is incorporated in the vector potential V, or μ_0 is left out of the definition of Φ. The meaning of ε is the flux per unit length in the axial direction of the structure on potential V, divided by V.

ε_S with excess potential drop is given by

$$\varepsilon_S = \frac{4}{\pi} \ln\left(D_1 + \sqrt{D_1^2 - 1}\right) \tag{11.2}$$

with

$$D_1 = \frac{h_1 + \frac{2}{\pi}\Delta L}{h_0 + \frac{2}{\pi}\Delta L}. \tag{11.3}$$

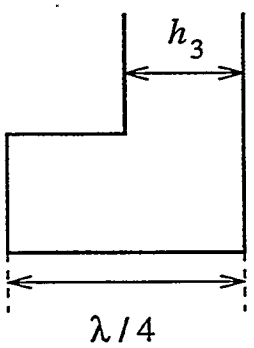

Figure 4.

$$\alpha = \frac{\lambda/4}{h_3} \quad \text{and} \quad \Delta L = \frac{h_3}{\pi}\left((\alpha+1)\ln(1+1/\alpha) + (\alpha-1)\ln(1-1/\alpha)\right). \tag{11.4}$$

The effect of ΔL will be very small under most circumstances. The excess flux

potential drop is too small to be of concern for ε_T.

3D Scalar Potential for Saturation-Caused Fields in the Insertion Device

This entails the same approach as for the case of $\mu = \infty$, except that the condition $\partial V/\partial x = 0$ at $y = h$ is to be dropped:

$$V = \sum \cos nk_z z \cdot g_n(x, y)\,,$$

$$\nabla^2 V = 0 \quad \Longrightarrow \quad \nabla^2 g_n = n^2 k_z^2 g_n\,.$$

We introduce $nk_z x = u$, and $nk_z y = v$:

$$\nabla^2_{u,v} g = g\,. \tag{1}$$

We construct $g(u, v)$ that has the following properties: odd in y, $g(-v) = -g(v)$, and gives field approximating $\cosh \varepsilon u - 1$ for $y = 0$. ε is arbitrary, real or imaginary, and the field equals 0 for $u = 0$ when letting $\varepsilon \to 0$ at end.

We try $g = \cosh \varepsilon u \sinh av$. To satisfy (1):

$$\varepsilon^2 + a^2 = 1 \quad \text{and thus} \quad \boxed{a = \sqrt{1 - \varepsilon^2}}$$

has to hold. We add a function of v, such that g'_v is proportional to $\cosh \varepsilon u - 1$ for $v = 0$. The only odd function of v that will satisfy this requirement and also satisfy (1) is $-a \sinh v$, thus

$$\boxed{g = \cosh \varepsilon u \sinh av - a \sinh v\,.} \tag{2}$$

One can use the superposition of such functions with different ε, but this would probably not be practical.

The expansion for $\varepsilon \to 0$ is

$$\boxed{g = \frac{\varepsilon^2}{2}\left(u^2 \sinh v - v \cosh v + \sinh v\right).} \tag{3}$$

For $v = 0$, we obtain the expected sextupole field:

$$g'_v(u, 0) = \frac{\varepsilon^2}{2} u^2\,. \tag{4}$$

At the pole, where $v_h = nk_z h$,

$$g'_u(u, v_h) = \frac{\varepsilon^2}{2} 2u \sinh v_h\,, \tag{5}$$

It is this field in the x-direction that is responsible for the sextupole field in the midplane.

February, 1992. Note 0125u-w.

(5) allows us to make an estimate of the saturation effects in the midplane during the design phase. Thus,

$$\frac{g'_v(u,0)}{g'_u(u,v_h)} = \frac{u}{2\sinh v_h} = \frac{nk_z x}{2\sinh nk_z h} = \frac{x}{2h}\cdot\frac{nk_z h}{\sinh nk_z h}. \tag{6}$$

It is interesting to note that every additional expansion of (2) in ε^2 leads to a new solution to (1) describing the fields in the midplane to the highest orders $\sim x^4, x^6$, etc.

To check on (3), its expansion in k_z up to the 3rd order terms in $\{u,v\}$ gives, as expected,

$$\begin{aligned} g &= \frac{\varepsilon^2}{2}\left(u^2 v - v\left(1+\frac{v^2}{2}-\left(1+\frac{v^2}{6}\right)\right)\right) \\ &= \frac{\varepsilon^2}{2}\left(u^2 v - \frac{v^3}{3}\right) \\ &= \frac{\varepsilon^2}{6}\Im(u+iv)^3. \end{aligned} \tag{7}$$

Scalar Potential for 3D Insertion Device Fields

In the 2D case,

$$(1) \qquad V = \sum_{n=\text{odd}} b_n \cos nk_z z \cdot \sinh nk_z y \quad \text{with} \quad k_z = \frac{2\pi}{\lambda}.$$

In order to simplify matters, we drop the sum, and re-introduce it at the end.

The effects of lateral ends are equally periodic in z, thus $nk_z \Rightarrow k_z$, and

$$(2) \qquad V_{LE} = \cos k_z z \cdot g(x,y).$$

Where $g(x,y)$ is valid only in the vacuum region of the $\{x,y\}$ space.

Further, we have that

$$(3) \qquad \nabla^2 V = 0 \quad \Longrightarrow \quad \nabla^2 g = k_z^2 g,$$

where g is the Fourier expansion coefficient as a function of x, y,

At the pole surface, for integer μ, $z = \mu\lambda/2$ and $y = h =$ half gap, $B_x = B_y = 0$. We expand g in a Fourier series in y. We have that $g \sim \sin mk_y y$ for $k_y = \pi/h$, and

$$g = \sum a_m \sin mk_y y \cdot \cosh k_m x,$$

with $k_m^2 = k_z^2 + m^2 k_y^2$. We use $a_m = b_0 b_m / \cosh k_m W$, where W is half the pole width, and we expect b_m to be only weakly dependent on W.

$$(4) \qquad \begin{cases} V = \displaystyle\sum_{n=\text{odd}} b_{n_0} \cos nk_z z \cdot (\sinh nk_z y + g_n), \\ g_n = \displaystyle\sum_{m=1} \frac{b_{nm} \sin mk_y y \cdot \cosh k_{nm} x}{\cosh k_{nm} W}, \\ k_{nm}^2 = n^2 k_z^2 + m^2 k_y^2, & \text{with } k_z = 2\pi/\lambda,\ k_y = \pi/h, \\ k_{nm}^2 = m^2 k_y^2 \left(1 + \dfrac{n^2}{m^2}\left(\dfrac{k_z}{k_y}\right)^2\right), & \text{with } \dfrac{k_z}{k_y} = \dfrac{2h}{\lambda} = \dfrac{\text{gap}}{\lambda}. \end{cases}$$

Under most circumstances, $\dfrac{k_z}{k_y} \leq .5$. For $n = 1$, $k_{nm} \approx mk_y$.

February, 1992. Note 0124u-w.

In the region of interest, only the case of $m = 1$ is of importance. That is, the dominant term is

$$g_1 = \frac{b_{11} \sin k_y y \cdot \cosh k_{11} x}{\cosh k_{11} W}. \tag{5}$$

We may now proceed to conclude that

$$-H_y = k_z \sum n b_{n_0} \cos n k_z z \left(\cosh n k_z y + \sum b_{nm} \frac{m k_y}{n k_z} \cdot \frac{\cos m k_y y \cdot \cosh k_{nm} x}{\cosh k_{nm} W} \right). \tag{6}$$

From (6), we expect $b_{nm} < 0$, and $\frac{m k_y}{n k_z} |b_{nm}|$ to be in the order of 1, but probably less than 1.

Suggestions for Magnetic Measurements.

Make all measurements as function of z, filter out random errors, and then do the harmonic analysis by measuring the quantities derived from $\sinh n k_z y + g_n$. To measure field components, measure B_y at $y = 0$ for a number of values of x close enough to the lateral edge to get values of b_{n1} and b_{n2}. Then measurements of B_x close to the lateral ends are made, at $y \simeq h/2$, to check the validity of $V(x, y, z)$. If agreement is reached, an investigatation of whether b_{nm} are more easily obtained from B_x measurements is to be done. To verify the model, compare the measurements at individual points, without the harmonic analysis, to the model calculations.

After sufficient measurements, make a table that lists the b_{nm} coefficients as functions of two dimensionless products (i.e. h/λ and W/h), and possibly find a practical formula to represent the data. A possible complication may result from saturation in the iron which may dominate the behavior of the field as a function of x.

Examination of experimental data shows that decay of field errors as one moves away from the lateral edge of the insertion device can be much slower than this description indicates. A possible cause of this may be H_x at pole surface caused by saturation.

Gradient Measurement in Insertion Device

The beam is in the z direction. The midplane is the $\{x, z\}$ plane. We use a vibrating coil to measure $\partial B_y/\partial x$.

As a general mechanical design principle, make the wanted resonance frequency and its harmonics different from the resonance frequencies of other vibrating modes.

We want to measure $\partial B_y/\partial x$. We move a B_y-coil in the x direction that is "long" in z and short in x. The problem arises that this motion may excite vibration in the y direction, adding a $\partial B_y/\partial y$ signal. A better way to collect the same information is to measure $\partial B_x/\partial y$, by vibrating a B_x-coil in the y direction such that it is "long" in z and short in y. Possible contamination due to $\partial B_x/\partial z$ drops out in the Fourier analysis in z.

February, 1992. Note 0120u-w.

Undulator Trajectory and Radiation

We begin with the following definitions:

$$\ddot{\mathbf{r}}\gamma m = -e(\mathbf{e}_x\dot{x} + \mathbf{e}_y\dot{y} + \mathbf{e}_z\dot{z}) \times \mathbf{e}_y B,$$

$$\ddot{x}\gamma m = e\dot{z}B = e\dot{z}A'_z,$$

$$\dot{x}\gamma m = \epsilon A(z),$$

$$dt\beta c = ds = dz\sqrt{1+x'^2}, \quad \dot{x} = x'\frac{\beta c}{\sqrt{1+x'^2}},$$

$$A = B_0 \int \cos kz dz = \frac{B_0}{k}\sin kz$$

$$\frac{x'}{\sqrt{1+x'^2}} = \varepsilon \sin kz, \quad \varepsilon = \frac{B_0/k}{\beta\gamma mc/e} = \frac{K}{\gamma},$$

$$\frac{1}{x'^2} + 1 = \frac{1}{\varepsilon^2 \sin^2 kz}, \quad \boxed{x' = \frac{es}{\sqrt{1-\varepsilon^2\sin^2 kz}}.}$$

Thus,

$$J = \int \dot{x} e^{i\varphi} dt,$$

where

$$\varphi = \omega\left(t - \frac{z}{c}\right) = \frac{\omega}{\beta c}(\beta ct - \beta z) = \frac{\omega}{\beta c}\int \left(\sqrt{1+x'^2} - \beta\right) dz,$$

$$1 + x'^2 = \frac{1}{1-\varepsilon^2\sin^2 kz},$$

$$\beta = \sqrt{1-\frac{1}{\gamma^2}} \simeq 1 - \frac{1}{2\gamma^2}.$$

and furthermore,

$$\sqrt{1+x'^2} - \beta = 1 + \frac{\varepsilon^2\sin^2 kz}{2} - 1 + \frac{1}{2\gamma^2} = \frac{1}{2\gamma^2}(1 + \varepsilon^2\gamma^2\sin^2 kz),$$

March, 1990. Note 0101u-w.

and

$$\varphi = \frac{\omega}{2\beta c\gamma^2}\int (1 + K^2 \sin^2 kz)dz = \boxed{\frac{\omega}{2\beta c\gamma^2}\int \left(1 + \frac{K^2}{2} - \frac{K^2}{2}\cos 2kz\right)dz,}$$

where, for $\beta \approx 1$,

$$\varphi = \frac{\omega}{2c\gamma^2}\left(1 + \frac{K^2}{2}\right)z - \frac{\omega}{2c\gamma^2}\frac{K^2}{2}\frac{\sin 2kz}{2k}.$$

Therefore,

$$J = \int x' dz \cdot e^{i\varphi}, \quad \text{with} \quad \frac{\omega}{c} = k_L,$$

$$J = \frac{\varepsilon}{2i}\int e^{i\left(\frac{k_L}{2\gamma^2}\left(1+\frac{K^2}{2}\right)-k\right)z - i\left(\frac{k_L}{2\gamma^2}\frac{K^2}{2}\frac{\sin 2kz}{2k}\right)}dz,$$

where

$$\Delta k = \left(\frac{k_L}{2\gamma^2}\left(1 + \frac{K^2}{2}\right) - k\right),$$

$$e^{iu\sin x} = \sum J_n(u)e^{inx}, \quad \text{with} \quad u = \frac{k_L K^2}{8\gamma^2 k} \quad \text{and} \quad x = kz.$$

Thus,

$$J = \frac{\varepsilon}{2i}\int e^{i(\Delta kz - 2nkz)}J_n(u)dz.$$

Further, from

$$\frac{k_L(1 + K^2/2)}{2\gamma^2} - (2n+1)k = 0,$$

and solving for $\frac{k_L}{k}$, we have

$$u = \frac{(n + 1/2)K^2/2}{1 + K^2/2}.$$

Mathematical Representation of Undulator and Wiggler Fields

Undulator and wiggler fields that are not uniform in the transverse direction are usually derived from

$$V = V \cosh k_1 x \sinh k_2 y \cos z \quad \text{with} \quad k_1^2 + k_2^2 = k^2. \tag{1}$$

Starting with $\nabla^2 V$ in cylindrical co-ordinates, we have

$$r^2 \nabla^2 V = \left(r^2 \frac{\partial^2}{\partial r^2} + r \frac{\partial}{\partial r} + \frac{\partial^2}{\partial \varphi^2} + r^2 \frac{\partial^2}{\partial z^2} \right) V = 0.$$

Assuming, without loss of generality, midplane symmetry, we write

$$V = \sum F_n \sin n\varphi \cos kz, \tag{2.1}$$

thus getting

$$\left(r^2 \frac{\partial^2}{\partial r^2} + r \frac{\partial}{\partial r} - n^2 - k^2 r^2 \right) F_n = 0. \tag{3}$$

and therefore,

$$F_n = a_n I_n(kr). \tag{2.2}$$

An interesting consequence is that whether one uses (1) or (2), one would get the same fields and pole shapes for a sufficiently small kr.

$$\sum a_n I_n(kr) \sin n\varphi = V_0 \cosh(k_1 r \cos\varphi) \sinh(k_2 r \sin\varphi), \tag{4}$$

and, in particular, this means that

$$a_n I_n(kr)\pi = V_0 \int_0^{2\pi} \cosh(k_1 r \cos\varphi) \sinh(k_2 r \sin\varphi) \sin n\varphi d\varphi. \tag{5}$$

This must hold in particular for $kr \ll 1$, i.e. by comparing the lowest order term in r and executing the trivial integrations, one gets a_n which then leads to an extremely interesting integral representation of $I_n(kr)$.

July, 1986. Note 0055u-w.

Publications of Klaus Halbach

(October 1994)

1. E. Baldinger, K. Halbach: "Berechnung der Zählversluste von Untersetzern nach der Theorie von Jost," Helv. Phys. Acta **24**, 315 (1951).
2. K. Halbach: "Berechnung linearer, realisierbarer Netzwerke zur Erzielung optimaler Signal/Rauschverhältnisse," Helv. Phys. Acta **26**, 65 (1953).
3. F. Alder, K. Halbach: "Das magnetische Kernmoment von Cr53," Helv. Phys. Acta **26**, 426 (1953).
4. K. Halbach: "Ueber eine neue Methode zur Messung von Relaxationszeiten und Åber den Spin von Cr53," Helv. Phys. Acta **27**, 259 (1954).
5. K. Halbach: "Modellunabhängige Beschreibung von Modulationseffekten bei der Kerninduktion," Helv. Phys. Acta **29**, 37 (1956).
6. K. Halbach: "Modulation-Effect Corrections for Moments of Magnetic Resonance Line Shapes," Phys. Rev. **119**, 1230 (1960).
7. K. Halbach, R. W. Layman: "Production of a Hot Rotating Plasma," Phys. Fluids **5**, 1482 (1962).
8. W. B. Kunkel, W. R. Baker, A. Bratenahl, K. Halbach: "Boundary Effects in Rotating Plasma Experiments," UCRL-10399; Phys. Fluids **6**, 699 (1963).
9. K. Halbach, W. R. Baker: "Plasma Gun Aspects of an E × B System," UCRL-10208; Phys. Fluids **7**, 562 (1964).
10. K. Halbach: "Matrix Representation of Gaussian Optics," Am. J. Phys. **32**, 90 (1964).
11. K. Halbach, D. B. Hopkins: "Operation of the Homopolar Gun II Coil System," *Proceedings of the Symposium on Engineering Problems of Controlled Thermonuclear Research* (1966).
12. K. Halbach: "A Program for Inversion of System Analysis and Its Application to the Design of Magnets," *Proceedings of the International Conference on Magnet Technology* (1967), p. 47.
13. R. M. Main, K. Halbach, P. Kennedy, R. Yourd, A. Watanabe, D. Kolody: "High Gradient Magnetic Drift Tube Quadrupoles," *Proceedings of the 1968 Proton Linear Accelerator Conference*, p. 52.
14. K. Halbach: "Application of Conformal Mapping to Evaluation and Design of Magnets Containing Iron with Nonlinear B(H) Characteristics," Nucl. Instrum. Methods **64**, 278 (1968).
15. K. Halbach: "Calculation of the Stray Field of Magnets with POISSON," Nucl. Instrum. Methods **66**, 154 (1968).
16. K. Halbach: "First Order Perturbation Effects in Iron Dominated Two Dimensional Symmetric Multipoles," Nucl. Instrum. Methods **74**, 147 (1969).
17. K. Halbach, R. Yourd: *Tables and Graphs of First Order Perturbation Effects in Iron Dominated Two-Dimensional Symmetrical Multipoles*, UCRL-18916, May 1969, 30 pp.
18. K. Halbach: "Fields and First Order Perturbation Effects in Two Dimensional Conductor Dominated Magnets," Nucl. Instrum. Methods **78**, 185 (1970).
19. K. Halbach, O. A. Anderson, D. Fuss: "Systematic Shaping of |B| on Flux Surfaces in Axisymmetric Toroidal Systems," Plasma Phys. **12**, 207 (1970).
20. K. Halbach: "Effect of Drift Tube Tolerances on the Electric Field Distribution Along the Length of an Alvarez Cavity," *Proceedings of the Proton Linear Accelerator Conference* (1970).
21. K. Halbach: "Field Correction Windings for Iron Magnets," Nucl. Instrum. Methods **107**, 529 (1973).
22. K. Halbach: "Some Eddy Current Effects in Solid Core Magnets," Nucl. Instrum. Methods **107**, 529 (1973).

23. K. Halbach: "A Magnetic Field Clamp with Beneficial Saturation Effects," Nucl. Instrum. Methods **119**, 327 (1974).

24. K. Halbach: "Rapid Measurement of the EFB of Homogeneous Field Magnets," Nucl. Instrum. Methods **119**, 329 (1974).

25. W. S. Cooper, K. Halbach, S. B. Magyary: "Computer Aided Extractor Design," *Proceedings 2, Symposium on Ion Sources and Formation of Ion Beams*, Berkeley, CA (1974).

26. K. Halbach: "Design Considerations for a Lumped Solenoid," *Proceedings of the 1975 PEP Summer Study*, Berkeley, CA (1975); LBL-4270.

27. K. Halbach: *Effect of Variable Measurement Coil Displacement on the Determination of the Harmonic Content of a Multipole*, SLAC, PEP-0208, February 1976, 8 pp.

28. F. Lobkowicz, U. Becker, K. Berkelman, Michael A. Green, E. Groves, K. Halbach, J. A. Kadyk, N. Mistry, A. Sessoms, M. Strovink: "A General Users Magnet Design," *Proceedings of the 1975 PEP Summer Study*, Berkeley, CA (1975), pp. 46–75.

29. K. Halbach: *Analysis of Some Errors in the Experimental Determination of the Harmonic Content of Multipole Magnets*, SLAC, PEP-0209 (February 1976), 13 pp.

30. H. D. Ferguson, J. E. Spencer, K. Halbach: "A General Ion-Optical Correction Element," Nucl. Instrum. Methods **134** (1976).

31. K. Halbach: *Mathematical Models and Algorithms for the Computer Program 'WOLF'* (1975); LBL-4444.

32. A. Abdel-Gawad, A. Hardt, S. Martin, J. Reich, K. L. Brown, K. Halbach: "Design Procedures for the Julich QQDDQ High Resolution Spectrometer," *Proceedings 7, International Cyclotron Conference*, Zurich (1975).

33. H. Ferguson, J. Spencer, K. Halbach: "A General Ion Optical Element," Nucl. Instrum. Methods **137**, 409 (1976).

34. K. Halbach: "A Simple Class of Beam Transport Systems with Optically Axisymmetric Transfer Properties," Nucl. Instrum. Methods **136**, 441 (1976).

35. K. Halbach, R. Holsinger: "SUPERFISH—A Computer Program for Evaluation of RF Cavities with Cylindrical Symmetry," Particle Accelerators **7**, 217 (1976).

36. K. Halbach, R. Holsinger, W. Jule, D. Swenson: "Properties of the Cylindrical RF Cavity Evaluation Code SUPERFISH," *Proceedings of the Proton Linear Accelerator Conference*, Chalk River (1976).

37. K. Halbach: *Coil Tolerance Effects in PEP Dipole*, SLAC, PEP-PTM-090 (February 1977).

38. K. Halbach: "Reply to the Comment by P. W. Hawkes on My Paper: A Simple Class of Beam Transport Systems with Optically Axisymmetric Transfer Properties," Nucl. Instrum. Methods **144**, 339 (1977).

39. Zebelman, W. Meyer, K. Halbach, A. Poskanzer, R. Sextro, G. Gabor, D.A. Landis: "A Time Zero Detector Utilizing Isochronous Transport of Secondary Electrons," Nucl. Instrum. Methods **141**, 439 (1977).

40. A. Colleraine, D. Doll, M. Holland, J. Kamperschroer, K. Berkner, K. Halbach, L. Resnick, A. Cole: "Parametric Study of the D3 Neutral Beam Injection System," *Proceedings of 10th Symposium on Fusion Technology*, Padua (1978).

41. R. Reimers, J. Peterson, R. Avery, K. Halbach, M. Kaviany, A. Lake, R. Main, D. Nelson, R. Nissen, J. Singh: "Magnets in the PEP Injection Line," *Proceedings of the 1979 Particle Accelerator Conference.*

42. R. Main, J. Tanabe, K. Halbach: "Measurements and Correction of the PEP Interaction Region Quadrupole Magnets," *Proceedings of the 1979 Particle Accelerator Conference*.

43. R. Avery, T. Chan, K. Halbach, R. Main, J. Tanabe: "PEP Insertion Quadrupole Design Features," *Proceedings of the 1979 Particle Accelerator Conference*.

63. D.H. Nelson, M. I. Green, K. Halbach, E. Hoyer: "Magnetic Measurements for Tuning and Operating a Hybrid Wiggler," J. Phys. (Paris) **45** (1984).

64. E. Hoyer, T. Chan, J.W.G. Chin, K. Halbach, K.-J. Kim, H. Winick, J. Yang: "The Beam Line VI REC—Steel Hybrid Wiggler for SSRL, IEEE Trans. Nucl. Sci. **NS-30**, 3118 (1983).

65. T. J. Orzechowski, M. C. Moebus, F. A. Penko, D. Prosnitz and D. Rogers (LLNL); C. S. Chavis, K. Halbach, D. B. Hopkins, R. W. Kuenning, A. C. Paul, A. M. Sessler, R. M. Yamamoto, and J. S. Wurtele (LBL): "The Status of the Lawrence Berkeley Laboratory and Lawrence Livermore National Laboratory Free Electron Laser (FEL)," presented at the 4th Workshop on FEL Devices (1983).

66. K.-J. Kim, J. J. Bisognano, A. A. Garren, K. Halbach, J. M. Peterson, A. M. Sessler, J. S. Wurtele (LBL); E. T. Scharlemann (LLNL): "A Design of a High Gain FEL-Storage Ring System," *Proceedings of the International Workshop on Coherent and Collective Properties in the Interaction of Relativistic Electrons and Electromagnetic Radiation*, Milan, Italy, September 13–16, 1984.

67. K.-J. Kim, J. J. Bisognano, A. A. Garren, K. Halbach, J. M. Peterson: "Issues in Storage Ring Design for Operation of High Gain FELs, *Proceedings of the International Workshop on Coherent and Collective Properties in the Interaction of Relativistic Electrons and Electromagnetic Radiation*, Milan, Italy, September 13–16, 1984; Nucl. Instrum. Methods **A239**, 54 (1985).

68. J. M. Peterson, J. J. Bisognano, A. A. Garren, K. Halbach, K.-J. Kim, and R. C. Sah: "A Storage-Fing FEL for the VUV," *Proceedings of the 1984 Free Electron Laser Conference*, Castelgandolfo, Italy, September 1984.

69. K.-J. Kim, K. Halbach, and D. Attwood: "Coherent VUV and Soft X-ray Radiation from Undulators in Modern Storage Rings," *Laser Techniques in the Extreme UV*, AIP Conference Proc., No. 119 (1984), p. 267.

70. D. Attwood, K. Halbach, and K.-J. Kim: "Partially Coherent X-rays," *Proceedings of the Workshop on VUV and X-Ray Sources*, National Research Council, November 9, 1984.

71. G. E. Fischer, M. Anderson, R. Byers, K. Halbach: "SLC Arc Transport System—Magnet Design and Construction," *Proceedings of the 1985 Particle Accelerator Conference*, Vancouver, B.C., Canada, May 13–16, 1985; SLAC-PUB-3612.

72. K. Halbach: "Permanent Magnets for Production and Use of High Energy Particle Beams," *Proceedings of the 8th International Workshop on Rare-Earth Magnets and their Applications*, Dayton, OH, May 6–8, 1985; LBL-19285.

73. K. Halbach: "Application of Permanent Magnets in Accelerators and Electron Storage Rings," J. Appl. Physics **57**, Part IIA, 3605–3608 (1985).

74. K. Halbach, B. Feinberg, M. I. Green, R. MacGill, J. Milburn, J. Tanabe: "Hybrid Rare Earth Quadrupole Drift Tube Magnets," *Proceedings of the 1985 Particle Accelerator Conference*, Vancouver, B.C., Canada, May 13–16, 1985; LBL-18960.

75. K. Halbach, E. Hoyer, S. Marks, D. Plate, D. Shuman: "CSEM-Steel Hybrid Wiggler/Undulator Magnetic Field Studies," *Proceedings of the 1985 Particle Accelerator Conference*, Vancouver, B.C., Canada, May 13–16, 1985; LBL-19584.

76. D. Attwood, K. Halbach, K. J. Kim: "Tunable Coherent X-rays," Science **228**, 1265–1272 (1985).

77. D. Attwood, K. J. Kim, K. Halbach, M. R. Howells: "Undulators as a Primary Source of Coherent X-rays," *Proceedings of the International Conference on Insertion Devices for Synchrotron Sources*, SPIE **582**, 10 (1985); LBL-20569.

78. K. Halbach: "Some New Ideas About Undulators," *Proceedings of the First International Conference on Insertion Devices for Synchrotron Radiation Sources*, SPIE **582**, 68 (1985).

79. K. G. Tirsell, T. C. Brown, P. J. Ebert, W. C. Dickinson, E. M. Lent, E. Hoyer, K. Halbach, S. Marks, D. Plate, D. Shuman, R. Tatchyn: "Development of a NdFe-Steel Hybrid Wiggler for SSRL," SPIE **582**, 177 (1985).

44. K. Halbach: "Strong Rare Earth Cobalt Quadrupoles, *Proceedings of the 1979 Particle Accelerator Conference.*

45. R. Holsinger, K. Halbach: "A New Generation of Samarium Cobalt Quadrupole Magnets for Particle Beam Focusing Applications," *Proceedings of 4th International Conference on Rare Earth Cobalt Magnets and Their Applications* (1979).

46. K. Halbach: "Design of Permanent Multipole Magnets with Oriented Rare Earth Cobalt Material," Nucl. Instrum. Methods **169**, 1 (1980).

47. K. Halbach: "Physical and Optical Properties of Rare Earth Cobalt Permanent Magnets," Nucl. Instrum. Methods **187**, 109 (1981).

48. K. Halbach, J. Chin, E. Hoyer, H. Winick, R. Cronin, J. Yang, Y. Zambor: "A Permanent Magnet Undulator for SPEAR," *Proceedings of the 1981 Particle Accelerator Conference*, IEEE Trans. Nucl. Sci. **NS-28**, 3136 (1981).

49. K. Halbach: "Design of Focussing and Guide Structures for Charged Particle Beams Using Rare Earth Cobalt Permanent Magnets," *Proceedings of the 5th International Conference on Rare Earth Cobalt Permanent Magnets and Their Applications* (1981).

50. H. Winick, G. Brown, K. Halbach, J. Harris: "Wiggler and Undulator Magnets," Phys. Today **34**, 50 (1981).

51. R. L. Gluckstern, R. F. Holsinger, K. Halbach. G. Minerbo, "ULTRAFISH—Generalization of SUPERFISH to m>1," *Proceedings of 1981 Linear Accelerator Conference*, p. 102.

52. B. Feinberg, G. Brown. K. Halbach, W. B. Kunkel: "A Method for Improving the Quality of the Magnetic Field in a Solenoid," Nucl. Instrum. Methods **203**, 81 (1982).

53. K. Halbach: "Perturbation Effects in Segmented Rare Earth Cobalt Multipole Magnets," Nucl. Instrum. Methods **198**, 213 (1982).

54. K. Halbach: "Conceptual Design of a Permanent Quadrupole Magnet with Adjustable Strength," Nucl. Instrum. Methods **206**, 353 (1983).

55. K. Halbach: "Permanent Magnet Undulators, Journal de Physique, Colloque Cl, supplement au no. 2, Tome 44, p. C1–211 (1983).

56. T. J. Orzechowski, D. Prosnitz, K. Halbach, R. Kuenning, A. Paul, D. Hopkins, A. Sessler, G. Stover, J. Tanabe, J. Wurtele: "A High Gain Free Electron Laser at ETA," UCRL-88705, National Conference on High Power Microwave Technology, Harry Diamond Labs (1983).

57. H. Winick, H. Wiedemann, I. Lindau, K. Hodgson, K. Halbach, J. Cerino, A. Bienenstock, R. Bachrach: "An All Wiggler and Undulator Synchrotron Radiation Source," IEEE Trans. Nucl. Sci. **NS-30**, 3097 (1983).

58. K. Halbach: "Permanent Multipole Magnets with Adjustable Strength," IEEE Trans. Nucl. Sci. **NS-30**, 3323 (1983).

59. S. A. Martin, A. Hardt, J. Meissburger, G. Berg, U. Hacker, W. Hurlimann, J. Romer, T. Sagefka, A. Retz, O. Schult, K. Brown, K. Halbach: "The QQDQ Magnet Spectrometer 'Big Karl'," Nucl. Instrum. Methods **214**, 281 (1983).

60. C. Bahr, T. Chan, J. Chin, T. Elioff, K. Halbach, G. Harnett, E. Hoyer, D. Humphries, D. Hunt, K. Kim, T. Lauritzen, D. Lindle, D. Shirley, R. Tafelski, A. Thompson, LBL; S. Cramer, P. Eisenberger, R. Hewitt, J. Stohr, Exxon; R. Boyce, G. Brown, A. Golde, R. Gould, N. Hower, I. Lindau, H. Winick, J. Yang, SSRL; J Harris, B. Scott, SLAC: "A New Wiggler Beam Line for SSRL," Nucl. Instrum. Methods **208**, 117 (1983).

61. E. Hoyer, T. Chan, J. Chin, K. Halbach, K.-J. Kim, H. Winick, J. Yang: "The REC Steel Hybrid Wiggler for SSRL," IEEE Trans. Nucl. Sci. **NS-30**, 3118 (1983).

62. G. Brown, K. Halbach, J. Harris, H. Winick: "Wiggler and Undulator Magnets—A Review," Nucl. Instrum. Methods **208**, 65 (1983).

80. A. Jackson, J. Bisognano, S. Chattopadhyay, M. Cornacchia, A. Garren, K. Halbach, K. J. Kim, H. Lancaster, J. Peterson, M. S. Zisman, C. Pellegrini, G. Vignola: "Optimization of the Parameters of a Storage Ring for a High Power XUV Free Electron Laser," SPIE **582**, 131 (1985).

81. K.-J. Kim, J. Bisognano, S. Chattopadhyay, M. Cornacchia, A. A. Garren, K. Halbach, A. Jackson, H. Lancaster, J. Peterson, M. S. Zisman, C. Pellegrini, and G. Vignola: "Storage Ring Design for a Short Wavelength FEL," IEEE Trans. Nucl. Sci. **32**, 3377–3379 (1985).

82. M. Cornacchia, J. Bisognano, S. Chattopadhyay, A. Garren, K. Halbach, A. Jackson, K.-J. Kim, H. Lancaster, J. Peterson, M. S. Zisman, C. Pellegrini, G. Vignola: "Design Concepts of a Storage Ring for a High Power XUV Free Electron Laser," Nucl. Instrum. Methods **A250**, 57 (1986).

83. J. Bisognano, S. Chattopadhyay, M. Cornacchia, A. Garren, A. Jackson, K. Halbach, K.-J. Kim, H. Lancaster, J. Peterson, M. S. Zisman, C. Pellegrini, G. Vignola: "Feasibility Study of a Storage Ring for a High Power XUV Free Electron Laser," Particle Accelerators **18**, 223 (1986); LBL-19771.

84. K. Halbach: "Concepts for Insertion Devices that will Produce High-Quality Synchrotron Radiation," Nucl. Instrum. Methods **A246**, 77 (1986); LBL-20174.

85. K. Halbach: "Some Concepts to Improve the Performance of DC Electromagnetic Wigglers," Nucl. Instrum. Methods **A250**, 115 (1986); LBL-20502.

86. K. Halbach: "Desirable Excitation Patterns for Tapered Wigglers," Nucl. Instrum. Methods **A250**, 5 (1986); LBL-20564.

87. K. Halbach: "Magnet Innovations for Linacs," *1986 Linear Accelerator Conference Proceedings*, SLAC Report 303 (1986), p. 407.

88. K. Halbach: "Specialty Magnets," *Physics of Particle Accelerators*, AIP Conference Proceedings, No. 153 (1987), p. 1277; LBL-21945.

89. B. Feinberg, J. Tanabe, K. Halbach, G. Koehler, M.I. Green: "Adjustable Rare Earth Quadrupole Drift Tube Magnets," *Proceedings of the 1987 IEEE Accelerator Conference*, p. 1419.

90. K. Halbach: "Use of Permanent Magnets in Accelerator Technology: Present and Future," *Proceedings of the Symposium on Permanent Magnet Materials*, MRS Spring Meeting., Anaheim, CA, April 23–25, 1987.

91. E. Hoyer, K. Halbach, D. Humphries, S. Marks, D. Plate, D. Shuman (LBL); V. P. Karpenko, S. Kulkarni, K. G. Tirsell (LLNL): "The Beam Line X NdFe-Steel Hybrid Wiggler for SSRL," *Proceedings of the 1987 IEEE Accelerator Conference*, p. 1508.

92. K. Halbach: "Description of Beam Position Monitor Signals with Harmonic Functions and Their Taylor Series Expansions," Nucl. Instrum, Methods **A260**, 14–32, 1987; LBL-22840.

93. G. A. Deis, A. R. Harvey, C. D. Parkison, D. Prosnitz, J. Rego, E. T. Scharlemann (LLNL); K. Halbach (LBL): "A Long Electromagnetic Wiggler or the Paladin Free-Electron Laser Experiments," *Proceedings of the Tenth International Conference on Magnet Technology*, September 23–26, 1987.

94. G. A. Deis, M. J. Burns, T. C. Christensen, F. E. Coffield, B. Kulke, D. Prosnitz, E. T. Scharlemann (LLNL); K. Halbach (LBL): "Electromagnetic Wiggler Technology Development at the Lawrence Livermore National Laboratory," *Proceedings of the Tenth International Conference on Magnet Technology*, September 23–26, 1987.

95. M. J. Burns, G. A. Deis, R. H. Holmes, R. D. Van Maren (LLNL); K. Halbach (LBL): "Development of the Strong Electromagnet Wiggler," *Proceedings of the Tenth International Conference on Magnet Technology*, September 23–26, 1987.

96. T. C. Christensen, M. J. Burns, G. A. Deis, C. V. Parkison, D. Prosnitz (LLNL); K. Halbach (LBL): "Development of a Laced Electromagnetic Wiggler," *Proceedings of the Tenth International Conference on Magnet Technology*, September 23–26, 1987.

97. K. Halbach: "Consequences of Tolerances in Undulators," *Proceedings of the Workshop on Scientific and Technological Applications of Synchrotron Radiation*, Miramare, Trieste, Italy, May 14–15, 1987.

98. D. B. Hopkins, E. H. Hoyer, K. Halbach, A. M. Sessler, W. A. Barletta, R. A. Jong, L. L. Reginato, S. S. Yu, J. R. Bayless, R. B. Palmer: *A FEL Power Source for a TeV Linear Collider*, LBL-25936-mc, October 1988.

99. B. Feinberg, G. U. Behrsing, K. Halbach, J. S. Marks, M. E. Morrison, D. H. Nelson: "Laced Permanent Magnet Quadrupole Drift Tube Magnets, *Proceedings of the IEEE Particle Accelerator Conference*, Chicago, IL, March 20–23, 1989; also, *Proceedings of the Linear Accelerator Conference*, Williamsburg, VA, October 2–7, 1988.

100. D. B. Hopkins, K. Halbach, E. H. Hoyer, A. M. Sessler, E. J. Sternbach: "Elements of a Realistic 17-GHz FEL/TBA Design," *Proceedings of the 1989 Workshop on Advanced Accelerator Concepts*, Lake Arrowhead, CA, January 9–13, 1989.

101. W. Hassenzahl, J. Chin, K. Halbach, E. Hoyer, D. Humphries, B. Kincaid, and R. Savoy: "Insertion Devices for the Advanced Light Source at LBL," *Proceedings of the 1989 IEEE Particle Accelerator Conference*, Chicago, IL, March 20–23, 1989.

102. M. Cornacchia, K. Halbach: "Study of Modified Sextupoles for Dynamic Aperture Improvement in Synchrotron Radiation Sources," SLAC-PUB-5096; Nucl. Instrum. Methods **A290**, 19 (1990).

103. E. Hoyer, J. Chin, K. Halbach, W. Hassenzahl, D. Humphries, B. Kincaid, H. Lancaster, D. Plate, and R. Savoy: "The U5.0 Undulator Design for the Advanced Light Source at LBL," *Proceedings of the 6th National Conference on Synchrotron Radiation Instrumentation*, Berkeley, CA, August 7–10, 1989.

104. R. Savoy, K. Halbach, W. Hassenzahl, E. Hoyer, D. Humphries, and B. Kincaid: "Calculation of Magnetic Error Fields in Hybrid Insertion Devices," *Proceedings of the 6th National Conference on Synchrotron Radiation Instrumentation*, Berkeley, CA, August 7–10, 1989; Nucl. Instrum. Methods **A291**, 408 (1990).

105. J. Tanabe, R. Avery, R. Caylor, M. I. Green, E. Hoyer, K. Halbach, S. Hernandez, D. Humphries, Y. Kajiyama, R. Keller, W. Low, S. Marks, J. Milburn, D. Yee: "Fabrication and Test of Prototype Ring Magnets for the ALS," *Proceedings of the 1989 IEEE Particle Accelerator Conference,* Chicago, IL, March 20–23, 1989.

106. K. Halbach: Insertion Device Design: 16 lectures presented from October 1988 to March 1989, LBL-V8811-1.1-16.

107. K. Halbach: "Understanding Modern Magnets through Conformal Mapping," *Proceedings of the Bloch Symposium*, Stanford, CA, October 27, 1989; International Journal of Modern Physics B **4**, 1201 (1990); LBL-28395.

108. K. Halbach: Magnet Technology: 6 lectures presented from February to April 1990, LBL-V920-2.1-6.

109. K. Halbach: *Summary of the 3-D Hybrid Theory, with some Applications to the Assessment of Perturbation Effects*, ALS Note LSBL-034 (1990).

110. R. Savoy, K. Halbach: "Design Considerations for a Fast Modulator in a 'Crossed Undulator'," *Proceedings of the IEEE 1991 Particle Accelerator Conference.*

111. C. Pellegrini, D. Robin, D. Cline, J. Kolonko, C. Anderson, W. Barletta, A. Chargin, M. Cornacchia, G. Dalbacka, K. Halbach, E. Lueng, F. Kimball, D. Madura, L. Patterson: "A High Luminosity Superconducting Mini Collider for Phi Meson Production and Particle Beam Physics," *Proceedings of the IEEE 1991 Particle Accelerator Conference*.

112. E. Hoyer, J. Chin, K. Halbach, W. V. Hassenzahl, D. Humphries, B. Kincaid, H. lancaster, D. Plate: "The U5.0 Undulator for the ALS," *Proceedings of the IEEE 1991 Particle Accelerator Conference.*

113. M. Cornacchia, W. J. Corbett, K. Halbach: "Study of Modified Octupole Magnets for Landau Damping with Dynamic Aperture Preservation," *Proceedings of the IEEE 1991 Particle Accelerator Conference.*

114. E. Hoyer, J. Chin, K. Halbach, W. Hassenzahl, D. Humphries, B. Kincaid, H. Lancaster, D. Plate, R. Savoy: "The U5.0 Undulator Design for the Advanced Light Source at LBL," Nucl. Instrum. Methods **A291**, 383 (1990).

115. E. Hoyer, J. Chin, K. Halbach, W. V. Hassenzahl, D. Humphries, B. Kincaid, H. Lancaster, D. Plate: "ALS Insertion Devices," *Proceedings of the Topical Conference on Vacuum Design of Synchrotron Light Sources* (1990).

116. T. J. Orzechowski, J. L. Miller, J. T. Weir, Y. P. Chong, F. Chambers, G. A. Deis, A. C. Paul, D. Prosnitz, K. Halbach, J. Edighoffer: "Free-Electron Laser Results from the Advanced Test Accelerator," Proceedings of the 1988 Linear Accelerator Conference.

117. K. Halbach: "Integration of Beam Position Monitor Signals," Nucl. Instrum. Methods **A297**, 531 (1990).

118. M. I. Green, P. Barale, L. Callapp, M. Case-Fortier, D. Lerner, D. Nelson, R. Schermer, G. Skipper, D. Van Dyke, C. Cork, K. Halbach, *et al.*: "Magnetic Measurements at Lawrence Berkeley Laboratory," IEEE Trans. Magn. **28**, 797 (1992).

119. M. A. Green, K.-J. Kim, P. J. Viccaro, E. Gluskin, K. Halbach, R. Savoy, R. Trzeciak: "Rapidly Modulated Variable Polarization Crossed Undulator Source," Rev. Sci. Instrum. **63**, 336 (1992).

120. E. Hoyer, J. Chin, K. Halbach, W. V. Hassenzahl, D. Humphries, B. Kincaid, H. Lancaster, D. Plate: "The U5.0 Undulator for the Advanced Light Source," Rev. Sci. Instrum. **63**, 359 (1992).

121. E. Blum, K. Halbach: "Performance of Electro Magnet and Permanent Magnet Quadrupoles with Iron Poles," Nucl. Instrum. Methods **A320**, 432 (1992).

122. C. Pellegrini, J. Rosenzweig, G. Travish, K. Bane, ... K. Halbach, *et al.*: "The SLAC Soft X-ray High Power FEL," Nucl. Instrum. Methods **A341**, 326 (1994).

123. R. D. Schlueter, K. Halbach: "Harmonics Suppression of Fields Arising from Vacuum Chamber Eddy Currents, with Applications to SSC Low Energy Booster Magnets," IEEE Trans. Magn. **30**, 2130 (1994).

124. R. D. Schlueter, K. Halbach: "Skew Harmonics Suppression in Electro Magnets, with Applications to the Advanced Light Source Storage Ring Corrector Magnet Design," IEEE Trans. Magn. **30**, 2126 (1994).

125. H. Winick, K. Bane, R. Boyce, J. Cobb, ... K. Halbach, *et al.*: "Short Wavelength FEL's Using the SLAC Linac," Nucl. Instrum. Methods **A347**, 199 (1994).

Technical Notes of Klaus Halbach

Database Reference	Title	Year
0001bpm	"Notes on a beam position monitor	86
0002bpm	Beam position error due to error in electric signals	86
0003bpm	2D pickup electrode design (square box)	86
0004bpm	Position monitor signal for finite size beam	86
0005bpm	Justification for treating beam position monitors 2D and statically	86
0006bpm	2D pickup electrode system design (diamond box)	86
0007bpm	Moments $g_m = \int z^m \rho(x,y) dxdy$ of charge distributions, and properties of Gaussian distribution	86
0008bpm	Measurement of harmonic coefficients of beam pos. monitor model	86
0009bpm	Harmonics for various mixing patterns of beam position detector signals & their use	86
0010bpm	Algorithms for evaluation of fields from electrode in diamond duct	86
0011bpm	Formula summary	86
0012bpm	Specific design options; double electrode systems	86
0013bpm	Length normalization, and desirable duct size	86
0014bpm	F from dipole moment $q'\|\Delta z\|$ on duct surface	86
0015bpm	Actual integrated charge on electrode	86
0016bpm	Map of duct with photon slot onto circular disk	86
0017bpm	Expansion coefficients of finite size round electrodes flush in 2D duct	86
0018bpm	Reciprocity theorem for current → pickup loop	86
0019bpm	Outline for calculation of integrated harmonics along an axis that is skewed relative to axis of finite length multipole	86
0020bpm	Algorithm for calculation of beam position from measurements	86
0021bpm	$W = \int_{-\infty}^{+\infty} V(z) dz$ from finite length electrode in 2D geometry	86
0022bpm	Exact, complete proofs of reciprocity theorems for electrostatic and magnetostatic beam monitors	86
0023bpm	Design objectives to be achieved by electrode placements in duct	86
0024bpm	Performance requirements for BPM signal processing system	86
0025bpm	Details about model time domain transfer functions for BPM signal process	86
0026bpm	Farler method to design single and double integrator	86
0027bpm	Design of wide flat top $F(u)$	86
0028bpm	Some thoughts on integrators	86

0062bpm	Multipole expansion of field produced by circular electrode in circular duct	89
0063bpm	Proof that for reciprocity potential in BPM duct $G(x,y,s)=\left(\frac{\partial}{\partial x^2}+\frac{\partial}{\partial y^2}\right)\int V_3(x+sz,y,z)dz \neq 0$ *for* $s \neq 0$	89
0064bpm	Uniqueness of beam position from BPM signals	93
0065bpm	BPM data reduction program BPM5	93
0066bpm	Proper signs of coefficients for $F(z)$ for electrostatic BPM	93
0067bpm	Uniqueness of beam location from BPM signals	93
0068bpm	BPM designed to measure p_2	93
0069bpm	BPM in parallel plate duct, without harmonic expansion	93
0070bpm	BPM in parallel plate duct, with harmonic expansion	93
0071bpm	Map of interior of Gm1 onto circular unit disk for BPM creation	93
0001csem	Description of REC material in magnetic circuit	78
0002csem	Analytical fields for 4-pole with 2 REC blocks in 45 d sector	78
0003csem	REC quadrupole with continuously changing M direction	78
0004csem	Permanent REC multipole with continuously changing magnetization direction	78
0005csem	Properties of REC magnetic buckets with geometry invariant against rotation by $2\pi/M$	78
0006csem	Ideas about manufacturing procedures for REC quads	78
0007csem	Production of solenoidal fields with REC	78
0008csem	Properties of REC multipole buckets (includes easy axis rotation theorem)	78
0009csem	Reduction of REC material in "my" REC quadrupoles by replacing part of it with $\mu = \infty$ steel	78
0010csem	Magnetization of hexagon and triangle for quadrupole production	78
0011csem	Tuning parameters for 16-piece REC quad	78
0012csem	Multipiece REC quad: design and tolerances	78
0013csem	Multipiece REC multipole	78
0014csem	Efficiency of REC use in continuous quadrupole	78
0015csem	Multipiece quad with Ron-shaped pieces	78
0016csem	Properties of Ron-shaped poles	78
0017csem	Recommended geometry for PIGMI quads	78
0018csem	Memo to Swenson, Farrell, Knapp	78
0019csem	Quad from magnetized REC circular rods of given size	78
0020csem	Magnetic fields produced by some REC configurations	78

0021csem	Different method to drive fields for continuous REC multipoles and optimum design	78
0022csem	Segmented REC multipole in $\mu = \infty$ shell	78
0023csem	Linear array of REC magnets as plasma bucket wall (with bucket physics)	78
0024csem	Data for Ron's 16-piece quad, and general REC price information	78
0025csem	Elimination of first allowed harmonic in multipiece REC multipoles	78
0026csem	REC quad with circular rods	79
0027csem	Various methods to calculate fields produced by REC pieces	79
0028csem	Fields produced by rectangular charge sheet	79
0029csem	Nomogram for wiggler design	79
0030csem	Helical wiggler performance evaluation	79
0031csem	Continuous helical REC wiggler; Fourier expansion of $\mathbf{H}_c$	79
0032csem	Helical wiggler fields, with all Fourier components	82
0033csem	Fourier decomposition of $\mathbf{H}_c$ in segmented helical multipoles	82
0034csem	Continuous helical multipole magnet	79
0035csem	Rough comparison between REC wiggler and REC wiggler with steel pole	79
0036csem	REC in circular $\mu = \infty$ shell	79
0037csem	Fringe fields at the ends of REC multipoles (general properties)	79
0038csem	A possible REC undulator for SSRL	79
0039csem	Periodic solenoidal fields with continuous REC easy axis orientation	79
0040csem	Optimum easy axis orientation of REC to produce solenoidal field $\approx \sin kz_0$	79
0041csem	REC dipole with $\mu = \infty$ steel	79
0042csem	Field on axis produced by REC rings with fixed easy axis	79
0043csem	List of problems to be done for prod of solenoidal fields with pure REC structures	79
0044csem	Finite REC structure (for solenoidal fields) with $H_{z,\text{center}} = \text{Max}$ with given r_1	79
0045csem	Optimization of field at center of single cylindrical REC shell	79
0046csem	Perturbation effects in segmented REC multipoles	79
0047csem	Numbered equations of my REC multipole paper	79
0048csem	Fields on axis of 1/0 long filamentary helix	79
0049csem	Fringe fields of REC undulator in direction perp beam: primitive model	79
0050csem	Forces between 2 halves of linear undulator	79
0051csem	Stray field from continuous REC undulator in direction perp beam	79

0082csem	Conversion between coordinate system used in iron and REC perturbation papers and conventional measurement coordinate system	81
0083csem	EFB of REC quad next to steel plate	81
0084csem	REC and steel quadrupole design	82
0085csem	Different methods for understanding, or design, of REC magnets	82
0086csem	CTR multi-aperture magnet MAM	82
0087csem	A new method to design REC and steel (hybrid) magnets	82
0088csem	Fields produced by a REC helical undulator (summary)	82
0089csem	Fields produced by coils with rectangular cross section (ELF #51)	82
0090csem	Formulas for REC-steel (hybrid) dipole corner: excess flux and flux from REC	82
0091csem	Excess flux in Gm2	82
0092csem	Excess flux in Gm3 corner $3\pi/4$ corner	82
0093csem	Excess flux in Gm3 corner with arbitrary angle	82
0094csem	Excess flux in Gm5 corner with arbitrary angle	82
0095csem	Flux deficiency of Gm6 corner with arbitrary angle	82
0096csem	Flux deficiency of 90° inside corner	82
0097csem	Summary of formulas for calculation of excess flux and flux deficiencies at corners	82
0098csem	Hybrid dipole formulae	82
0099csem	Incorporation of finite $\mu - 1$ of REC into hybrid design	82
0100csem	Flux deposition by magnetic charge between two parallel plates (3D)	82
0101csem	HFIX notes (old)	81
0102csem	3D quad fringe field note (old)	81
0103csem	Hybrid wiggler/undulator optimization - notes	81
0104csem	Hybrid wiggler design information	82
0105csem	Fraction of magnetic charge deposited on steel plate	82
0106csem	Harmonics produced by a rectangular block	82
0107csem	Excess flux into "open end" of steel of hybrid dipole/wiggler	82
0108csem	Excess flux into Gm7	82
0109csem	Analytical hybrid wiggler model	82
0110csem	Ideas and program to develop a variable strength hybrid quadrupole and dipole	82
0111csem	Conjecture about charge deposited (in V-Q model) by dipole	82
0112csem	Charge deposition on 3D steel surfaces of V-Q model by magnetic charge and dipole	82
0113csem	Force, torque on rotatable ring in VSHQ	82

0173csem	Fraction of charge deposited on several surfaces on $V = 0$	82
0174csem	"DNA-Project" (Vachette)	82
0175csem	Investigation of possible geometries for dipoles and quadrupoles suitable as elements of an e-storage ring	82
0176csem	Reprints left at Orsay	82
0177csem	Use of HD1P2, VHYBQ6, 7; LEFF	82
0178csem	Optimum operating point of CSEM	83
0179csem	Effectiveness of CSEM in "unused" corner of 2D box magnet, and in a 3D magnet	83
0180csem	Calculation of $\int_{-\infty}^{0} \frac{V(x)dx}{V_0}$ for Gm11	83
0181csem	Calculation of $\int_{-\infty}^{0} \frac{V(x)dx}{V_0}$ for Gm11 (more concise)	84
0182csem	Excess flux into corner in Gm12	83
0183csem	Excess flux into Gm13	83
0184csem	Conceptual design procedure for hybrid wiggler with superimposed "uniform" field	83
0185csem	Charge deposition in wiggler excited as a dipole	83
0186csem	Excess flux in Gm14 and Gm15	83
0187csem	Hybrid undulator with superimposed quadrupole field	83
0188csem	Practical approximations for flux deposition from charge sheet in Gm16	83
0189csem	SC transf. of Gm17, and excess flux, for POLE	83
0190csem	Design procedure for a hybrid-hybrid wiggler (ELF #93)	84
0191csem	2D hybrid-hybrid design formulae (ELF #94)	84
0192csem	Hybrid wiggler with 1/0-thin pole	84
0193csem	H^* and F produced by trapezoidal block of CSEM	84
0194csem	Calculation of H^* and F produced by "polygonal" block of CSEM	84
0195csem	Measurement of magnetic properties of trapezoidal block of CSEM for multiple magnet	84
0196csem	Estimate of Leff of hybrid quad without field clamp	84
0197csem	Minimization of excitation errors in hybrid quads	84
0198csem	$\int B^2\, dx$ – deficiency in midplane of Gm8	84
0199csem	Design of CSEM damping wiggler - (for DW1 program)	84
0200csem	Summary of excess flux formulae and copies	82
0201csem	Calculation of gradient off axis from gradient on axis	84
0202csem	Formulae for optimization of volume of ring magnet to produce given field	84
0203csem	Program for development of balloon magnet	84

0204csem	Program and printout of optimum dipole ring magnet for given field	84
0205csem	Tolerances that lead to field errors in hybrid U/W	84
0206csem	"Simple flux" into conical surfaces in cyl. geometry	84
0207csem	Ring-magnet design program LA1	84
0208csem	Antisymmetric Undulator to make vertically polarized or circularly polarized light	84
0209csem	Hybrid pole width optimization (neomax)	84
0210csem	CSEM "no center piece" septum magnet	84
0211csem	Thoughts on the design of antisymmetric hybrid W/U	84
0212csem	Antisymmetric hybrid W/U analysis/design	84
0213csem	HDIP5	84
0214csem	Field produced by rectangular charge sheet (87 - Zylin note)	82
0215csem	$\int Vdx$ in Gm18 corner	84
0216csem	Representation of hybrid W/U by ladder network	84
0217csem	V, A in Gm19	85
0218csem	SC transformation and fields in Gm20	85
0219csem	Scheme to achieve cancellation of net flux into beam region of U due to change gap	85
0220csem	Flux load on V-bus due to statistical fluctuations in CSEM flux deposition on poles	85
0221csem	Direct flux to midplane due to half-gap change of one pole	85
0222csem	Flux deposition on V = constant surface from magnetic charges, with anisotropic medium	85
0223csem	Even vs. odd number of poles in U/W	85
0224csem	New approximation for flux deposition from charge sheets in Gm16	85
0225csem	Explicit expansion of fields for $x \rightarrow \infty$ in Gm16	85
0226csem	Charge deposition from coil on pole in 2D	85
0227csem	An apparent paradox associated with charge deposition from coil on pole in 3D	85
0228csem	"Excess" flux at inside corner of Gm3	83
0229csem	Flux into end of hybrid quad	84
0230csem	End flux in VHBQ (for HQ1)	84
0231csem	VHBQ end flux formulas for comp. progr.	84
0232csem	2D hybrid U/W that is equivalent to helical hybrid U/W	85
0233csem	"Flux" seen by straight trajectory under one CSEM block pair in pure CSEM undulator	85
0234csem	Measurement of properties of CSEM block to be used in CSEM-iron circuit	85
0235csem	Fields in Gm16	85

0271csem	Design of bucket system (Physics)	86
0272csem	Thoughts on CSEM and iron solenoid magnet for Ed Rowe	86
0273csem	Excess voltage in Gm16	86
0274csem	Excess voltage in Gm16 (see work of 10/86 note)	88
0275csem	Ideas on producing strong solenoidal fields with a hybrid CSEM system (for Aladdin user)	86
0276csem	Execution of strong hybrid solenoid design	86
0277csem	Excitation of cylindrical box magnet/hybrid solenoid	86
0278csem	CSEM ring dipole assembled with square blocks	86
0279csem	Analysis of low field performance of PM assisted em	86
0280csem	HQ1, B_{max} for HQ1	86
0281csem	Laud quad	86
0282csem	V = constant surfaces inside CSEM multipole ($n \geq 2$)	87
0283csem	Solenoid fields from CSEM cylinder, axially magnetized (for Ian Brown)	87
0284csem	Stan Ruby's problem	87
0285csem	New version of bitter map for Gm17	88
0286csem	An important theorem, and a new map for Gm17	87
0287csem	Manageable integrals for map of Gm17	88
0288csem	F_{01} and F_{12} for small n for Gm5	88
0289csem	$\int B' dz$ for CSEM quad with conical ends	88
0290csem	Some excess flux geometries that are very easily analyzed	88
0291csem	Fields, flux, etc. in 2D hybrid wiggler with 0 thickness poles	88
0292csem	Calculation of flux entering $\mu = \infty$ surfaces	88
0293csem	ΔB^* due to displacement of rectangular 2D CSEM block in vacuum	88
0294csem	Use of 2D excess flux formulae in cylindrical geometry and for 3D edges	88
0295csem	Excess flux into pole in Gm34	88
0296csem	Excess flux into Gm35	88
0297csem	Preliminary design of hybrid orange spectrometer	88
0298csem	Orange spectrometer ray tracing in midplane	88
0299csem	Excess flux in Gm2	88
0300csem	Efficiency of use of CSEM in Ian B.'s magnet	88
0301csem	Hybrid U/W design in dipole geometry	88
0302csem	Excess flux in Gm36	88
0303csem	Excess flux coefficients/calculation for the end of hybrid multipoles	88
0304csem	H^* at edge of CSEM block, with recipe for $\Im \ln \frac{z-z_2}{z-z_1}$	88
0305csem	Laced cylindrical electromagnet	88

0338csem	Fields from charge sheet in xy-plane at $z = 0$	93
0001ctr	Field perturbation of homogeneous field by sphere	76
0002ctr	$2K = \int \frac{B(B_o - B)}{B_o^2} dz$ for Gm24	76
0003ctr	$2K = \int \frac{B(B_o - B)}{B_o^2} dz$ for Gm42	76
0004ctr	Flux and EFB for corner magnet (Gm24)	76
0005ctr	At least one focus for any hard edge magnet	76
0006ctr	First order optics for swap magnet without space charge	76
0007ctr	First order matrices for bending magnet	76
0008ctr	Bend magnet with two EFBs parallel to each other	76
0009ctr	Some optical properties of reflection sweep magnet	76
0010ctr	Extrapolated penetration for exponential field	76
0011ctr	Achromatization condition for displacement in reflection magnet	76
0012ctr	Continuation of 0011ctr	78
0013ctr	Two-step field distribution to give minimum of extrapolated penetration	76
0014ctr	Results of transmission magnet and various notes	77
0015ctr	How to deal with multiple beams in bendplane	76
0016ctr	Space charge effects on a straight line in phase space	76
0017ctr	Effects of constant **E** on phase space point	76
0018ctr	Space charge effects in band beam	76
0019ctr	Scraping of beam at walls parallel to the midplane (two versions)	76
0020ctr	Minimum spot size and maximum density in bend magnet	76
0021ctr	Production of second half of reflection matrix	76
0022ctr	Analytical bend plane matrix properties	76
0023ctr	Actual numbers for power deposition normalization	76
0024ctr	First order matrix in bend plane for $B_z(x,y) = B(y)$	76
0025ctr	Matrix perpendicular to bendplane (two versions)	77
0026ctr	Trajectories in strip magnet III	76
0027ctr	Trajectories in strip magnet II (Reference trajectory in midplane)	76
0028ctr	Trajectories in strip magnet I	76
0029ctr	Fluxes in Gm25 for three stacked dipoles	77
0030ctr	Three stacked dipoles with three power supplies	77
0031ctr	Summary of optics formulae	77
0032ctr	Eddy currents effects from cylinder excited by multipole field	77
0033ctr	Conducting cylinder in time dependent homogenous field perpendicular to axis	77

0034ctr	Eddy currents in cylinder in time dependent field parallel to axis	77
0035ctr	Strip magnet orientation	77
0036ctr	Power density perpendicular to reference trajectory	77
0037ctr	New method to calculate power densities, including Gaussian distributions	77
0038ctr	Eddy currents in ferromagnetic spherical shells and balls	77
0039ctr	Summary of eddy currents formulae	77
0040ctr	Transmission through two apertures	77
0041ctr	$C = BA$	77
0042ctr	Aperture projection for curved source and drift I	77
0043ctr	Aperture projection for curved source and drift II	77
0044ctr	Aperture projection	77
0045ctr	Transmission through two half apertures	77
0046ctr	Transmission through apertures with general m_{11} and m_{12}	77
0047ctr	General aperture projection	77
0048ctr	Flux exclusion from Gm1	77
0049ctr	Superconducting circular pipe in multipole field	77
0050ctr	Thoughts on eddy current problem	77
0051ctr	A potentially useful conformal transformation	77
0052ctr	Superconducting and $\mu = \infty$ elliptical pipe	77
0053ctr	Approximation to S-C transform of outside of Gm1 to outside of Gm37	77
0054ctr	Eddy current distribution in a special box	77
0055ctr	Phase space transform	77
0056ctr	Field perturbation by superconducting box	77
0057ctr	Shielding bar optimization results	78
0058ctr	Steel grid with maximum pumping	77
0059ctr	Aperture projection for curved source and drift space, and application	77
0060ctr	Absolute duct protection program	77
0061ctr	Projection of general duct into starting phase space, for general transform matrix	77
0062ctr	Eddy current fields from $D3$, neutral beam boxes (and other notes)	77
0063ctr	Pressure distribution in neutralizer tube	77
0064ctr	Properties of molecular flow in general duct	78
0065ctr	Probability treatment of molecular flow in general duct	77
0066ctr	Optimization of flow role through neutralizer	78
0067ctr	Chevron transmission coefficient	78

0068ctr	Transmission of fields through shielding bars	78
0069ctr	Field penetration through shielding bars	78
0070ctr	Duct with changing cross-section A and circumference U	78
0071ctr	Temperature rise in insertion device, two layer structure	77
0072ctr	Transmission numbers through duct, with absolute protection	77
0073ctr	Angular distribution for 2D flow, if 3D distribution follows Lambert's law (Original and Corrected version)	77
0074ctr	Absolute protection of tilted duct	78
0075ctr	What is $\frac{d^2T}{\partial m_{11}^2}$ for $m_{11} = \partial$	78
0076ctr	Transmission through aperture with general m_{11}, m_{12}, for *TI59*	78
0077ctr	Simple representation of "streaming" into duct	78
0078ctr	Behavior of eddy current caused power dissipation	78
0079ctr	Eddy current power dissipation in thin walled, infinitely long cylinder with field parallel and perpendicular to axis	78
0080ctr	Eddy current — energy deposition	78
0081ctr	Eddy current — energy deposition	78
0082ctr	Working formulas for eddy current energy deposition	78
0083ctr	Power density perpendicular beam	78
0084ctr	Extreme location of full energy	78
0085ctr	Eddy current energy deposition in whale bone pipe structure	78
0086ctr	*TI59* program for shielding bar calculations	78
0087ctr	Pressure changes due to change of conductance or pumping speed	78
0088ctr	Summary of formulas of interest for 2D-shielding	78
0089ctr	Two shielding problems	78
0090ctr	Magnetic field inside eddy current shielded box	78
0091ctr	Loss of beam on poleface	78
0092ctr	Feasibility of decreasing power density at calorimeter at the expense of some transmission loss at symmetric collimator down, by choosing appropriate focal point	78
0093ctr	Calorimeter power density and collimator transmission versus FP	78
0094ctr	Calorimeter power density and collimator transmission versus FP for various z'_{00}	78
0095ctr	Absolute duct protection geometry in vertical direction	78
0096ctr	Ellipse made of superconductor, or steel, or both	78
0097ctr	Cylindrical shielding with conductors, steel, conducting steel	78
0098ctr	Tapered shielding finger system with maximum conductance	78
0099ctr	Realistic $\mu = \infty$ finger shielding factor	78
0100ctr	Shielding of inside of Gm40 against dipole field	78

0101ctr	T-measurement in plate	78
0102ctr	A useful procedure for measurement of total power in an isolated ion species on D3 injector beam dump	78
0103ctr	Point on inclined plate where power density is independent (to 1st order) of z'_{00}	78
0104ctr	Thermistor location procedure	78
0105ctr	Temperature rise in solid insertion device plate	76
0106ctr	Temperature distribution on ion dump resulting from non-uniform energy deposition	78
0107ctr	Summary of *TI59* runs to determine best location for thermistor array on beam dump	79
0108ctr	Aperture projection program for *TI59*	79
0109ctr	Effect of collimator on power density in beam dump	79
0110ctr	Beam dump sensors problem	79
0111ctr	Insertion device power density on axis perpendicular to beam for ZEPHYR	80
0001u-w	Analysis of bus system	85
0002u-w	Analysis of undulator with *V*-busses	85
0003u-w	Formulas for new POLE/HH progr.	85
0004u-w	Summary of formulas for new POLE/HH progr.	85
0005u-w	Optimization of wiggler coil area	85
0006u-w	Flux into pole Gm23 from end of CSEM block	85
0007u-w	Design of pole of EM wiggler with rectangular coil	85
0008u-w	2nd optimization of EM wiggler pole shape	85
0009u-w	Trajectory displacement due to a single pole (above and below midplane), and ± pairs of poles, of an iron wiggler array	85
0010u-w	Design of wiggler taper adjustment system that avoids trajectory displacement	85
0011u-w	Trajectory displacement due to γ-change in wiggler consistency of 1 –2 1 modules	85
0012u-w	$\int_{-\infty}^{+\infty} B(z)z^2 dz$ for $B(-z) = B(z)$ from ELF wiggler	85
0013u-w	Steering strategy for ATA wiggler: definition of problem	85
0014u-w	Summary of work on displacement in EM w, and methods to avoid it (chronologically)	85
0015u-w	Translation of excitation patterns in EM W/U into CSEM needed for excitation of hybrid U/W	85
0016u-w	Recent work talk, 3/26/85	85
0017u-w	Error of pattern 1-2 3-4 3-2 1	85

0018u-w	Detailed formulae for design of tapered EM U/W (with no focusing) that gives no deflection and displacement	85
0019u-w	Formulas for design of tapered W/U: asymmetric derivation	85
0020u-w	Tapered W/U excitation with patterns encompassing an even or an odd number of poles (displacement, but there are errors)	85
0021u-w	Flux traversed by e when in flat region of U/W with iron poles	85
0022u-w	Flux traversed by e in U/W with iron poles	85
0023u-w	Parabolic wiggler profile with γ = constant: comparison between continuous field amplitude change, ± pole pairs with same excitation, and poles with individual excitation	85
0024u-w	Achievable field in EM U with rectangular pole and coil	85
0025u-w	Different formulation of achievable *B* in EM with straight pole and coil	85
0026u-w	Achievable field in EM U with shaped pole and rectangular coil	85
0027u-w	Achievable field in EM U with shaped pole and two rectangular coils	85
0028u-w	Achievable field in EM U with shaped pole and coil that fills all non-iron space between poles	85
0029u-w	Achievable field in CSEM assisted EM U with rectangular pole and coil	85
0030u-w	Notation in 8/85 notes on EM U with straight shaped poles, and computer runs	85
0031u-w	Vertical steering due to horizontal displacement of Ted poles	85
0032u-w	Effect of steering in the presence of focusing	85
0033u-w	Calculation of flux associated with horizontal steering	85
0034u-w	Displacement of electron beam in flat part of undulator/wiggler for γ = constant	85
0035u-w	Excitation pattern for U/W with focusing	85
0036u-w	Switching from U/W excitation pattern 1-2 1 to 1-3 3-1	85
0037u-w	A possible reason for the increase of $\Delta B/B$ with g/λ in hybrid undulator/wiggler	85
0038u-w	Overlapping area of straight line poles of SU	85
0039u-w	Design formulas and progr. for (PM assisted) strong EM U/W	85
0040u-w	Coil system to measure "non-zero-ness" of field integrals of Ted poles excited with flux = 0 pattern	85
0041u-w	Detailed flux analysis in pole of PM assisted em U/W	86
0042u-w	OHFX	86
0043u-w	Implementation of non-linear tapers with order 4 binomial coefficients	86

0076u-w	Execution of design of 1. order W/U compensation system, to 1st order in wiggler focusing	88
0077u-w	Path length error in 1 $\lambda_u \rightarrow$ phase shift	88
0078u-w	Effect of small angle between two halves of U/W	88
0079u-w	Capacity between ID poles, next to midplane, for poles filling all available space	89
0080u-w	Signal from 2d easy axis error measurement apparatus	89
0081u-w	Propagation of field errors on 3-C ladder system	89
0082u-w	Error in ID field integral caused by gap error of one pole and CSEM orientation error close to midplane	89
0083u-w	$\int B_y dz$ produced by easy axis orientation error of "short" CSEM blocks	89
0084u-w	Steering caused by end-rotation	89
0085u-w	Zero-steering insertion device entry system with one, and two, parameter	89
0086u-w	Formulas for insertion device entry design, and one for design of end of ID	89
0087u-w	Insertion device Parameter Calculation WH-RS-01 (Roland Savoy)	89
0088u-w	Steering produced by two tuners and use to tune U	89
0089u-w	Coil to measure steering in U/W	89
0090u-w	Excitation of semi-infinite U in vicinity of an end, and flux into pole 0	89
0091u-w	Decay eigenvalues for three-capacitor ladder array	89
0092u-w	Steering in hybrid U from indirect fields	89
0093u-w	Systematic classification of perturbations and tolerances in hybrid ID	89
0094u-w	Indirect flux contributions to displacement without steering	89
0095u-w	Direct flux sources for generation of displacement without steering	89
0096u-w	Excess coefficient for $\int F^{-2} dz$ on pole of Gm16	89
0097u-w	Calculation of steering in hybrid insertion device from $\lambda/2$ model measurements	89
0098u-w	2D force and torque on CSEM rotators	89
0099u-w	Effect of pole saturation in ID	89
0100u-w	Calculation of $\frac{B(g)}{B(g_o)}$ and $\frac{\Delta B(g)}{\Delta B(g_o)}$	89
0101u-w	U trajectory and radiation	90
0102u-w	Femtosecond time resolution with a two undulator system (discussed with S. Ruby and K. Halbach)	90
0103u-w	Helical U with "quads"	87
0104u-w	Geometry of central pole	90

0105u-w	Asymmetric W	90
0106u-w	C_0' / C_2' as function of gap for small gaps	90
0107u-w	Flux split and excess potential drop in Gm16	90
0108u-w	Design of hybrid asymmetric (Goulon) wiggler	90
0109u-w	Entry into Goulon-W	90
0110u-w	Entry into Goulon-W	90
0111u-w	Entry into Goulon-W	90
0112u-w	Displacement-free iron free undulator for $M' = 4$	90
0113u-w	Decay cond. for Goulon-W	90
0114u-w	Line integrals over fields produced by line changes	90
0115u-w	Steering from a round finite length block of CSEM	90
0116u-w	Displacement from around finite length block of CSEM	90
0117u-w	Steering without displacement with 2 round blocks of CSEM	90
0118u-w	Coil system to measure steering between field free region at end of ID, and periodic part of ID	92
0119u-w	Steering with flooding pole 0	92
0120u-w	Gradient measurement in ID	92
0121u-w	Displacement-free entry system for "2-wire" helical U	90
0122u-w	Procedure to correct ends of ID	90
0123u-w	Determination of B_r/H_c of CSEM with Helmholtz coil	91
0124u-w	Scalar potential for 3D ID fields	92
0125u-w	3D scalar potential for saturation caused fields in ID, Vers. 2	92
0126u-w	3D scalar potential for saturation caused fields in ID, Vers. 1	92
0127u-w	Direct flux from CSEM corrector in ID	92
0128u-w	"Impedance" for hybrid ID	92
0129u-w	Flux transport along axial direction of EM wiggler	93
0130u-w	Flux into top of rectangular block on $V = 1$	93
0131u-w	Excess flux into pole, and flux into side of Gm40	93
0132u-w	Effects of excess potential drop on flux into side of pole	93
0133u-w	Error of flux calculation for finite pole width with excess flux coefficient	93
0134u-w	NPOLE	93
0135u-w	Wiggler parameter K definitions	93
0136u-w	Simple analytical model for fields from one pole of hybrid ID	93
0137u-w	ρ, A_0/B_1 for hybrid insertion device	93
0138u-w	Connection between undulator field errors and optical phase	93
0139u-w	Comparison of first and second order contributions of error fields to phase shift	93

0140u-w	Normalization factors ε_1 and ε_2 for comparison of first order to second order phase shifts, with analytical model for $b(z)$	93
0141u-w	Least square fit of $f(z)$ with $a + bz$ in $0 \leq z \leq 1$	93
0142u-w	Magnetic measurement and data reduction to identify some specific (undesirable) error field consequences (Talk ANL)	93
0143u-w	Field integrals for iron-free ID	93
0144u-w	Scalar Potential for 3D Fields in "Business Region" of insertion device with finite width poles	92
0145u-w	Consequences of Field Perturbations in ID	92
0001misc	Solenoid lens, different derivation	67
0002misc	Solenoid lens, solenoid field on axis	67
0003misc	Multipole shielding	67
0004misc	Velocity selector	67
0005misc	Homopolar ion source	67
0006misc	Matrix describing 2nd order effects to 2nd order, in one dimension	66
0007misc	"Resonances" in r and z directions, without coupling	
0008misc	Beam optics in periodic machine, with no acceleration	67
0009misc	Weak focusing	67
0010misc	Phase space matching of ellipses and parallelograms (2D phase space only)	71
0011misc	Matching of two beam ellipses with single lens	71
0012misc	Description and some simple properties of phase space parallelograms	71
0013misc	Doublett optimization	71
0014misc	Transmission of periodic sequence of quadrupoles	71
0015misc	Bad method	71
0016misc	Gas filled magnetic spectrometer	71
0017misc	Velocity selector	71
0018misc	Homogeneous field velocity separator with fringe fields to first order	71
0019misc	Strong focusing vel. separator to first order (only strong focus modification)	71
0020misc	Phase space matrix, and achromatic spot size	71
0021misc	"Optimum" dispersive system	71
0022misc	Optimized dispersive system	71
0023misc	Polynomial $a_o x + a_1 x^2 + a_2 x^3 = y$ having same y value for $x_1 = 1, x_2 = \frac{1+c}{2}, x_3 = c$	71
0024misc	Vel. spectrometer	71
0025misc	Vel. spectrometer	71

0026misc	Twister, achromatic	71
0027misc	Achromatic twister	71
0028misc	Twister condition	71
0029misc	Easy to design twister with periodic system	71
0030misc	Four quadrupole twister	70
0031misc	Impossibility to make any twister (i.e. it does not have to have a simple drift space) with symmetrical system having only four magnets	71
0032misc	Impossibility to make symmetrical twister with 4 thin lenses	71
0033misc	First order twister-theory	70
0034misc	Achromatic spot size in both planes	71
0035misc	Solenoid to first order	71
0036misc	Long, periodic, symmetric, beam transport line	71
0037misc	Elimination of singularities of integrand at ends of integration interval	69
0038misc	Linear least squares with erroneous matrix	71
0039misc	Fierz's planet orbits	71
0040misc	HAT-detector	72
0041misc	"Stiff catenary" = "axially stressed beam"	72
0042misc	Network to give $1 + \mu$ plot (Gm33)	72
0043misc	"Harmonic polynomials" for V in cylindrical geometry	70
0044misc	Exact "$\lambda/4$ plate" from two plates	72
0045misc	Integrator drift	72
0046misc	"Buffed" doublett	73
0047misc	Beam bending	73
0048misc	Vibrating beam, right end free, left end clamped	73
0049misc	Different method to derive formula for curvature of a mapped curve	73
0050misc	Change of curvature along tangent	75
0051misc	Heat conduction in cylindrical shells	73
0052misc	Foil thickness measurement with specular reflection measurements	72
0053misc	Dimensional analysis of space charge flow	73
0054misc	Bending angle for particle in φ-independent field	73
0055misc	ε_1 and ε_2 relaxation	73
0056misc	Optimum overrelaxation factor	73
0057misc	Δ-properties	74
0058misc	Optimization of ε for linearized P_e-cycle	74
0059misc	Difference equations from variational principle, specifically for geoth. transform with k^2 V term	74

0060misc	Determination of dominant eigenvalues and associated quantities	74
0061misc	$\int V^n \, d\upsilon$ over tetrahedron, for V = linear function of x, y, z	74
0062misc	$\int \pi \upsilon_\nu^{n\nu} da$ over triangle for υ_ν = linear function of x,y	74
0063misc	Current deposition in POISSON	74
0064misc	Explicit expressions for geothermal difference equations	73
0065misc	Kerr cell apodizer	74
0066misc	Potential distribution for 2D elst. lens	74
0067misc	2D and cylindrical elst. lens	74
0068misc	Increase of convergence rate of sums with integration	74
0069misc	Determination of width of distribution function with slit	74
0070misc	$\int_1^2 W^{*N-n} \, W^n dW$	74
0071misc	Young overrelaxation	71
0072misc	Push-pull effect from two parameters with nearly identical effects	74
0073misc	Input impedence of "bridged" op-amplifier	74
0074misc	Minimization of $\int y^2(x)dx$, y = joined straight lines in equidistant x-intervals (re-creation of 1966 work)	75
0075misc	Fast conventional Fourier series	75
0076misc	Evaluation of polynomial with real coefficients, but complex argument	75
0077misc	Simpler derivation of evaluation of polynomial of z	76
0078misc	Analytical $F(z)$ in upper half-plane from $F(x)$	75
0079misc	Analytical $F(z)$ in upper half-plane from $A(x)$; $V(x)$ (new version)	75
0080misc	Propagation of sound in layered structure	75
0081misc	Equation of motion in S-C-mapped geometry	75
0082misc	Two-plane imaging with doublett	75
0083misc	Phase space detected by detector of width $2x_0$	74
0084misc	Periodic doublett system for beam transport over long distances	75
0085misc	Representation of matrix by ideal lens and 2 drift spaces	75
0086misc	Hippi modification = design of strong focusing bending magnet	75
0087misc	Estimate of necessary aperture for Hippi-beam transport	75
0088misc	Proof that necessary aperture for infinite periodic beam transport system does not necessarily represent an upper limit for aperture of phase space matching system for same beam	75
0089misc	Buffed doubletts, distributed and lumped elements as cell for periodic system	75
0090misc	Graphical representation of transform. of phase space ellipse through drift space and thin lens	75

0091misc	Computation and graphical representation of transformation of phase space matrix through drift space and thin lens (from Steffer)	75
0092misc	PEP-interaction region solenoid compensation schemes	75
0093misc	Properties of total *H*-system that has pure drift matrix	75
0094misc	$M_x = M_y$ system	75
0095misc	Beam transport system with axisymmetric transfer matrices	75
0096misc	2 identical systems, but with opposite polarities, in series	76
0097misc	Triplett telescope (thin lenses)	75
0098misc	Optimization of $n = 1$, two compensated coil system for harmonic analysis	75
0099misc	Effect of field errors on observation in detector plane	75
0100misc	Analytical continuation of $1/(z-a)$ with *N*-term Taylor series	75
0101misc	Schwarz's formula, with z_0 inside or outside circle	75
0102misc	Some thoughts on analytical continuation for measurement evaluation	75
0103misc	Coil structure adjustment of 2D magnetic measurements	75
0104misc	Trajectories in some bending magnets	75
0105misc	Location of minimum aperture of 2D beam	75
0106misc	2D parallel duct as a virtual leak	75
0107misc	Properties of tape wound coil geometry	75
0108misc	Parabola extremum finder and equation solver	75
0109misc	Lawson's ring	75
0110misc	Simple method to determine location of focal plane of optical system	75
0111misc	Retroreflecting optical system	75
0112misc	Search routine for maximum finder	76
0113misc	An interesting data analysis and error analysis problem	76
0114misc	3 ways to calculate Fourier coefficients	76
0115misc	Trajectory with air resistance; slightly different approach	77
0116misc	Trajectory with air resistance	76
0117misc	Eriter Maclanrim formula derivation	76
0118misc	Expansions in y_o	76
0119misc	Trajectory with curvature concept	76
0120misc	Particle trajectories in $\mathbf{E} + \mathbf{B}$ field with $E_\varphi = 0, B_\varphi = 0$ with Lagrange function	76
0121misc	Particle trajectories in $\mathbf{E} + \mathbf{B}$ field with $E_\varphi = 0, B_\varphi = 0$ with equation of motion	76
0122misc	Particle trajectories in $\mathbf{E} + \mathbf{B}$ field with $E_z = 0; B_z = 0$	76
0123misc	1st order "radial" particle trajectory in electric field	76
0124misc	Coefficients of polynomial after factoring one or two roots (Horner)	76

0152misc	Minimum beam size in system described by $M=\begin{pmatrix} \cos\varphi & \sin\varphi/k \\ -k\sin\varphi & \cos\varphi \end{pmatrix}$	79
0153misc	Fourier series/transform facts, for FFT use	79
0154misc	EFB of dipole to produce desired beam spot location	80
0155misc	Power density produced on target by scanning	80
0156misc	Scanner optics	80
0157misc	Combination of scanning dipole with quadrupole to correct chromatic aberration of center trajectory	80
0158misc	Scanning properties of hard edge strip magnet	80
0159misc	Scanning caused by hard edge magnet with circular pole	80
0160misc	Exact equ. of motion in 2D multipole field	77
0161misc	Ray tracing in oriented wedge dipole-quadrupole (Ray's quad)	80
0162misc	2D multipole transmitter	80
0163misc	Strip transmission magnet for given deflection of two given in species	80
0164misc	Beam dump with arbitrary orientation	80
0165misc	Application of Bernoulli's equ. to water pipe system	80
0166misc	Trajectory displacement because of soft edge, composed to hard edge of magnet	80
0167misc	General midplane ray tracing with homog. fields, and straight and circular boundaries	80
0168misc	TRACE	80
0169misc	Axisymmetric quadrupole quadruplett	80
0170misc	Aperture projection into starting phase space for lumped optical system	80
0171misc	Trajectory and first order matrix in bend plane of 2D magnet	80
0172misc	Computation and properties of first order optics matrices	80
0173misc	Ultrafish variables	81
0174misc	Envelope of E_{critical} vs. θ curves	81
0175misc	Space charge limit on focusing of round zero-emittance beam in drift space	80
0176misc	Effect of exit impedance of duct on $\int pdx$ from outgassing	81
0177misc	Local interpolation with continuous function and its first N derivatives	81
0178misc	1st order optics of E = constant deflector	81
0179misc	Size of beam (of rhomboidal shape in phase space) in optical system	81
0180misc	Design of TRW spectrometer magnet	81
0181misc	Index and comments to notes sent to Phil Kidd (TRW)	81

0241misc	$F_2 = \int_{-\infty}^{+\infty} \frac{e^{-x^2}}{(x+z_o)} dx, \Im z_0 > 0$	86
0242misc	Multilayer mirrors 1) basics	86
0243misc	Multilayer mirrors 2) periodic structures	86
0244misc	Summary of multilayer design formulae and procedures	86
0245misc	Some thoughts on design of multilayer mirrors	86
0246misc	Jacobian $J = \begin{pmatrix} u'_x & v'_x \\ u'_y & v'_y \end{pmatrix}$ in complex notation	82
0247misc	Determination of circle that connects three points	86
0248misc	Map of straight line segment z_1, z_2 with $W = kz^2$	86
0249misc	Necessary condition for conformality	86
0250misc	Reflection magnet with achromatic zero offset	86
0251misc	Location and size of waist in driftspace from β_2, β_1, Δz	86
0252misc	Achromatic spots	86
0253misc	$[J_0(\xi) - J_1(\xi)]^2$	86
0254misc	$[J_0(\xi) - J_1(\xi)]^2$ for $x = \frac{1/2}{1+2/k^2} \leq \frac{1}{2}$	86
0255misc	Decay of error fields in (ideal) ← (not all is correct) symmetrical iron dominated quad	86
0256misc	Malcolm's mechanism, note #1	87
0257misc	Mechanism for Malcolm H., note #2 (on airplane from SFO to JFK)	87
0258misc	Synchrotron light phase shifter	87
0259misc	Trajectory in gradient magnet	88
0260misc	Least square fitting of function	88
0261misc	Design of quadrupole system with $M_x + M_y = 0$	88
0262misc	Twister condition (re-write of 1971 note, for SSRL)	88
0263misc	Twister condition	71
0264misc	Letter-Herman/Heinz (some notes)	88
0265misc	Expansion of Taylor series, raised to some power p, into a Taylor series (for Bozoki)	88
0266misc	Inversion of a Taylor series, with recursion formulae	88
0267misc	Analog integrator dynamics	89
0268misc	$F(x) = \int_0^{\pi} J_0(x\cos\varphi) d\varphi$	89
0269misc	New bumps	89
0270misc	$I_2 = \int_0^{+\infty} \frac{x^2}{\cosh x} dx$	89

0271misc	Chromaticity correction with sextupole	90
0272misc	Simple proof for "amusing geometry theorem"	90
0273misc	An amusing geometry theorem	90
0274misc	Radiative energy loss by accelerated charge	90
0275misc	Analysis of analog integrator	90
0276misc	Analysis of analog integrator (Milan)	90
0277misc	β function in unstructured focusing quadrupole	90
0278misc	Dimensional analysis of trajectory of non-relativistic charged particles in stationary electric and magnetic fields	92
0279misc	Gravity drive "train"	92
0280misc	Map of interior of unit circles with centers at $z = 0$, $\omega = 0$)	92
0281misc	Simpler map of interior of circular disks onto each other	92
0282misc	Map of circular unit circles onto each other, with given maps of two points on circumferences	93
0283misc	Mathematical framework for production of achromatic spot, using only quadrupoles and/or solenoids	77
0284misc	Production of achromatic spot with a beam transport system consisting only of quadrupoles and solenoids	77
0285misc	Memo to participants of the discussion on linear beam transport systems at LASL, November 3–4, 1977	77
0286misc	Fringe fields	??
0287misc	A simple derivation of the Lorentz transformation without talking about light	92
0288misc	General map of circular disks onto each other	92
0289misc	Math for MATROPT (document, programs and assorted notes)	93
0290misc	$J = \int_{-\infty}^{+\infty} [F(x) - F(x-a)]^2 dx$	93
0291misc	Multipole fields	67
0292misc	Statistics	67
0293misc	Statistics	67
0294misc	Mother-Daughter Detection	67
0295misc	Statistics for decay time measurements	67
0296misc	Application of generating function of two variables to specific problem	67
0297misc	Generating Function with several variables	67
0298misc	First order matrix-differential equation for relativistic particle	67
0299misc	Field in twisted symmetrical multipole	69
0300misc	Beam optics for long, twisted quadrupole	67
0301misc	I_q'' calculations	67

0018thry	Fields at center and on center of pole tip in 3-pole case	66
0019thry	Ideal quadrupole	66
0020thry	Perfect 6-pole	67
0021thry	Sheet current ellipse and $\mu = \infty$ shield for production of homogeneous field inside ellipse	67
0022thry	Current filaments in circular $\mu = \infty$ iron shell with $r = r_0$	67
0023thry	Septum problem	67
0024thry	Field perturbation in septum magnet	67
0025thry	Errors from non-uniform current distribution in return path (near yoke) of septum magnet	68
0026thry	Numerical solution of algebraic equations	68
0027thry	Measurement in 6-pole of second order contribution to signal measured with pick up coil	67
0028thry	Field perturbation produced by bump	68
0029thry	Effective length of a magnet	68
0030thry	Field produced by two superconducting current sheets	67
0031thry	Magnetic field inside of ellipse with uniform j over its total area	68
0032thry	Field energy for $\mathbf{B} \approx \mathbf{H}$	68
0033thry	Summary of formulas for energy, force and torque	67
0034thry	General force formula for cylindrical geometry	68
0035thry	Two-dimensional field produced by "odd"-shaped conductor with constant current density	68
0036thry	Vector potential measured by bundle of wires with polygon as boundary	68
0037thry	Pick up coil system for harmonic analysis with suppression of all harmonics up to n	68
0038thry	Experimental zero-field point determination in sextupole	68
0039thry	The number of zero-field points in the aperture region of a multipole magnet	68
0040thry	Octupole component produced by a sextupole run as a quadrupole	68
0041thry	Sextupole with one pair of poles having different excitation or different spacing	68
0042thry	Better method to drive error fields produced by error excitation of one pole of a symmetric 4-pole	68
0043thry	Symmetrical 4-pole with only one pole excited	68
0044thry	Amplitude and phase errors in harmonic analysis	68
0045thry	Current distribution and power dissipation in conductors in two-dimensional fields	68
0046thry	1/4 of Panofski quadrupole with non-constant current densities	68

0047thry	1/4 of Panofski quadrupole with unequal current densities	68
0048thry	1/4 of Panofski quadrupole	68
0049thry	Application of trim to a cavity problem	68
0050thry	Quadrupole with filaments to give sextupole	68
0051thry	End of septum magnet	68
0052thry	Field distribution in shielding plate (SLAC problem)	68
0053thry	Multipole expansion of the sector potential in a circular aperture	68
0054thry	Schwarz's formula	68
0055thry	Calculation of fields, gradients and multipole coefficients by contour integrals over circle	68
0056thry	Qualitative considerations concerning field corrections with special coil windings and "chunks" of iron, using the 2D current flow or fluid flow analogue	68
0057thry	More details about the "vane-skim"	68
0058thry	Minimization of stray fields of magnet by optimizing "steel shield"	68
0059thry	Fourier analysis of numerical data	68
0060thry	Fields in Gm8	68
0061thry	Combined skew 4-pole and normal 6-pole	68
0062thry	12-pole with straight slots for combined skew 4-pole - "normal" 6-pole	68
0063thry	Transformation of curvature under conformal map	68
0064thry	Methods to eliminate or reduce long time dynamical drift of systems ("creepy magnet")	68
0065thry	Optimization of a function of more variables than number of restraints plus one	68
0066thry	Heating of kicker magnet "coils"	68
0067thry	Integrated multipole strengths for skew axis	68
0068thry	Power with eddy currents in sheet	68
0069thry	Optimization of coil slot for combined 6-pole and skew 4-pole	68
0070thry	Multipole components with respect to displaced axis	68
0071thry	Sensitivity of solution of linear equations to change of an individual matrix element	68
0072thry	Change of determinant for small changes of one element of the matrix that describes a system that is least squares optimized with restraints and has least squares limitations on parameters	68
0073thry	Allowable relative errors of the elements of matrices describing system to be optimized	68
0074thry	Error analysis for parameters obtained from least squares optimization with restraints and least squares bound on parameters	68

0075thry	Efficient method to solve homogeneous system of linear diff. equ. with const coefficients	68
0076thry	Data analysis of stripping cross-section measurements	68
0077thry	Corner saturation	69
0078thry	Transmission of rotation angles through universal joint	69
0079thry	Summary of integrator roles from Dec. 63	69
0080thry	Fields in magnet with midplane symmetry in $r, \varphi z$	69
0081thry	2D fields in slab (no iron or singularities) in region of description	69
0082thry	Logarithmic spiral	69
0083thry	**B** and **H** variation in direction of center of curvature of V = constant and A = constant lines in 2D isotropic, homogeneous, nonlinear iron	69
0084thry	**B** and **H** variation in direction of center of curvature of V = constant and $rA\varphi$ = constant lines in cylindrical geometry for isotropic, homogeneous, nonlinear iron	69
0085thry	Reduction of $B(H)$ measurements on torus	69
0086thry	Capacitor stray field (for Bob Smith)	69
0087thry	Power dissipation in tape wound quadrupoles	69
0088thry	Field quality criterion	69
0089thry	Field error criterion for non-circular aperture	70
0090thry	Some general field relations expressed in complex form	69
0091thry	Effective length of quadrupole	70
0092thry	Comparison between $L_1 = [B]/B_0$ and $L_2 = 2\sqrt{3[x^2B]/[B]}$ for several $B(x)$	70
0093thry	Better formulation of effective length of 4-pole for first order optics	70
0094thry	Force between HILAC quadrupoles	67
0095thry	Total extinction lines produced by magneto-birefringent material between crossed polaroid jitters multipole magnet	69
0096thry	Weights for calculating potential from potentials at surrounding points if pot. satisfies Laplace's equation	69
0097thry	Resistance of specific 2D sheet structure	70
0098thry	Computation of upper and lower limits of impedances of 2D structures with variational principle	70
0099thry	Relation between H_x at pole face and H_y in midplane of magnet	69
0100thry	Measurement of Fourier coefficients of field between two $\mu = \infty$ plates	69
0101thry	Calculation of Fourier coefficients of H^*	69
0102thry	Representation of fields between two parallel plates of $\mu = \infty$ iron	69

0103thry	General relationships of fields in linear, location independent, anisotropic medium	70
0104thry	Effect of nonlinearity of iron on the effect of small perturbations in 3D	70
0105thry	Scalar potential and pole face for $\mu = \infty$ bending magnet with cylindrical symmetry, and given inhomogeneous field in midplane	70
0106thry	Scalar potential and $\mu = \infty$ poleface for inhomogeneous field with midplane symmetry in cylindrical magnet with axis outside field region	70
0107thry	Scalar potential and $\mu = \infty$ poleface to get given inhomogeneous field with midplane symmetry in cylindrical magnet with axis far outside of field region	70
0108thry	Correct POISSON equation for cylindrical geometry	74
0109thry	Effect of current sheet in midplane of windowframe magnet	70
0110thry	Additional effective "force" length and "field" length of corners	70
0111thry	$F(z) = \int_0^z \frac{\ln(1+t)}{t} dt$	70
0112thry	Orthogonal 2D analogue for 2D and cylindrical geometry magnetic fields	70
0113thry	Energy in magnetostatic field, and derivation of field equations from variational principles	70
0114thry	Derivation of TRIM equ's from variational principle	70
0115thry	TRIM equ's for anisotropic medium	70
0116thry	Evaluation of $b(H)$ curve from flux measurements on "washer"-shaped iron ring	70
0117thry	Evaluation of $b(H)$ curve from flux measurements on "washer"-shaped ring (without Fourier transform)	71
0118thry	Feeding of 4-poles	70
0119thry	Eddy current loss in Fe for $\overline{H} = \overline{H}_0 \cos \omega t$ with Pryntig reactor	74
0120thry	Eddy current loss in Fe for $\overline{B} \approx \sin \omega t$	71
0121thry	Rise time of magnetic field and eddy current - energy deposition in pulsed magnet (old version)	70
0122thry	Power dissipation and "μ_{eff}" of Cu conductor in pulsed magnet	71
0123thry	$\mathcal{L}^{-1}\left(\frac{e^{-\alpha\sqrt{p}}}{p^{3/2}}\right)$	73
0124thry	$\mathcal{L}^{-1}\left(\frac{e^{-\alpha\sqrt{p}}}{p^{5/2}}\right)$	73
0125thry	$\mathcal{L}^{-1}\left(\frac{\coth y \cdot \sqrt{p}}{p^{3/2}}\right)$	73

0126thry	$\mathcal{L}^{-1}\left(\frac{\coth y\cdot\sqrt{p}}{p^{5/2}}\right)$	73
0127thry	Energy dissipation in vacuum vessel	71
0128thry	Eddy current effects for ramp excitation (one pulse)	71
0129thry	Important eddy current formulae	74
0130thry	Eddy current effects in pulsed magnet	71
0131thry	Eddy currents (does not take nonlinearity-induced apparent anisotropy into account)	70
0132thry	Rotating E quadrupole and DC magnetic field as mass filler	71
0133thry	RF B_{ax}	71
0134thry	Matrix for cylindrical lens for $\varphi(z)=\varphi_o+\frac{\varphi_0 z}{1+kz}$	71
0135thry	Effect of gap above HT-conductor	71
0136thry	Effect of horizontal gap on Ht-distribution produced by Ht-filament (reformulation of 3/71 notes)	71
0137thry	Eddy current time constants in Fe-magnets	70
0138thry	Beneficial effects of saturation in yoke-connected field clamp	71
0139thry	Eddy currents for cylindrical geometry	72
0140thry	Turn-on procedure of magnet to avoid "overdriving" $B(H)$ curve	71
0141thry	$B(H)$ measurement with two rings; cancellation of contributions B', B', B'''	71
0142thry	Normal TRIM-equation	71
0143thry	Simultaneous compensation of two time constants	71
0144thry	Procedure to make small changes of field level in large magnet so that inhomogenieties in gap decay as fast as possible, and to reach new field level in shortest time	71
0145thry	Dynamical system to drive "loudspeaker"	71
0146thry	Coating of steel with Cu to reduce eddy current losses	71
0147thry	SLAC - bubble chamber eddy current problem	71
0148thry	Power loss in coil in limit of "small" cross section	71
0149thry	Eddy current power in the limit of "small" losses	71
0150thry	Losses in "loudspeaker" coil (SLAC)	71
0151thry	Qualitative considerations for SLAC bubble chamber - "loudspeaker"	71
0152thry	Numbers for bubble chamber "loudspeaker"	71
0153thry	Convergence test (originally done spring 1970; notes lost; this written in spring 1972)	72
0154thry	Windowframe tolerances	71
0155thry	Slit effect for $\mu=\infty$	71

0185thry	Reduction of bending length because of slit	73
0186thry	Harmonics production by symmetrical cut at pole ends of 4-pole, (a transcript of notes made during Dec 72–Feb 73)	73
0187thry	Excitation loss for $\mu = \infty$ laminations with finite insulation thickness	73
0188thry	Torque acting on ellipse with $\mu = \infty$ in homogeneous field	73
0189thry	Single shim first and second order	73
0190thry	First and second order shimming of *H*-magnet with slot	73
0191thry	Coil position for 1st and 2nd order corrected fields	73
0192thry	1st and 2nd order shimming with two filaments	73
0193thry	Mapping of magnet with pole with slanted side	73
0194thry	Jim Walter's lamination thickness	73
0195thry	2D eddy current distribution in lamination of anisotropic steel	73
0196thry	$W = -iz^2$, map of circular pole of 4-pole	73
0197thry	Saturating yoke and poles in 4-pole	72
0198thry	Analytical *B-H* curve description	73
0199thry	Long coil to measure $\partial B_y / \partial y$ in 2D	73
0200thry	Coil system to measure $\partial B_z / \partial z$ in 3D	73
0201thry	Coil system to measure $\partial B_z / \partial x$ in 3D	73
0202thry	Epics flux splitting	73
0203thry	Properties of magnetic line integrals	74
0204thry	Change of harmonic content of multipole due to change of width of (all) poles	74
0205thry	Pole shimming methods	74
0206thry	Shimming with knife edge pole and filaments	74
0207thry	Shimming of pole with filament at $t = -a$, strength m	74
0208thry	Power in thick storage ring wall	74
0209thry	Finite thickness current sheet on poleface (for HAT)	74
0210thry	Eddy currents when driving magnet very hard into saturation ("charging" permanent magnet with coil)	74
0211thry	Field modification in ideal quadrupole by round pipe, to first order in $\mu - 1$	73
0212thry	Seminar on 8/10/73 at LASL	73
0213thry	EFB - coil geometry - effect on EFB (done at LASL)	73
0214thry	Torque on vane in homogeneous field	70
0215thry	Ellipse in homogeneous field	70
0216thry	Evaluation of first vane run	70
0217thry	Position of vane in 2-vane correction system	70

0218thry	Multipoles produced by radial displacement of Fe-plate between poles of 4-pole	70
0219thry	Parameter to correct field errors in assembled 4-poles	70
0220thry	Force and torque calculations for vanes	70
0221thry	Q^2 distribution	70
0222thry	Notes for measurements of 4-poles	70
0223thry	LASL 4-poles	70
0224thry	Arch's "new" field quality normalization	70
0225thry	Achievable 4-pole quality	70
0226thry	Conclusions for ESCAR coil system	74
0227thry	Error analysis for dipole coil system	74
0228thry	$\overline{z^n}$ over square	74
0229thry	$\sum z^n$ over line perpendicular to z_{center}	74
0230thry	Stray field outside field clamp	75
0231thry	Effects of construction errors at the end of dipole magnets	75
0232thry	Field coil to test pick-up coil	75
0233thry	Quadrupole - pole width $\leftrightarrow$ dipole overhang	75
0234thry	Calibration of OAM	75
0235thry	Harmonics in dipole fringe field	75
0236thry	Harmonics to produce $B_y \approx x$ in midplane of quadrupole	75
0237thry	Quadrupole with $B_y \approx x$ in midplane	75
0238thry	Conventional dipole	75
0239thry	Recreation of "integrated multipole strengths for skewed axis"	75
0240thry	Eddy current energy deposition at yoke's edge	75
0241thry	Possible solutions to 2D grid problem	75
0242thry	Correct POISSON equation for cyl. geometry	74
0243thry	Diff. equation for cyl. geometry - POISSON	75
0244thry	1/2 - windowframe - sextupole	75
0245thry	Windowframe sextupole with wedge-shaped coil	75
0246thry	Windowframe sextupole with finite and constant thickness coil	75
0247thry	Method to calculate 2D field outside convergence radius from 2D harmonic measurements (recreation of notes from ~ early 75 that I cannot find)	75
0248thry	Eddy current force between solenoid and thick Cu plate	75
0249thry	"Octupus" fields	75
0250thry	Penetration of high frequency fields into dipole	75
0251thry	AC fields in windowframe magnet	75

0252thry	Measurement of pure quadrupole with displaced coil rotating about a skewed axis	75
0253thry	2D field in homogeneity $\leftrightarrow$ curvature and displacement of field line	75
0254thry	$\lvert\Delta B\rvert^2$ from allowed harmonics in symmetric quadrupole	76
0255thry	Magnetization data for Texas A&M magnet	76
0256thry	Multipole production by pole asymmetry of 4-pole	76
0257thry	Stored energy in permanent magnet assembly	76
0258thry	Alternate way to excite quadrupole with filaments on pole to give sextupole	77
0259thry	Production of $n = 3$ in quadrupole with poleface filament	77
0260thry	Production of sextupole field in quadrupole with current sheet on pole surface	77
0261thry	PEP staircase 4-pole	77
0262thry	Measurements to give field quality outside "normal" convergence radius of quadrupole	77
0263thry	AC force on 2D conducting steel plate	77
0264thry	Eddy currents for fast permanent magnet magnetization	77
0265thry	Stored energy in cylindrical and 2D geometry and in cylindrical geometry with rA = constant surface	77
0266thry	Field errors because of parabolic segment cut from pole	77
0267thry	Effect of circular arc carved into pole of dipole	77
0268thry	Polynomials for edit in cyl. geometry	78
0269thry	SC transform of Gm26 with ellipse integral	78
0270thry	SC transformation of Gm27	78
0271thry	Minimization of correction coil current	78
0272thry	"Superconducting" kicker magnet	72
0273thry	Shimming of pole with filament model	78
0274thry	Eddy currents in cylindrical yoke-ring	78
0275thry	Eddy current summary for TPC	78
0276thry	Error analysis for Don Sorenson's measurement coil system	78
0277thry	Decay of V in pipe	74
0278thry	Poleface for weak focusing bend magnet with cyl. symm.	78
0279thry	$\overline{B}$ through plate excited by two coils	78
0280thry	Lee Heflinger's notes on coil system stability	78
0281thry	Current increase necessitated by hole in steel	79
0282thry	Flux through $\mu = \infty$ bodies in uniform magnetic field	79
0283thry	Eddy current - caused force and torque on conducting circular plate	79
0284thry	Eddy current - force and torque on long thin sheet in 2D field	79

0285thry	Force and torque on 2D body with $\mu = \infty$ or $\sigma = \infty$ in 2D multipole field	79
0286thry	Model for eddy current forces and torques on 2D structures with incomplete flux exclusions	79
0287thry	Complex potential for $\mu = \infty$ or $\sigma = \infty$ ellipse in pure multipole field	79
0288thry	Summary for 2D, $\sigma = \infty$, or $\mu = \infty$ forces and torques	79
0289thry	$\int \mathbf{j} dv$	79
0290thry	Re-formulation of model for forces and torques on 2D structures with incomplete flux exclusion by eddy currents, and for $\mu = \infty$	79
0291thry	1/2 dipole magnet with hole in septum	79
0292thry	WNR stripping magnet	79
0293thry	Effect of hole in yoke of PSR dipole	79
0294thry	1/2 quadrupole with hole in mirror plate	79
0295thry	2D field model for D3 magnetic coil system	79
0296thry	Field distortion from bellows welds in Bevatron	79
0297thry	Corner flux	76
0298thry	1D model of eddy currents in non-linear steel	79
0299thry	Re-creation of optimization of 2-coil measurement system for quadrupoles	79
0300thry	Force on coil in 2D and cylindrical geometry	79
0301thry	Axial forces on HISS coil	79
0302thry	Decay of cylindrical symmetrical field between two parallel plates with $\mu = \infty$	79
0303thry	B. Price magnet	79
0304thry	Charged circle next to plane; minimization of E_{max} for given ΔV and center of circle	79
0305thry	"Closed" charged surface with constant $\|E^*\|$ next to conducting plane	79
0306thry	Curved electrodes with $\|E^*\|$ = constant, next to conducting plane	79
0307thry	Dipole steering with quadrupole	79
0308thry	Dipole steering with quad in 2 extreme cases	80
0309thry	Representation of laminated steel by anisotropic medium	79
0310thry	Analysis of cylindrically symmetric solenoid system with a symmetry-violating perturbation	80
0311thry	Approxim. calcul. of flux going into cyl. hoop, and consequences of satur. of hoop	80
0312thry	Effective edge associated with step in pole	80
0313thry	Jeff associated with coil-ends in HIF quadrupole	80
0314thry	Leff of HIF quadrupole	80

0315thry	Etst. field from plate with circular hole	80
0316thry	Axisymmetric elongated ellipsoid in field parallel axis	80
0317thry	NBS race track K-iron magnet	80
0318thry	Fringe field flux in some magnets	80
0319thry	Force estimates for ideal superconducting undulator	80
0320thry	Far field expansion of A_φ (cylindrical geometry)	80
0321thry	Simulation of "rest of universe" in cyl. geometry	80
0322thry	Deductive proof that for 2D fields, only A_z is needed	80
0323thry	Test for aberrations for far off midplane trajectories in strip magnet	80
0324thry	B_y = constant curves in Gm10	80
0325thry	3rd order kick at end of semi-infinite quadrupole	81
0326thry	Rogowski quadupole: formulation of problem	81
0327thry	Compensation of ripple from coil (for D3)	81
0328thry	Compensation of ripple from coil (for D3)	81
0329thry	Adaptive optics correction element	81
0330thry	VECAN; disk 52	81
0331thry	Fourier analysis of vector pot. in X/4-section	81
0332thry	Field penetration through 2D slit	81
0333thry	$\overline{B_r}, \overline{B_z}$ in cylindrical geometry, from $rA = V$ = linear function in Δ	81
0334thry	Eddy current in conductor with circular cross section exposed to (previously) uniform AC field	81
0335thry	Eddy currents in lamination	81
0336thry	Poleface correction of LANL AT2 quads	81
0337thry	1st order shim of pole	82
0338thry	Design of center part of "Rug's" quadrupole	81
0339thry	TRW undulator problem with floating wire	81
0340thry	Force on REC and small sphere of $\mu = \infty$ steel in external field	82
0341thry	Design and properties of Helmholtz coil system	82
0342thry	Superconducting wiggler with coil surface = field line with $\|B\|$ = constant	82
0343thry	Shielding inside of 2D "box" with elliptical outer contour	82
0344thry	Shielding of long box against transverse field in presence of longitudinal field	82
0345thry	Summary of formulas for shielding in transverse direction only	82
0346thry	Shielding considerations for neutral beam injection module containing 4 individual lines	82
0347thry	Production on quadrupole field modulated by sin kz	82
0348thry	Shielding of cylinder with superconducting sheet, or steel	82

0349thry	Production and properties of 2D **E** field that has on x-axis the properties $E_y = E_o$, $E_x = f(x)$, with Gm28	82
0350thry	Optimization of T-M coil system for quad	82
0351thry	**j** and **H** caused by two displaced solenoids with opposite polarities	82
0352thry	Force between charge sheet and pole (2D)	82
0353thry	Force on solenoid (between steel poles) due to radial motion	82
0354thry	Axial force on TPC coil due to axial displacement	82
0355thry	"Rogowski"-shield (for TRW)	82
0356thry	PSR stripper 2: magnet optimization	82
0357thry	PSR stripper 1: conformal map, fields	82
0358thry	Single stripping magnet with eddy current driven Cu sheet	82
0359thry	Pulsed wiggler field inside circular cylinder with thin conducting wall	82
0360thry	Timing of ELF wiggler use	82
0361thry	Fields in ribbon-beam-electrode system	82
0362thry	Foraday-rotator-magnet	82
0363thry	Fieldline bow $\leftrightarrow$ field error in cyl. geometry	82
0364thry	Jose Alonso magnet	81
0365thry	Measurement coil for small quads	82
0366thry	Questions about properties of 2D, 3D magnet codes	82
0367thry	Application of the V-Q theory to the design of electromagnets	82
0368thry	Decay of fields in $\mu = \infty$ steel box	83
0369thry	Stability of current carrying wire in magn. field	81
0370thry	Eddy currents in circular pipe in quadrupole	83
0371thry	Filament-wiggler (for Sandia)	83
0372thry	Production of quadrupole field with windings on cylinder surface, surrounded by shells of various properties	83
0373thry	Quadrupole with thin sheet excitation, surrounded, at a distance, by a thin sheet of finite conductivity	83
0374thry	Finite thickness plate in homogeneous field	83
0375thry	Thoughts on description of fringe fields of dipoles	83
0376thry	Comments to representation of 2D dipole fringe fields	83
0377thry	Thin sheet eddy current damper	83
0378thry	Behavior of F, $\int F dz$, F' in vicinity of a corner	83
0379thry	3rd order kick in fringe field of quadrupole	83
0380thry	Estimate of flux going into pole of multipole	83
0381thry	Treatment of 2D quadrupole, with excitation sheet, eddy current sheets, etc., with matrices (in Laplace domain) (Version 1)	83

0413thry	2D electrode system to produce prescribed $\|E\|$ on a V = constant surface of prescribed shape	85
0414thry	Exact solution for 2D electrodes that give $\|E\|$ = constant on $V = 0$ surface given by curvature ≈ cos(k·curve length)	85
0415thry	Re-creation of eddy current overshoot limit	85
0416thry	Penetration of potential (+ fields) into a hollow cylindrical shell of zero potential and semi-infinite length	70
0417thry	Magnetic spring constants for radial and axial displacement of SLD coil	84
0418thry	$B(H)$ interpolation function	85
0419thry	$\bar{j}$ for circular bend of conductor (for POISSON)	85
0420thry	Representation of a rectangular 2D conductor with non-uniform j by a rectangular conductor with uniform j	85
0421thry	BNL measurement system deficiencies (quad system)	85
0422thry	Fields around $x_o = y_o = z_o = 0$ from centered rectangular ± charge sheet pair at $\pm z$	85
0423thry	Beam spreader magnet optics	86
0424thry	Beam spreader quadrupole: first cut	86
0425thry	GM in source magnet	86
0426thry	Fields, and flux into center pole, of cyl. in source magnet	86
0427thry	Field in vicinity of corner	86
0428thry	Design of poles of quadrupole for general shape of good field region	86
0429thry	Quadrupole, made with filaments, inside a dipole	86
0430thry	Filaments for dipole field parallel to midplane in midplane of dipole	86
0431thry	Sextupole = 0 from linear superposition of contributions from vacuum and iron	83
0432thry	Field change inside circular μ = constant shell in sin $n\varphi$ multipole with circular outer iron shell	86
0433thry	ALS combined function bend magnet (Note #1)	86
0434thry	ALS combined function bend magnet (Note #2)	86
0435thry	ALS laminated combined function bend magnet (Note #3)	86
0436thry	Aberrations in a curved laminated combined function bend magnet	86
0437thry	Penetration of solenoidal field through conducting shell	86
0438thry	Characterization of dipole fringe fields with field integrals	86
0439thry	Field from four semi-infinite line charges	86
0440thry	Flux in shell of Richard's refrigerator	86
0441thry	Math details for "perfect" quad end	86
0442thry	Math details index	86

0475thry	$\overline{B}$, B_0 in bend dipole	87
0476thry	Description of the properties of an ellipse	88
0477thry	Fields produced by eddy currents in thin elliptical vacuum chamber in dipole with $\mu = \infty$ poles, to 1st order	88
0478thry	Procedure to get $f[g(x,y)]$ with $\nabla^2 f = 0$, when $\nabla^2 g \neq 0$	88
0479thry	Useful techniques for designing a 2D non-dipole in dipole geometry	88
0480thry	De-normalization of fields and currents in quadrupole	88
0481thry	Excess flux in Gm32	88
0482thry	Total flux into 1st quadrant pole of quad when excited as dipole	88
0483thry	Thoughts about the (asymmetric) ALS ring quadrupole	88
0484thry	"Production" of nonlinear I_0 (V_0) for quadrupole shunt	88
0485thry	Summary of properties of fringe fields of multipoles	88
0486thry	3rd order kick in fringe field region of semi 1/0 quad	88
0487thry	Force in cylindrical symmetry on 1/2 tones	88
0488thry	A general theorem about integrals over Cartesian vacuum field components, and applications to field integral measurements	88
0489thry	Propagation of fast perturbation in dipole	87
0490thry	Boundary condition vacuum-conducting iron	87
0491thry	Flux into rectangular box	88
0492thry	Boundary condition at iron-air interface for AC, and application to 2D circle	88
0493thry	AC shielding of circular cylinder	88
0494thry	Propagation of AC fields in 1D	88
0495thry	Decay of fields between parallel plates, and in circular cylinder, with eddy current boundary condition	88
0496thry	$\Omega(x)$ properties	88
0497thry	Summary of eddy current modified H in $\mu \geq 1$, $\sigma \geq 0$ material	88
0498thry	Inadequacy of ID eddy current analysis	88
0499thry	Quad measurement coil system on surface of cylinder	88
0500thry	Sextupole measurement coil system	88
0501thry	Effect of (thin) gap in yoke of quadrupole	88
0502thry	"Math part" of ID eddy current analysis in iron	88
0503thry	Model functions for $H(B)$ without hysteresis	88
0504thry	$\|B\|$ at the edge of a multipole pole, and $\overline{B}$ between edges	88
0505thry	Analytical design of dipoles with vanishing $N = 3$; and $N = 3, 5, 7$ (no success)	88
0506thry	Eddy currents in $\mu\sigma \neq 0$ spherically symmetric system	88

0533thry	Design of window-frame magnet coil that gives no sextupole even though it can not touch poles	90
0534thry	Flux carried by ferromagnetic conduction bolt	90
0535thry	$F(z)$ outside circle from A (or V) on circle (if well behaved outside circle)	90
0536thry	Mapping exterior of ellipse to exterior of unit circle	90
0537thry	Procedure to "fake nut of universe" outside elliptical boundary in POISSON	90
0538thry	Line integral measurement with circular coil of magnet with non-parallel straight EFB ideal	90
0539thry	Properties of field integral along circular arc through a magnet with a field that depends on x, y, but not z	90
0540thry	Europe Notes — POISSON	90
0541thry	Calculation of 2D harmonics from exotic measurements	89
0542thry	POISSON notes, Europe 1990	90
0543thry	Circular cyclotron magnet design	90
0544thry	Curvature of $\omega = z^2/2$ map of circle	90
0545thry	Curvature of $\omega = z^n$ map of circle	90
0546thry	Flux induced onto $\mu = \infty$ surface by coil with I	90
0547thry	Change in EFB due to movement of coil, to 1st order	90
0548thry	Coil system to measure precisely the (integrated) strength of a (small) quadrupole	90
0549thry	I' shimmed vertical steering magnet	89
0550thry	Penetration of external fields into gap of semi-infinite dipole	90
0551thry	Penetration of external field into gap of dipole with finite pole thickness	90
0552thry	Multipole expansion of skew fields produced by filaments and sheets	90
0553thry	Dipole field from environmental field in fig 8 quad	90
0554thry	General procedure to get perturbation effects in non-ideal 2D magnets "without" finite element code	91
0555thry	CERN Permeameter: primitive analytical model	90
0556thry	Techniques for evaluating $F(C,A) = \int_0^{2\pi} [G(C + A\cos\varphi)\cos\varphi d\varphi]$	90
0557thry	$\int_0^{2\pi} \cos k(C + A\sin\varphi)\sin\varphi d\varphi = J$	90
0558thry	Amplitude dependent shift correction for modified sextupoles	90
0559thry	Field in iron quadrupole from $I' = \cos 2\varphi$	91
0560thry	Currents $\approx \cos n\varphi$ on circle in iron multipole	91
0561thry	Thin walled circular conducting shell in multipole field	91

0562thry	Generation of 3rd harmonic in mapped geometry with filaments in ideal multipole	91
0563thry	Generation of 2nd harmonic in mapped geometry with filaments in ideal multipole	91
0564thry	Multipole from I_1 in dipole and quadrupole	91
0565thry	Stored energy inside I carrying conductor	91
0566thry	$\mathcal{L}'$ for correction conductor in dipole	91
0567thry	Minimizing stored energy in (2D) region around point with given field	91
0568thry	A theorem about fields produced by ± filaments on closed $\mu = \infty$ boundary	91
0569thry	Map of circular disk on unit circular disk with centers at $\omega = 0$ and $z = 0$, with $\omega(1) = 1$ and $\omega(0) = \omega_0$, $\|\omega_0\| < 1$	91
0570thry	Re-formulation of "large gap suspension" problem in 2D	91
0571thry	Cyclotron correction coil use (Juelich Note)	91
0572thry	Transmission of light through a substance between two polaroid filters	92
0573thry	V_1, H_z, H_z', H_z'' for semi-infinite solenoid of finite radial thickness	92
0574thry	AC fields onto conducting 2D iron cylinder	92
0575thry	Penetration of mid-plane symmetric fields into ends of 2D dipole	92
0576thry	PM solenoid for SLAC Klystron	92
0577thry	Penetration of fields parallel mid-plane of 2D dipole into ends of dipole	92
0578thry	Design of coil system to measure quadrupole (re-creation)	92
0579thry	Sextupole measurement coil design	92
0580thry	Field from finite size Helmholtz coil	92
0581thry	Ratio of fields at points in scale and mapped geometry	92
0582thry	Power of Panofski quadrupole	92
0583thry	T-distribution in magnet when cooled/heated on outside surface	93
0584thry	Field in vicinity of $\mu = \infty$	93
0585thry	Magnet axes notation — Folder (no transcription)	68
0586thry	Ht windings — Folder (no transcription)	70
0587thry	Conductor dominated magnets — Folder (no transcription)	70
0588thry	Iron dominated magnets — Folder (no transcription)	69
0589thry	Over-relaxation — Folder (no transcription)	75
0590thry	Ripple (Eddy currents) — Folder (no transcription)	75
0591thry	Dipole with small gap bypass	93
0592thry	Displacement-caused change of force on coil in coil slot	93
0593thry	LEB-MEB symmetrical H dipole	92